Investigation into reliability and performance of an implantable closed-loop insulin delivery device

Dolly Jacob

December 2014

A thesis submitted to De Montfort University for the fulfilment of the requirements of the degree of Doctor of Philosophy

De Montfort University

Leicester School of Pharmacy

Faculty of Health and Life Sciences

Declaration

This thesis contains the original work of the author except where otherwise indicated.

Abstract

An implantable closed-loop insulin delivery device (INsmart device) containing a glucose responsive gel has been developed within the INsmart research group, over a period of 10 years, to mimic pancreas. In this thesis, the reliability and performance capability of the INsmart device was studied for future clinical use.

Investigations into the device material compatibility with insulin solution, assessed by monitoring insulin loss and degradant formation over a period of 31 days using RP-HPLC have shown that stainless steel and titanium are the most compatible materials. Polycarbonate contributes to insulin loss after 11 days, resin might not be the best material and polyurethane is the least compatible for future device designs.

To study insulin delivery mechanism and kinetics from the device, fluorescently labelled human insulin (FITC-insulin) was synthesised and characterised using RP-HPLC and MS, to produce a product with predominantly di-labelled conjugate (>75%) with no unreacted FITC or native insulin. Clinically used insulin analogues were also fluorescently labelled to produce predominantly di-labelled FITC-insulin conjugate with potential future biological and *in vitro* applications.

The drug release mechanism from the glucose sensitive gel held in the INsmart device, studied using fluorescein sodium was determined as a Fickian diffusion controlled release mechanism. The diffusion coefficient (*D*) for FITC-insulin in the non-polymerised dex2M-conA gel (NP gel) determined using mathematical models, QSS and TL slope methods was $1.05 \pm 0.02 \times 10^{-11}$ m^2/s and in the cross-linked dex500MA-conAMA gel (CL gel) was $0.75 \pm 0.06 \times 10^{-11}$ m^2/s. In response to physiologically relevant glucose triggers in the NP gel, the diffusivity of FITC-insulin increases with increasing glucose concentrations, showing a second order polynomial fit, device thus showing glucose sensitivity and graded response, mimicking pancreas. Rheological measurements further confirmed the gel glucose responsiveness demonstrated by a third order polynomial fit between FITC-insulin *D* and the NP complex viscosity in response to increasing glucose concentration. The knowledge of FITC-insulin diffusion kinetics in the gel has aided in making some theoretical predictions for the capability and performance of the INsmart device. Alternate device geometry and design optimisation is also explored.

Acknowledgements

I would like to thank Prof. M Joan Taylor for allowing me the opportunity to undertake this study under her supervision. Prof. Taylor has been a constant support and a great mentor during the course of this research. Along with Prof. Taylor I would like to thank Dr Paul Tomlins whose guidance and support has been invaluable. I would like to thank Dr Tarsem Sahota for his helpful insights, suggestions and help throughout the course of this research. I would also like to thank Dr Ewa Jaroszkiewicz for her support and guidance.

I would like to acknowledge and thank the technical staff in the Pharmaceutics Department for their assistance, especially Mr David Ian Fletcher for the essential technical support.

I would like to dedicate this research to my family. To my supportive husband who is my guide, my conscience and my best friend without whom I never would have finished. To my parents, who have always encouraged me to pursue my goals and never give up. To my daughter and son who are my daily motivation and inspiration. To my dear sisters and friends for their support and encouragements.

Finally I would like to thank De Montfort University for the research studentship and EPSRC UK National Mass Spectrometry Facility, Swansea University for analytical support.

Contents

List of Figures

List of Tables

List of Equations

Abbreviations and Nomenclature

η^*	complex viscosity
% RSD	percent relative standard deviation
ACN	Acetonitrile
Approx.	approximately
AUPs	area under peaks
BG	blood glucose
CL gel	cross-linked dex500MA-conAMA gel
CL dexMA-conAMA mixture	-cross linked methacrylated dextran–methacrylated concanavalin A mixture
conA	Concanavalin A
conAMA	concanavalin A methacrylamide (methacrylated concanavalin A)
conc.	concentration
D	diffusion coefficient (m^2/s)
D_e	effective diffusion coefficient (m^2/s) (measured using the QSS method)
dex2M	dextran, average molecular weight 2000 kDa
dex500MA	methacrylated dextran 500 KDa, DS 3%
dexMA	dextran methacrylate (methacrylated dextran)
EDTA	Ethylenediaminetetra-acetic acid
erf	error function
erfc	*complementary error function*
FDA	Food and Drug Administration
FITC	Fluorescein isothiocyanate
FITC-insulin conjugate	- Fluorescein isothiocyanate insulin conjugate.
G'	storage modulus which is a measure of the stored energy, the elastic part
G''	loss modulus which is a measure of the energy lost as heat, the viscous part
HbA1c	glycated haemoglobin, covalent conjugation of glucose with

	haemoglobin
HCl	hydrochloric acid
HPLC	High performance liquid chromatography
Hrs	hours
ICH	International Conference on Harmonisation of Technical Requirements for Registration of Pharmaceuticals for Human Use
i.e.	that is
LVE	linear viscoelastic range
min	minutes
m-cresol	meta cresol
NaCl	sodium chloride
NaOH	sodium hydroxide
NP gel	non-polymerised dex2M-conA gel
NP dex2M-conA mixture	non polymerised dextran 2 million Da –concanavalinA mixture
NSI	nanospray ionisation
PC	polycarbonate
PDA	photo diode array detector
PU	polyurethane
QSS	quasi steady state
R	resin
rDNA	recombinant DNA technology
RMM	relative molecular mass
RP-HPLC	Reverse Phase High Performance Liquid Chromatography
Rt	retention time
RT	Room temperature
RP-HPLC	Reversed phase high performance liquid chromatography
rpm	rotations per minute
SS	stainless steel
Std	standard
tan delta	ratio of *G"/ G'*
T1DM	Type 1 diabetes mellitus
T2DM	Type 2 diabetes mellitus
TFA	Trifluoroacetic acid

Ti	titanium
TL	time lag
t_{lag}	lag time
USP	United States Pharmacopoeia
WFI	water for injection

Chapter 1 Introduction

The primary focus of the work presented in this thesis was to investigate the performance capability and reliability of an implantable closed-loop insulin delivery device, INsmart for clinical use in treatment of sufferers of type 1 diabetes. A basic understanding of the disease and associated complications are presented in this chapter; a detailed account of the numerous effects on the body however is too vast to be studied here. Insulin structure and stability aspects are also presented, followed by current disease management strategies.

1.1 Control of blood sugar

Plasma glucose levels are normally maintained within a narrow range of 3.5-5.5 $mmolL^{-1}$ through the insulin-glucose-glucagon regulatory mechanism and are governed by a negative biochemical feedback (‘closed-loop’) that operates continuously and automatically and provides an appropriate response to the glucose levels. Normal glucose control is maintained through the antagonistic action of the two pancreatic hormones, insulin and glucagon. An overview of normal glucose homoeostasis is presented in **Figure 1-1**.

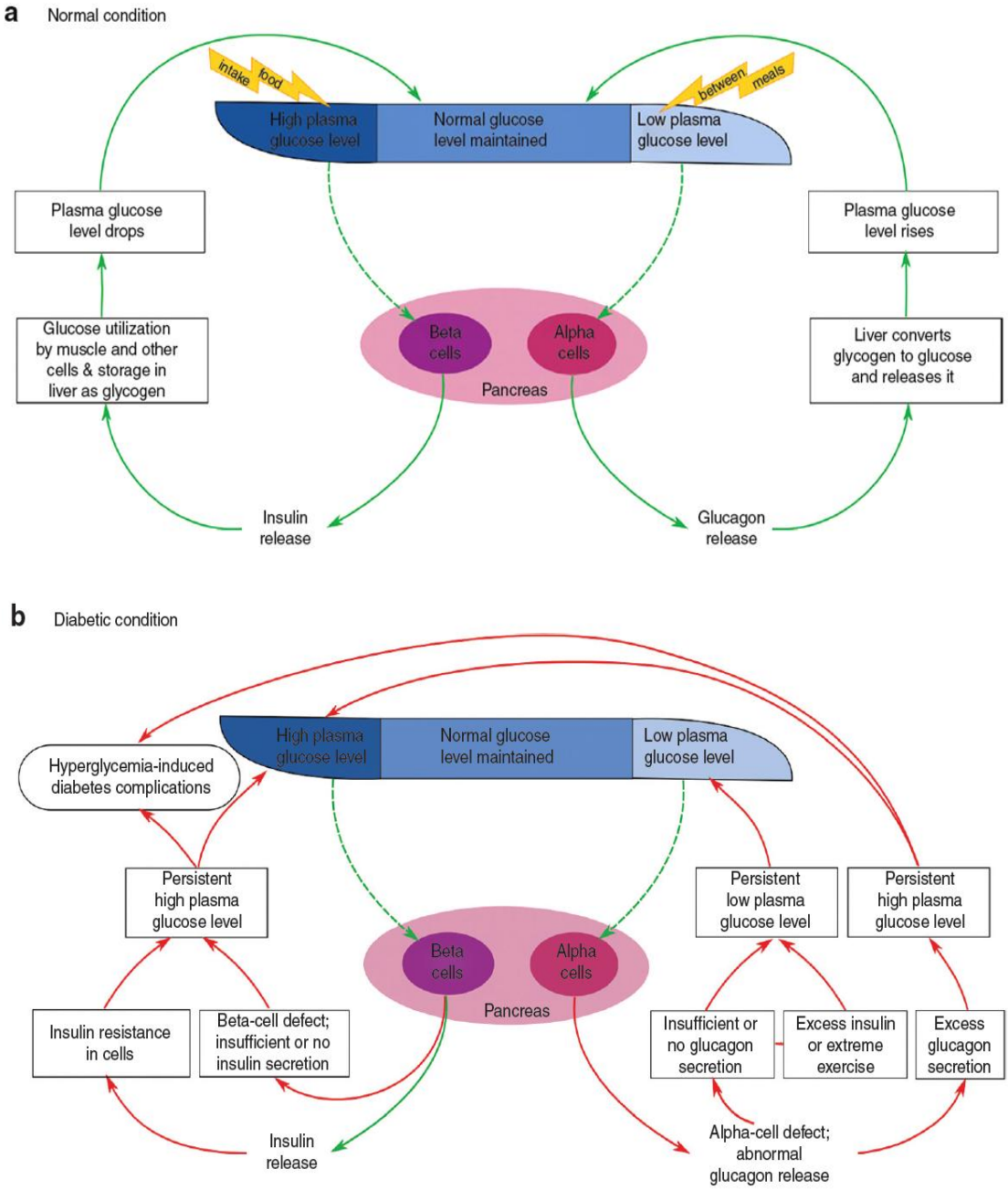

Figure 1-1: Overview of glucose homoeostasis under normal and diabetic condition (Ajmera et al., 2013).

In normal individuals, high blood glucose levels (post meal) stimulates insulin secretion by pancreatic islet β-cells and suppresses glucagon secretion from α-cells, which enables the muscle and other cells to take up glucose for energy and store them as

glycogen in liver. In low glucose conditions, glucagon secretion by pancreatic α-cells counter regulates the glucose level by inducing the breakdown of glycogen into glucose (refer to **Figure 1-1a**). When this synchronised regulatory mechanism is disrupted, it leads to diabetes (Ajmera et al., 2013).

Inefficient uptake of plasma glucose in diabetic individuals occur due to insufficient or lack of insulin production by β-cells, or the insulin resistance of target cells. This result in persistent high plasma glucose levels (hyperglycaemia) (refer to **Figure 1-1b**). This condition is often accompanied by absolute or relative excess of glucagon which causes higher rate of hepatic glucose production than utilisation, which further contributes to hyperglycaemia (refer to **Figure 1-1b**) (Dunning and Gerich, 2007; Puri and Hebrok, 2012; Talchai et al., 2012). Another defect observed in diabetic patients is impaired secretory response of α-cells to low-glucose concentrations, which leads to the risk of episodes of severe hypoglycaemia, especially in patients exposed to excessive insulin during treatment or to extreme physical activities carried out as part of self-management (refer to **Figure 1-1b**) (Cryer, 2002).

The mechanism of insulin release from normal pancreatic beta cells is more or less constant within the beta cells, irrespective of blood glucose levels. It is stored within vacuoles pending release via exocytosis and release into plasma is primarily triggered by concentration of glucose in the plasma as shown in **Figure 1-2**.

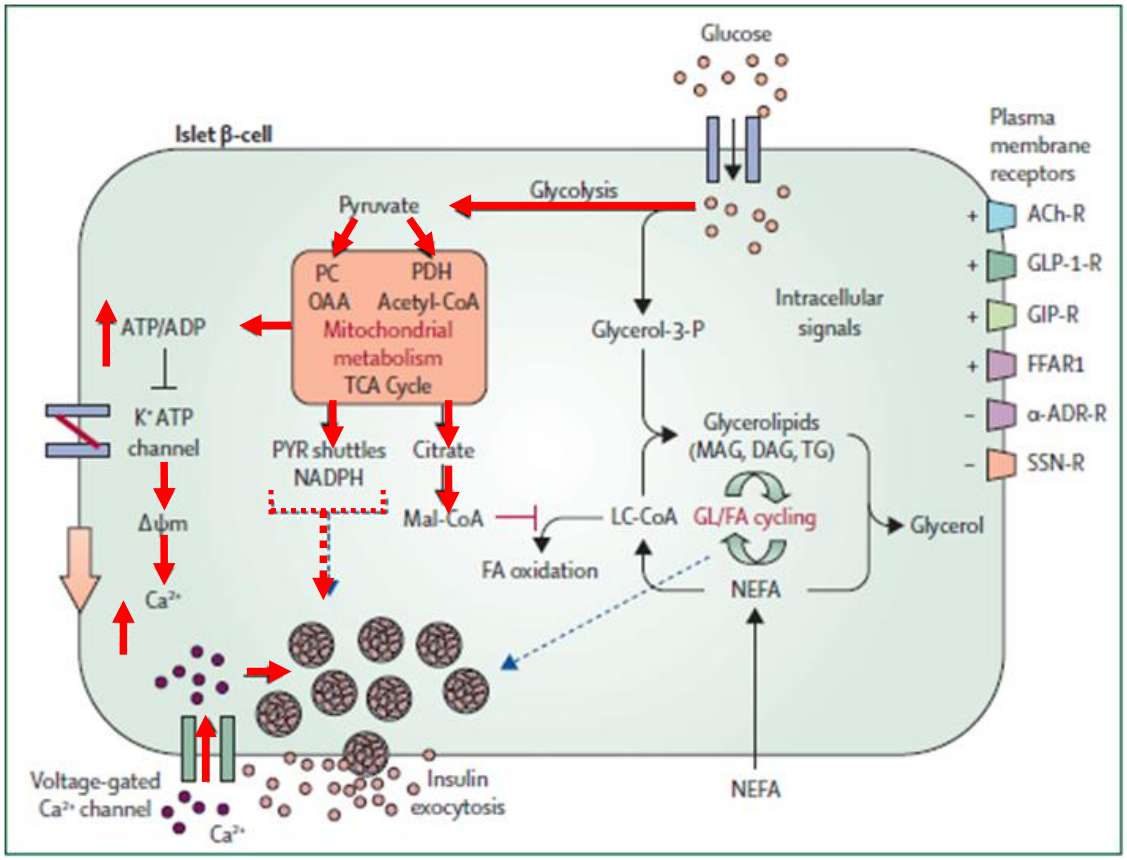

Figure 1-2: Role of islet β-cell metabolic activation by fuels and neurohormonal agonists in insulin secretion (main pathway highlighted in red), PC=pyruvate carboxylase. PDH=pyruvate dehydrogenase. Ach-R, GIP-R, GLP-1-R, FFAR1, α-ADR-R are all receptor on β-cell surface.OAA, oxaloacetate; CoA=coenzyme A. Δ_m=change in plasma membrane potential. Mal-CoA=malonyl-CoA. LC-CoA=long-chain acyl-CoA (Nolan, Damm and Prentki, 2011).

A pancreatic beta cell senses the concentration of glucose in plasma as glucose can equilibrate rapidly across the β-cell membrane due to the expression of the high capacity, low affinity glucose transporter-2 (MacDonald, Joseph and Rorsman, 2005). Glucose enters the β-cell by facilitated diffusion through glucose transporters (GLUT1 and 2). The next irreversible step of glucose phosphorylation catalysed by a single enzyme glucokinase (GK) appears to be rate limiting for β-cell glycolytic flux under normal physiological conditions, so that GK is regarded as the β-cell 'glucose sensor',

underlying the dependence of the β-cell insulin secretory response to glucose in the physiological range (Fridlyand and Philipson, 2010).

Once phosphorylated, glucose is metabolised via glycolysis to pyruvate and in the mitochondria to acetyl-CoA, which is then oxidised in the TCA cycle. These actions lead to an increased cytosolic ratio of ATP to ADP, which closes the K^+ ATP channels, depolarises the plasma membrane potential, and opens voltage-gated Ca^{2+} channels, causing influx of Ca^{2+} and the triggering of insulin-granule exocytosis. A number of other processes also simultaneously occur which enhance the pathway and augment insulin secretion. The β-cell also responds to other neurohormonal and metabolic extracellular signals via various plasma membrane receptors.

In diabetic individuals, the targets for self monitored blood glucose levels before meals are 4-8 mmol/L for children, and 4-7 mmol/L for adults and 2 hours post prandial is < 10 mmol/L for children and < 8.5 mmol/L for adults (Montague, 1983; Shier, Butler and Lewis, 2003; Gandy, 2014; NICE, 2004; NICE, 2008). Concentrations outside of this range for a long period can be harmful, particularly in the brain for which glucose is the primary fuel. In hypoglycaemic conditions the brain will become starved of glucose and the patient can become comatose. In the long term, hypoglycaemia and hyperglycaemia can cause a range of problems. Most diabetic individuals maintain glycaemia control by measuring their blood glucose several times a day or with occasional HbA1c readings. HbA1c is the level of the covalent conjugation of glucose with haemoglobin which is a descriptor and predictor of likely health outcomes. Internationally, the target HbA1c level for most people is 53 mmol/mol (7.0%) or less (Gandy, 2014).

1.2 Diabetes mellitus

Diabetes mellitus can be described as a group of metabolic diseases characterised by persistent hyperglycaemia due to inefficient uptake of plasma glucose by muscles and other cells, which is caused by deficient insulin secretion or by resistance to the actions of insulin combined with relative insulin deficiency. Insulin resistance and insulin deficiency lead to the abnormalities of carbohydrate, fat, and protein metabolism that are characteristic of diabetes mellitus, chronic hyperglycaemia which is characteristic of

diabetes causes long-term damage, dysfunction, and failure of various organs, especially the eyes, kidneys, nerves, heart, and blood vessels (American Diabetes Association, 2008). "Diabetes mellitus" means "excessive excretion of sweet urine", based on the characteristic symptoms of the condition which is excretion of large amounts of glucose in the urine, a condition known as glucosuria.

Diabetes mellitus is a relatively common disease; the affected population shows some degree of abnormality in glucose metabolism that is indicative of diabetes itself or a tendency towards it. Some key facts published by WHO (Fact sheet No312, reviewed October 2013), state that 347 (314-382) million people in 2008 worldwide (representing nearly 5% of the world's population) have diabetes. This is an increase from 153 (127-182) million in 1980 and is expected to affect 552 million people by 2030. This provides some idea of escalation of the condition. The study published in *Lancet* by Danaei, Finucane et al summarised that diabetes is rising globally, driven by population growth, ageing and by increasing age-specific prevalence. The study highlighted the necessity for effective preventive interventions and for health systems to be prepared to detect and manage diabetes and its follow-on effects (Danaei et al., 2011). An estimated 3.4 million people died from consequences of diabetes in 2004 (World Health Organization, 2009). According to WHO, diabetes will be the 7th leading cause of death in 2030 (World Health Organization, 2011a).

The International Diabetes Federation (IDF) in 2013 estimated that (of the adult world population of 4.6 billion) the five countries with the largest numbers of people with diabetes were China (98.4 million), India (65.1 million), the United States of America (24.4 million), Brazil (11.9 million) and Russian Federation (10.9 million). The IDF also reported that in 2013 the five countries with the highest diabetes prevalence in the adult population were Tokelau (37.5%), Federated States of Micronesia (35.0%), Marshall Islands (34.9%), Kiribati (28.8%) and Cook Islands (25.7%). Low and middle income countries face the greatest burden of diabetes (Diabetes UK, 2012; International Diabetes Federation, 2013).

Based on the 2011 study of prevalence of diabetes in the adult population across the UK, gives an average prevalence of 4.45 per cent in adults. It is estimated that more than one in 20 people in the UK has diabetes (diagnosed or undiagnosed). Most health

experts agree that the UK is facing a huge increase in the number of people with diabetes. By 2025 it is estimated that five million people will have diabetes. Most of these cases will be T2DM diabetes, because of the ageing population and rapidly rising numbers of overweight and obese people. The figures are alarming and confirm that diabetes is one of the biggest health challenges facing the UK today. To curb this growing health crisis with reduction in associated deaths from diabetes and its complications, Diabetes UK propose increasing awareness of the risks along with lifestyle changes, improving self-management and access to integrated diabetes care services (Diabetes UK, 2012).

The financial burden from diabetes management on the individual and the health services are immense. In the UK it is currently estimated that about 10 per cent of the NHS budget is spent on diabetes. The challenge for producing effective affordable treatments is therefore large, growing and global (Diabetes UK, 2012).

Reduction in the risk of complications has been shown with good diabetes management; however failure to do so has been associated with serious complications including heart disease, stroke, blindness, kidney disease and amputations leading to disability and premature mortality. There is also a substantial financial cost to diabetes care as well as costs to the lives of people with diabetes. Half the people with type 2 diabetes show signs of complications by the time they are diagnosed. These complications may begin five to six years before diagnosis and the actual onset of diabetes may be ten years or more before clinical diagnosis (Diabetes UK, 2012).

There are three main types of diabetes;

Type 1 diabetes mellitus (T1DM) – TIDM results from the metabolic defect that stems from an autoimmune destruction of pancreatic β-cells in the pancreatic islets of Langerhans with a consequent inability to produce sufficient insulin. The causes of T1DM are not yet known but have been shown to be due to a combination of genetic predisposition and environmental conditions, such as exposure to certain viruses or other associated autoimmune condition (Holt and Kumar, 2010)(TEDDY Study Group, 2008). T1DM has an early onset in life and symptoms quickly become severe. The classical symptoms include polydipsia (intake of large volumes of water), polyuria (frequent urination), hyperglycaemia, and (usually) recent unexplained loss of weight

along with at least two of the following characteristic features – rapid onset of symptoms over days or weeks, glucosuria or blood glucose markedly raised, ketones in the urine or blood or family history of T1DM. T1DM is a condition wherein the insulin activity is not impaired but there is an absolute insulin deficiency causing persistent hyperglycaemia. The condition therefore responds to insulin replacements.

T1DM requires both insulin therapy and careful lifelong control of the balance between dietary intake and insulin dose. Without insulin replacement, people developing T1DM risk surviving and with which they can participate normally in the usual daily activities, but still are at risk of associated complications. T1DM individuals are at risk of ;

- metabolic complications such as hyperglycaemic ketoacidosis, hypoglycaemia, dyslipidaemia;
- macrovascular complications such as cardiovascular, cerebrovascular, peripheral vascular disease;
- microvascular complications such as retinopathy, nephropathy, sensory, motor, and autonomic neuropathy;
- psychological complications such as depression and anxiety.
- other complications associated with non-adherence to recommended management in children and young adults due to family conflict or risky behaviour. Pregnant women have increased risks of complications, such as: hypertension and pre-eclampsia, foetal and neonatal complications such as congenital malformations, and macrosomia (Brownlee, 2001; Brownlee, 2005).

Type 2 diabetes mellitus (T2DM) – T2DM is caused by insulin resistance and a relative insulin deficiency resulting in persistent hyperglycaemia. T2DM is slow to develop (typically in older, obese individuals); the symptoms are milder and often go unrecognized at first often with complications developing before diagnosis. Excessive thirst, polyuria, polydipsia are characteristic symptoms (similar to T1DM) of T2DM (Nelson and Cox, 2008).

T2DM is often referred to as insulin–resistant diabetes but in fact is a group of diseases where the regulatory activity of insulin is disordered due to a combination of insulin resistance, pancreatic beta-cell failure resulting in insufficient insulin secretion or some

feature of the insulin-responsive system being defective, in spite of insulin production. People with T2DM differ in the levels of increased insulin resistance and decreased insulin secretion. Genetic susceptibility is linked to increased body weight, physical inactivity and age-related weight gain (Williams, 2003; American Diabetes Association, 2008). T2DM is often associated with a strong familial predisposition and thus a positive family history confers a 2.4-fold increased risk for T2DM, however the genetics of T2DM are complex and not clearly defined. Only a handful of genes have been identified: genes for calpain 10, potassium inward-rectifier 6.2, peroxisome proliferator-activated receptor gamma, insulin receptor substrate-1, and some others (Stumvoll, Goldstein and van Haeften, 2005). Ethnicity affects the prevalence of T2DM; a greater than 10-fold difference is seen between high-risk and low-risk ethnic groups. Also T2DM is more prevalent in adults who had low birth weight for gestational age (BMA, 2004; National Diabetes Support Team, 2006). Polycystic ovary syndrome can increase the risk of impaired glucose tolerance and diabetes.

The additional risk factors for T2DM include obesity, lack of physical activity, history of gestational diabetes, impaired glucose tolerance, impaired fasting glucose, drug therapy, cigarette smoking, low fibre and high glycaemic index diet (Hundal and Inzucchi, 2003, Srinivasan et al., 2008, Hu et al., 2001). The so-called metabolic syndrome (a combination of obesity, hypertension, and dyslipidaemia) increases the likelihood of T2DM (Srinivasan et al., 2008).

Individuals with T2DM diabetes are at increased risk of developing microvascular and macrovascular complications (Khunti et al., 2006; Srinivasan et al., 2008). The complications of T2DM diabetes are associated with high blood pressure, high lipid levels, muscle damage, foot, eye, renal problems (nephropathy) and neuropathy (NICE, 2008). Randomized controlled trials have suggested that high BP values in people with T2DM diabetes are linked to a rapid decline in renal function. Higher levels of triglycerides present immediate risks of pancreatitis. Intensive BP control can reduce progression of microvascular complications. Reviewing the feet of people with diabetes regularly and keeping blood glucose, blood fats and blood pressure under control can prevent some of the complications associated with the feet. Diabetes is the most common cause of lower limb amputations.

Though the complications of T1DM and T2DM diabetes are essentially the same, in poorly controlled individuals microvascular complications tend to be more common in T1DM diabetes where as macrovascular complications are more common in T2DM diabetes. The major causes of mortality are similar, though there is a greater reduction in life expectancy in T1DM diabetes than T2DM diabetes.

The association between obesity, diabetes, the metabolic syndrome and cancer (Giovannucci et al., 2010; Renehan et al., 2008), have been investigated over a long period of time and hyperinsulinemia and /or insulin resistance have been established as major factors in its pathogenesis. T2DM has been associated with a range of cancers including breast, colorectum and bladder (Johnson et al., 2012), while association of T1DM and cancer remains more speculative.

Gestational diabetes mellitus (GDM) - GDM is defined as a condition that arises during pregnancy (usually during the second or third trimester) in a previously undiagnosed female and occurs as the body cannot produce enough insulin to meet the extra needs of pregnancy resulting in abnormally high glucose levels. GDM results from an increased severity of insulin resistance as well as an impairment of the compensatory increase in insulin secretion during pregnancy. Pregnancy serves as a metabolic stress and uncovers underlying insulin resistance and beta cell dysfunction (Singh and Rastogi, 2008). GDM affects up to 5 per cent of all pregnancies and is normally transitory and resolves after delivery. Women who are overweight or obese are at a higher risk of GDM and approximately 7% are at risk of going on to developing T2DM diabetes. Children born to mothers with GDM also have a higher risk of suffering from obesity and T2DM in later life.

Other specific types of diabetes include monogenic diabetes which is due to a single gene defect. It was previously known as 'Maturity-Onset Diabetes in the Young', MODY which is related to lifestyle/obesity in teenagers and is in fact T2DM. Other specific types include diabetes secondary to pancreatectomy or pancreatitis (Holt, Kumar 2010).

1.3 Insulin

1.3.1 Insulin structure

One of the outstanding achievements of modern medicine has been the discovery of use of insulin as an injected therapeutic agent for the treatment of diabetes**.** Due credit goes to (Banting and Best, 1922) for the isolation of insulin from pancreas in 1922, which has been one of the exciting discoveries in medicine of the last century. Since then, insulin has been one of the most extensively studied molecules of biochemistry. Banting and Best were successful in isolating a concentrated pancreatic secretion which demonstrated lowering of blood glucose in animals and under careful control in humans with diabetes with relatively low toxicity. Following this discovery, crude extracts of cow, pig and sheep pancreas were used to treat diabetes until purified insulin was successfully crystallized by (Abel, 1926) and by (Scott, 1934), when zinc – insulin was crystallized.

Structure at synthesis

The insulin molecule is originally synthesised in the human body as preproinsulin composed of 110 amino acids in the beta cells of the pancreas. The ‘signal peptide’ comprising of 24 amino acids are removed by enzyme action from one end of the chain when it passes through the endoplasmic reticulum, leaving another form (pro-insulin) behind. Further 2 amino acids are removed by another enzyme carboxypeptidase E. The proinsulin, as shown in **Figure 1-3** folds and bends to give the molecule its final structure. The middle C-peptide section ("the C chain") of 33 amino-acids is then removed by the action of the enzymes prohormone convertase 1 and 2, converting it into the final structure with 2 chains, A and B. Insulin and C-peptide are packaged together in the secretory granule. On stimulation of the beta cell, C-peptide and insulin are secreted in equimolar proportions. Thus, C-peptide levels reflect beta cell functional capacity.

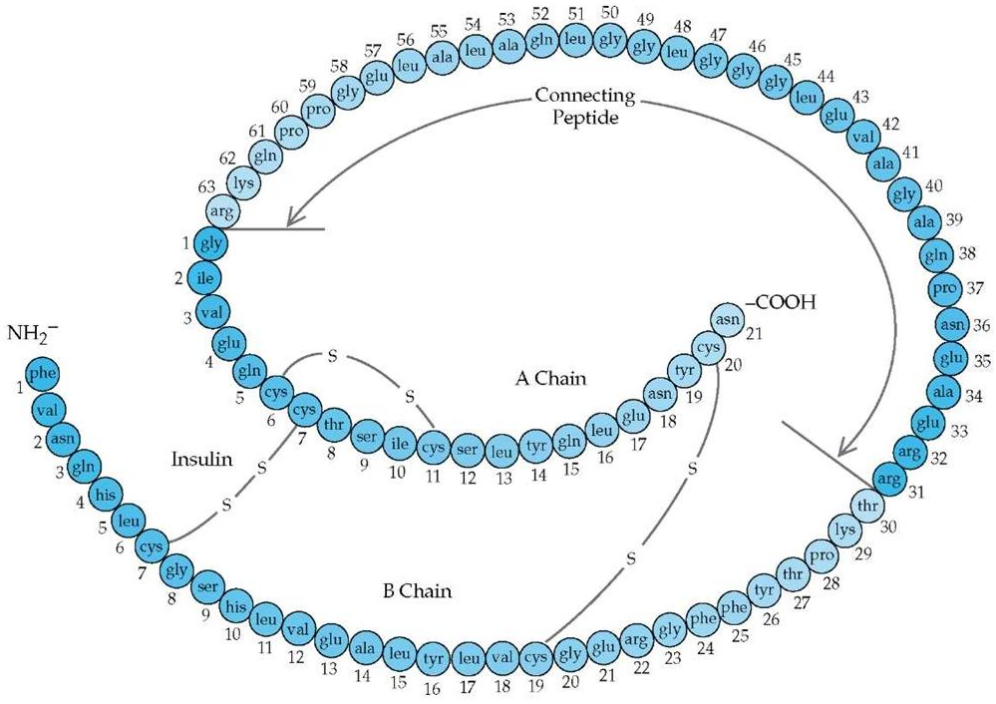

Figure 1-3: The structure of human proinsulin, the precursor molecule to insulin. The 33 amino acid peptide that connects the amino terminus (NH2-) of the A chain to the carboxyl terminus (-COOH) of the B chain is called connecting peptide (C-peptide) (taken from (Voet and Voet, 1995), p.193).

The human insulin molecule consists of two polypeptide chains (A and B), linked to each other by two disulfide bonds, containing 51 amino acid residues and is illustrated in **Figure 1-3**. The A chain consists of 21 residues with an additional disulfide loop between A6 and A11 whereas the longer B chain consists of 30 residues. The three-dimensional structure of the insulin molecule is formed of three α-helices (residues A1–A8, A12–A18 and B9–B19) and a β-strand from B21 to B30 constrained by the intra- and two interchain disulphide bonds. The nonpolar cysteine residues A6-A11 and the aliphatic side chains of residues A2, A16, B11 and B15 constitute the hydrophobic core of the insulin monomer and the surface is covered by both polar and nonpolar residues. The A chain and the B9-B19 helix form a stable structural unit, whereas the B25-B30 and B1-B8 segments are variable in conformation. Phenol or *m*-cresol is usually added to insulin preparations to promote α-helical conformation of the B-chain segment, B1-B8.

Insulin imparts its biological effects as a monomer. Insulin exists in its active monomeric form (Cahill Jr, 1971), in solutions at neutral pH, only at low concentrations of < 0.1 µM, ~ 0.6 µg/mL. Insulin is in circulation in the blood at a concentration of 10^{-8} to 10^{-10}M (physiological concentrations ~ 1 ng/mL) (Frank, Pekar and Veros, 1972; Blundell et al., 1972).

Despite the variations in amino acid sequence in insulin from other animal species, the folding and packing of the two chains into their three dimensional conformation are essentially the same in all insulins. Insulin from the hystricomorph rodent family show the highest number of amino acid substitutions; for example guinea pig insulin contains 18 residues different from the respective positions in human insulin. Of the other insulin used for pharmaceutical preparations, porcine (refer to **Figure 1-4**) and bovine insulins contain alanine in position B30 and bovine insulin contains alanine in position A8 and valine in A10.

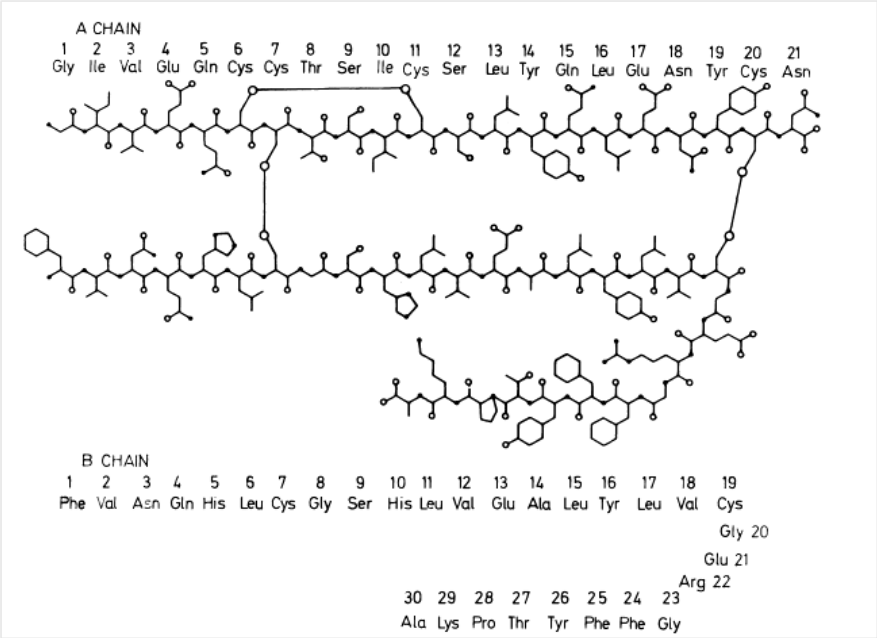

Figure 1-4: The chemical structure of pig insulin as determined by (Brown, Sanger and Kitai, 1955).

At higher concentrations the insulin monomers self-associates to form dimers where two identical monomers come together to form an antiparallel β-sheet between the two COOH-terminal of B23 and B30 residues, this further packs ProB28 against B20 to B24 residues. The two molecules in a dimer are held together by, hydrophobic interactions, nonpolar forces and stabilized by four hydrogen bonds between monomer residues B24 and B26 (Baker et al., 1988; Brange et al., 1990).

In the presence of zinc and in higher concentrations at acidic or neutral pH, three dimers assemble to form a soluble, globular protein structure, a hexamer as shown in **Figure 1-5** (Baker et al., 1988). Though the insulin monomer represents a small motif of protein folding, the zinc-hexamers exhibits key features of globular proteins; such as secondary structure elements (the α-helix, 3_{10}-helix, β-sheet and the β-turn), tertiary organisation of hydrophobic core, specific interfaces for self-assembly and allosteric regulation through ligand-dependent conformational changes (Baker et al., 1988; Weiss, 2013). The zinc ions are situated in the polar channel in the centre of the hexamer coordinated to B10 His. The hexamer can adopt two different states – T-state and R-

state which refers to an extended or a α-helical conformation of the B-chain N-terminal respectively. The R-state which is more stable and has lesser tendency to dissociate is induced by phenol in the presence of zinc ions and thus is a property of the hexamer (Brange and Langkjaer, 1993). This R-state where the B1-B8 α-helices are stabilized at the dimer-dimer interface of a hexamer occurs in the presence of phenol or cresol molecules and its position restricts the zinc-ion diffusing out of the hexamer (Derewenda et al., 1989; Kaarsholm, Ko and Dunn, 1989).

In aqueous and neutral solutions and at higher concentrations ≥ 2mM, insulin molecules have a propensity to dimerise and it further assembles into hexamers in the presence of zinc ions which ensures its stability. However, as insulin binds to its receptor as a monomer, this property of forming hexamer is not necessary for the biological activity of the hormone.

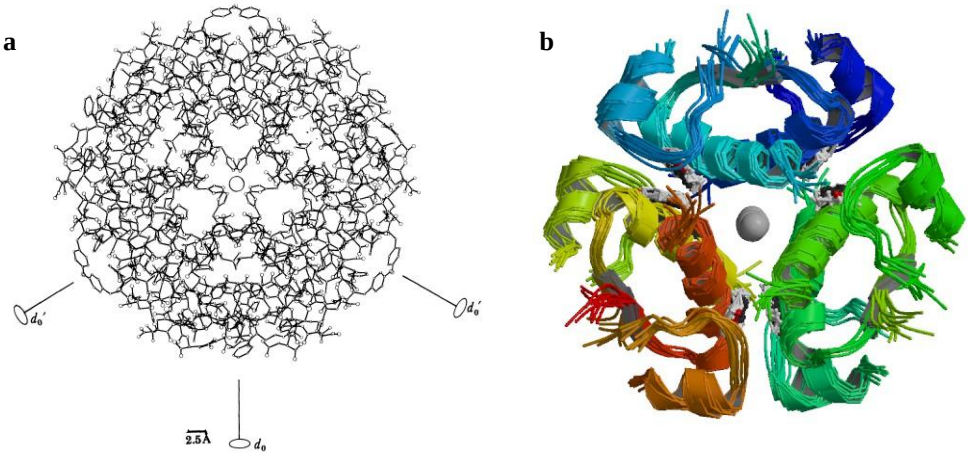

Figure 1-5: **a:** Atoms in the 2Zn insulin hexamer viewed along the crystal threefold axis, as determined by (Baker et al., 1988); **b:** The R6 Human insulin hexamer (non-symmetric), NMR structure. Protein chains are coloured from the N-terminal to the C-terminal using a colour gradient (Chang et al., 1997).

Insulin Analogues: The insulin hexamer crystal structure elucidated by Hodgkin et al in 1969 still continues to provide insight for biosynthesis processes and forms the basis for modern efforts to optimize its molecular properties for use in treatment of diabetes (Brange et al., 1987; Dodson et al., 1993; Berenson et al., 2011). Advances in protein

design have immensely helped in modifying the insulin molecule to modulate its pharmacokinetic and pharmacodynamic properties (Brange, 1997; Freeman, 2009). This has been made possible as it has been demonstrated that surface amino acids residues in a native insulin molecule, including dimers and hexamers can be altered independent of the receptor binding surfaces (Shoelson et al., 1992).This has resulted in insulin analogue formulations currently used clinically which are rapid-acting formulations intended for bolus injection before meals or use in pumps and long-acting basal formulations intended for once-a-day injections. Some of the insulin analogues created in this manner, along with the strategies used for creating them are described in **Chapter 4**.

1.3.2 Insulin stability

The structural integrity of a therapeutic protein is essential for the maintenance of its physiological and pharmacological activity, thus its efficacy. Insulin stability is critically dependent on the conformational flexibility within the insulin molecule which controls the rate of spontaneous structural transformation and can be categorized as physical or chemical alterations in the molecule. These have mutual influence; changes in conformation affect the susceptibility of the molecule for chemical attack and vice versa. A variety of physical modifications of the secondary and quaternary structure (which include denaturation, adsorption, precipitation, fibrillation and aggregation) and chemical changes of the primary structure (yielding insulin derivatives) are known to affect insulin and insulin preparations during storage and use.

1.3.2.1 Physical stability

Physical instability is manifested as macroscopically visible changes observed when handling or use of insulin such as increase in solution viscosity, precipitation from solutions, changes in physical appearance of suspensions or visible signs of insulin adsorption.

Denaturation or unfolding is the loss of the physical native three-dimensional or globular structure with no change to their chemical composition. Denaturation could be thermal denaturation induced by elevated temperatures resulting in formation of irreversible aggregates, cold denaturation occurring well below the freezing point of water or chemical denaturation due to binding of chaotropes such as urea and guanidinium hydrochloride that disrupt the 3D molecular structure of proteins(Manning et al., 2010).

The insulin lost due to **adsorption/adhesion** is inversely proportional to insulin concentration (negligible for higher concentrations such as 5 IU/ml (~ 0.2 mg/ml)) and varies with the material, being more prone to be adsorbed to hydrophobic than to hydrophilic surfaces. Insulin adsorption can be counteracted by addition of 0.1 – 1% of albumin.

Precipitation

Precipitation can occur in insulin solutions due to a number of factors. Generally reduction in insulin solubility due to pH changes or introduction of Zn^{2+} or other divalent metal ions results in formation of amorphous or crystalline precipitates in insulin solutions as shown in the adapted illustration, **Figure 1-6** (Brange et al., 1987). The isoelectric precipitation (pI) value for native insulin is 5.4 (Jensen, 2009). Small amounts of leachable material from device materials or container closure systems could bring the insulin solution in its isoelectric precipitation zone (pH 4.5 – 6.5), especially if the solution is unbuffered (Melberg et al., 1988). Also, absorption of buffer leading to drop in pH of insulin solutions, and/or absorbed phenol from insulin preparations can cause precipitation.

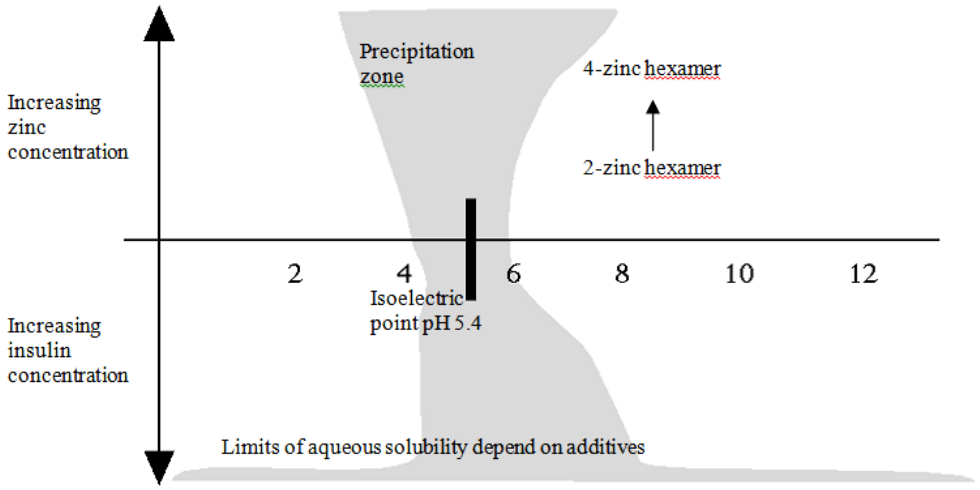

Figure 1-6: Schematic diagram showing the influence of increasing zinc and insulin concentration on precipitation of insulin (adapted from (Brange et al., 1987)). The shaded area represents the insulin precipitation zone.

Fibrillation

Under the influence of heat, insulin has a tendency to undergo conformational changes resulting in linear aggregation or fibrillation which precedes precipitation. Waugh has shown that observable fibrillation precedes precipitation by a nucleation growth mechanism involving three or four insulin monomers (Waugh, 1946a; Waugh, 1946b; Waugh et al., 1953, Weiss, 2013). Elevated temperatures are required for nucleus formation; however subsequent growth into fibrils can occur at low temperatures (Waugh et al., 1953). The fibril nuclei formation probably proceeds via monomerisation of oligomeric insulin. A mechanism for fibrillation using computer simulations of insulin aggregation has been reported where partially unfolded insulin monomers have shown to associate and form intermediate assemblies (Sluzky et al., 1991; Sluzky, Klibanov and Langer, 1992). The slow formation of intermediates, commonly observed as a lag time in fibrillation, reaches a critical size (170nm in diameter corresponding to ~100 molecules) which has sufficient surface area for stability and for interactions with native insulin molecules.

Neutral solutions containing low concentrations of hexameric insulin are more prone to fibrillation. It is thought that fibrillation, which involves dissociation of insulin hexamers and conformational changes of the monomer, probably precedes adsorption (Phillips et al., 2012). Addition of glycerol and some polysaccharides to insulin solutions significantly increase physical stability however they significantly decrease the chemical and biological stability. Addition of calcium and zinc ions improves the physical stability of neutral insulin preparations at higher concentrations. A marked fibrillation-inhibitory effect is obtained by low concentrations of lecithin or a synthetic detergent for example 400U/mL pump insulin marketed by Aventis has detergent (Genapol®). The most effective stabilization is seen when these methods are combined. Bovine insulin is more prone to fibrillation than human or porcine insulins, due to A8 Alanine residue on the hexameric surfaces aiding interactions with hydrophobic surfaces. It has been shown that in the presence of higher molecular contaminants such as covalent dimer, proinsulin etc. insulin has lesser propensity to fibrillation (Brange et al., 1982).

Aggregation

There is no single pathway by which aggregation occurs and a number of factors can contribute to protein aggregation such as incorrect folding during protein expression, perturbation of the native conformation during purification, formulation, freeze-thawing, freeze-drying, ultrafiltration/diafiltration, vial and syringe filling, pumping, transportation or storage. It is thus important to consider the intrinsic conformational stability of the protein as well as the protein-protein interaction (Manning et al., 2010). General mechanisms of protein aggregation as described by Philo (Philo and Arakawa, 2009) are association of native monomers e.g. assembly of insulin hexamers, aggregation of conformationally altered monomers, aggregation of chemically modified monomers, nucleation controlled aggregation which involves formation of nucleus or seed and surface induced aggregation. Non-native aggregation can cause a number of undesirable effects such as adverse immunological effects during therapy, reduced efficacy, unacceptable physical state and appearance.

1.3.2.2 Chemical stability

Chemical instability involves covalent modification of the protein amino acid sequence (primary structure) leading to bond formation or cleavage. Chemical instabilities can be classified as following;

Hydrolytic reactions

The principle hydrolytic products in acidic and neutral solutions are acid-catalysed deamidation of residue Asn ^{A21} (A21 desamido insulin) (Sundby, 1962) and base-catalysed deamidation of residue Asn ^{B3} (B3 desamido insulin). The B3 transformation leads to formation of a mixture of isoAsp and Asp derivatives (Brange et al., 1992b). Deamidation is discussed in detail in **Chapter 3**. Hydrolytic chain cleavage of the A-chain at A8-A9 occurs in crystalline suspensions of rhombohedral crystals in presence of additional free zinc ions (Brange, 1992c).

Formation of covalent dimers and oligomers

Covalent insulin dimers (CID) and oligomers are formed at ambient or higher temperatures during storage in neutral solutions and in amorphously precipitated insulin (Brange and Langkjaer, 1993). These are formed through transamidation wherein amine groups on one molecule (predominantly the B1 α-amino group) reacts with side chain carboxyamide groups on another molecule (usually in the A chain) (Weiss, 2013). The rate of CID formation varies with composition, formulation and in some instances the concentration of the preparations and is only slightly influenced by species. In crystalline insulin zinc suspensions, following prolonged storage at temperatures above 25°C, successive transamidation of insulin molecules with already formed insulin dimers lead to formation of trimers and tetramers (Brange, Havelund and Hougaard, 1992a). Insulin analogues with the B1 α-amino group blocked by direct addition of polyethylene glycol or thyronine have been investigated to avoid B1-mediated transpeptidation (Hirsch, 2005).

Disulfide Interchange Reactions

Disulfide interchange reactions which require juxtaposition of disulfide bridges from different insulin molecules are initiated by cleavage of cystine A7-B7 by hydrolysis or β-elimination (Manning, Patel and Borchardt, 1989). In regular formulations such polymers are detected (Brange, Havelund and Hougaard, 1992a).

1.3.2.3 Influence of pH, auxiliary substances and temperature

Deterioration due to different hydrolysis reactions is at a minimum at around pH 6.5, whereas acidic pH 4 is optimum for formation of covalent dimers and oliogomers. In alkaline media (pH >9) accelerated formation of covalent oligomers and polymers is observed as a function of pH. With increasing pH, increasing formation of B3 deamidation products has been observed (Brange, Havelund and Hougaard, 1992a). Isotonic substances and preservatives influence the stability of insulin preparations by their effect on deamidation and CID formation. Among preservatives, it was found that there is a gradation in the stabilizing effect namely phenol > *m*-cresol > methylparaben and for isotonic agents, NaCl > glycerol > glucose (Brange and Langkjaer, 1992e). Temperature is a major influence in all pharmaceutical insulin preparations. The rate of deamidation and formation of higher molecular weight (HMWT) products increases with increase in temperature (Brange, Havelund and Hougaard, 1992a; Brange et al., 1992b; Brange and Langkjaer, 1993).

1.4 Disease management

Over the past 30 years, dramatic changes have occurred in the management of T1DM diabetes mellitus. Insulin replacement strategies, administering smaller doses of insulin (basal doses) throughout the day and appropriate insulin doses (bolus doses) as needed to supplement for additional anticipated carbohydrate intake or subtract for exercise have made it possible to maintain near-normal glycaemia in most patients, though very stringent regimen is required. The aim of insulin replacement therapy in general is to normalize blood glucose in order to prevent rapid death from ketoacidosis and to delay and reduce the associated complications of diabetes. The following diabetes management strategies are currently used;

1.4.1 Orally administered drugs

Getting the support for intensive lifestyle behaviour change which include healthy diet, regular physical activity, maintaining a normal body weight and avoiding tobacco use can prevent or delay the onset of T2DM diabetes (Hirsch, 1999; THE COST OF DIABETES: REPORT, 2014). However, most people with T2DM diabetes will eventually need treatment with oral hypoglycaemic agents. The agents currently widely used include metformin, sulphonylureas, meglitinides (nateglinide, repaglinide) or combined oral drug treatment (may reduce HbA1c levels more than monotherapy). These show a reduction in HbA1c in a range from 0.4 to 2% but also have been associated with developing hypoglycaemia (Diabetes UK, 2012). Sulfonylureas act by improving insulin action and secretion following a meal, however, sulfonylureas do not show a dose-dependent relationship with efficacy (Groop, 1992; Moser, Morris and Garg, 2012). Sulfonylureas alone may become inadequate with the progression of the disease and many patients may need to add insulin to their regimen or combine with a dimethylbiguanide to reach treatment goals (Wright et al., 2002). Dimethylbiguanide (metformin) acts by increasing insulin sensitivity thereby decreasing insulin resistance in T2DM and also works to decrease gluconeogenesis by the liver, further decreasing fasting glucose (Bailey and Turner, 1996; Moser, Morris and Garg, 2012). Some other drugs in development for T2DM include glucokinase activators, which increase glucose uptake by the liver, sodium-glucose transporter-2 (SGLT2) inhibitors, which increase glucose loss in the urine resulting in weight loss and modest improvement in glycaemic control (Bailey et al., 2013) and organ (liver) specific medications. Some studies, have pointed out that individual or group intensive educational programmes may also contribute to reduce HbA1c compared with usual care (Hundal and Inzucchi, 2003). Structured education courses to help understand and manage their condition and annual checks of blood glucose levels, blood pressure, cholesterol, eyes, feet, kidneys, weight and smoking status are all recommended by NICE and are essential for people to keep on top of their diabetes. There are now widely-used cost-saving drugs to reduce blood pressure, cholesterol and kidney damage.(THE COST OF DIABETES: REPORT, 2014)

1.4.2 Subcutaneous injections

Since the discovery of insulin, various formulations have been developed for subcutaneous delivery in an attempt to imitate the physiological insulin response. This has dramatically improved the prospects of people with diabetes. However, the initial unmodified insulin preparations varied greatly in potency, contained many impurities, resulted in significant elevation of circulating insulin antibodies and had short duration of action which meant that multiple daily subcutaneous injections were required. Formulations with additives such as protamine and zinc ("intermediate-acting" neutral protamine Hagedorn (NPH) insulin in the 1940s and the lente family of insulins in the 1950s) were the first successful attempts to prolong insulin's action (Hirsch, 2010). However, these formulations were still associated with considerable variability of effect and a pronounced peak in their time–action profile. As the pharmacokinetics of these preparations given subcutaneously, did not match the profiles of physiological insulin secretion, new long-acting insulin analogues with altered properties which would better satisfy basal insulin requirements over the entire day were developed with the advance of the rDNA technology in the 1980s. Significant efforts have been made since to alter the physicochemical and pharmacological properties of insulin to aid development of optimal basal-bolus strategies for improved insulin therapy (Brange and Vølund, 1999). A basal-bolus regimen is now common for T1DM patients. Long-acting insulin (insulin glargine and insulin detemir) administered once daily at bedtime or, ideally, twice daily to meet basal needs in combination with rapid acting bolus insulin at either mealtime or premeal taking into account the content of a specific meal are now firmly established as key tools in the battle against diabetes (Hirsch, 2010). Patients with T1DM diabetes typically require an insulin dosage of 0.5 to 1.0 units per kg per day, however newly diagnosed patients may require lower amounts because of some continued endogenous insulin production. The flexible insulin regimens are based on response to self-monitoring of blood glucose levels and carbohydrate intake (Owens, 2002). Insulin degludec, which demonstrates comparable efficacy to insulin glargine, is now being evaluated for administration at less frequent intervals (Owens, 2011).

This treatment regimen however does not always maintain normoglycaemia and the resulting hyperglycaemia is responsible for the long term complications in patients such as eye disease leading to blindness, kidney damage, renal failure, nerve damage and loss

of various organs (Graves and Eisenbarth, 1999). The effectiveness of an insulin regimen is influenced by physicochemical factors such as onset, peak and duration of action plus patient factors such as individual variations in insulin absorption, levels of exercise and types of meals consumed.

1.4.3 Pumps

Open-loop systems

Continuous subcutaneous insulin infusions (CSII) delivered using pumps has a number of advantages over multiple daily injections (MDI) including better glycaemic control as measured by HbA1c, modest reduction in insulin dose and higher patient compliance and satisfaction (Skyler, 2010). Disadvantages include higher costs of therapy, risk of incidence of non delivery and diabetic ketoacidosis and the need to be attached to the system (Meneghini and Sparrow-Bodenmiller, 2010). Advances in technology have improved the functionality of pumps and added features that provide greater control of insulin delivery such as programming of delivery of multiple doses by time, ability to calculate recommended bolus dose based on meal carbohydrate content, memory displays of past insulin delivery and wireless uploading of blood glucose values to the pump from blood glucose meter (Moser, Morris and Garg, 2012). Patch-pumps where the infusion component sits directly on skin offers increased ease of use by eliminating pump tubings (Skyler, 2010).

Diabetic patients still need to read glucose content from the blood and use these blood glucose values to decide their insulin dosages. Finger prick glucose measurements, often regarded as cumbersome and uncomfortable by patients, only provide information about a single point in time, so it is difficult to discern trends in decline or raises in blood glucose levels. In non-diabetic individuals normal HbA1c values are maintained without risking hypoglycaemia because of the meticulous interplay of the humoral signalling. Therefore there have been attempts to mimic these using informative feedback systems using pump systems with which dose rates can be intelligently adjusted and ultimately automated (Kerr and Partridge, 2011). Continuous glucose monitoring systems (CGM) measure interstitial fluids continually and use several

algorithms to calculate current blood glucose values. They consist of a small needle which is inserted in the abdominal subcutaneous fat, the tip of the needle houses a small glucose sensor which can measure glucose levels in the fluid which surrounds the fatty tissue. However, despite the small size of glucose molecule there is a delay (approximately 18 to 30 minutes) associated with equilibration of glucose in subcutaneous tissue fluids and blood glucose content as the glucose molecules have to diffuse through tissues and then to the sensor (Taylor and Sahota, 2013b; Nielsen et al., 2005). There is limited evidence for the effectiveness of real-time continuous glucose monitoring use in children, adults and patients with poorly controlled diabetes. The largest improvements in glycaemia control were seen for sensor-augmented insulin pump therapy in patients with poorly controlled diabetes who had not used an insulin pump before. There are indications that higher compliance of wearing the CGM device improves the HbA1c levels for patients using MDI or CSII therapy (Garg et al., 2011);(Gilliam and Hirsch, 2009). Examples of CGM devices in current clinical use include DexCom SEVEN* PLUS, Medtronic MiniMed Paradigm®, REAL-Time and Guardian®.

Closed-loop insulin delivery systems

Diabetic condition is characterised by real-time calorie turnover as well as chronically raised prandial glucose levels, thus control needs a basal and boost dose of insulin. In addition to this there are changes imposed by secondary factors such as exercise which might use glucose from glycogen mobilised by glucagon or glucose from blood which need insulin to move it into cells depending on blood glucose levels at start of exercise. Another affecting factor is physiological stresses which are thought to be mediated by the sympathetic, counter-regulatory systems and can raise insulin requirements by more than half. Therefore the delivery systems must achieve real-time response and cope with the variations with basal and boost doses. A closed-loop system, which automatically monitors the change in glucose levels and accordingly dispenses an accurate dose of insulin, would present an ideal insulin therapy for long-term routine patient care. Closed systems are completely automated systems which should calculate and administer the required dose accurately and continuously in real time. The main concept for closed

systems is based on its ability to maintain near normal glycaemic levels real-time, to prevent long term effects of hyperglycaemia caused by the lag time, to drive the healthcare cost down especially the cost associated with complications and to improve the quality of life for patients.

The closed loop system should accomplish the following criteria; be glucose-specific and respond in an acceptable timescale and in a dose-related manner, be able to transmit the variable release rate in real time to plasma, impart detailed control without undue oscillation, deal with local visceral insulin and glucose levels, operate long term without leak of insulin or components or creation of other harm, should not produce increased need (‘down regulation’), deliver readily available insulin or analogues and not need specific conjugates such as glycosylated forms (Taylor and Sahota, 2013b).

There are several potential routes forward to use closed loop ideology for the practical management of diabetes. Implanting pancreatic islet is a biological solution to delivering insulin via a closed loop system (Senior et al., 2012). Islet transplantation is currently an accepted modality to treat selected diabetic patients with frequent hypoglycaemias and severe glycaemic liability. However the main deterrents to this solution include chronic graft function most likely associated with immune rejection, recurrence of autoimmunity or chronic exposure to potentially carcinogenic immunosuppressant agents (Pepper et al., 2013).

There have been many biological, electronic and chemical approaches to designing of closed loop systems but no fully operational portable system exists. Electronic systems have attempted to close the loop, but these still need some sort of manual intervention. Electronic systems as described by Hovorka group (Hovorka et al., 2010) comprising of an electronic sensor, namely a CGMS sensor, pump delivery system in combination with advanced control algorithm to compute the quantum dose per unit time is a half way solution between a conventional pump use and a closed loop system. The major shortcoming of this system was suboptimum accuracy of the sensing device. Most of the systems available show a failure to give a timely pre-prandial dose to control the later surge and then giving an over compensation leading to hypoglycaemic condition much akin to conventional dose systems (Taylor and Sahota, 2013a).

A closed-loop artificial pancreas is being attempted to be developed using the Medtronic implantable pump (Renard, 2008) or the Diaport (Taylor and Sahota, 2013a) and a model based controller which uses a control algorithm to regulate glucose levels by adjusting insulin delivery. The Medtronic Veo system is half way between conventional pump and a closed loop system, here the electronic sensor is in communication with the pump but must still receive manual instruction for insulin dose. It is capable of automatically suspending insulin delivery for up to two hours if an impending hypo is detected electronically, however with a risk of hyperglycaemia. Diaport is a simpler and more practical surgically implanted device for continuous intraperitoneal infusion of insulin, aimed at reducing the long lag associated with subcutaneous insulin delivery. These still are not the ideal systems as both suffer from sensor delays relating to the subcutaneous environment or peritoneal cavity environment and thus postprandial surge cannot yet be controlled automatically.

Innovative technologies

The closed loop delivery system comprising electronic sensor and pump systems have been so far been well represented commercially and in clinical studies. However technology with these systems still has to overcome sensor associated time lags and inability to mimic real-time responses. Alternative systems are being researched based on chemically controlled reservoirs where insulin can be delivered through a glucose sensitive membrane or hydrogel as a function of glucose present (Abdekhodaie and Wu, 2009; Zhang et al., 2006; Tanna et al., 2006a; Tanna et al., 2006b)

One such innovation, wherein the sensor and the delivery system is the same component, is the device using a glucose sensitive biomaterial developed by Taylor et al. The system has been shown to perform satisfactorily in diabetic rats and pigs. (Taylor, Tanna and Sahota, 2010b; Taylor and Sahota, 2012)

Chapter 2 Development of an implantable closed-loop insulin delivery device, INsmart

In this chapter the design of the implantable closed-loop insulin delivery device, INsmart device is presented, including its performance in previous *in vivo* experiments. The various aspects that need consideration for further development of the device are presented along with the aims and objectives for the work covered in this project.

2.1 Design of device

The device in this investigation is an innovative system in terms of insulin delivery. The device is a completely implantable peritoneal artificial pancreas. It houses a novel glucose-sensitive gel, kept in place by a rigid casing, which forms a gateway to the insulin reservoir and it is designed to both sense glucose and deliver insulin in the peritoneal cavity. The gel exhibits a fast gel-sol transition with a primary and practically specific response to glucose. The formulation of this biomaterial and its specific properties are further discussed in the section below. The device would be implanted between the lowest rib and the hip and topped up with insulin every few weeks. The device can be refilled with insulin via subcutaneous ports. The device is in preclinical development stage. The original concept, originated within the INsmart group, is covered by patents (Taylor, 1992); (Taylor, 1993), the current and operating patents which cover the glucose sensing gel and device design include (Taylor, 2001; Taylor, 2013b; Taylor, 2013a). The working prototypes were designed and manufactured by Renfrew International, Leicester, UK (refer to **Figure 2-1** for the **interim working prototype)**.

Advantages of this device

- A closed-loop device.

- Based on a glucose –specific chemical response
- Rapid response and accurate dose administered, removes the need to inject insulin manually
- No electronic or moving parts
- Simple and cheap solution for all diabetes patients.
- Simple to implant and easily refillable
- Needs no immunosuppressive drugs
- Not visible externally and hence socially preferable to external portable pumps.

Figure 2-1: Figure of the device (CAD), the actual device with Luer connections (interim working prototype) and the device with refill needle ports (Taylor, 2013b).

The parts of an interim working prototype, which was used for this project, are discussed below;

2.1.1 Components

The design has sequential arrangements of membranes, gel spacer and grids as shown in **Figure 2-2**. The design prevents any distortion of the membranes during assembly and prevents any internal swelling. All the parts of the device can be removed and cleaned

(for the experimental model). The working model parts contain stainless steel (Grade 316), polycarbonate (a thermoplastic polymer containing monomer bisphenol A) and resin (a polyurethane two part thermosetting resin made of polyol and isocyanate mixed). In future designs, there are plans to replace the resin part with polyurethane (a long chain thermoplastic polymer made up of polyol and isocyanate mixed) and make the device entirely of polycarbonate in order to make it lighter. The tubing connecting the luer connections from the device to the fill ports under the skin are polyethylene-lined polyurethane (manufactured by SAI, Strategic Applications Incorporated) to give bio and insulin compatibility, refer to **Figure 2-3**.

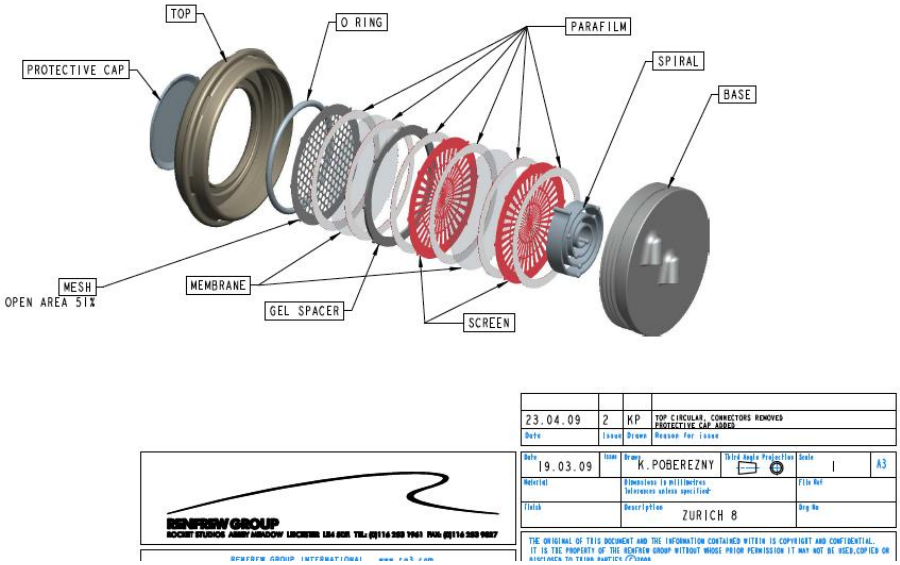

Figure 2-2: Figure showing the parts of the device (developmental model) (Taylor, 2013b).

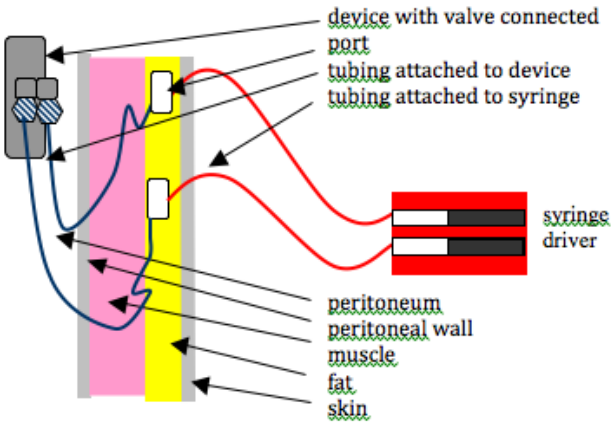

Figure 2-3: Figure showing the refill plumbing circuits.

2.1.2 Glucose responsive gel

The gel, which exhibits a fast gel-sol transition with a primary and practically specific response to glucose is a viscoelastic, hydrophilic material that is formed from an interaction between a branched glucose polymer, dextran (produced by Leuconostoc mesenteroides) and the lectin concanavalin A (con A) from Canavalia ensiformis (Jack bean) (Type VI) with glucose-specific receptors (Tanna et al., 2006a; Tanna et al., 2006b). The lectin, con A, itself is a protein (RMM 104kDa) which exists as a dimer below pH 5.8 and as a tetramer at physiological pH with identical components. Each component has a binding subunit for the cooperative accommodation of two divalent metal ions and appropriately configured carbohydrates with terminals such as mannose, glucose or fructose (Benzeval, Bowyer and Hubble, 2012; Kaushik, Mohanty and Surolia, 2009). Admixtures of lectin in solution with polysaccharides that are effectively multivalent form precipitates and gels.

The gel which formed part of a implantable insulin delivery device used in the *in vivo* pig studies was a partially polymerised product of dextran methacrylate (dex-MA) and con A methacrylamide (con A-MA) that create large molecular structures with covalent bonds but not a solid hydrogel. Both simple mixtures (dex and con A) and the polymerised counterpart, form gels that produce a reversible change in consistency on

contact with glucose to modulate insulin transport and thus act as a self-adjusting system (Taylor, Tanna and Sahota, 2010a)(refer to **Figure 2-4**).

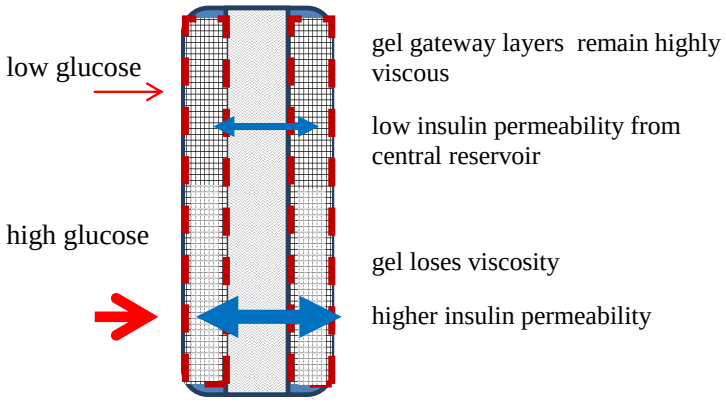

Figure 2-4: Overview of the gel action contained in insulin delivery device

Figure 2-5 shows a comparison of the polymerised and mixture systems with interstitial areas which become free when free glucose is introduced and allow insulin monomer transport. In the device the polymerised gel was retained between two porous membranes (~ MWCO 100kDa) which allows the ingress of glucose (180Da) and the delivery of insulin as the monomer (~6kDa) but prevents ingress of bacteria (0.2 -30 μm), enzymes and other proteins larger than the pore size of the retaining membranes, such as those present in the peritoneum or other relevant implant site fluids as shown in **Figure 2-4**. A stability study conducted within the INsmart group, has shown that in the presence of chymotrypsin (25kDa), a tryptic enzyme present in the peritoneum, the polymerised acrylic gels maintained stability when encased in dialysis membrane MWCO 50kDa for over 500 days. Other biochemicals that may be present in the peritoneum include alkaline phosphatise (89kDa), aspartate aminotransferase (dimer; 94kDa), albumin (66kDa), bilirubin (585Da), cholesterol (387Da) and urea (60.05Da) (Simmen et al., 1995).

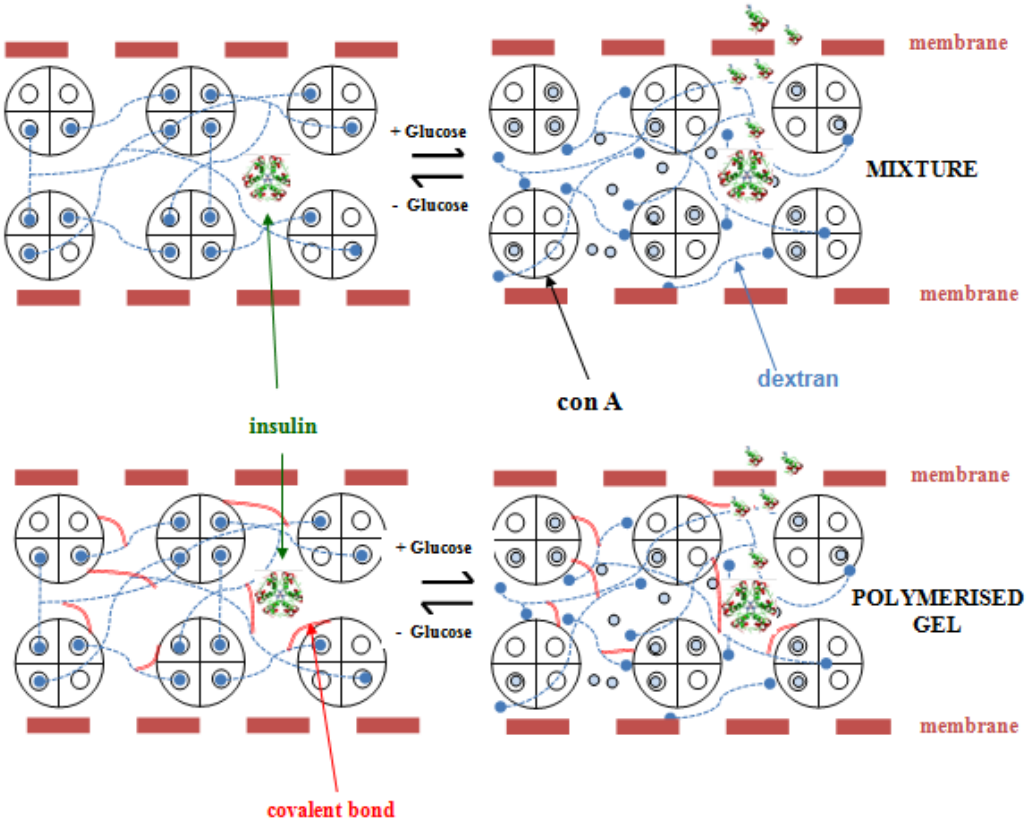

Figure 2-5: Sol-gel transition of glucose-sensitive dextran and conA gel. Key- Large circles represent cross-section of conA, small closed blue circle represent dextran chain terminal glucose and open blue circle represent glucose.

2.1.3 Insulin formulation

The insulin solution contained in the device reservoir is another essential part of the device system. Commercially available high concentration insulin formulations which have been stabilised with phenol or *m*-cresol are required to minimise the device refilling cycles.

A different working device type designed with double the surface area called the **"modified works-like"** (double sided device design) was used for the pig experiments to increase the amount of insulin delivered. It was difficult to predict if the initial prototype (**interim working prototype** as described earlier) would output enough insulin for a diabetic pig even with the maximum concentration commercially available

(500 IU/mL) insulin preparation. The difficulty in prediction was because of the following reasons;

- Previous *in vitro* simulations suggested that output would be suitable but the bulk receptor fluid conditions are inevitably different from the peritoneum in which the device is in contact with fluid but not immersed. Delivery *in vivo* was lower than the *in vitro* output suggested.
- Insulin solubility: At high concentrations of 500 IU/mL, the formulation is stabilised by phenol or *m*-cresol. The phenol is not merely present as a bacterial preservation but also as an agent which complexes with insulin molecule. This produces a stable hexamer that is soluble at higher concentrations than if phenol were not present. The phenol concentration could drop below the critical concentration over time through device material absorption or diffusion out of the reservoir.
- Also, the physical and chemical stability of insulin could be compromised by even marginal pH fluctuations.

A third prototype called the **"advanced looks-like"** was built to depict a clinically acceptable appearance (refer to **Figure 2-6**). The design conveys simplicity of shape, comfort, ease of sterilisation, suggests simpler surgery, the slot-in cartridge of gel, and the economy of the dual lumen refill plumbing that will interface with a standard but slim low-profile dual port such as the Bard type pictured below right.

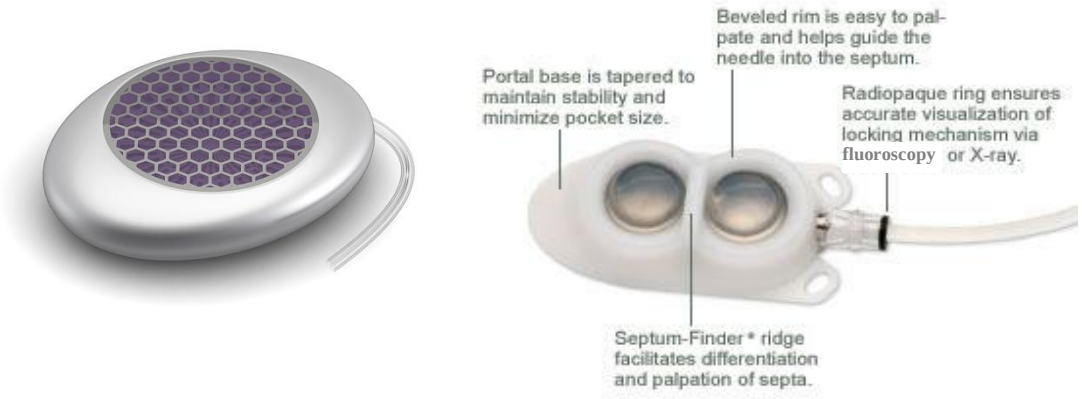

Figure 2-6: The **"advanced looks-like"** prototype.

The **interim working prototype** and **modified works-like** models are the working models designed to be assembled and dissembled repeatedly for experiments, though a little bulky and less sleek than the future implantable advanced looks-like prototype.

The interim working prototype was used in *in vitro* experiments presented in this thesis. The device was too bulky for use in *in vivo* because it has a substantial lid that fits a bespoke spanner and it has luer connections angled to the back for filling, all of which were later improved, however it is a good working prototype.

In vitro testing with the device

Some *in vitro* testing of the device have been performed in the past using tartrazine dye. Tartrazine was used because of its availability, its cost, its stability, its compatibility with the gel; and its ease of UV/Vis. assay for repeated readings. In these early studies a non-polymerised gel with a 3 mm path length and 10 mm diameter, was used. It was found to respond to a 1% glucose challenge with a prompt but sustained fourfold increased rate of dye delivery when tested *in vitro*. The pathlength and gel concentration influenced the magnitude of response with high gel concentrations producing osmotic gel swelling.

2.2 *In vivo* performance in animal models

In vivo study in rats

A recent study in diabetic rats assessed the feasibility of a simple device version of the intraperitoneal (IP) implantable closed-loop insulin delivery device. The performance of the system was compared over time in diabetic rats with a control system. The protocol involved using oral glucose challenges and daily assessments of BG and body weight. The automated response regimen of the active system was quantified by comparison with IP multiple dose injection (MDI) results in the same rat model. Successful control was found for the device containing active gel when assessed daily and when challenged with large glucose doses in comparison with an inactive gel analogue as a

control. The device was well tolerated and was found to operate to further advantage when vascular omentum grew into the perforated front of the device. The response from the device was estimated at outputting approximately 0.5 IU/kg/h basal with 2 IU/kg boosts in order to match the demand of the challenges. The seemingly high response from the device could be attributed to a higher metabolic rate in rats than humans and hence requiring a higher wgt/wgt dose. The device eventually did exhaust and hence highlighted the need for a refill mechanism in future device models (Taylor, Tanna and Sahota, 2010b).

In vivo study in pigs

Following the study in rats, the next steps were to scale the device to be relevant for humans. To this end, the device engineered with filling circuit was surgically implanted in the domestic pig. For both rats and pigs, the diabetic model closely simulates human diabetes. The weight for weight insulin requirements for rodent is higher than humans but for pigs is the same. The study was approved by the respective ethical committees to be conducted on 10 pigs in two sites, Nottingham and Huntington. The study was conducted at the Nottingham site on ten animals in total, four were used to develop the surgery, two were used to implant single sided device design and check dose by injection and four received the double sided device design. Of the four that received the double sided device, one died of peritonitis, one did not become diabetic and two responded to the insulin, one perfectly and one sub-optimally.

Surgery was developed and streptozotocin was used to induce diabetes in pigs and they were observed to ensure that blood glucose levels reached at least 33 mmol/L. The device was filled with insulin solution in situ using the subcutaneous port and the animal was observed for several weeks, during which time there was normal access to food and water. During this time the pig was given several oral glucose challenges.

The study showed that blood glucose levels dropped from >33 to under 10 mmol/L five days after filling the device. Glucose challenge responses improved so that ultimately the blood glucose (BG) peak was 18 mmol/L and normalised about half an hour afterwards, contrasting with attempts to control the diabetes by intravenous insulin injections. The residual reservoir insulin solution was removed after 10 days of good

glycaemic control and diabetic BG levels >33mmol/L (>600 mg/dL) occurred only after a further 24 days implying a depot of insulin had remained after removal of the reservoir solution. About 62.5 IU per 24 hours was needed to control the diabetes including the increased output needed to control the large oral glucose challenges implying the successful operation of the automatic bolus system, with no manual intervention needed. Using information from injected insulin and the observation that the pig ate its food about eight times daily, it was calculated that this translates to a basal dose of about 1.3 IU/h and boost doses of about 3.9 IU. The inference from the study was that the implantable device controlled the basal and bolus needs for more than four weeks without any manual insulin adjustment, including a period where residual insulin in the gel acted as a depot source. The implanted system eventually caused peritonitis (because of abrasion) after several uneventful weeks but improvements in how and where the device is located are planned to solve this.

Another interesting finding from the pig experiment was with regards to the gel pathlength in the device. When the single sided device was initially used *in vivo* in the pig, there was almost no observed effect after filling the insulin reservoir; this could be due to a much longer *in vivo* lag time with the 3 mm gel path length. Hence, the delivery device was modified to a double sided system and the path length was reduced by half. The gel path length is very important in the design of reservoir delivery devices because it affects both the lag time and the steady state flux. In the experiment where the path length was 1 mm the lag time was apparently 5.5 days, given that following the fill, the BG had settled to its lowest point by that time and that a steady-state BG plateau was established. In theory lag time is proportional to the square of the path length and this suggests that the lag time for a 1.5mm path would be $(1.5)^2$ x 5.5 = 12.3 days. Interestingly, the effect of the extra dose in one of the pigs where the gel pathlength was 1.5 mm started to have an effect about 12 days after its administration and supports this analysis. For the 3mm path used in the initial pig where no response was observed, the lag time would have been about 50 days (Unpublished results).

2.3 What are the next steps for this device?

A recent survey was undertaken by the INsmart group to determine both positive and negative experiences of T1DM patients currently using open-loop continuous subcutaneous insulin infusion (CSII) pumps to ascertain their interest in and to define the desirable performance characteristics from the implantable closed loop insulin pump, INsmart. Most respondents with T1DM diabetes with well controlled blood glucose, based on self-reported HbA1c results reported a reduction in this value after transferring to CSII from multi-dose injections. However, 70% of pump users experienced more than three hypoglycaemic episodes per week. 80% reported self-measured BG values above 10mmol/L three or more times per month. The majority of respondents felt that the current external insulin pumps had a number of disadvantages such as their constant visible presence, rotation of insertion sites and skin inflammation. The INsmart pump is implanted in the peritoneal cavity and works on instant feedback mechanism for controlling insulin release just like a normal pancreas would, hence could easily overcome the highlighted limitations of an external pump (Taylor et al., 2014) and there clearly is a interest and willingness from T1DM sufferers to accept an implantable closed-loop device as part of their treatment strategy.

The animal studies have highlighted the need to understand the design capabilities of the device with respect to insulin delivery mechanism and kinetics to gain confidence in the performance of the device. The aim of this work was to investigate and understand some key device reliability and performance related aspects.

Reliability and Performance

The INsmart implantable insulin delivery device aims to mimic pancreas, by monitoring the change in BG levels and achieving real-time responses and coping with the BG variations with basal and bolus doses. The next goal in the development of the INsmart device is human clinical trials. The following device reliability and performance related aspects were investigated in this work;

Insulin formulation stability and compatibility with device materials

As discussed in **Chapter 1, Section 1.3.2**, insulin is inherently quite unstable, given to degradation mediated by both chemical and enzymatic means. In addition, the physical stability of solutions is a problem so that although phenols, surfactants and other stabilisers are used, the tendency to aggregate, precipitate and crystallise is a problem that limits the use of insulin formulations for purposes such as pumps. Though commercially available insulin formulation was used within the implantable device, its stability will be subjected to some of the deleterious influences mentioned above.

Aggregation of aqueous insulin solutions is still a serious obstacle in the development of stable formulations for delivery devices (Florence, 2010). A number of factors have been implicated as having an effect on insulin aggregation which lead to plugging of the devices namely, abrupt changes in flow path, motion, elevated temperatures, metal ion contamination, impure insulin formulations, CO_2 diffusion, pH drop, dissimilar metal pump components, salt concentration, inappropriate diluents, refrigeration temperatures, processing, insulin heterogeneity, and buffering systems (Lougheed et al., 1980). A study by Fiengold et al on the effect of contact material on vibration induced insulin aggregation tested a number of materials suitable for pump reservoirs which included metals (stainless steel, titanium and a titanium alloy) and various plastics (polypropylene, polytetrafluoroethylene, polyvinylchloride PVC, polyamide, cellulose butyrate and silicone elastomer) (Feingold, Jenkins and Kraegen, 1984). The study findings showed that insulin solution delivered through the PVC infusion set showed reduction in preservative content to less than 30% of initial content and an increased chemical transformation product formation. However, polyethylene PE infusion system showed a minor decrease in preservative content and no increase in chemical transformation. The study also highlighted the effect of the method of sterilization performed on PVC and PE catheters on the chemical stability of insulin solution. Gamma irradiated PVC catheters were markedly harmful to insulin solution (gamma irradiation could potentially break the polymer chains), while the ethylene oxide sterilization (which has the potential of absorbing into the material) did not affect the chemical stability of insulin. Silicone rubber has been found to be the most active in promoting insulin aggregation of all the medical grade materials likely to be used in pumps(Lougheed et al., 1983). These studies have highlighted the fact that careful

selection and combinations of insulin formulation and materials can minimise insulin aggregation and denaturation, it also highlighted the need for testing of the proposed reservoir components and insulin formulations with an aim to detect denaturation in solution and precipitation of insulin.

Chapter 3 covers a study performed to understand the stability of insulin formulation and compatibility with each of the material used in the device over a period of a month. This was done by monitoring the loss of insulin and formation of degradants by reverse phase high performance liquid chromatography (RP-HPLC) over a period of a month.

Insulin delivery mechanism and kinetics

For the *in vitro* diffusion experiments performed to understand insulin delivery mechanism and release profiles from the device, insulin was fluorescently labelled with fluorescein isothiocyanate (FITC) to improve its detection and for quick quantification purposes. The details of the synthesis and identification of the FITC-insulin conjugates produced are presented in **Chapter 4**. Clinically used insulin analogue formulations were also fluorescently labelled and conjugate species produced were identified.

The aim of the device is to mimic the real-time response in human. Based on the design of the INsmart device (interim working prototype) the various factors that could be responsible for a lower or higher insulin response are listed in **Table 2-1**.

Table 2-1: Factors affecting insulin delivery from the device.

Factors responsible for inappropriate insulin delivery affect	
Factor	**Affects**
Device wrong place	Correct positioning of the implanted device is vital for the performance. Device needs to be in contact with an appropriate fluid and facing a permeable membrane.
Device leak	This would result in insulin overdose.
Device blockage	This would result in insufficient insulin dose.
Gel Thickness	Thicker gel means increased pathlength which will result in greater lag time before insulin is released from device. Very thin layer of gel can alter the uniformity of the gel thickness and thus affect the release kinetics.
Insufficient insulin in reservoir	This will affect the diffusion kinetics and hence affect the delivery rates.
Area	Based on Fick's law of diffusion, the rate of diffusion is directly proportional to the area available for insulin to diffuse through.
Gel polymer content	Polymer content inversely affects the diffusion coefficient of insulin. Higher polymer content will result in lower diffusivity and lower polymer content will result in higher diffusivity.
Gel response time	The response time is affected by gel characteristics or polymer content.

One of the main factors affecting the insulin delivery from the device is the response of the gel to glucose levels. The intensity and the duration of the glucose trigger also influence the recovery of the gel. This highlighted the need to understand the insulin release kinetics from the device. The diffusion of insulin and glucose through the gel was determined. This was achieved by using model dyes and gel initially to develop an experimental protocol for selection of an appropriate mathematical model for measuring diffusion. The development of the experimental protocol for measuring diffusion is presented in **Chapter 5.**

The design of the INsmart device for the management of diabetes is based on the small changes occurring in the glucose responsive gel in response to the diabetic physiological glucose levels and its corresponding ability to modulate the diffusion of insulin through the material. Glucose sensitivity of the gel which forms the basis of the insulin delivery mechanism of the gel was assessed by rheological testing of the gel which is presented in **Chapter 6**.

The diffusion kinetics of FITC-insulin conjugate through the gel and its response to glucose triggers are presented in **Chapter 7**.

Predicting the performance of the INsmart device

The importance of knowing the mechanism and kinetics lies in getting the dose right for each challenge but also in predicting the service intervals and what affects these. The service intervals apply to the gel and the insulin in the reservoir, the intervals at which the gel would need to be replaced and the insulin solution replenished.

Long term stability studies have been performed on the biomaterial within the INsmart group which has given confidence in the long term performance capability of the gel (Sahota and Taylor, 2013). Acrylic polymerised gels and also dextran and concanavalin A at 20 and 37°C when stored with and without 0.1%w/w glucose have shown by rheological characterisation to have a stable complex viscosity for over 730 days indicating that over time they do not undergo degradation. Gel integrity in presence of chymotrypsin contained in dialysis membranes of 50kDa were found to be resistant to degradation over long term (>500 days). Thus giving confidence in the gel stability and integrity for use in the INsmart device.

When considering the use of device in humans, one of the fundamental questions that needs to be answered is how long the insulin in the reservoir will last and how frequently it will need to be replaced. The service intervals for the insulin formulation in the reservoir would depend on the insulin concentration and volume in reservoir. The depletion of the insulin in the reservoir and replacement strategies depends on daily insulin consumption by the individual with diabetes. This consumption depends on a number of factors such as onset, peak and duration of action, patient factors such as

individual variations in insulin absorption affecting the basal dose required, levels of exercise and types of meals consumed. An idealised insulin release profile from the device should mimic the natural pattern of insulin release from a normal pancreas in the human body. **Chapter 8** focuses on using the insulin diffusion kinetic data to make so theoretical estimations regarding the performance of the INsmart device.

The following key questions with respect to reliability and performance of the device are investigated in this work;

1. What are the factors that affect the stability of insulin in the device?
2. How stable is the insulin formulation with the materials used in the device?
3. What is the mechanism (pharmacokinetics) of insulin delivery from the INsmart device?
4. What are the diffusion coefficient values of insulin through the glucose responsive gel?
5. Does the gel respond to glucose triggers?
6. How does gel pathlength affect insulin release rates?
7. Is the device capable of delivering the daily insulin requirement (basal insulin amounts)?
8. Can the device deliver post-prandial insulin doses (bolus amounts) and how fast?
9. Should alternative device geometries be explored?
10. How long will the insulin in the reservoir last? What is the insulin replenishment strategy?

Chapter 3.Insulin solution stability and compatibility with current and potential INsmart device materials

3.1 Introduction

The stability of insulin in solution is essential for the efficacy of therapeutic preparations used in continuous pumps and controlled release polymeric devices. The efficacy of insulin solution can be significantly reduced by a number of chemical changes of its primary structure yielding insulin derivatives and physical modifications of the secondary and quaternary structures resulting in denaturation, aggregation and precipitation. These chemical and physical changes lead to drastic reduction of biological potency and obstruction of delivery routes, creating serious problems for drug delivery systems (Brange and Langkjaer, 1993). The general modes of physical and chemical instabilities of insulin in solution and the factors that promote them have been discussed in detail in **Chapter 1**.

The importance of investigating insulin aggregation in an environment which is relevant to the implantable delivery system has been discussed in **Chapter 2**. The most relevant factors for investigation include; effect of body temperature, vibration and contact with the reservoirs' material. Undesirable aggregation of aqueous insulin solutions is still a serious obstacle in the development of stable formulations for delivery devices. Careful selection and combinations of insulin formulation and materials have been shown to minimise insulin aggregation and subsequent precipitation. This further highlights the need for testing the proposed reservoir components and insulin formulations with an aim to detect insulin precipitation in solution (Sluzky, Klibanov and Langer, 1992; Melberg et al., 1988; Feingold, Jenkins and Kraegen, 1984; Lougheed et al., 1983). In order to design and develop the implantable artificial pancreas, INsmart device, its materials need to be biocompatible not only with the surrounding tissue but also internally they need to be compatible with the novel glucose responsive gel and insulin.

Presented below is a brief description of insulin and its degradants and the analytical methods investigated to determine them.

3.1.1 Stability of insulin in solution

Insulin like many other proteins is not very stable in solution and is liable to modification by chemical reactions with molecules in its vicinity; chemical stability for insulin has been discussed in **Chapter 1**. During storage and use, insulin in pharmaceutical preparations deteriorate by two main chemical reactions; deamidation due to hydrolytic reactions and polymerisation due to formation of intermolecular covalent bonding with other insulin molecules to form higher molecular weight transformation products (Fisher and Porter, 1981; Oliva, Fariña and Llabrés, 1996). Both mechanisms accelerate at higher temperatures. Here, insulin deterioration due to the chemical transformation mechanism of deamidation was investigated.

Deamidation of Asn residues is one of the most common protein degradation pathways, and has been used as a marker for the stability of protein drugs (Bischoff and Kolbe, 1995). Deamidation, the most prominent nonenzymatic degradation reaction of insulin, occurs due to loss of the amide $–NH_2$ groups. Insulin has six residues that are potential deamidation sites: Gln^{A5}, Gln^{A15}, Asn^{A18}, Asn^{A21}, Asn^{B3}, and Gln^{B4} (glutamine (Gln) residues at positions A5, A15, B4 and asparagine (Asn) residues at A18, A21 and B3). The Asn residues are more prone to deamidation than the glutamine residues. These positions do not play any part in the immunogenicity of the insulin molecule; hence formation of desamido insulin does not affect the potency of insulin (Fisher and Porter, 1981).

In acid solutions, pH <2, direct hydrolysis of the side chain amide leading to deamidation at residue Asn ^{A21} (Sundby, 1962), generates aspartate as the sole product and forms desamido insulin (A21 desamido insulin).

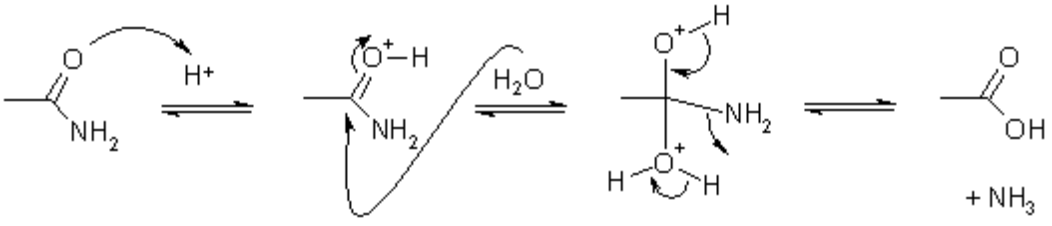

This changes charge and hydrophilic/hydrophobic properties of insulin which are the key forces controlling its tertiary structure and responsible for its biological activity.

In neutral solutions, deamidation primarily occurs at residue Asn^{B3} but at a reduced rate. Deamidation of Asn^{B3} and hydrolysis of the peptide bond between residues A8 and A9 leads to the formation of a mixture of isoAsp and Asp derivatives (B3 desamido insulin) (Brange et al., 1992b; Nilsson and Dobson, 2003).

This deamidation mechanism (beta-aspartyl shift mechanism) primarily occurs through intramolecular rearrangement as shown in **Figure 3-1**. Whereby an intermediate five-membered cyclic succinimide (A) is formed due to the peptide bond nitrogen (reactive anion) of the N+1 amino acid attacks the carbonyl carbon of the asparagines or asparate side chain. The succinimide is then rapidly hydrolysed to yield iso-asparate (beta-asparate) and asparate in a ratio of approximately 3:1 (Yomota et al., 1996).

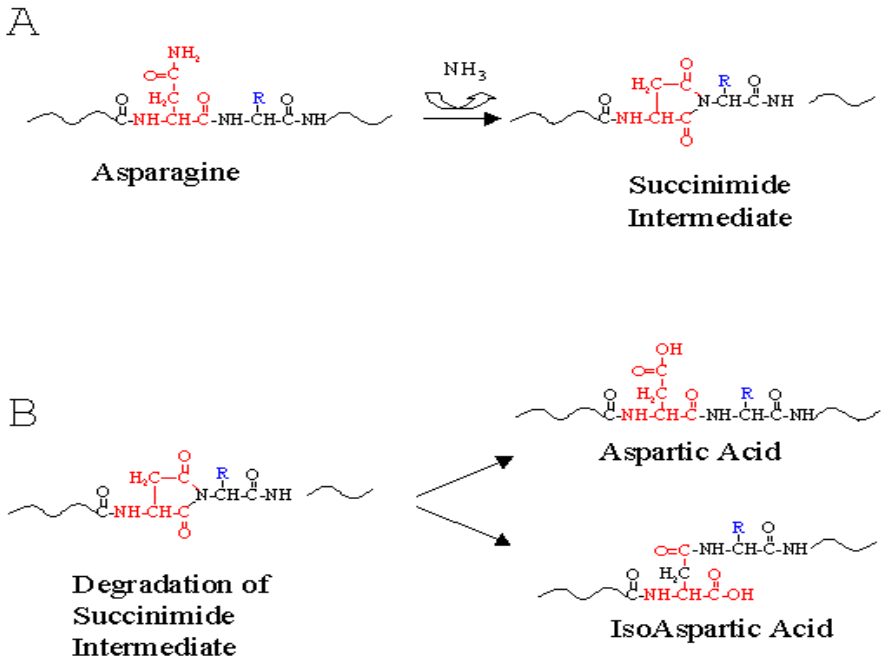

Figure 3-1: Mechanism of deamidation of insulin residue Asn^{B3} under neutral conditions (taken from http://www.ionsource.com/Card/Deamidation/deamidation.htm).

The rate limiting step for formation of B3 desamido insulin is the rate of cyclic succinimide intermediate formation; which is highly temperature dependent and pH dependent, more alkaline pH increases deprotenation of peptide bond hydrogen and rate

of succinimide formation. However, the ratios at which the two B3 derivatives (isoAsp/Asp) are formed are independent of time and temperature but vary with the type of formulation e.g. whether the formulation is a neutral suspension of crystals, or amorphous insulin, or neutral solution containing phenol or cresol. Thus the maximum stability against deamidation is at around pH 6, where reaction is 5 to 10-fold slower than at pH 7.4. The physical and chemical deterioration of insulin is almost entirely governed by the capacity of the B-chain terminals to undergo the structural changes necessary for these reactions to take place. By careful formulation e.g. addition of phenol or zinc ions the insulin molecules can be constrained (by forming hexamers) and their flexibility and tendency to disassemble reduced thus making them less prone to fibrillation and chemical degradation, these formulations are neutral hexameric solutions that dissociate into monomers on injection and are rapidly absorbed, hence the peritoneal pH of approximately 7.6 do not aid deamidation.

3.1.2 Determination of insulin and its degradants

A review of the literature highlights several immunoassay and non-biological analytical methods for the determination of human insulin in *in vivo* and *in vitro* conditions. Immunoassays reported include enzyme (Bürgi et al., 1988), electrochemiluminescence (Sloan et al., 2012; Cassidy et al., 2012), gravimetric and radiolabel immunoassay (Dezier et al., 1987) just to name a few. Other than these, capillary electrophoresis (Staub et al., 2010; Yeh et al., 2010), high performance liquid chromatography (Mohd Hafiz et al., 2013; AbuHeshmeh et al., 2013), liquid chromatography-tandem mass spectrometry (Chen et al., 2013), size exclusion chromatography (Tantipolphan et al., 2010) have also been widely used for determination of human insulin.

Oliva et al have discussed reverse phase high performance liquid chromatography (RP-HPLC) and size exclusion chromatography (SEC) HPLC methods for the analysis and characterisation of insulin and its degradation products in pharmaceutical preparations. The results of the validation procedure showed that their methods were specific, precise, reproducible and robust. The RP-HPLC method used by them for the determination of both A21 and B3 desamido insulin degradants however was able to detect these degradants only in samples stored under stress conditions of high temperatures (60°C

with shaking or in suspension samples at 50°C without shaking)(Oliva, Fariña and Llabrés, 2000).

RP-HPLC is now a technique of choice used to separate proteins based on their hydrophobicity, where the hydrophobic interactions between the column packing and the hydrophobic regions of the protein are exploited (Aguilar, 2004). RP-HPLC is the most used analytical method for separation and determination of peptides and proteins in an extensive range of applications and is considered to be the most suitable method for meeting most of the criteria for quantitative analysis within the pharmaceutical industry (Crowther, 2001). This analytical technique has been widely used to develop and validate simple, rapid, accurate and specific method with short run times for determination of insulin in both artificial and biological environments (Mohd Hafiz et al., 2013; Rajan et al., 2006; AbuHeshmeh et al., 2013; Sarmento et al., 2006). Most of these determinations of insulin control the degree of ionisation on insulin by using a mobile phase with low pH or high salinity.

The official monographs (USP 26 and BP 2014, Ph. Eur. Monograph 0854) detail HPLC methods for the assay of insulin for "Insulin preparations". They provide information about potency (evaluated by assay by comparison with certified standard), purity (quantification of related proteins) and presence of covalent aggregation products (with molecular masses greater than that of insulin). The Pharmacopoeia limits and specifications for the insulin preparations are: A21 desamido insulin is not greater than 5% of total area of peaks, sum of area of other peaks apart from those due to insulin and A21 desamido insulin is not greater than 6% of the total peak areas. Impurities with molecular masses greater than that of insulin: not greater than 2% of total area of peaks (British Pharmacopoeia Volume III, 2014). The liquid chromatography method described in the official BP for the assay of human insulin and detection of its A21 desamido human insulin is a gradient method and has a run time of 50 min while the official USP HPLC method for analysis of human insulin has even longer run time of 90 min.

For the purposes of the present project it is important to determine the loss of insulin and also detect formation of degradants in an environment which is relevant to the

implantable device, therefore sensitive methods which can detect insulin and the two desamido insulin are required.

An isocratic HPLC method used by Moslemi et al (Moslemi, Najafabadi and Tajerzadeh, 2003) uses an ion-pairing reagent, tetraalkylammoniumhydroxide to acquire peaks with better resolution. However it was found that in the reported method A21 desamido was prepared by storing human insulin in 0.01MHCl at 40°C for 48 hours in order to detect it and also the peak appeared very close to the human insulin peak.

The **RP-HPLC acidic analytical method** validated and used in this project for determination of insulin and A21 desamido insulin is an isocratic method with a short analysis time (30 mins) and sensitive to detect small amounts of A21 desamido insulin. The usual reported acidic HPLC method (like the ones discussed above) allows the A21 peak to be well separated, but the B3 desamido peak is usually included in the main insulin peak. Contrasting with acidic analytical methods, Yomota et al have developed a HPLC method for separation of B3 desamido insulin by using pH stable octadecylsilyl (C18) column and an alkaline eluent (0.1M phosphate buffer pH 9.0 containing 26% acetonitrile), by which two peaks corresponding to B3 desamido insulin derivatives (isoAsp/Asp) were eluted in front of the insulin peak. These results were in agreement with capillary zone electrophoresis method used to separate human insulin and A21 and B3 desamido insulin (Yomota et al., 1996). The **RP-HPLC neutral analytical method** used for this project was based on this study. A C18 column from Phenomenex and an alkaline mobile phase at pH 7.4 was used for the determination of insulin and B3 desamido insulin.

Thus two RP-HPLC methods, the acidic and neutral analytical methods were used for the determination of insulin and its desamido insulin degradants.

A RP-HPLC method for the determination of fluorescently labelled insulin (FITC-insulin) was also investigated for identification of the synthesised FITC-insulin conjugates and for material compatibility studies using FITC-insulin. The **FITC-insulin method** used for the determination of FITC-insulin conjugates was as described in the published paper by Hentz et al (Hentz et al., 1997).

Thus the following three RP-HPLC methods were developed;

1. Acidic analytical method for determination of insulin and A21 desamido insulin
2. Neutral analytical method for determination of insulin and B3 desamido insulin
3. FITC-insulin method for determination of FITC-insulin conjugates

This chapter has two sections; the first presents the validation results for the three methods and demonstrates the suitability of these methods for determination of insulin and its degradants and FITC-insulin conjugates. The second section presents the results from compatibility studies of insulin with various device materials that were used for the *in vitro* studies and was used/or have a potential to be used as part of an *in vivo* device.

3.2 Materials and Methods

3.2.1 Chemicals and reagents

Humulin® R (Hum R) 500 IU manufactured by Eli Lilly and Co was used. Diluting fluid manufactured by Novo Nordisk was used. HPLC grade acetonitrile, sodium dihydrogen phosphate, disodium hydrogen phosphate, ortho-phosphoric acid and ethanolamine were purchased from Fischer Chemicals, Loughborough, UK. Nylon membrane filters, 0.45µm, 47 mm were purchased from Whatman International Ltd, England. Distilled water was used. FITC-insulin synthesised in-house (synthesis as discussed in Chapter 4) was used.

3.2.2 Preparation of Humulin R standards

The Hum R standard solutions from 50 to 500 IU/mL (50, 100, 150, 200, 250, 300, 350, 400, 450, 500 IU/mL) were prepared by dilution of the standard stock solution with diluting fluid. A calibration graph was constructed in the range of 50 to 500 IU/mL for Hum R (n=6).

3.2.3 Preparation of FITC-insulin standards

A standard stock solution containing FITC-insulin was prepared in distilled water at a concentration of 5 mg/mL and pH was adjusted to 7.6. The standard solutions from 0.025 to 5 mg/mL (0.025, 0.05, 0.10, 0.15, 0.20, 0.25, 0.50, 1, 3, 5 mg/mL) were prepared by dilution of the standard stock solution with distilled water (pH 7.6). A calibration graph was constructed in the range of 0.025 to 5 mg/mL for FITC- insulin (n=6).

3.2.4 RP-HPLC Chromatographic system

The chromatographic analyses were performed using a Shimadzu Prominence HPLC system consisting of an in-line DGU-20AS Prominence degasser, LC-20AD Prominence quaternary pump, SIL-20A Prominence auto sampler, CTO-20AC Prominence column oven, SPD-M20A Prominence diode array detector and RF-10AXL Fluorescence Detector for detection of fluorescent peaks.

3.2.5 Acidic analytical method for determination of insulin and A21 desamido insulin degradant.

A Jupiter 5 µ C18 300 Å, 250 × 4.6 mm column from Phenomenex, Cheshire UK was used for the separation preceded by a 0.5mm in-line filter and a widepore C18 4 × 3 mm guard column. For detection of insulin and degradant Asn ^{A21} desamido insulin an acidic mobile phase was used. The mobile phase consisted of 74:26 (v/v) aqueous sodium sulphate pH 2.3: acetonitrile. The aqueous sodium sulphate solution was prepared by dissolving 28.4 g/L sodium sulphate in distilled water. 2.7 ml ortho-phosphoric acid was then added and the pH adjusted to 2.3 with ethanolamine. The aqueous solution was filtered through nylon membrane of 0.45 µm pore size. Elution was isocratic with a flow rate of 1.5 mL/min, a column temperature of 40 °C and sample injection of 20 µl. The detector was set to scan from 190 to 400 nm and had a channel set at 215 nm to detect insulin and its degradation products.

3.2.6 Neutral analytical method for the determination of insulin and B3 desamido insulin degradant.

A Jupiter 5 µ C18 300 Å, 250 × 4.6 mm column from Phenomenex, Cheshire UK was used for the separation preceded by a 0.5 mm in-line filter and a widepore C18 4 × 3 mm guard column. The mobile phase consisted of 73:27 (v/v) 0.1 M sodium phosphate buffer pH 7.4: acetonitrile. 0.1 M sodium phosphate buffer was prepared by dissolving 3.5 g/L of sodium dihydrogen phosphate and 13.8 g/L of disodium hydrogen phosphate in distilled water and pH adjusted to pH 7.4. The buffer was filtered through nylon membrane of 0.45 µm pore size. Elution was isocratic with a flow rate of 1.5 mL/min, a column temperature of 40°C and sample injection of 20 µl. The detector was set to scan from 190 to 400 nm and had a channel set at 215 nm to detect insulin and its degradation product.

3.2.7 FITC-insulin method for determination of FITC-insulin conjugates.

A Luna (3 µ) C18 (2) 100 Å, 150x4.60 mm column from Phenomenex, Cheshire UK was used for the separation preceded by a 0.5mm in-line filter and a widepore C18 4 × 3 mm guard column. Elution was using a gradient method using mobile phase A; 0.1% trifluoroacetic acid (TFA) in water and mobile phase B; 90% acetonitrile and 10% water containing 0.1% TFA with a flow rate of 1.0 mL/min, a column temperature of 40°C and sample injection of 20 µl. The following gradient was used: 0-15 min (85% to 65%A), 15-25 min (65% to 35%A), and 25-32 min (35%A).

The peaks were monitored by fluorescence detection where the excitation and emission wavelengths were set at 494 and 518 nm, respectively. The photo diode array detector (PDA) was also set to scan from 190 to 400 nm and had a channel set at 215 nm to detect presence of unlabelled native insulin.

3.3 Validation

3.3.1 Method validation parameters

The three methods were subjected to an assessment of validation capabilities and was based on the FDA guidance document – *'Guidance for Industry, Q2B Validation of Analytical Procedures: Methodology'* (*FDA Guideline for Industry Q2B Validation of Analytical Procedures: MethodologyID - 1524* 1997). This Guidance was developed within the Expert Working Group (Quality) of the International Conference on Harmonisation of Technical Requirements for Registration of Pharmaceuticals for Human Use (ICH) and has been subject to consultation by the regulatory parties in accordance with the ICH process. The guidance document is complementary to the ICH guidance entitled '*Text on Validation of Analytical Procedures (ICH Q2A)'.* The objective of validation of these three analytical methods is to demonstrate their suitability for the intended purpose. In accordance with the ICH guidelines a design of experiment approach was utilised in order to provide a sound, overall knowledge of the validation capabilities.

Validation capabilities such as Selectivity, System suitability, Linearity, Range, Accuracy, Precision and Detection and Quantitation limits, as detailed in the FDA guidance, for the three RP-HPLC methods were determined and are presented below. For detailed FDA guidance acceptance criteria and details for each parameter, refer to **Appendix 1**.

Selectivity

To demonstrate selectivity of the RP-HPLC methods a diluting fluid which contained the same excipients as those present in HumR without human insulin was used. Diluting fluid and HumR were injected into the HPLC system under the optimised test conditions and corresponding chromatograms were recorded. Representative chromatograms were generated to show that excipients present in the diluting fluid were not interfering with the signal from insulin and desamido insulin degradants.

System suitability

The system (integral system which comprises of the equipment, electronics, analytical operations and samples to be analysed) suitability for the three methods was assessed by six replicate analyses of HumR and FITC-insulin at a selected concentration. The acceptance criterion from the guidance referred to above was ±2% for percent relative standard deviation (% RSD) for the peak areas and retention times (Rt) for HumR and FITC-insulin.

Linearity

A series of standard solutions containing 50-500 IU/mL of HumR (10 concentrations) and 0.025-5.0 mg/mL of FITC-insulin (10 concentrations), sample volume of 20 µl each were analysed using the method-specific chromatographic conditions described in **Section 3.2**. Calibration plots from six replicate experiments were constructed for HumR standard solutions and FITC-insulin solutions by plotting the concentration of compounds versus peak area response (area under peaks, AUP). The regression equation was calculated from the calibration curves, along with the standard deviations of the slope and intercept on the ordinate.

Range

The concentration range, within or at the extremes of which the three analytical methods show acceptable degree of linearity, accuracy, and precision, was derived from the linearity studies.

Accuracy

Accuracy is defined as the closeness of the agreement between a test result and the accepted reference value (combination of random and systematic errors) (Crowther, 2001).

Accuracy of the methods was determined by injecting four different concentrations, with three replicate each, of HumR and FITC-insulin into the HPLC system. The same procedure as described for linearity was followed. AUP for each insulin solution was recorded and the recovery percent of insulin was calculated using the regression equation.

Precision

Precision of an analytical method expresses the closeness of agreement between a series of measurements obtained from multiple sampling of the same homogenous sample under the prescribed conditions (Crowther, 2001).

Precision of the assay was determined by repeatability (intra-day) and intermediate precision (inter-day) by injecting four different concentrations, with three replicate each, of HumR and FITC-insulin into the HPLC system. Repeatability which refers to the use of the analytical procedure within a laboratory over a short period of time was evaluated by assaying the samples the same day. Intermediate precision was assessed by comparing the assays on different days using different insulin standards, using freshly prepared mobile phase. The AUPs were recorded and RSD % was calculated.

Detection and Quantitation limits (Sensitivity)

Limits of detection (LOD) and quantitation (LOQ) were calculated based on standard deviation of the analytical response represented by AUP (for the lowest concentration used) and slope of the calibration curve. The following equations **Equation 3-1 and Equation 3-2** were used;

$$LOD = 3.3\frac{\sigma}{S} \qquad \textbf{Equation 3-1}$$

$$LOQ = 10\frac{\sigma}{S} \qquad \textbf{Equation 3-2}$$

Where σ is the standard deviation of the response and S is the slope of the calibration curve. The regression data obtained from the linearity studies were used.

3.3.2 Results and Discussion

Validation capabilities; selectivity, system suitability, linearity, range, accuracy, precision and detection and quantitation limits for the three RP-HPLC methods were assessed and results are as discussed below. For the FITC-insulin method the validation results for only the di-labelled FITC-insulin conjugate are presented here, the mono and tri-labelled conjugates gave similar results.

Selectivity

The developed RP-HPLC acidic analytical method, under the chromatographic conditions, achieved a run time of 30 minutes with elution of HumR insulin at Rt of 13.3 min, *m*-cresol at Rt 5.6 min and degradation product A21 desamido insulin at Rt 24.1 min. The comparison of the chromatograms of the placebo and HumR revealed that there were no additional peaks co-eluting with the peaks of insulin and A21 desamido insulin, refer to **Figure 3-2**.

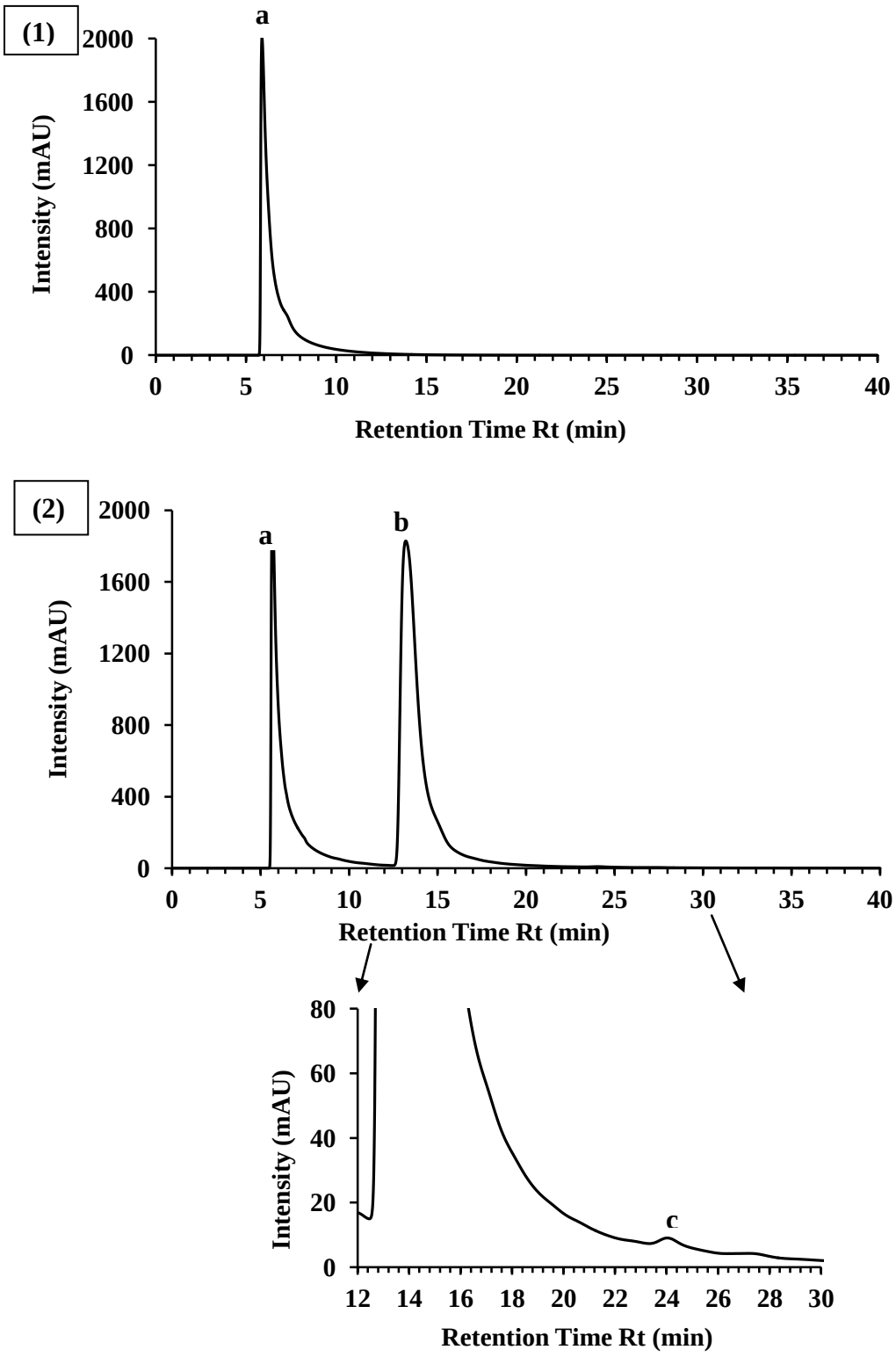

Figure 3-2: RP-HPLC chromatogram using the acidic analytical method of **(1)** Placebo (diluting fluid), **a:** *m*-cresol peak at Rt 5.6 min and **(2)** HumR (400 IU/mL), **a:** *m*-cresol peak at Rt 5.6 min, **b:** insulin peak at Rt 13.3 min, **c:** A21 desamido insulin at Rt 24.1 min.

The developed RP-HPLC neutral analytical method, under the chromatographic conditions, achieved a run time of 30 minutes with elution of HumR insulin at Rt of 16.6 min, *m*-cresol at Rt 5.4 min and degradation product B3 desamido insulin at Rt 12.6 min and Rt 13.4 min. The comparison of the chromatograms of the placebo and HumR revealed that there were no additional peaks co-eluting with the peaks of insulin and B3 desamido insulins, refer to **Figure 3-3**.

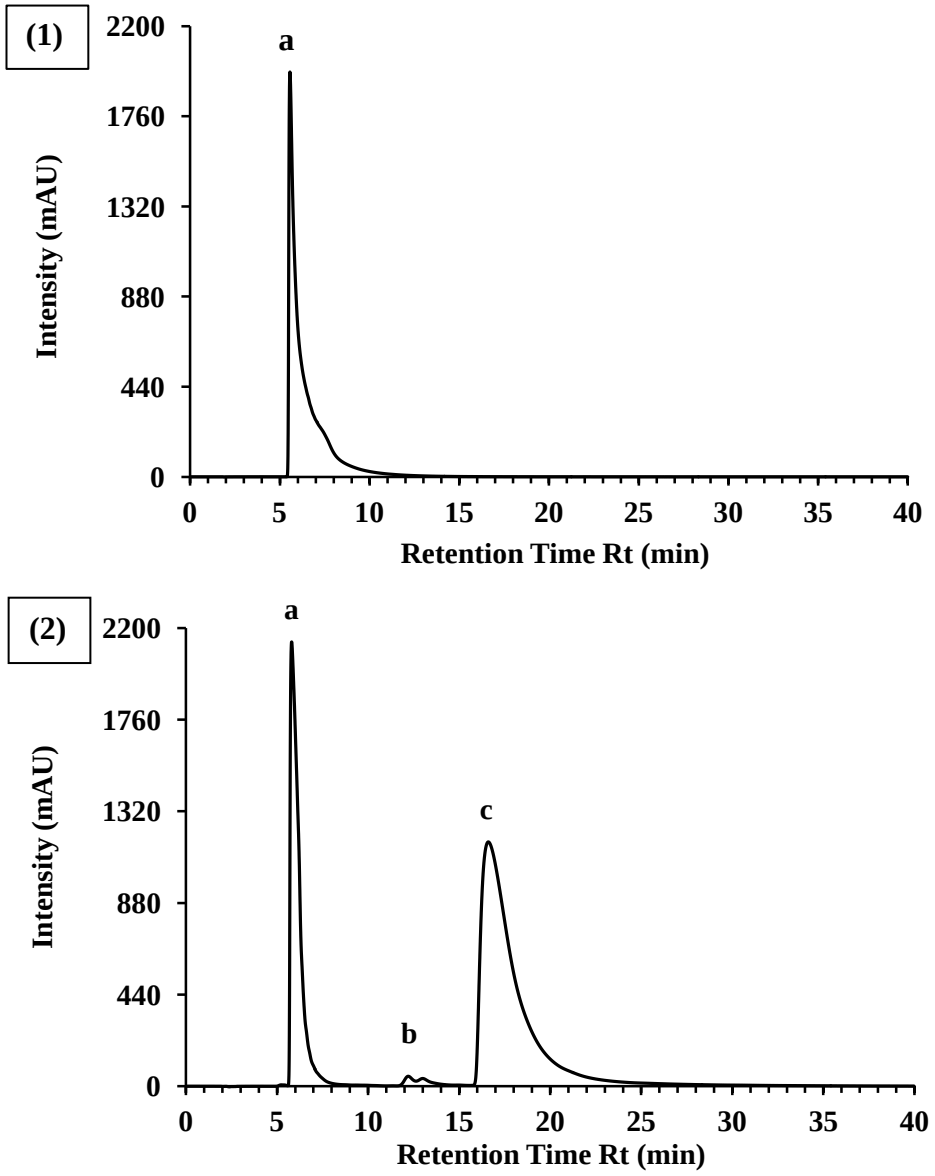

Figure 3-3: RP-HPLC chromatogram using the neutral analytical method of **(1)** Placebo (diluting fluid), **a:** *m*-cresol peak at Rt 5.4 min and **(2)** HumR (400 IU/mL), **a**: *m*-cresol peak at Rt 5.4 min, **b**: B3 desamido insulin peaks at Rt 12.6 and 13.4 min, **c**: insulin peak at Rt 16.6 min.

The RP-HPLC FITC-insulin method has shown that FITC-insulin had mono-labelled FITC-insulin conjugate peak with Rt of 21.8 min, di-labelled FITC-insulin conjugate peak with Rt 22.5 min and tri-labelled FITC-insulin conjugate peak with Rt 23.5 min (refer to **Figure 3-4**). This has been determined and confirmed using RP-HPLC and MS as discussed in **Chapter 4**.

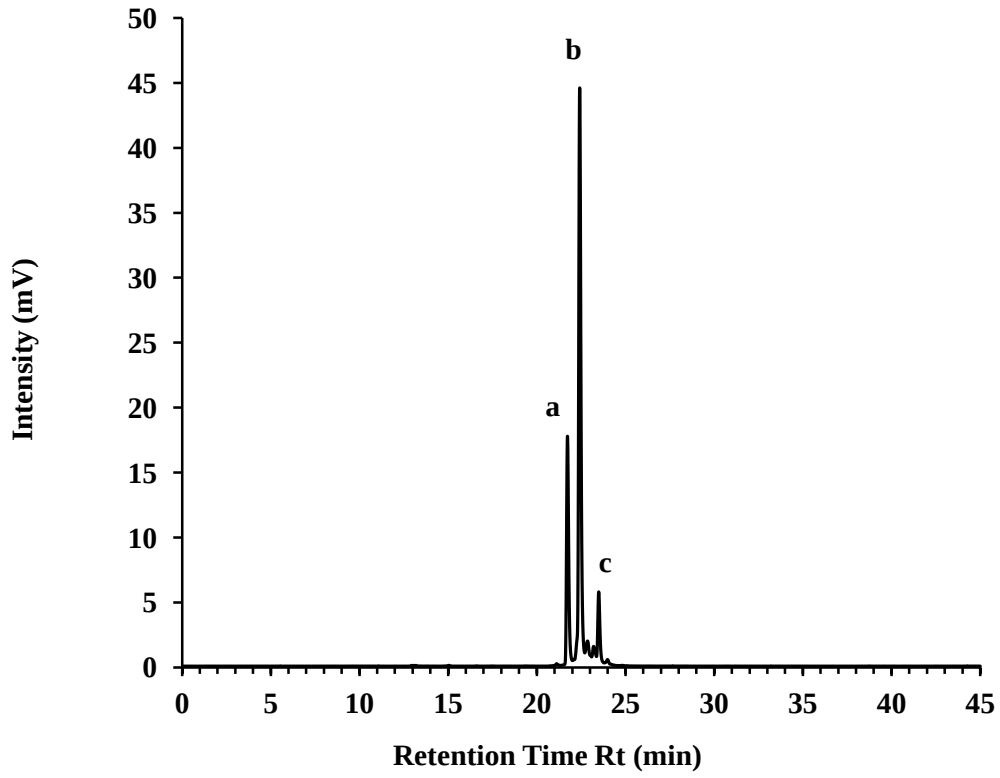

Figure 3-4: RP-HPLC chromatogram of FITC-insulin (5 mg/mL) using the FITC-insulin method, **a**: mono-labelled at Rt 21.8 min, **b**: di-labelled at Rt 22.5 min, **c**: tri-labelled FITC-insulin conjugate at Rt 23.5 min.

System suitability

The system suitability results for the acidic, neutral and FITC-insulin methods are as presented in **Table 3-1**, **Table 3-2** and **Table 3-3**, respectively.

Table 3-1: System suitability study of HumR (concentration 200 IU/mL) using acidic analytical method for determination of insulin and its A21 desamido insulin degradant.

System suitability parameters	Rt in min	Peak Area
Mean (n=6)	13.3	114,382,890
SD	0.05	473811
% RSD	0.41	0.41

Table 3-2: System suitability study of HumR (concentration 250 IU/mL) using neutral analytical method for determination of insulin and its B3 desamido insulin degradant.

System suitability parameters	Rt in min	Peak Area
Mean (n=6)	16.6	92,426,999
SD	0.25	419828
% RSD	1.49	0.45

Table 3-3: System suitability study of di-labelled FITC-insulin conjugate (concentration 0.25 mg/mL) using FITC-insulin method for determination of FITC-insulin conjugates.

System suitability parameters	Rt in min	Peak Area
Mean (n=6)	22.5	19,111
SD	0.01	279
% RSD	0.06	1.46

The % RSD of peak area and Rt for HumR using the acidic and neutral analytical methods and for di-labelled FITC-insulin using the FITC-insulin method are within ±2% (acceptance criteria) indicating the suitability of the corresponding systems.

System suitability results thus suggest that the chromatographic system and conditions used in the three methods are suitable for the samples analysed.

Linearity

Figure 3-5 and **Figure 3-6** show the linear relationship between AUP and insulin concentration over the concentration range 50-500 IU/mL for the acidic and neutral analytical methods, respectively. **Figure 3-7** shows the linear relationship between AUP and FITC-insulin concentration over the concentration range 0.025-5.0 mg/mL for the FITC-insulin method. The calibration curves constructed for the six replicate experiments were evaluated by their correlation coefficient.

The calibration equation for the acidic analytical method from six replicate calibration curves, y=387,831x + 2,089,296 (R^2 = 0.9966), demonstrated the linearity of the method. Standard deviations of the slope and intercept for the calibration curves were 8,986 and 1,506,488, respectively. The regression equation with all the linearity parameters for the acidic analytical method from six replicate calibration curves is as presented below in **Figure 3-5**, where R^2 is correlation coefficient, r is Pearson correlation coefficient and CI is confidence interval.

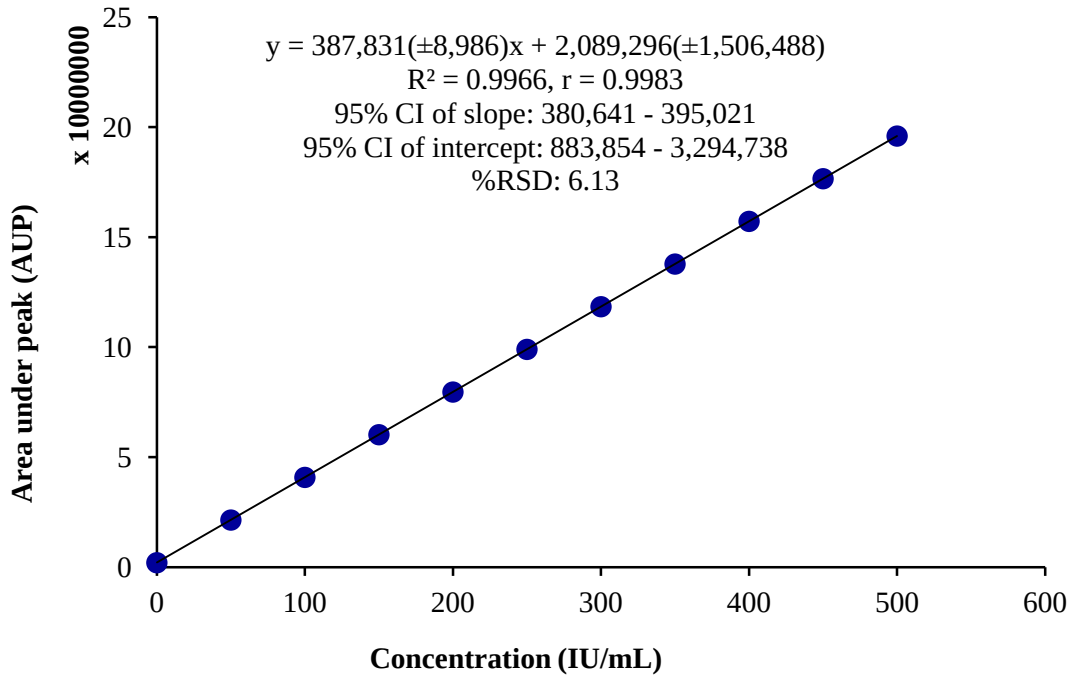

Figure 3-5: Parameters of regression equation, relating HumR concentration to analytical response (AUP) using acidic analytical method.

The regression equation with all the linearity parameters for the neutral analytical method from six replicate calibration curves is as presented below in **Figure 3-6**;

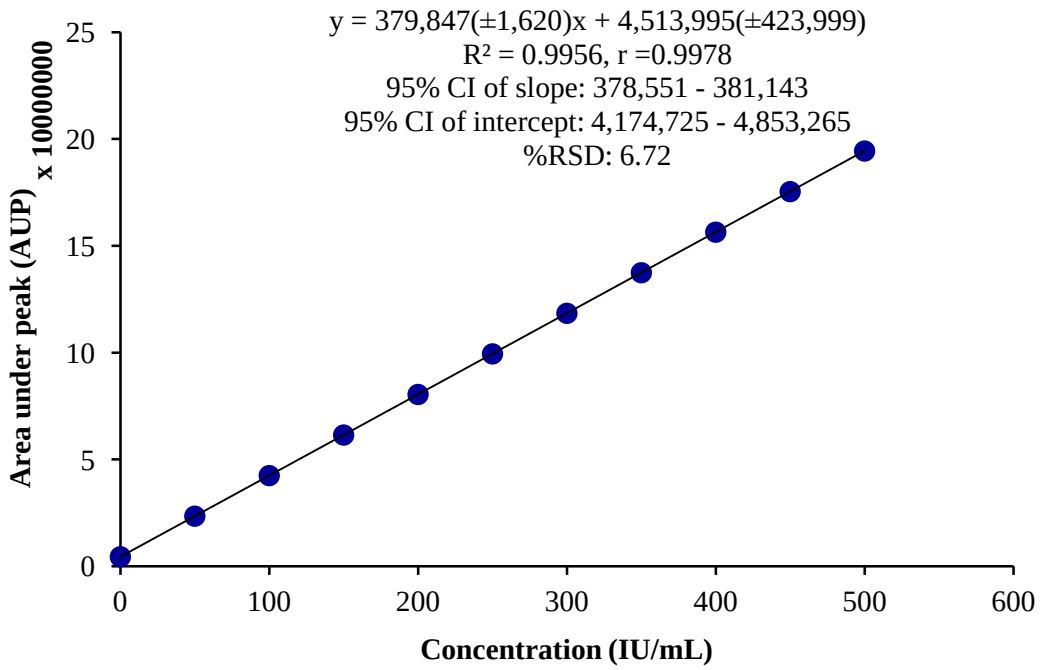

Figure 3-6: Parameters of regression equation, relating HumR concentration to analytical response (AUP) using neutral analytical method.

The regression equation with all the linearity parameters for the FITC-insulin method from six replicate calibration curves is as presented below in **Figure 3-7**;

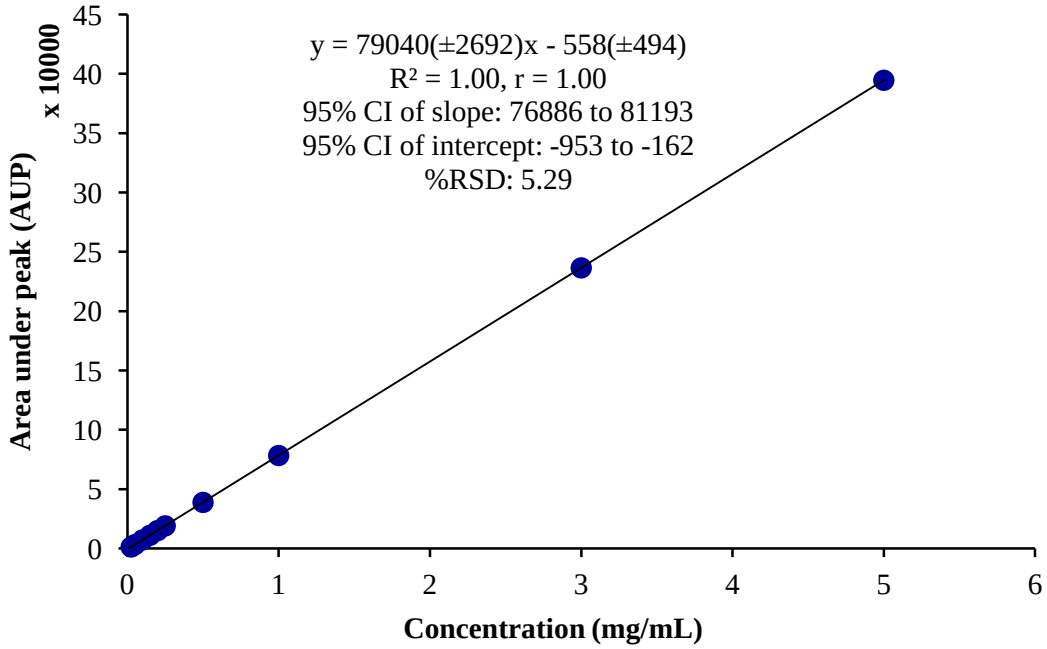

Figure 3-7: Parameters of regression equation, relating di-labelled FITC-insulin conjugate concentration to analytical response (AUP) using FITC-insulin method.

Linearity studies have shown a linear relationship between AUP and concentration of HumR across the concentration range 50 – 500 IU/mL as indicated by the correlation coefficient using both the acidic and neutral analytical methods. Also, linear relationship was shown for di-labelled FITC-insulin across the concentration range of 0.025-5.0 mg/mL (correlation coefficient was 1) using the FITC-insulin method.

Range

The linearity ranges studied using the acidic, neutral and FITC-insulin methods are as shown in **Figure 3-5**, **Figure 3-6** and **Figure 3-7**, respectively. The linearity results suggest that all three analytical methods provide an acceptable degree of linearity within, and at the extremes of the concentration ranges studied.

Accuracy

The accuracy results for the acidic, neutral and FITC-insulin methods are shown as in **Table 3-4**, **Table 3-5** and **Table 3-6,** respectively.

The AUPs corresponding to insulin concentrations were used to calculate the recovery percent of insulin using the regression equation. The recovery was 100.48 ± 0.63% and 101.27 ± 1.46% for HumR using the acidic and neutral analytical method, respectively and was 100.02 ± 0.26% for di-labelled FITC-insulin conjugate using the FITC-insulin method.

Table 3-4: Accuracy of the acidic analytical method for determination HumR**.**

Std conc. IU/mL	**AUP Mean ±SD**	**RSD %**	**Cal. conc.±SD IU/mL**	**Recovery %**
150	59,082,209±519,203	0.88	150.50±3.14	100.33
200	81,130,312±321,212	0.40	202.74±0.89	101.37
350	136,853,506±1,181,152	0.86	351.11±4.33	100.32
500	197,502,242±1,337,885	0.68	499.43±2.52	99.89
			Average Recovery %	100.48
			SD	0.63
			RSD	0.63

Table 3-5: Accuracy of the neutral analytical method for determination HumR.

Std conc. IU/mL	AUP Mean ±SD	RSD %	Cal. conc.±SD IU/mL	Recovery %
150	64,732,780±149.388	0.23	150.62±0.34	100.41
200	82,944,396±184,091	0.22	206.79±0.09	103.39
300	124,611,907±190,231	0.15	303.12±0.46	101.04
400	156,927,295±1,166,927	0.74	400.91±1.43	100.23
			Average Recovery %	101.27
			SD	1.46
			RSD	1.44

Table 3-6: Accuracy of the FITC-insulin method for determination of di-labelled FITC-insulin conjugate.

Std conc. mg/mL	AUP Mean ±SD	RSD %	Cal. conc.±SD mg/mL	Recovery %
0.05	3,483±29	0.82	0.0500±0.00	99.92
0.20	15,216±160	1.06	0.2000±0.00	100.00
0.50	39,393±470	1.19	0.5019±0.01	100.38
1.00	79,149±339	0.43	0.9978±0.00	99.78
			Average Recovery %	100.02
			SD	0.26
			RSD	0.26

Accuracy results demonstrate the suitability of the methods for quantitative determination of insulin.

Precision

Precision calculated for the HumR samples during the intra- and inter-day run using acidic and neutral analytical methods are presented in **Table 3-7** and **Table 3-8**, respectively. Precision calculated for the FITC-insulin samples using FITC-insulin method are given in **Table 3-9**. The % RSD value for intra-day precision was ≤ 1.01 and for inter-day precision was ≤ 0.75.for acidic analytical method, intra-day precision was ≤ 0.74 and for inter-day precision was ≤ 0.30 for neutral analytical method and intra-day precision was ≤ 1.05 and for inter-day precision was ≤ 0.83 for FITC-insulin method. Thus all three methods show suitable repeatability and intermediate precision.

Table 3-7: Precision of acidic analytical method for determination of insulin in HumR.

Std conc.	**Intra-day**		**Inter-day**		**Overall RSD**
IU/mL	**AUP Mean±SD**	**RSD %**	**AUP Mean±SD**	**RSD %**	**%**
200	80,511,102±8,10,141	1.01	81,130,312±321,212	0.40	0.80
300	114,116,991±502,655	0.44	114,648,789±310,602	0.27	0.41
500	197,502,242±1,337,885	0.68	197,061,936±1,478,956	0.75	0.65

Table 3-8: Precision of neutral analytical method for determination of insulin in HumR.

Std conc.	**Intra-day**		**Inter-day**		**Overall RSD**
IU/mL	**AUP Mean±SD**	**RSD %**	**AUP Mean±SD**	**RSD %**	**%**
100	45,340,751±79,090	0.17	44,156,436±133,078	0.30	1.47
200	82,944,396±184,091	0.22	86,743,903±37,292	0.04	2.46
400	156,927,295±1,166,927	0.74	162,635,381±141,610	0.09	2.01

Table 3-9: Precision of FITC-insulin method for determination of di-labelled FITC-insulin conjugate.

Std conc.	Intra-day		Inter-day		Overall RSD
mg/mL	AUP Mean±SD	RSD %	AUP Mean±SD	RSD %	%
0.05	3,483±29	0.82	3,493±29	0.83	0.75
0.20	15,216±160	1.05	15,806±84	0.53	2.21
1.00	79,149±339	0.43	80,421±238	0.30	0.93

Precision studies have demonstrated the repeatability and intermediate precision of the three analytical methods with respect to the chromatographic conditions under which they are intended to be used.

Detection and Quantitation limits (Sensitivity)

LOD and LOQ were calculated based on standard deviation of the analytical response represented by AUP for the lowest concentration used in linearity studies and slope of the calibration curve. The LOD and LOQ for HumR using acidic analytical method were 0.79 and 2.41 IU/mL, respectively. The LOD and LOQ for HumR using neutral analytical method were 0.98 and 2.97 IU/mL, respectively. The LOD and LOQ for di-labelled FITC-insulin conjugate using FITC-insulin method were 0.0013 and 0.0039 mg/mL, respectively. The results thus demonstrate the sensitivity of the three methods.

3.4 Compatibility with device materials results and discussion

3.4.1 Background

The objective of the compatibility studies was to investigate insulin stability and compatibility with materials that formed part of the implantable closed-loop insulin

delivery device, INsmart, or have a potential to be considered for use in future device designs.

Insulin has a tendency to come out of solution in several forms, possibly even when the formulations are optimised for stability in the product as presented for sale (containing additives such as pH adjusters, phenol and zinc). Some precipitated and/or aggregated forms are permanently inactivated whereas some are reversible, but in precipitated form, all cause problems for the working of devices with membranes and fine tubes. Some preliminary work was performed by the INsmart group at National Physical Laboratory (Teddington) to understand the effect of formulation adjuncts and the conditions relevant to the INsmart device that could have an effect on insulin stability. A design of experiment approach (power analysis -Taguchi approach) was employed to select key influential factors. The following were selected;

- Formulations (insulin 0.4% and 2%),
- Temperature (20°C and 37°C),
- Glucose concentrations (0 and5%),
- Phenol concentrations (0 and 0.4%),
- 2 different shear rates achieved using different tube diameter
- Stirring using orbital motion at 20 rpm.

These were studied over a period of 21 days. The study has found that the most significant factors were phenol, insulin concentration, temperature and the combination of phenol and temperature. The worst case conditions were 0% phenol, 2% (500 IU/mL, the top commercial concentration) insulin and 20°C. The effect of agitation seemed much less significant and the passage of the solutions through fine tubing (shear) was not found to be significant under the conditions. Agitation and shear are known to be factors that can cause insulin to come out of solution but here the movement may have been gentler than needed to produce the effect and the single passage of insulin through tubing may be an insignificant insult, though representative of the *in vivo* refilling condition (and also of pump-delivered insulin).

As an extension of this work material compatibility studies were performed and are presented here. This chapter describes experiments conducted to look at the potential adverse effects of material type on insulin stability. Five materials were investigated of

which polycarbonate (a thermoplastic polymer containing monomer bisphenol A) and stainless steel (Grade 316) are present in current device design, polyurethane (a long chain thermoplastic polymer made up of polyol and isocyanate mixed) and titanium (99.99% purity) are potential future materials of interest and resin (a polyurethane two part thermosetting resin made of polyol and isocyanate mixed) was a material which was used in very early designs which might have potential future use.

HumR 500 IU/mL concentration was used in *in vivo* pig experiments as described in **Chapter 2**. It was therefore important to simulate these *in vivo* conditions where compatibility could be assessed using a similar concentration and with each of the material used to fabricate the device. The material compatibility study was therefore conducted with HumR (500 IU/mL) which it was reasoned would give valuable information with regard to selection of material for future design. FITC-insulin was used in all *in vitro* diffusion studies discussed in this thesis. Therefore material compatibility study was also conducted with FITC-insulin which would provide understanding of solution stability for the duration of *in vitro* experiments. The material compatibility was assessed by measuring insulin recovery and degradation products formed over the study period using the three validated RP-HPLC methods discussed in the previous section.

3.4.2 Experimental set-up

3.4.2.1 Materials

HumR 500 IU/mL manufactured by Eli Lilly and Co was used. It has a composition of 500 IU/mL insulin, 2.5 mg/mL *meta*-cresol, and 16 mg/mL glycerine, zinc oxide to supplement the endogenous zinc to obtain a total zinc content of 0.017 mg /100 units, and water for injection. The pH (reported as between 7.0 and 7.8) was adjusted to 7.4.

FITC-insulin solution (5mg/mL, pH 7.6) was prepared by dissolving FITC-insulin (synthesised in-house) in distilled water and then adjusting the pH (refer to **Chapter 4** for details on synthesis of FITC-insulin). The FITC-insulin solution was prepared immediately before use.

Sample bottles were acquired from Fisher Scientific, Loughborough. These were clear 1.8 mL Vial (E-C sample Wheaton 33 low extractable borosilicate glass 12 x 35 mm dia. x ht (cap on) 8-425 screw cap size) with septum top, rubber lined black cap.

Machined material samples of polycarbonate (a thermoplastic polymer containing monomer bisphenol A) (PC), polyurethane (a long chain thermoplastic polymer made up of polyol and isocyanate mixed) (PU), resin (a polyurethane two part thermosetting resin made of polyol and isocyanate mixed) (R) and stainless steel (Grade 316) (SS) were acquired from Renfrew Group. These were rounded rods, dia.: 2.8±0.2 mm, ht: 44±1 mm with polish and finish matching those on the device. Titanium wire (Ti) manufactured by Sigma Aldrich, 0.5 mm diameter, 99.99%, 50cm wire was used. These were cut to size to fit the sample bottles.

3.4.2.2 Experimental set-up and method

The material rods were secured in the sample bottles by inserting in the sample bottle lids through the septum as shown in **Figure 3-8** below;

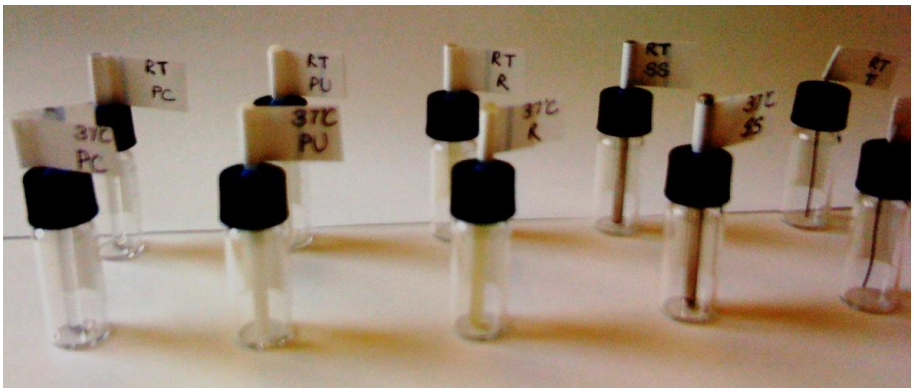

Figure 3-8: Sample bottles with material rods secured in the lid.

1mL of the insulin solution was placed in the 2 mL test sample bottles each with PC, PU, R, SS rod and Ti wire. In addition, insulin solutions placed in sample bottles without any test materials and stored at 20°C were used as control standards. The test sample bottles were stored at 20°C and 37°C. Three sets of sample bottles with material

rods (3x10 sample bottles) were set up to provide for the three RP-HPLC methods. Two sets had HumR solution and one set had FITC-insulin solution. Sampling was performed after 0.083 (2hr), 1, 3, 7, 11, 21 and 31 days and analysed by RP-HPLC. The sample bottles with FITC-insulin solutions were placed in a dark container and protected from light.

For the HumR samples RP-HPLC the acidic analytical method was used in order to determine the amount of insulin remaining in the sample and to assess the amount of A21 desamido insulin degradant. The RP-HPLC neutral analytical method was used to determine the amount of insulin remaining in the sample and to assess the amount of B3 desamido insulin degradant. In addition the recovery of meta- cresol (*m*-cresol) in the HumR samples was determined. Insulin and *m*-cresol recovery were determined by comparison with control samples stored at 20°C but without the test material rods. A calibration curve using the control samples was generated at each time point.

The FITC-insulin method was used for the determination of the amount of FITC-insulin conjugates remaining in the FITC-insulin samples. FITC-insulin recovery was determined by comparison with control samples stored at 20°C but without the test materials (rods). A calibration curve using the control samples was generated at each time point.

The test sample set-up for the studies is as shown in **Figure 3-9**;

Figure 3-9: Experimental set-up of the study sample bottles with test materials.

3.4.3 Results and discussion

The compatibility study results for HumR samples with test materials using the RP-HPLC acidic and neutral analytical methods are presented together followed by the results for FITC-insulin samples.

3.4.3.1 Compatibility study results for HumR with device materials at 20°C and 37°C using the RP-HPLC acidic and neutral analytical methods

The visual observation results for the HumR samples for both analytical methods, acidic and neutral, are presented in **Table 3-10**. Same visual observations were noted for both sample sets as the visual observations are independent of the HPLC methods used and are just duplicates at this stage.

Table 3-10: Visual observation table for material compatibility study from both sets (acidic and neutral analytical methods).

20°C		**Test material**				
Time (days)	**Control**	**PC**	**PU**	**R**	**SS**	**Ti**
0.08	clear	clear	clear	clear	clear	clear
1	clear	clear	clear	fine suspended particles	clear	clear
3	clear	clear	fine suspended particles	fine suspended particles	clear	clear
7	clear	clear	fine suspended particles	increased fine suspended particles	clear	clear
11	clear	clear	increased suspended particles	increased fine suspended particles	clear	clear
21	clear	clear	white sediment	increased suspended particles	clear	clear
31	clear	clear	white sediment	increased suspended particles	clear	clear
37°C		**Test material**				
Time (days)	**Control**	**PC**	**PU**	**R**	**SS**	**Ti**
0.08	clear	clear	clear	clear	clear	clear
1	clear	clear	fine suspended particles	fine suspended particles	clear	clear
3	clear	clear	fine suspended particles	fine suspended particles	clear	clear
7	clear	clear	white suspended particles	fine suspended particles	clear	clear
11	clear	clear	white sediment	increased fine suspended particles	clear	clear
21	clear	clear	white sediment	increased suspended particles	clear	clear
31	clear	clear	white sediment	increased suspended particles	clear	clear

The control HumR solution stored at 20°C without any material remained clear over the entire study period, it can be concluded that the effects observed were due to the device materials present. Solutions with PC, SS and Ti remained clear throughout the study as shown in **Table 3-10**. From 1 day onwards, R seems to initiate aggregation and/or precipitation at 20°C and 37°C. PU initiating aggregation and/or precipitation from 1 day onwards at 37°C and from 3 days at 20°C. Time limitations prevented analysing the suspended particles observed.

3.4.3.1.1 Effect on insulin recovery over time

The insulin recovery values were normalised over the entire time period based on values observed at initial time point. The insulin recovery results using the acidic and neutral analytical methods are presented below in **Figure 3-10** and **Figure 3-11**, respectively;

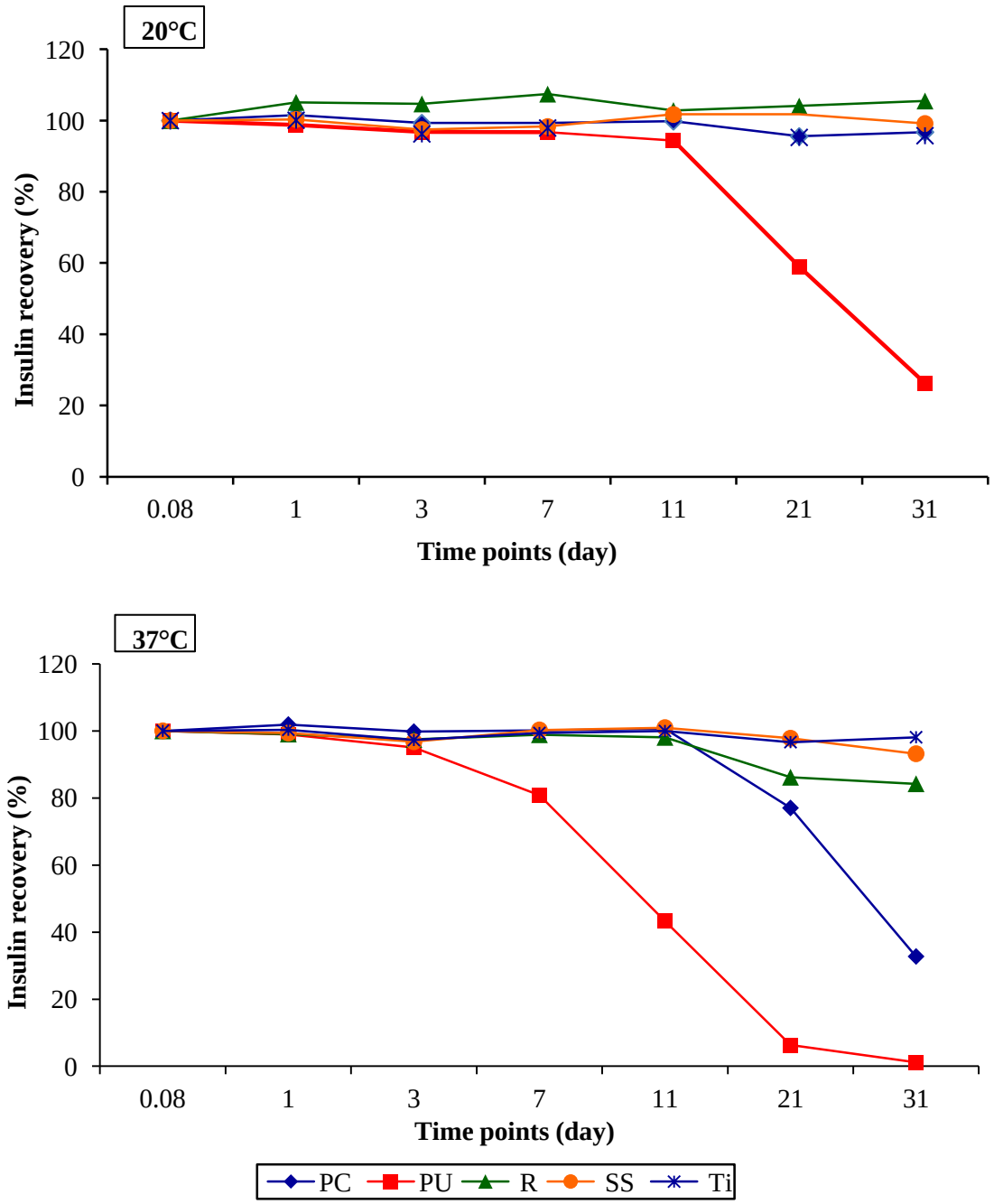

Figure 3-10: Insulin recovery over time for each test material at 20°C and 37°C using the acidic analytical method.

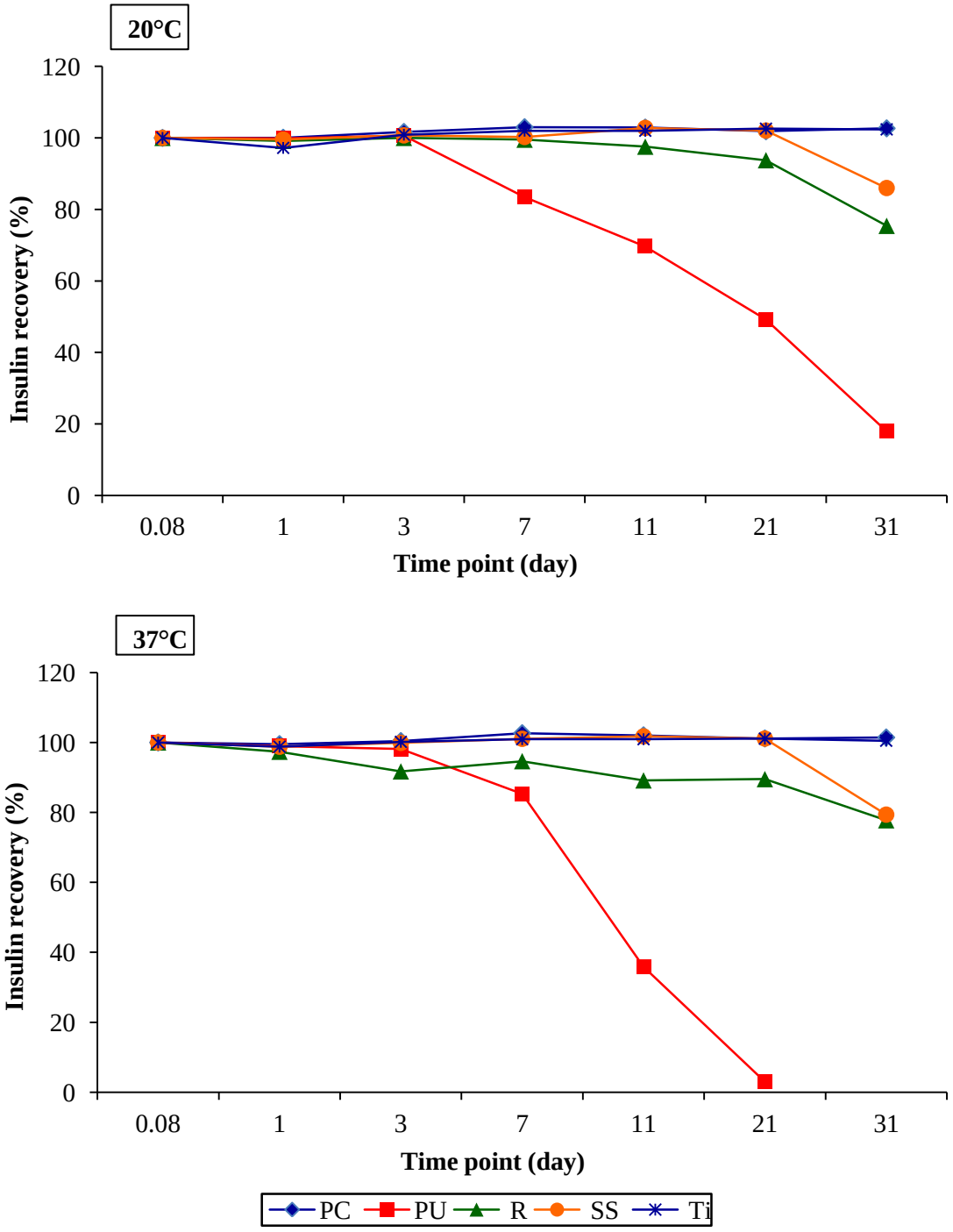

Figure 3-11: Insulin recovery over time for each test material at 20°C and 37°C using the neutral analytical method.

Using the acidic analytical method, as shown in **Figure 3-10**, solutions in contact with PC, R, SS and Ti show negligible loss of insulin after 31 days at 20°C. However, PU showed a loss of ~74% after 31 days at 20°C. At 37°C, solutions in contact with Ti showed negligible loss of insulin, with SS showing a loss of ~7%, R showing ~16%, PC showing ~ 67% and PU showing complete loss of insulin after 31 days.

Using the neutral analytical method, as shown in **Figure 3-11**, solutions in contact with PC and Ti show negligible loss of insulin after 31 days at 20°C. However, R showed a loss of ~25%, SS showed a loss of ~ 15% and PU showed a loss of ~82% after 31 days at 20°C. At 37°C, solutions in contact with PC and Ti showed negligible loss of insulin, with SS and R showing a loss of ~22% and PU showing complete loss of insulin after 31 days.

The insulin recovery results suggest that at 20°C HumR solution is compatible with PC and Ti for up to 31 days and with R and SS up to 21 days. At 37°C HumR solution is compatible with Ti for up to 31 days, with SS for up to 21 days and PC and R up to 11 days. The results show that PU looks like the least compatible of all the materials.

3.4.3.1.2 Formation of A21 and B3 desamido insulin over time

A21 desamido insulin

The levels of A21 desamido insulin formed in the insulin solutions with the test materials over 31 days at 20°C and 37°C are as presented in **Figure 3-12**.

Low levels of A21 desamido insulin were observed over time for all materials at 20°C and 37°C, the maximum values observed were well below Pharmacopoeia specified limits for insulin preparations of not more than 5% of total area of peaks.

The maximum levels observed over 31 days at 20°C was with R (0.34%) and the maximum levels observed at 37°C was with SS and Ti (0.49%).

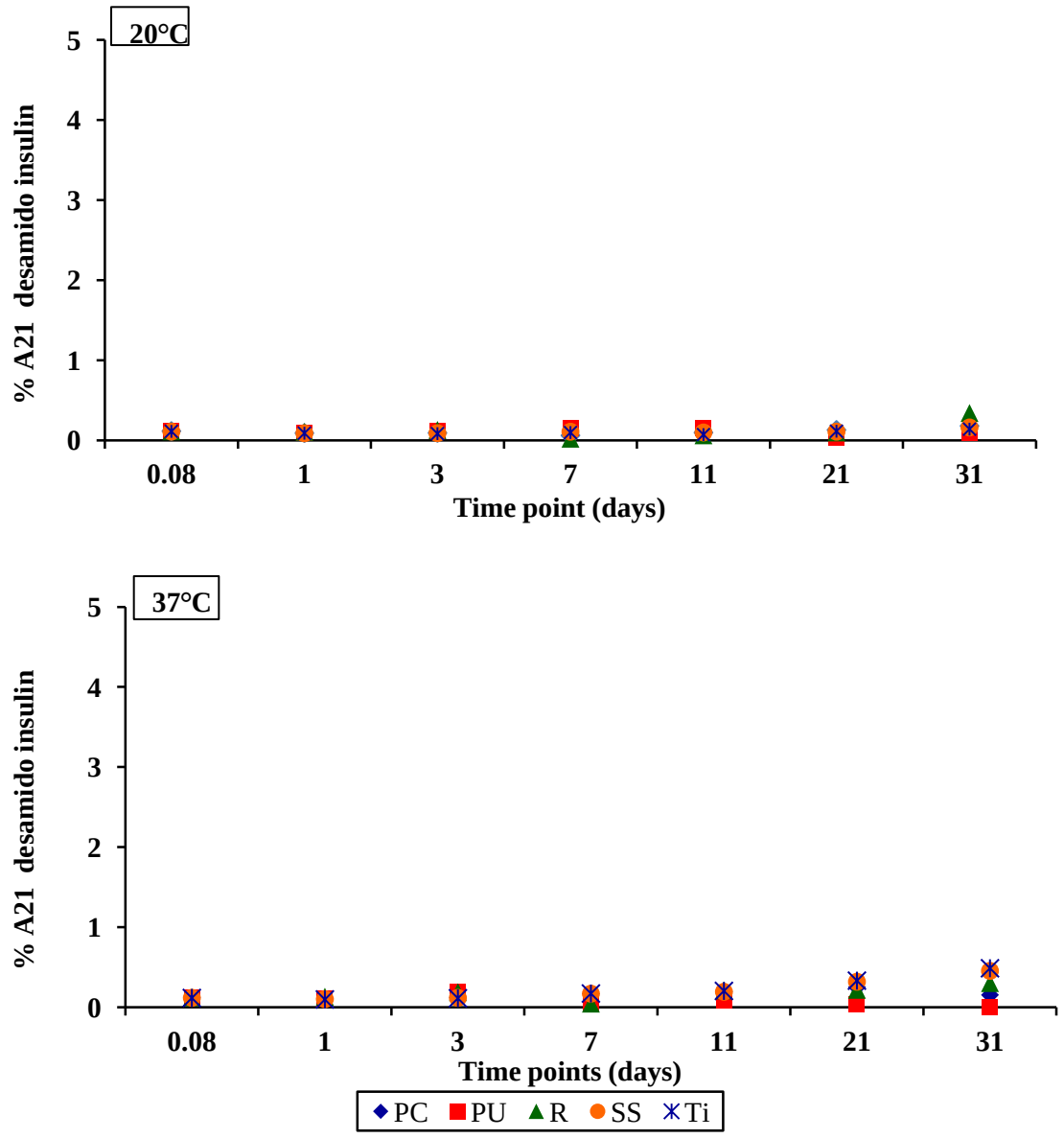

Figure 3-12: A21 desamido insulin formed over time at 20°C and 37°C as a percentage of the total insulin peak area using acidic analytical method.

B3 desamido insulin

The levels of B3 desamido insulin formed are as presented in **Figure 3-13**. Formation of B3 desamido insulin is largely unaffected by any of the materials at 20°C and 37°C except for R, which shows an increase after 3 days. Polycarbonate seems to contribute to the formation of B3 desamido insulin after 21 days at 37°C. For all materials, except R (maximum level was 7.5%), the B3 desamido insulin values observed were below the

Pharmacopoeia specified limit which states that all other peaks (other than A21and insulin peak) should not be more than 6%.

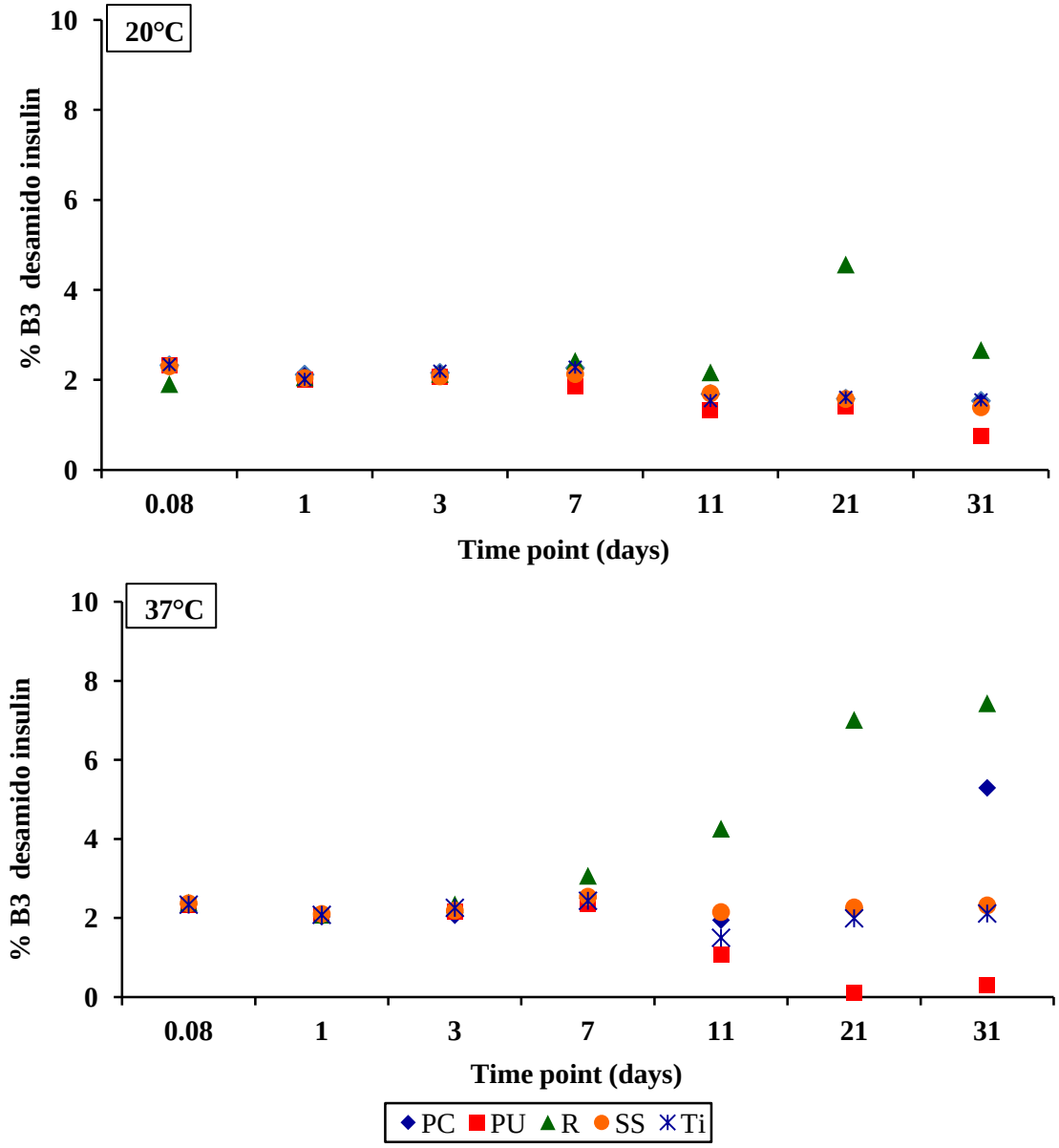

Figure 3-13: Total B3 desamido insulin (isoAsp and Asp) formed over time at 20°C and 37°C as a percentage of the total insulin peak area using neutral analytical method.

3.4.3.1.3 Effect on m-cresol recovery over time

The *m*-cresol recovery values were normalised over the entire time period based on values observed at initial time point. The *m*-cresol recovery levels from the insulin solutions with the test materials over 31 days at 20°C and 37°C are as presented in **Figure 3-14**.

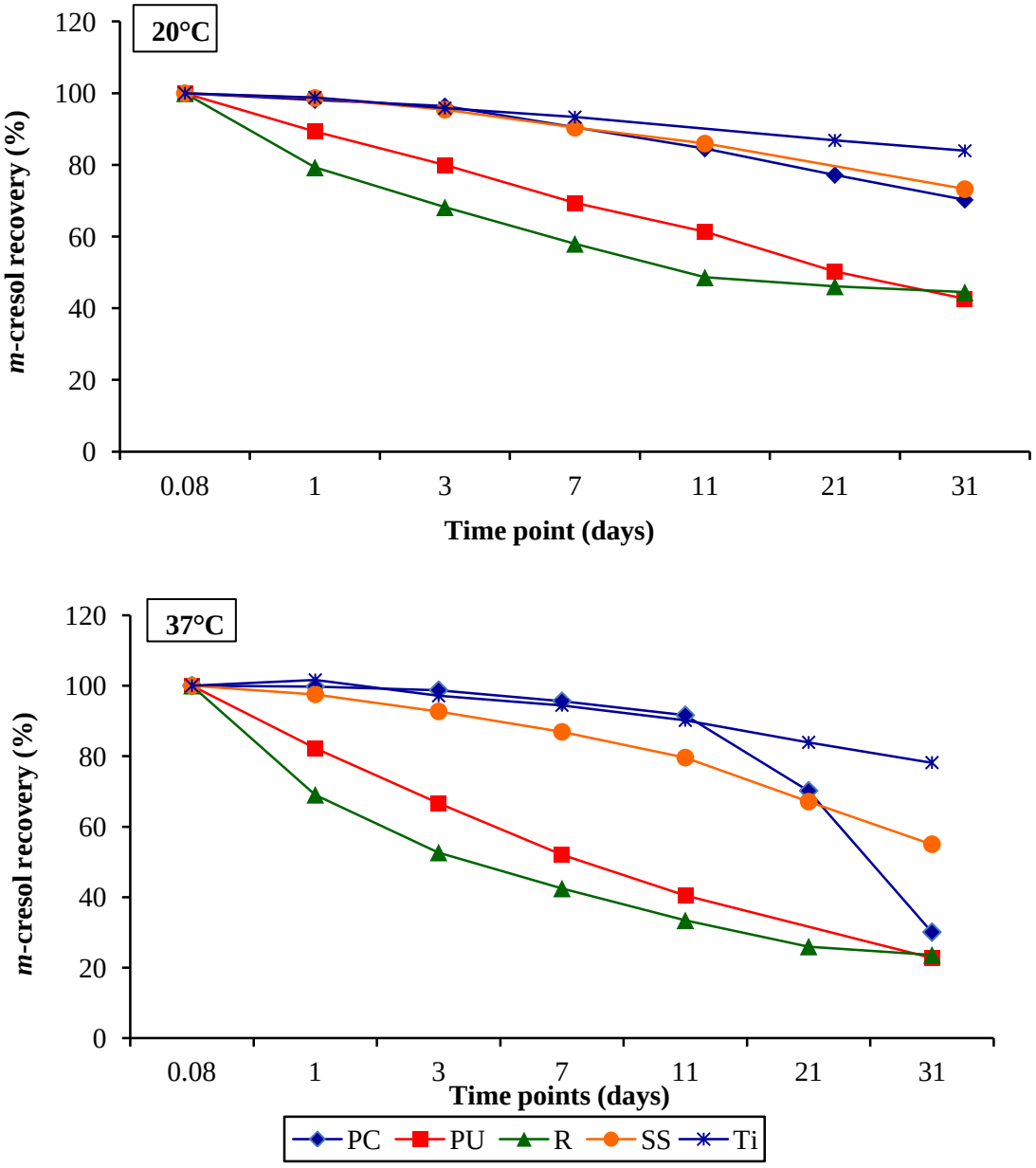

Figure 3-14: *m* – cresol recovery over time for each test material at 20°C and 37°C using the acidic analytical method.

Insulin solutions in contact with all five materials show loss of *m*-cresol over the 31 day test period at 20°C and 37°C. At 20°C, solution with Ti showed the least loss of *m*-cresol, with PU and R showing a loss of ~56% and SS and PC showing a loss of ~28% after 31 days.

At 37°C, solution with Ti showed least loss of *m*-cresol, with PC, PU and R showing a loss of ~74% and SS showing a loss of ~45% after 31 days.

Comparison of the insulin and *m*-cresol recovery trends reveal that recovery of *m*-cresol decreases with increase in loss of insulin at 20°C and 37°C.

Combining all findings from the visual observations, insulin recovery, *m*-cresol recovery, formation of A21 and B3 desamido insulin the following conclusions can be made for the materials tested;

PC – HumR is found to be compatible with PC at 20°C with negligible loss of insulin and very low levels of desamido insulin degradants formed though there is some loss of *m*-cresol observed. At 37°C there appears to be insulin loss after 11days (using the acidic method) which is proportional to *m*-cresol loss observed after 11 days, here the insulin loss can be linked to the loss of protection of the insulin molecule by *m*- cresol and not formation of degradants.

SS and **Ti** – At 20°C and 37°C , the HumR solutions were compatible over 31 days with no aggregation observed, low levels of desamido insulin degradants observed and some loss in insulin observed for SS at 37°C after 21 d can be linked to loss in *m*- cresol observed.

PU – Aggregation of the HumR solutions were observed at 20°C and 37°C which can be linked to insulin loss from 11d at 20°C and 3d at 37°C. This loss in insulin was due to loss of protection by *m*-cresol observed and not due to formation of the desamido insulin degradants as very low levels of these were observed.

R – Aggregation of the HumR solutions were observed at 20°C and 37°C after 1d and increased over 31 days, insulin loss was less compared to other materials. The *m*-cresol loss is linked to higher levels of B3 (>7%) formed. Here aggregation observed is not linked to insulin loss, but loss of *m*-cresol (which could have been absorbed by Resin) and formation of B3 desamido insulin instead.

3.4.3.2 Compatibility studies for FITC-insulin with device materials at 20°C and 37°C using the RP-HPLC FITC-insulin method

Observation table for material compatibility study for FITC-insulin method are presented in **Table 3-11**. FITC-insulin control solutions stored at 20°C without any material remained clear for up to 7 days. Solutions with PC, SS and Ti showed signs of precipitation from 3 days onwards at 20°C and 37°C. Solution with PU showed signs of precipitation from 3 days at 20°C and from 1 day at 37°C, whereas R seems to initiate precipitation from 1 day onwards at 20°C and 37°C.

The visual observations indicate that precipitation occurs in FITC-insulin solution between 7 and 14 days when stored alone in glass and with the test materials it starts much sooner. A point to be noted here is that the FITC-insulin solution has no formulation additives or stabilisers. For the purposes of the diffusion *in vitro* experiments, FITC-insulin solutions were always freshly prepared just before use.

Table 3-11: Observation table for material compatibility study for FITC-insulin method.

20°C		**Test material**				
Time (days)	**Control**	**PC**	**PU**	**R**	**SS**	**Ti**
0.08	clear	clear	clear	clear	clear	clear
1	clear	clear	clear	fine suspended particles	clear	clear
3	clear	hazy	hazy	hazy	Slightly hazy	Slightly hazy
7	clear	hazy	hazy	hazy	Slightly hazy	Slightly hazy
14	hazy	hazy	hazy	hazy	hazy	hazy
36	hazy	hazy	hazy	hazy	hazy	hazy
37°C		**Test material**				
Time (days)	**Control**	**PC**	**PU**	**R**	**SS**	**Ti**
0.08	clear	clear	clear	clear	clear	clear
1	clear	clear	fine suspended particles	fine suspended particles	clear	clear
3	clear	hazy	hazy	hazy	hazy	clear
7	clear	hazy	hazy	hazy	hazy	hazy
14	hazy	hazy	hazy	hazy	hazy	hazy
36	hazy	hazy	hazy	hazy	hazy	hazy

3.4.3.2.1 Effect on FITC-insulin recovery over time

The percent FITC-insulin conjugates were determined for each sample solution at each time point by comparing to the same solution stored at 20°C with no materials using the FITC-insulin method, the results are as presented in **Figure 3-15** and **Figure 3-16**.

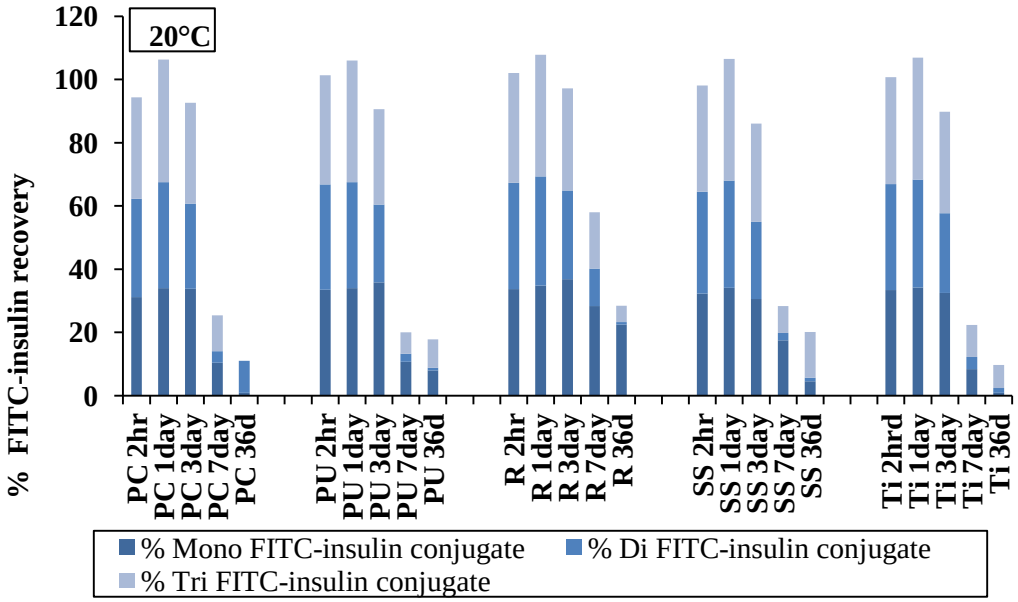

Figure 3-15: Percentage recovery of FITC-insulin conjugates at 20°C over time compared to the same solution stored without material at initial time point using FITC-insulin method (data presented is normalised against control).

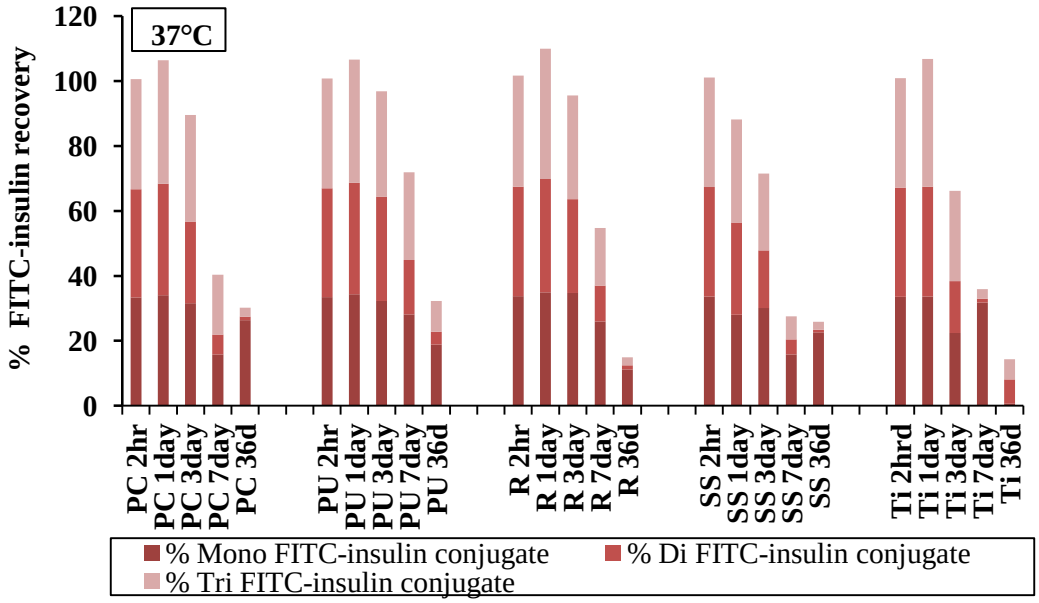

Figure 3-16: Percentage recovery of FITC-insulin conjugates at 37°C over time compared to the same solution stored without material at initial time point using FITC-insulin method (data presented is normalised against control).

The percentage recovery of FITC-insulin conjugates over time indicate the loss of the conjugates from 3 day time point at 20°C and 37°C as shown in **Figure 3-15** and **Figure 3-16**, respectively for all the materials tested. The results suggest that the FITC-insulin solution would need some formulation adjuncts and stabilisers if the solution is to be used with the device for a longer period.

3.5 Chapter summary

- The validation capabilities; selectivity, system suitability, linearity, range, accuracy, precision and detection and quantitation limits determined for the three RP-HPLC methods were assessed based on the FDA guidelines. The RP-HPLC acidic and neutral analytical methods can be used to detect and quantify insulin and two of its main deamidation degradants. The RP-HPLC FITC-insulin method enables quantification of the FITC-insulin conjugates in samples.
- The validation studies have demonstrated the suitability of the three methods for the determination of insulin and its degradants and FITC-insulin conjugates with reduced

analysis times and with accuracy across the concentration ranges intended to be studied for the INsmart device material compatibility studies.

- The objective of the compatibility studies was to investigate insulin stability and compatibility with materials that formed part of the device or have a potential to be considered for use in future device designs. The main conclusions from the material compatibility studies are as follows;
  - HumR was found to be compatible with PC, SS and Ti for up to 31 days at 20°C showing no visible aggregation, negligible loss of insulin, low levels of desamido insulin degradants and some loss of *m*-cresol. At 37°C, similar observations were made for SS and Ti, except for some loss in insulin observed for SS at 37°C after 21 d which can be linked to loss in *m*-cresol observed. At 37°C for PC there appears to be insulin loss after 11days (using the acidic method) which can be linked to loss of protection of the insulin molecule by *m*- cresol and not to the formation of degradants.
  - With PU, visual aggregation of HumR solutions were observed at 20°C and 37°C which can be linked to insulin loss from 11d at 20°C and 3d at 37°C. This loss in insulin was due to loss of protection by *m*-cresol observed and not due to formation of the desamido insulin degradants as very low levels of these were observed.
  - With R, aggregation of the HumR solutions were observed at 20°C and 37°C after 1d and increased over 31 days, insulin loss was less compared to other materials. The *m*-cresol loss is linked to higher levels of B3 (>7%) formed. Here aggregation observed is not linked to insulin loss, but loss of *m*-cresol (which could have been absorbed by Resin) and formation of B3 desamido insulin instead.
  - The material compatibility results suggest that the current device materials, SS and PC are suitable for *in-vivo* use with HumR for up to 11 days, but after that PC could contribute towards loss of insulin at 37°C. SS is compatible for up to 21 days at 37°C. Ti showed negligible loss of insulin for the entire duration of the study suggesting that it is a good material to consider in future device designs. R might not be the best material to consider and PU is definitely the least compatible and hence not suitable for future device designs.

- In comparison to the conclusions from the experiments performed at NPL which concluded that the worst case conditions were 0% phenol, 2% (500 IU/mL, the top commercial concentration) insulin and 20°C, the material compatibility study conclusions here confirm the necessity for presence of phenolic compound (*m*-cresol) for maintaining the stability of insulin solution but in contrast highlighted greater loss in insulin recovery at 37°C.
- FITC-insulin which is being used as a tool in *in vitro* experiments, the solution was found to be compatible with the device materials up to only 3 days. The control FITC-insulin solution showed signs of precipitation between 7 and 14 days and with materials it started much sooner, with PC, SS and Ti showing visual signs of precipitation from 3 days onwards at 20°C and 37°C while PU and R showing signs 1 day onwards. These visual observations matched the FITC-insulin conjugate recovery results.
- This did not pose a problem for the *in vitro* studies as such as FITC-insulin solutions were always freshly prepared just before use and the same solution was never used for periods greater than 3days. However, it has highlighted the fact that FITC-insulin solution needs formulation adjuncts and stabilisers, which should be assessed for stability if it is intended to be used in experiments with the device over a period of more than 3 days.

Chapter 4 Synthesis and identification of FITC-insulin conjugates

4.1 Introduction

Several immunoassay and non-biological analytical methods, especially high performance liquid chromatography (HPLC) are available for assay and determination of human insulin in *in vivo* and *in vitro* conditions. Though these methods are suitable for routine assay measurements, they are time consuming and not suitable for quick real time experimental measurements. This shortfall was overcome by the use of fluorescently labelled insulin for quick minute by minute quantification of insulin delivered from the INsmart device. Fluorescently labelled insulin was synthesised for use in i*n vitro* experiments to monitor and understand insulin delivery mechanism from the INsmart device.

In this chapter the synthesis of FITC-insulin conjugates (Fluorescein isothiocyanate insulin conjugates) using native human insulin will be described. FITC-insulin conjugates produced at various reaction times and in the presence of phenol or meta cresol (*m*-cresol) which are known to promote stability of insulin solution are investigated. FITC-insulin conjugate species synthesised using various clinically used insulin injection preparations are also presented. Further, conjugate species present in FITC-insulin products (synthesised by Sigma Aldrich) were examined and are presented.

4.1.1 Fluorescent probes

Fluorescence technologies are widely used in bioanalytical applications for detection purposes and have often superseded radiolabeling. Small molecule - based fluorescent probes have been extensively used in biological sciences over the last several decades (Lavis and Raines, 2008; Jameson and Ross, 2010). They have been routinely used by researchers to tag non fluorescent molecules of interest for detection purposes

(Giepmans et al., 2006). In addition to aiding in visualization, functional fluorescent probes have become indispensable tools in modern biology because they provide dynamic information concerning the localization and quantity of molecules of interest (Ueno and Nagano, 2011). The small size of a fluorophore in comparison to a protein/peptide is advantages with respect to potentially low impact on the protein's biological activity and at the same time can impart high detection sensitivity.

Fluorescein isothiocyanate isomer I (**Fluorescein 5-isothiocyanate, FITC**) (empirical formula: $C_{21}H_{11}NO_5S$, molecular weight: 389.38 Da) is yellow-orange in colour and is widely used to fluorescently label proteins via the amine group in various biological applications. The isothiocyanate group reacts with terminal amine residues and primary amines in proteins. FITC isomer I has the thiocyanate group on the 4 carbon of the benzene ring, whereas isomer II has the thiocyanate on the 5 carbon (**Figure 4-1**). The two isomers are indistinguishable spectrally, by wavelength or intensity. Isomer I is the commonly used isomer due to the fact that it more easily isolated in pure form and hence is less expensive, though mixed isomers are perfectly suitable for many applications.

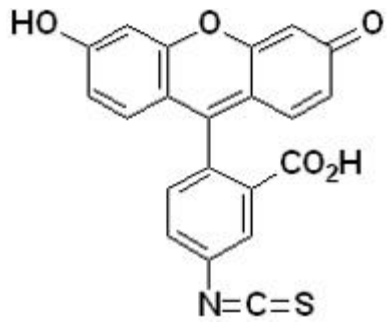

FITC isomer I
[Fluorescein-5-isothiocyanate]

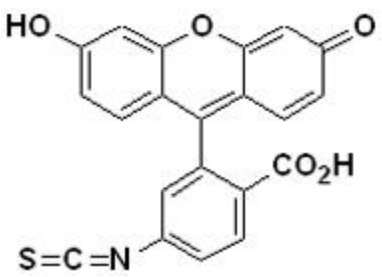

FITC isomer II
[Fluorescein-6-isothiocyanate]

Figure 4-1: Structure of fluorescein isothiocyanate isomers.

Biological applications of this amine-reactive fluorescent probe include fluorescent labelling of proteins, fluorescent reagent for protein tracing, microsequencing of

proteins and a reagent in the fluorescent antibody technique for the rapid identification of pathogens (Choi et al., 2013; Shelma and Sharma, 2013; Rodríguez-Sáinz et al., 2013). FITC is a fluorophore of choice due to its high molar absorptivity and quantum yield. It is soluble in acetone at 1 mg/mL, in anhydrous dimethyl sulfoxide (DMSO) at 5 mg/mL, in water at less than 0.1 mg/mL in water. An organic solvent is normally used for stock solutions which can be diluted in basic buffer for coupling procedures immediately prior to use, displaying absorption maximum excitation at 495 nm and emission at 525 nm in the visible range of the spectrum. FITC (isomer 1) was used to fluorescently label insulin to synthesise FITC-insulin conjugates for *in vitro* use.

4.1.2 Insulin, insulin receptor structure and binding mechanism

Despite more than three decades of investigation, the details of the mechanism of insulin–insulin receptor binding has still not been fully understood, this is partly due to the fact that the three-dimensional structure of the insulin–insulin receptor complex has proved elusive aggravated by the complexity of producing the receptor protein (Menting et al., 2013; Vashisth, 2014). Here, information highlighting the importance of certain regions of insulin residue involved in insulin-receptor recognition and binding are presented. This is important with respect to understanding the impact of fluorescent labelling on certain sites on the insulin molecule.

Studies of insulin analogues have allowed mapping of the interactive residues on the surface of the molecule and have demonstrated how activity depends on the integrity of the insulin fold. Two surfaces of insulin are understood to interact with the insulin-receptor (De Meyts, 2004; Schaffer, 1994), as shown in **Figure 4-2**. It appears that both these regions are involved in binding; the classical binding site is labelled as 'binding-site 1' and binding site on the hexamer surface as 'binding site 2'(Schaffer, 1994). The classical binding site is usually considered to comprise a number of residues in the dimer-forming surface (B12, B24, B25) and probably also some of the hydrophobic residues buried beneath the C-terminus of the B chain.

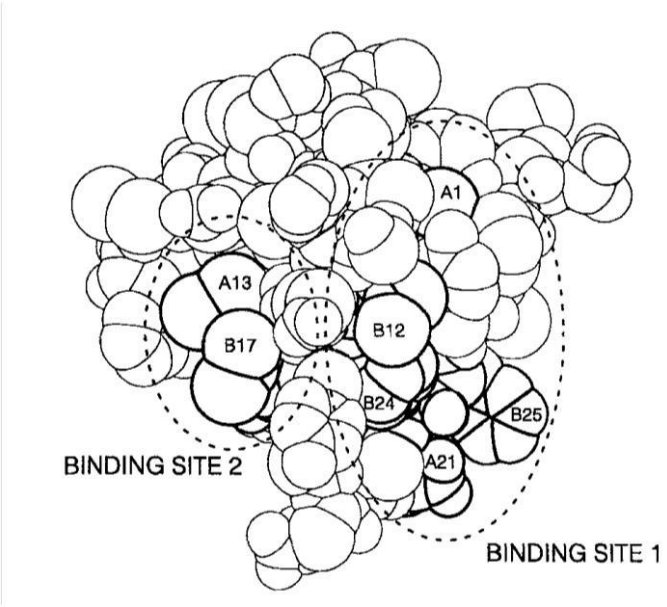

Figure 4-2: Model of human insulin showing binding sites 1 and 2. Note that binding-site 1 is partially covered by the C-terminus of the B chain (Schaffer, 1994).

The insulin receptor is a cell surface receptor for insulin, comprising a tetramer of two alpha (α) and 2 beta (β) subunits derived from cleavage of a single precursor protein. It is a disulphide-linked $(\alpha\beta)_2$ homodimer; the extracellular portion of each αβ protomer contains six domains (L1, CR, L2, FnIII-1, FnIII-2 and FnIII-3) and an insert domain (ID) within FnIII-2, refer to **Figure 4-3**.

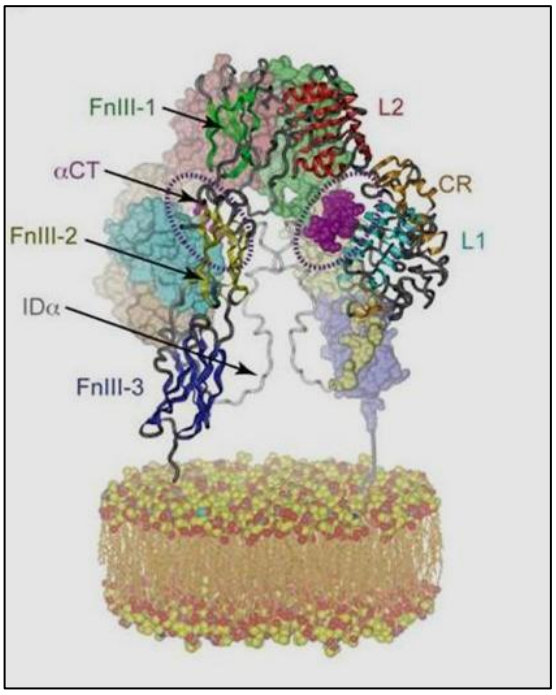

Figure 4-3: Three dimensional structure of the insulin receptor system with the dashed ellipses showing the primary and secondary insulin-binding sites (Menting et al., 2013).

The homodimer has a two-fold symmetric inverted "V" conformation, with the L1-CR-L2 module of one insulin receptor monomer packed against the FnIII-1,-2,-3 module of the alternate insulin receptor monomer. The tandem L1-β2 / αCT element forms site 1, the primary insulin-binding site (dashed ellipse). Site 2, the secondary insulin-binding site, is formed by residues at the junction of the FnIII-1 and FnIII-2 domains of the opposite α-chain to that contributing the L1 domain to site 1 (Menting et al., 2013; Hubbard, 2013; Ward and Lawrence, 2012; Ward and Lawrence, 2011).

Menting et al have studied and presented the interaction of insulin with the insulin-receptor binding sites. The insulin-binding sites 1 and 2 interact with the primary and secondary receptor binding sites. It has been proposed that at the receptor primary binding site insulin rearranges itself by displacing the C-terminal B chain residues B20-B30 from its helical core upon receptor engagement (Menting et al., 2013; Whittaker et al., 2008). The receptor contains an intrinsic tryrosine kinase domain that is located within the β subunit which upon activation by insulin results in numerous changes including uptake of glucose into the liver, muscle and adipose tissue (Kido, Nakae and Accili, 2001; Saltiel and Kahn, 2001).

4.1.3 Clinically used insulin injection preparations

Variant forms of insulin, known as insulin analogues, with modified amino-acid sequences and improved pharmacokinetic properties have been produced since human insulin was successfully made using recombinant-DNA (rDNA) technology in the early 1980s. Design of insulin analogues are based on general principles of protein folding and assembly (Berenson et al., 2011). Short acting insulin analogues, present in commercially available injections Humulin® R and Actrapid®, have been produced using rDNA technology with same structure as natural human insulin which show absorption similar to natural human insulin. After subcutaneous injection, the maximal effect is at approx. 3 hrs (range: 20 min to 7 hrs) and terminates after approx. 8 hrs (range: 3 to 14 hrs).

Rapid acting insulin analogues, insulin aspart, insulin glulisine and insulin lispro present in NovoRapid®, Apidra® and Humalog® respectively, have been produced with reduced self-association properties or accelerated hexamer dissociation properties to achieve rapid absorption than regular insulin (Brange, 1997; DeFelippis, Chance and Frank, 2001),(Weiss, 2013). Following subcutaneous injection, the time to maximum concentration is 40 – 60 min and duration of action is about 3 - 5 hrs.

Long acting insulin analogues, insulin determir and insulin glargine present in Levemir® and Lantus® respectively, have been synthesised either by introducing amino-acid changes that increase the isoelectric point of insulin whereby reducing its solubility at physiological pH, or by covalent acylation. After subcutaneous injection, insulin levels rise slowly to a plateau within 6–8 hrs and remain essentially unchanged for up to 24 hrs, suitable for once-daily administration (Owens, 2002). The differences between the insulin analogues are as presented in **Figure 4-4** and **Table 4-1** to **Table 4-3**, the information was largely derived from manufacturers' data and product monographs. It is important to know the differences between the insulin analogues in terms of amino-acid substitutions and formulation details to understand the impact of fluorescent labelling on certain sites on the insulin molecule.

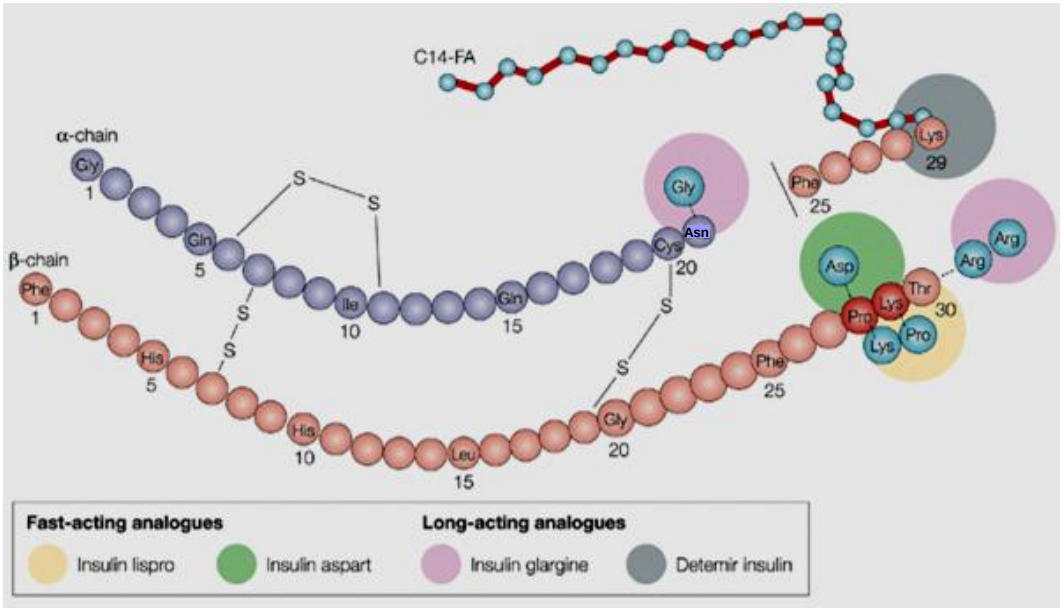

Figure 4-4: Figure showing the differences in the insulin analogues (Owens, 2002).

Table 4-1: Types of short - acting insulin preparations commercially available with description of insulin present.

Insulin, Brand & Manufacturer	**Difference from Human Insulin and mode of action**	**Molecular formula & mass**	**Formulation details**
Human insulin **Regular insulin** **Humulin® R U-500** Eli Lilly	Structurally identical to natural human insulin. Mode of action is same as natural insulin.	$C_{257}H_{383}N_{65}O_{77}S_6$ 5807.57 Da	Humulin® R U-500 is a sterile, clear, aqueous and colourless solution that contains human insulin (produced by rDNA technology in a special non-disease-producing laboratory strain of *Escherichia coli* bacteria) 500 units/mL, 16 mg/mL glycerine, 2.5 mg/mL metacresol and 0.005 mg/mL zinc oxide and water for injection (WFI). The pH is 7.0 to 7.8. HCl and/or NaOH may be added during manufacture to adjust the pH. Also available as Humulin R U-100.
Human insulin (rys) **Actrapid® U-100** **Novo Nordisk**	Structurally identical to natural human insulin. Mode of action is same as natural insulin.	$C_{257}H_{383}N_{65}O_{77}S_6$ 5807.57 Da	Actrapid® is a neutral, clear and colourless solution of human insulin (rys). One IU (International Unit) of human insulin corresponds to 0.035 mg of anhydrous human insulin (rys) (produced by rDNA technology using *Saccharomyces cerevisiae*).Also contains: glycerol, meta-cresol, zinc chloride and WFI. HCl and/or NaOH added to adjust the pH.

Table 4-2: Types of rapid - acting insulin preparations commercially available with description of insulin present.

Insulin, Brand & Manufacturer	**Difference from Human Insulin and mode of action**	**Molecular formula & mass**	**Formulation details**
Insulin aspart NovoRapid®/ NovoLog® U-100 Novo Nordisk	Human insulin analogue in which proline has been replaced by aspartic acid in the B-chain position 28, which creates charge repulsion and steric hindrance due to a local conformational change at the carboxyl terminus of the B chain. Reduced tendency to self-associate into hexamers due to electrostatic repulsion at the dimer interface resulting in rapid absorption leading to an earlier peak and a shorter duration of action than soluble insulin.	$C_{256}H_{381}N_{65}0_{79}S_6$ 5825.8 Da	NovoRapid® 100 U/mL, is a sterile, aqueous, clear, and colourless solution, that contains insulin aspart (produced by r DNA technology in Saccharomyces cerevisiae) 100 Units/mL (3.5mg), 16 mg/mL glycerin, 1.50 mg/mL phenol, 1.72 mg/mL metacresol, 19.6 mcg/mL zinc, 1.25 mg/mL disodium phosphate dihydrate, 0.58 mg/mL sodium chloride and WFI. The pH is 7.2-7.6, HCl 10% and/or NaOH 10% may be added to adjust pH.
Insulin glulisine Apidra® U-100 Sanofi-Aventis	Human insulin analogue in which the amino acid asparagine at position B3 is replaced by lysine and the lysine in position B29 is replaced by glutamic acid. The glucose lowering activities of Apidra® and of regular human insulin are equipotent when administered by the intravenous route, however after subcutaneous administration; the effect of Apidra® is more rapid in onset and of shorter duration compared to regular human insulin.	$C_{258}H_{384}N_{64}O_{78}S_6$ 5823 Da	Apidra® is a sterile, aqueous, clear, colourless solution in vials or cartridges for use as an injection. Each millilitre of Apidra® contains 100 units (3.49 mg) insulin glulisine (produced by rDNA technology utilising a non-pathogenic laboratory strain of Escherichia coli (K12),3.15 mg *m*-cresol, 6 mg tromethamine, 5 mg sodium chloride, 0.01 mg polysorbate 20, and WFI. The pH is adjusted to approx. 7.3 by addition of aqueous solutions of HCl and/or NaOH.

Insulin lispro **Humalog® U-100** **Eli Lilly**	Human insulin analogue in which the amino acid proline at position B28 is replaced by lysine and the lysine in position B29 is replaced by proline. Mode of action same as regular insulin, however the change in amino acid sequence creates steric hindrance and a reduced ability to self-associate, as a result is absorbed more rapidly than regular soluble insulin from subcutaneous injection sites and also has a shorter duration of action.	$C_{257}H_{383}N_{65}O_{77}S_6$ 5807.57 Da	Humalog® is a sterile, aqueous, clear, and colourless solution. Each millilitre of Humalog® contains insulin lispro (produced by rDNA technology utilising a non-pathogenic laboratory strain of *Escherichia coli*) 100 units, 16 mg glycerine, 1.88 mg dibasic sodium phosphate, 3.15 mg *m*-cresol, zinc oxide content adjusted to provide 0.0197 mg zinc ion, trace amounts of phenol, and WFI. Insulin lispro has a pH of 7.0 to 7.8. The pH is adjusted by addition of aqueous solutions of HCl 10% and/or NaOH 10%.

Table 4-3: Types of long - acting insulin preparations commercially available with description of insulin present.

Insulin, Brand & Manufacturer	**Difference from Human Insulin and mode of action**	**Molecular formula & mass**	**Formulation details**
Insulin determir Levemir® U-100 Novo Nordisk	Insulin detemir differs from human insulin in that threonine in position B30 has been omitted and acylation of a C14 fatty acid chain (myristic acid) to the lysine residue at B29. This modification results in delayed absorption due to increased self-association into hexameric form at injection site and high degree of reversible albumin binding (by fatty acid chain), thereby delaying its absorption from the subcutaneous tissue and transport across the capillary endothelium of skeletal muscle.	$C_{267}H_{402}N_{64}O_{76}S_6$ 5916.9 Da	Levemir® is a clear, colourless, aqueous, neutral sterile solution. Each mL of Levemir® contains 100units(14.2mg/mL) insulin detemir (produced by rDNA expression in *Saccharomyces cerevisiae* followed by chemical modification.), 65.4mcg zinc,2.06mg *m*-cresol,16.0mg glycerol, 1.80mg phenol,0.89mg disodiumphosphatedihydrate, 1.17mg NaCL and WFI. HCl and/or NaOH added to adjust pH to approx. 7.4.
Insulin glargine Lantus® U-100 Sanofi-Aventis	Insulin glargine differs from human insulin in that A21 asparagine is replaced by glycine (to stabilise the molecule) and two arginines are added to the B-chain C-terminus resulting in a shift of isoelectric point to neutrality. After subcutaneous injection, the insulin glargine acidic solution (pH 4) is neutralised; leading to formation of microprecipitates from which insulin glargine is slowly released, resulting in a relatively constant conc./time profile over 24 hrs with no pronounced peak. This profile allows once-daily dosing as a patient's basal insulin.	$C_{267}H_{404}N_{72}O_{78}S_6$ 6063 Da	Lantus® is a clear aqueous fluid. Each millilitre of Lantus® injection contains 100 IU (3.6378 mg) insulin glargine (produced by rDNA technology utilising a non-pathogenic laboratory strain of *Escherichia coli* (K12)). 10mL vials contain the following inactive ingredients per mL: 30 mcg zinc, 2.7 mg *m*-cresol, 20 mg glycerol 85%, 20 mcg polysorbate 20, and WFI. The pH is adjusted by addition of aqueous solutions of HCl and/or NaOH to approx. 4.

4.1.4 Background and outline

From previous work carried out within the INsmart group with labelling bovine insulin it was understood that labelled insulin can be produced which display higher aqueous solubility than native human insulin. Thus, for the *in vitro* experiments higher concentrations could be used in the insulin reservoir without the risk of precipitation. Also, synthesis of stable (in solution) biologically active labelled insulin in-house could be useful in wider biological and *in vitro* applications. Human FITC-insulin and bovine FITC-insulin synthesised by Sigma Aldrich are available but are very expensive (~£240 per 5 mg). Therefore a method to fluorescently label insulin was further developed to produce the material in house.

FITC-insulin complexes have been produced in the past but they have yielded mixtures with reduced biological activities (Maggi, 1966; Tietze, Mortimore and Lomax, 1962; Ciencialová et al., 2004). Fluoresceinthiocarbamyl insulin derivatives of bovine insulin prepared by Bromer et al (Bromer, Sheehan et al. 1967) under aqueous conditions have yielded mixtures of monosubstituted, disubstituted and tri substituted species with the monosubstituted fraction retaining only 40% of the native activity.

The FITC-insulin synthesis method used here was based on the work carried out by Hentz et al (Hentz et al., 1997). The method described by Hentz et al is the only exhaustive method described in literature for synthesis of FITC-insulin and has been repeatedly used by researchers. Although there is a much recent work done by Liu et al (Liu, Kohn and Mayer, 2012) where a N-trifluoroacetyl- based protecting group scheme is used to selectively label human insulin at positions A1, B1 and/or B29. In Hentz's work, human insulin was labelled with FITC to produce four distinct FITC-insulin conjugates by changing the reaction conditions (i.e. pH, reaction time, buffer and FITC/insulin ratio) which alter the selectivity of the fluorescein conjugation. The four isolated FITC-insulin conjugates were labelled at the following residues; A1(Gly), B1(Phe), A1(Gly)B1(Phe) and A1(Gly)B1(Phe)B29(Lys) as shown in **Figure 4-5**.

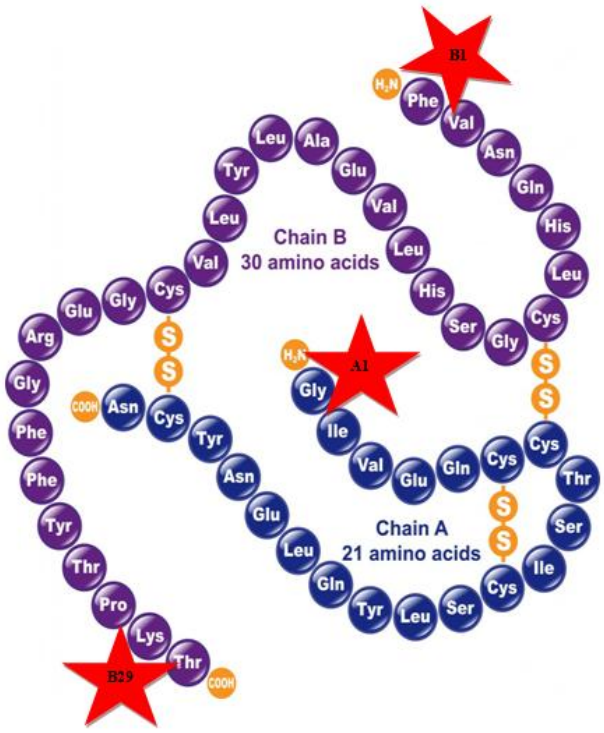

Figure 4-5: Diagram showing primary structure of human insulin with red stars indicating reactive primary amine sites for FITC conjugation (diagram modified from Shutterstock).

The characterisation of the conjugates shows that the degree and position of substitution affects the structural conformation and thus the biological activity of the FITC labelled insulin. Hentz found that FITC-insulin conjugates labelled at the A1 or B1 positions exhibited similar binding toward anti-insulin antibodies. Biological activity was measured using a tryrosine kinase phosphorylation assay for all four FITC-insulin conjugates. Refer to **Section 4.1.2** where insulin-insulin receptor binding was discussed highlighting the importance of certain sites on insulin molecule in insulin receptor recognition, receptor compatibility and biological activity *in vivo*. Based on biological activity results for FITC-insulin conjugates from the Hentz paper, the FITC-labelled insulin conjugate at B1 had equivalent activity as native insulin thus confirming that B1 position was not significantly involved in the binding to the insulin receptor, as can be understood from the discussion in **Section 4.1.2**. The A1 and the A1B1 FITC-insulin conjugates which showed a ~10 fold decrease in biological activity suggesting the

involvement of the A1 site in binding with the insulin receptor which can be understood as it forms part of the classical binding site for the receptor. The A1B1B29 showed almost ~100 fold decrease in biological activity indicating the importance of the B29 residue in receptor binding as discussed in **Section 4.1.2.** The proposed detachment of the C-terminal B-chain residues B20-B30 from the helical core of insulin upon receptor binding is understood to be crucial for the hormone–receptor recognition mechanism. The labelling of the insulin molecule at B29 could affect the conformation of the FITC-insulin conjugate and render it unrecognisable by the receptor and thus is likely to significantly reduce its biological activity.

The synthesis protocol detailing the various factors considered and different starting materials used are discussed below. The work described here is an extension of Hentz's work.

Synthesis of FITC-insulin conjugates using human insulin

FITC-insulin conjugate was synthesised using native human insulin and the synthesised conjugate species were identified using reversed phase high performance liquid chromatography (RP-HPLC).Mass spectrometry (MS) was used as an additional analytical tool to confirm the identity of the conjugate species produced. The effect of varying reaction time and adding phenolic compounds on the conjugates produced was assessed.

Effect of reaction time

In this study human insulin from Sigma Aldrich was labelled with FITC using the method described by Hentz et al and effect of varying reaction time on the FITC-insulin conjugate species produced was investigated.

Effect of phenol or m-cresol

Phenolic compounds are commonly used in insulin pharmaceutical preparations for dual purposes as anti-microbial preservatives and allosteric effectors due to their stabilising effect on the hexamer conformation of insulin (Berenson et al., 2011). Phenol promotes formation of an additional helical segment from B1-B8 and induces a structural change in the insulin from the T to the R state. Thus in the presence of phenol, the more stable

R-state formed has less tendency to dissociate, the B1-B8 α-helices are stabilised at the dimer-dimer interface and its position restricts zinc-ion diffusion out of the hexamer. This structural transition is induced by phenol in the presence of zinc ions and thus is a property of the hexamer. (Brange and Langkjaer, 1993).

The FITC-insulin conjugation method has zinc removed by chelating with EDTA, which dissociates the hexamer structure, and also does not include any phenolic compounds. Phenol or *m*-cresol was included in the reaction solution to study effect of phenolic compounds on the FITC-insulin conjugates produced in the absence of zinc. This will further give an insight into the conjugates produced using clinically used insulin injection preparations which always contain either phenol or *m*-cresol.

Synthesis of FITC-insulin conjugates using clinically used insulin injections

Different starting materials such as clinically used insulin injections which were either monomeric or hexameric were used to obtain conjugates which were then identified.

Short-acting human insulin analogues (Humulin®R and Actrapid®), rapid-acting insulin analogues which are monomeric [NovoRapid® (insulin aspart), Apidra® (insulin glulisine), Humalog® (insulin lispro)], and long-acting insulin analogues [Levemir® (insulin determir), Lantus® (insulin glargine)] which are hexameric were labelled with FITC to obtain mono-labelled active FITC-insulin conjugates with future biological and *in vitro* applications for tracing and relevant specific receptor binding studies.

Comparison to FITC-insulin products (synthesised by Sigma Aldrich)

Fluorescently labelled insulin products, FITC-bovine insulin and FITC-human insulin from Sigma Aldrich were analysed to compare with the FITC-insulin conjugate species synthesised in-house. FITC-insulin conjugate using bovine insulin was also synthesised in-house as it was required for comparison with the Sigma Aldrich commercial product. As shown in **Figure 4-6** bovine insulin differs from human insulin at the following positions: alanine for threonine at A8, valine for isoleucine at A10, and alanine for threonine at the carboxyl terminal of the B-chain (B30). Bovine insulin ($C_{254}H_{377}N_{65}O_{75}S_6$) has a molecular mass of 5733.5 Da.

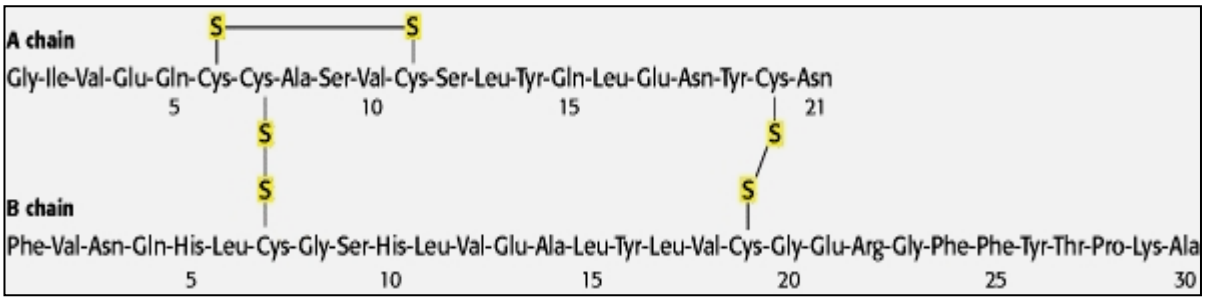

Figure 4-6: Primary structure of bovine insulin (Berg, Tymoczko and Stryer, 2002).

4.2 Materials and Methods

4.2.1 Chemicals and reagents

Human insulin, recombinant, expressed in yeast (12643, Pcode 1001188651, CAS: 11061-68-0), insulin from bovine pancreas (15500, CAS: 11070-73-8), fluorescein isothiocyanate isomer I (F-7250, CAS: 3326-32-7) were purchased from Sigma-Aldrich (St. Louis, MO). NovoRapid® , Actrapid® and Levemir® manufactured by Novo Nordisk, Apidra® and Lantus® by Sanofi-Aventis, Humalog® and Humulin® R manufactured by Eli Lilly were used. HPLC grade acetonitrile, trifluoroacetic acid, acetone, NaOH, HCl and buffer salts were purchased from Fischer Chemicals (Loughborough, UK). Ethylenediaminetetra-acetic acid disodium salt was from Hopkins & Williams and phenol, *m*-cresol were purchased from Sigma Aldrich. Distilled water was used throughout.

4.2.2 Synthesis of FITC-insulin conjugates

The FITC-insulin conjugate synthesis protocol was as presented below;

4.2.2.1 Preparation of 0.1M potassium phosphate buffer with 0.2M EDTA

1.07g dipotassium hydrogen phosphate (K_2HPO_4) and 0.52g of potassium dihydrogen phosphate (KH_2PO_4) were dissolved in ~50 mL distilled water and 0.2M EDTA was added. After dissolution of EDTA the volume was made up to 100 mL with distilled water. The pH of the buffer was adjusted to 7.0 with either 0.1M NaOH or 0.1M HCl.

For FITC-insulin conjugate synthesis in the presence of phenol or *m*-cresol, 0.4% w/v phenol or 0.25% w/v *m*-cresol were added to the 0.1M potassium phosphate buffer with 0.2M EDTA and the pH of the buffer was adjusted to 7.0 with either 0.1M NaOH or 0.1M HCl.

4.2.2.2 Preparation of human insulin/bovine insulin solution

A 10mg/mL human insulin/bovine insulin solution (5 mL) was prepared. Human insulin/bovine insulin was dissolved in hydrochloric acid (50mg in 10 drops of 0.1M HCl). About 4 mL of 0.1M phosphate buffer containing 0.2M EDTA was added resulting in a cloudy solution, followed by drops of 1M NaOH using a 1mL syringe until a clear solution was obtained. Buffer was added to just below the 5 mL mark and the pH was adjusted to 7.0 with acid or alkali.

4.2.2.3 Preparation of FITC solution

A 5 mg/mL solution of FITC in acetone was prepared just before use and protected from light, by covering in foil and kept in dark until use.

4.2.2.4 Method for FITC-insulin conjugation

Insulin solutions/ clinically used insulin preparations volume equivalent to 50 mg human insulin/ bovine insulin/insulin analogue was labelled with FITC using a 3 moles to 1 mole(FITC: insulin) ratio. Based on insulin/insulin analogue molecular weight and FITC molecular weight (389.39 Da), for a 3:1 molar FITC: insulin ratio, the quantity of FITC required was calculated. The calculated quantity of FITC solution (5 mg/mL) was added drop wise to the human insulin solution/insulin preparation, the pH of the solution was adjusted to 7.0, and the solution was protected from light and allowed to mix on a magnetic stirrer at room temperature for required reaction time. The quantities of FITC (5 mg/ml) solution used for insulin solution/insulin preparation are as detailed below.

Human insulin solution

Based on human insulin (5807.57 Da) and FITC (389.39 Da) molecular weight, 10.06 mg of FITC (2.01 mL of 5 mg/ml solution) was required for 5 mL (10mg/mL) human insulin solution.

Bovine insulin solution

Based on bovine insulin (5733.5 Da) and FITC (389.39 Da) molecular weight, 10.19 mg of FITC (2.04 mL of 5 mg/ml solution) was required for 5 mL (10 mg/mL) bovine insulin solution.

Short-acting insulin

Humulin®R U-500 and Actrapid® U-100

Based on human insulin (5807.57 Da) and FITC (389.39 Da) molecular weight, 10.06 mg of FITC (2.01 mL of 5 mg/ml solution) was required for 2.87 ml of Humulin®R U-500 and 14.33 mL of Actrapid® U-100

Rapid-acting insulin

NovoRapid® U-100

Based on insulin aspart (5825.8 Da) and FITC (389.39 Da) molecular weight, 10.03 mg of FITC (2.01 mL of 5 mg/ml solution) was required for 14.29 mL of NovoRapid® U-100

Apidra® U-100

Based on insulin glulisine (5823 Da) and FITC (389.39 Da) molecular weight, 10.03 mg of FITC (2.01 mL of 5 mg/ml solution) was required for 14.33 mL of Apidra® U-100.

Humalog® U-100

Based on insulin lispro (5808 Da) and FITC (389.39 Da) molecular weight, 10.06 mg of FITC (2.01 mL of 5 mg/ml solution) was required for 14.33 mL of Humalog® U-100.

Long-acting insulin

Levemir® U-100

Based on insulin determir (5916.9 Da) and FITC (389.39 Da) molecular weight, 9.87 mg of FITC (1.97 mL of 5 mg/ml solution) was required for 3.52 mL of *Levemir®* U-100.

Lantus® U-100

Based on insulin glargine (6063 Da) and FITC (389.39 Da) molecular weight, 9.63 mg of FITC (1.93 mL of 5mg/ml solution) was required for 13.74 mL of Lantus® U-100.

4.2.3 Separation of FITC-Insulin conjugate produced:

The FITC-insulin conjugate synthesised was separated by gel permeation chromatography (GPC) using Buchii apparatus chromatography pump B-688, peak detector B-686, fraction collector B-684 and a gel permeation column. The GPC column was a borosilicate plastic-glass column containing Sephadex ™ G25 (bead size: dry 50-150 µm and wet 86-258 µm). Sephadex ™ G25 is a cross-linked dextran which minimises nonspecific adsorption and gives high recoveries when used in group separations to remove small molecules or free labels from larger protein molecules.

Sephadex ™ G25 which was supplied as a dry powder was first swollen before use by adding sufficient distilled water to cover the surface of the powder and then allowed to stand at room temperature for 3 hrs. The Sephadex ™ G25 slurry was resuspended and poured into the column in one continuous motion to prevent introduction of any air bubbles. Sephadex ™ G25 was packed by passing distilled water at 10 mL/min until the bed had reached a constant height. The column adapter was locked in position on the gel bed surface and packing was continued until the gel bed was stable. The column was equilibrated first with distilled water for at least 2 hrs before use. A sample volume of up to 20 was injected for separation. The flow rate for elution was maintained at 10 mL/min. Between separation runs, the column was rinsed with 0.1M acetic acid and then equilibrated with distilled water before re-use.

After the required reaction time, the FITC-insulin conjugation mixture was injected into the gel permeation column and the fractions separated were collected. As shown in

Figure 4-7 two distinct bands visible on the column were collected separately. The first band collected should be the larger molecules of FITC-insulin conjugates and second band should be the smaller unreacted FITC molecules.

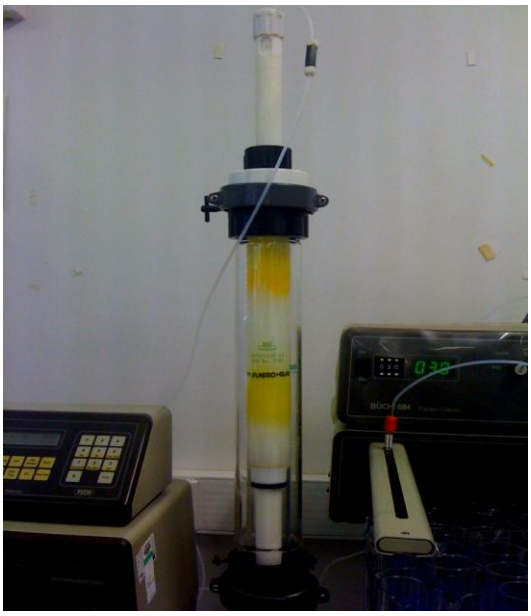

Figure 4-7: Figure showing bands (corresponding to FITC-insulin conjugates and FITC molecules) separated using gel permeation chromatography.

4.2.4 Analytical procedures for identification of FITC-insulin conjugates synthesised

The FITC-Insulin conjugate bands collected following GPC were analysed using reversed phase high performance liquid chromatography (RP-HPLC) and mass spectrometry (MS) to identify the species produced and confirm the absence of any unreacted FITC in the FITC-insulin conjugate band.

RP-HPLC chromatographic analyses

The RP-HPLC chromatographic analyses were performed using a Shimadzu Prominence HPLC system consisting of an in-line DGU-20AS Prominence degasser,

LC-20AD Prominence quaternary pump, SIL-20A Prominence auto sampler, CTO-20AC Prominence column oven and SPD-M20A Prominence diode array detector. A Luna (3 µ) C18(2), 150 x 4.60 mm column from Phenomenex, Cheshire UK was used for the separation preceded by a 0.5mm in-line filter and a widepore C18, 4 × 3 mm guard column. Elution was achieved using a gradient method with a flow rate of 1.0 mL/min, a column temperature of 40°C and sample injection of 20µl. The following gradient was used in HPLC determinations: 0-15 min (85% to 65%A), 15-25 min (65% to 35%A), and 25-32 min (35%A) where A was mobile phase A: 0.1% trifluoroacetic acid (TFA) in distilled water and B was mobile phase B: 90% acetonitrile/ 10% water/0.1% TFA.

The sampling was performed by SIL-20A Prominence autosampler and the sample volume used throughout was 20µL. The peaks were monitored by fluorescence detection where the excitation and emission wavelengths were set at 494 and 518nm, respectively. The Photo Diode Array (PDA) detector was also set to scan from 190 to 400nm and had a channel set at 215 nm to detect presence of unlabelled native insulin.

This RP-HPLC method for identification of FITC-insulin conjugates has been validated and the results are as presented in **Chapter 3**.

MS analyses

MS to determine the mass of the FITC-insulin conjugates produced was performed using a Thermofisher LTQ Orbitrap XL (a high resolution instrument giving accurate mass measurement over the mass range: m/z 50–2000 or m/z 200–4000) using the nanospray ionisation mode (NSI) at the EPSRC National Mass Spectrometry Facility, Swansea University.

The NSI mode is a low energy process creating very few fragments and yields positive and negative mass spectra with typical positive ions $[M + H]^+$, $[M + Na]^+$, $[M + nH]^{n+}$ and negative ions $[M - H]^-$, $[M + X]^-$ produced. The solvent used for sample preparation was a mixture of water/1:1 water: methanol + 0.1% formic acid. Hence the ions being produced may contain sodium (Na, m wt: 22.99 Da, formic acid (CH_2O_2, 46.03 Da) or methanol (MeOH, CH_4O, 32.04 Da). Samples were infused into the source of the mass spectrometer using a syringe pump at a flow rate of 10 µL/min. Analyses

were performed in the positive ion detection mode. Scans were acquired over a range of m/z 50–2000 or m/z 200–4000.

4.3 Results and discussion

4.3.1 Synthesis of FITC-insulin conjugates using human insulin

As discussed in **Section 4.1.2** the insulin binding sites involving residues A1,A13, A21,B12, B17 and B-chain residues B20-B30 play a crucial role in the binding of insulin to insulin receptors. The objective of the synthesis was to produce the B1 mono-labelled FITC-insulin conjugate, which has an equivalent biological activity to native insulin. Human insulin from Sigma Aldrich was thus labelled with FITC using the synthesis method described in **Section 4.2.2**.

The RP-HPLC chromatogram for FITC, **Figure 4-8**, show the peaks at retention times (Rt) 13 min, 16 min, 24 min and 28 min. The absence of these peaks in a synthesised product would confirm the removal of all unreacted FITC from the reaction.

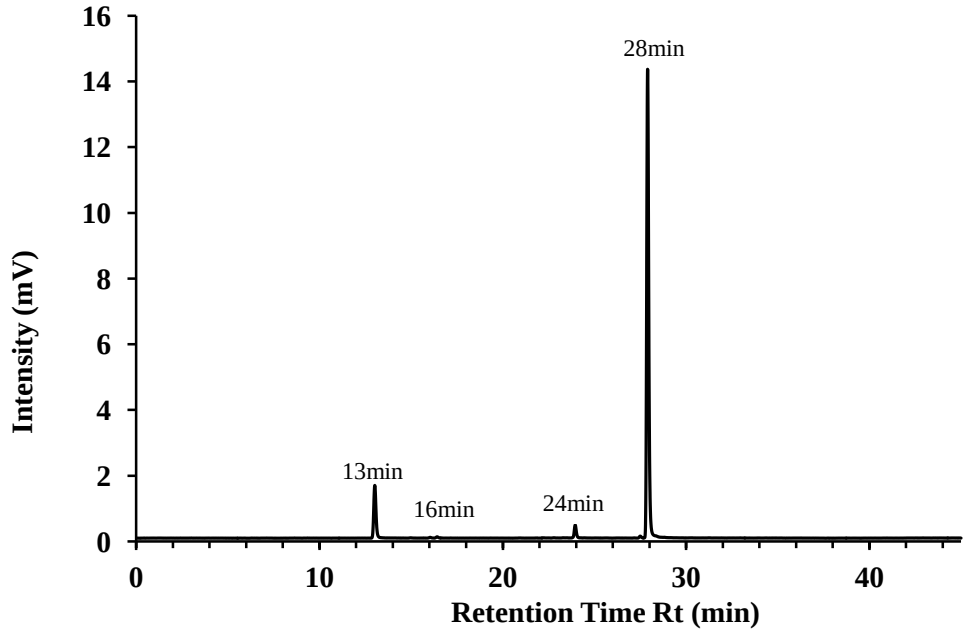

Figure 4-8: RP-HPLC fluorescence chromatogram of FITC showing peaks at Rt 13 min, 16 min, 24 min and 28 min.

The HPLC fluorescence chromatograms were checked for no unreacted FITC present. The PDA chromatograms were checked for any unlabelled native insulin, insulin peak appears at Rt 20.5 min on the PDA as shown in **Figure 4-9** for human insulin solution.

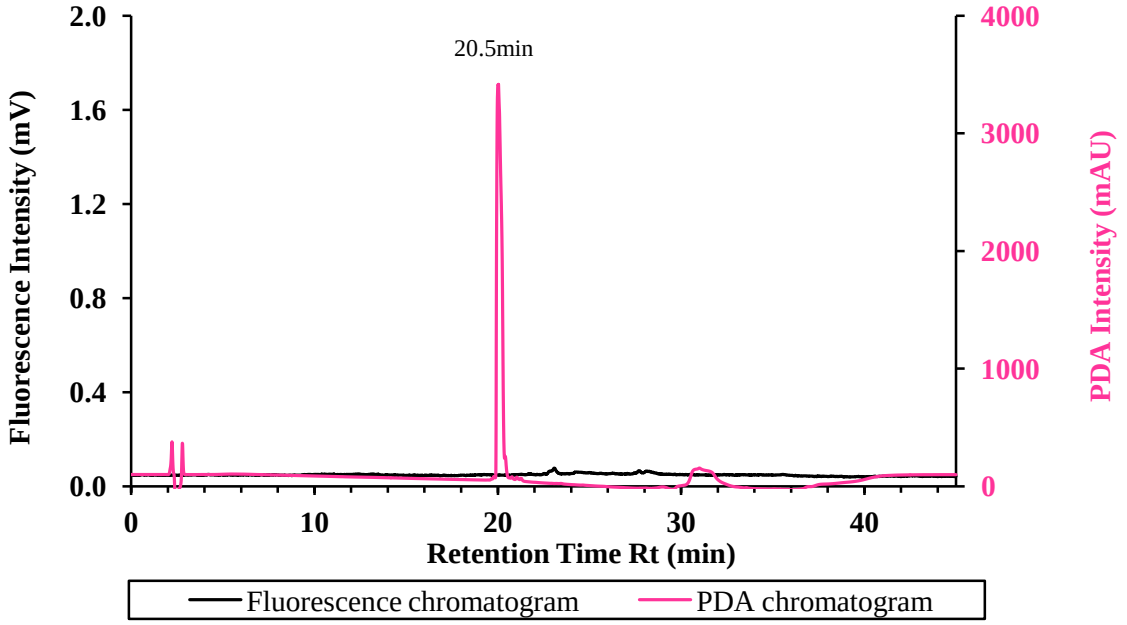

Figure 4-9: RP- HPLC fluorescence chromatogram and PDA UV chromatogram (showing peak at Rt 20.5 min) for Human insulin solution.

4.3.1.1 Effect of reaction time

The FITC-insulin conjugation reactions were monitored at different time intervals by RP-HPLC over a 45-hrs period. As shown in **Table 4-4** and **Figure 4-10** reaction time of 1 hr and 2 hrs produced predominantly mono-labelled conjugate (Rt 21.8 min) and as the reaction time increased over 45 hrs more di-labelled FITC- insulin conjugate (second peak, Rt 22.5 min) was produced with the appearance of tri-labelled conjugate (a third peak, Rt 23.5 min) after 20 hrs reaction time. The switch in ratio in favour of more di-labelled FITC-insulin conjugate produced occurs between reaction times 9 and 20 hrs. There was unlabelled native insulin present up to 5 hrs, suggesting that it is not long enough for all the insulin molecules present to be labelled with FITC.

Table 4-4: RP-HPLC area % of FITC-insulin conjugates formed at retention times over a period of 45 hrs.

Reaction time (hrs)	**Area (%)**			**Unlabelled native insulin (Rt 20.5 min on PDA)**
	Mono-labelled (Rt 21.8 min)	**Di-labelled (Rt 22.5 min)**	**Tri-labelled (Rt 23.5 min)**	
1	89	9	none	yes
2	57	36	none	yes
5	77	23	none	yes
9	61	39	none	no
20	36	62	none	no
22	22	74	3	no
25	11	80	5	no
45	6	79	9	no
Note: Instances where area % is not equal to 100% are due to small unresolved peaks present on the chromatogram.				

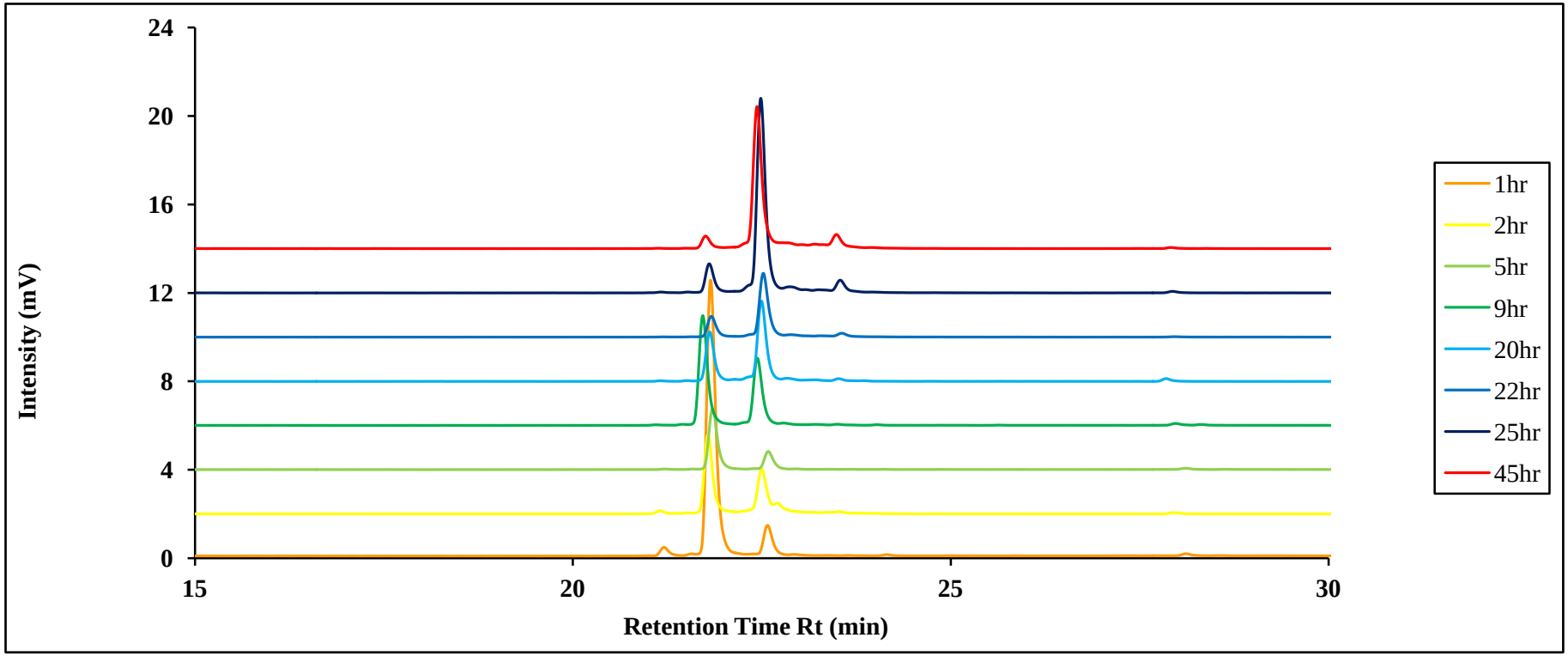

Figure 4-10: RP-HPLC fluorescence chromatograms of FITC-insulin conjugates produced at reaction times over a period of 45 hrs.

Using the mass spectra for the reaction times 1 hr and 45 hrs where predominantly one conjugate species (recognised by retention time) was produced it is possible to identify the conjugates. The RP-HPLC fluorescence and PDA chromatograms for FITC-insulin conjugates produced after reaction times of 1 hr and 45 hr are presented in **Figure 4-11** and **Figure 4-12**. The mass spectra and corresponding molecular mass for conjugates produced were compared against the theoretical molecular mass for FITC-insulin conjugate species as presented in **Table 4-5** and their identities ascertained. **Figure 4-13**, **Figure 4-14** and **Figure 4-15** show the mass spectra (full scan) for reaction times 1 hr, 5hrs and 45 hrs. Raw MS data is available from EPSRC UK National Mass Spectrometry Facility, Swansea University. The molecular mass of the conjugates produced after reaction times 1 hr, 5 hrs and 45 hrs are as presented in **Table 4-6**.

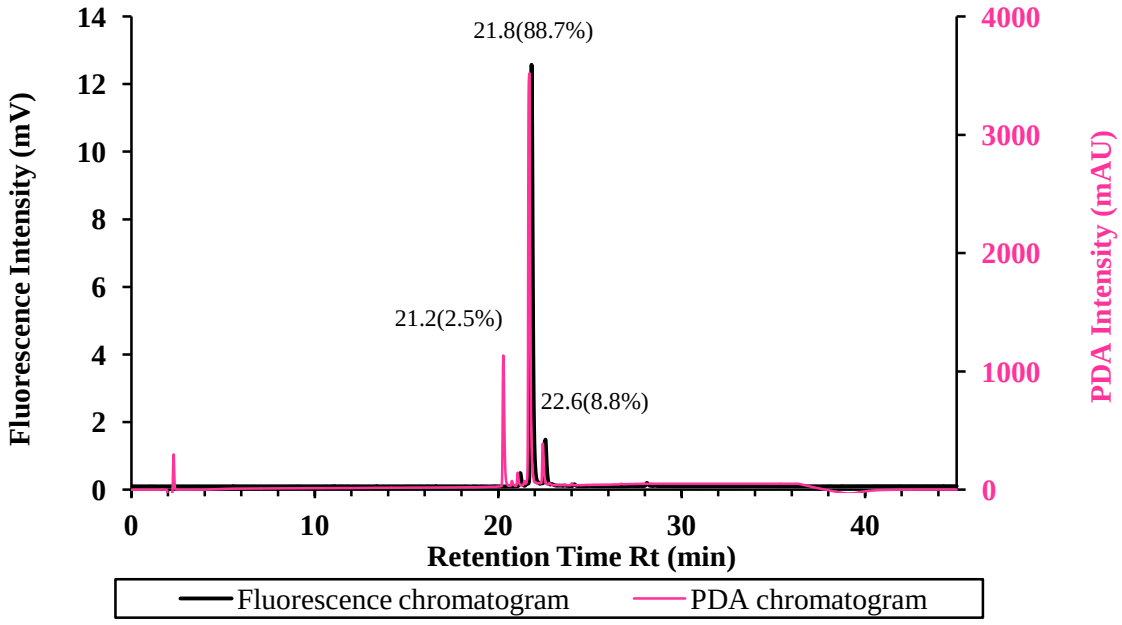

Figure 4-11: RP- HPLC fluorescence chromatogram (showing peaks with Rt (%Area)) and PDA UV chromatogram (showing peak at Rt 20.5 min) for FITC-insulin conjugates produced after a reaction time of 1 hr.

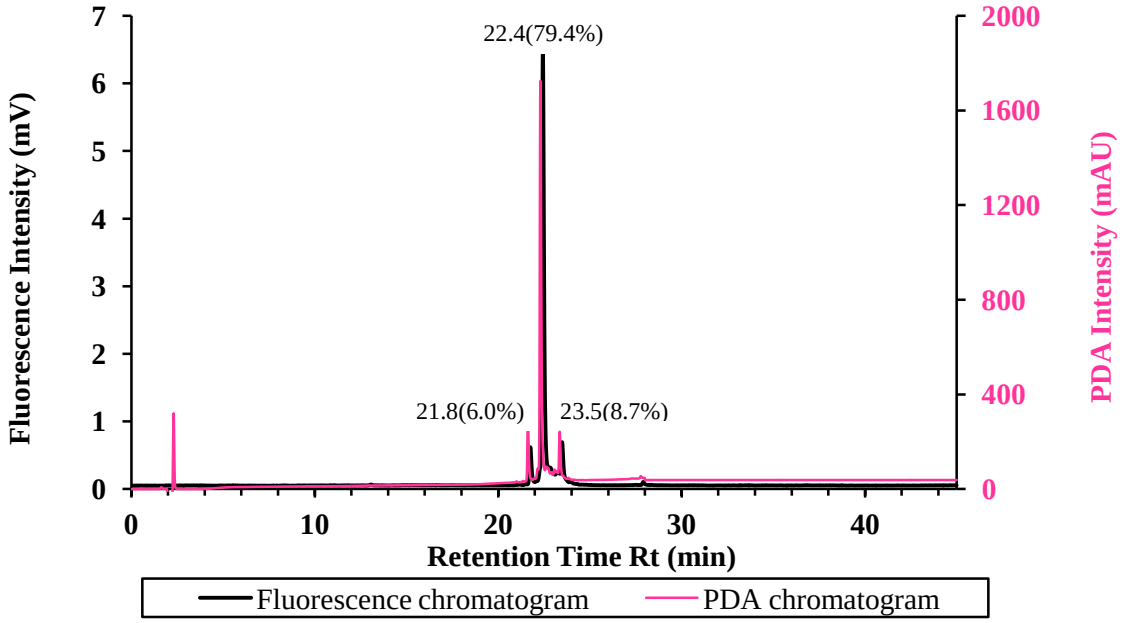

Figure 4-12: RP- HPLC fluorescence chromatogram (showing peaks with Rt(%Area)) and PDA detector UV chromatogram (no peak at Rt 20.5 min showing absence of unlabelled native insulin) for FITC-insulin conjugates produced after a reaction time of 45 hrs.

Table 4-5: Theoretical molecular mass of FITC-insulin conjugate species and their identity.

No of FITC labels	Theoretical mass M (Da)	Identity of conjugate
0	**5807.6**	**Insulin**
1	**6197.0**	**A1 or B1 FITC-insulin conjugate (Mono-labelled)**
2	**6586.3**	**A1B1 FITC-insulin conjugate (Di-labelled)**
3	**6975.7**	**A1B1B29 FITC-insulin conjugate (Tri-labelled)**

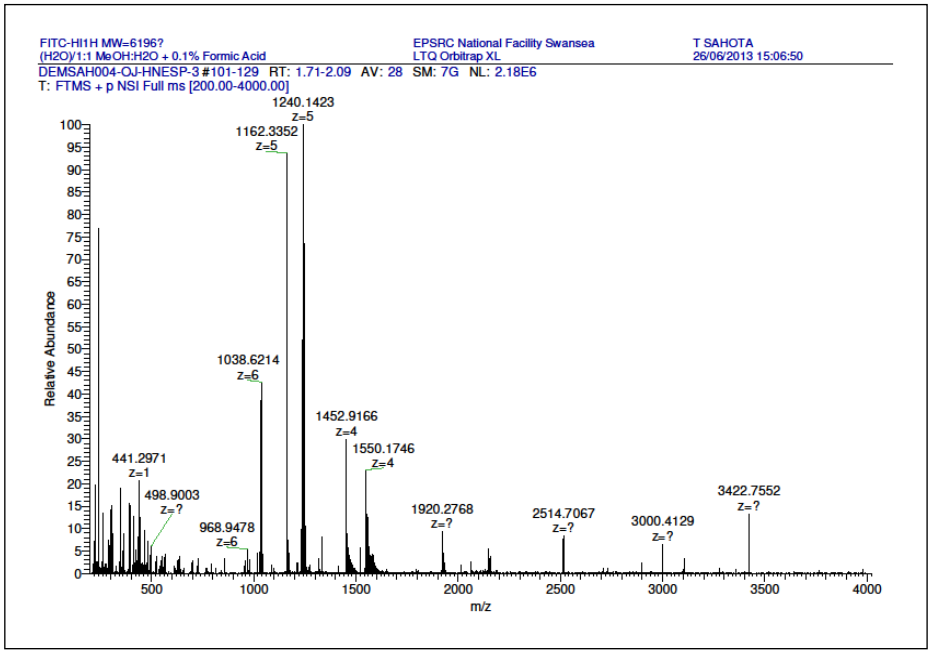

Figure 4-13: Mass spectra data for FITC-insulin conjugates produced after reaction time of 1 hr (peaks present in raw data at m/z 1317.7478, z5 corresponding to di-labelled conjugate not labelled in spectra)

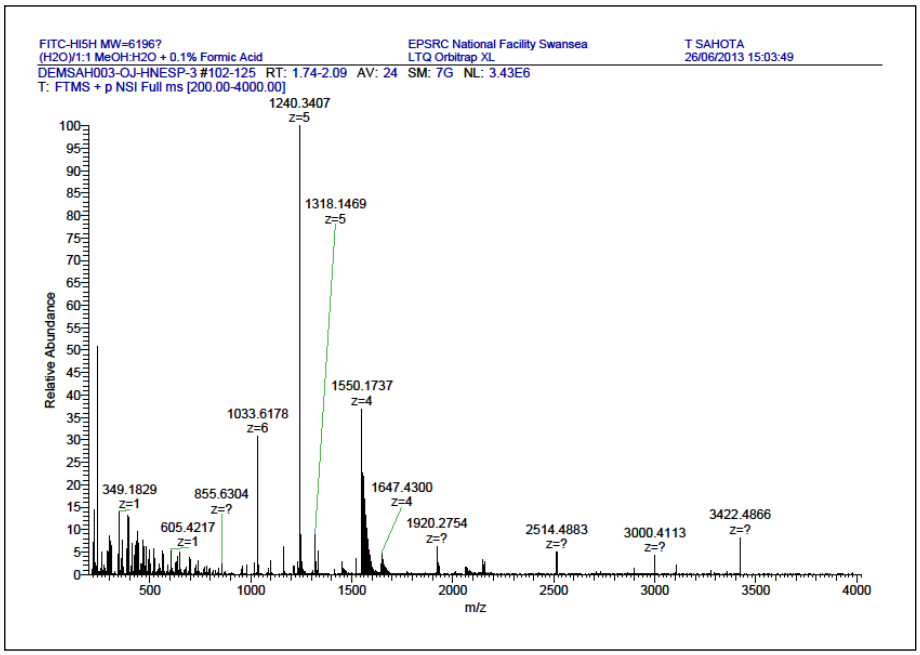

Figure 4-14: Mass spectra data for FITC-insulin conjugates produced after reaction time of 5 hr (peaks present in raw data at m/z 1162.5338 z5 and 1452.6644 z4 corresponding to unlabelled human insulin; peak at m/z 1098.6242 z6 corresponding to di-labelled conjugate not labelled in spectra).

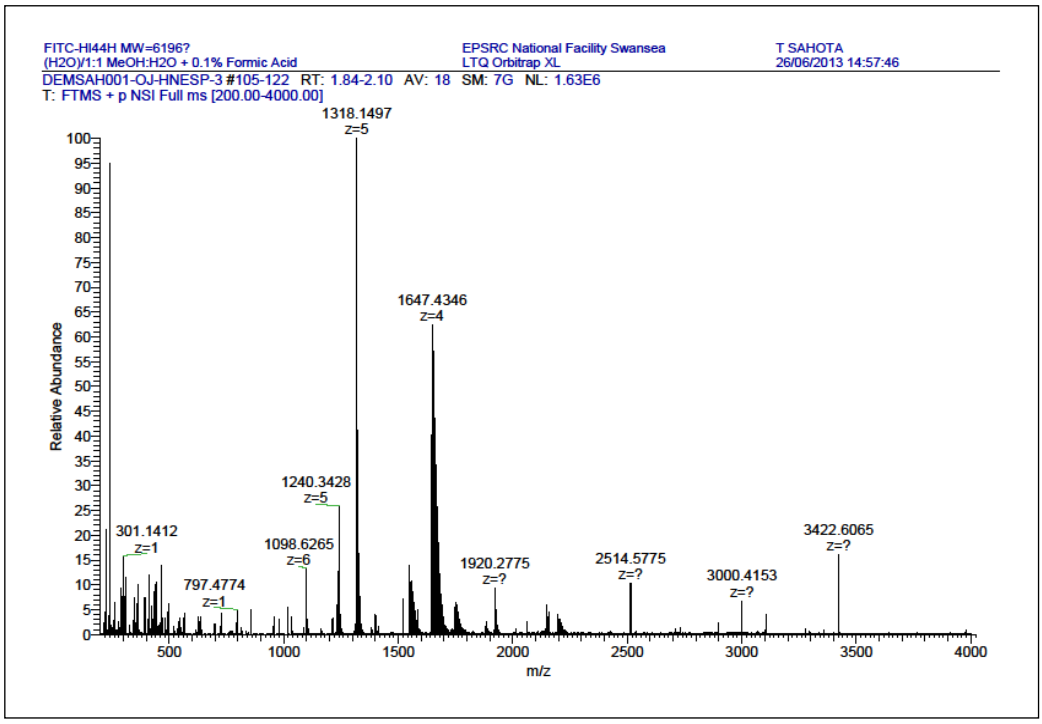

Figure 4-15: Mass spectra data for FITC-insulin conjugates produced after reaction time of 45 hrs (peak present in raw data at m/z 1549.9247 z4 corresponding to mono-labelled conjugate; peaks at m/z 1395.9559 z5 and 1750.1864 z4 corresponding to tri-labelled conjugate not labelled in spectra).

Table 4-6: Fluorescence chromatogram peaks, corresponding mass spectra data and identification of FITC-insulin conjugates produced after reaction times of 1 hr, 5 hrs and 45 hrs (key: M - mass, H - hydrogen, MeOH – methanol, Na - sodium, PDA – Photo Diode Array detector).

Reaction Time	**Chromatogram peaks Rt (min) (Area %)**	**Theoretical mass M (Da)(# FITC)**	**Molecular mass of conjugate ions produced (Da)**	**Identity of conjugates**
1 hr	20.5 (PDA)	5807.6 (0)	5813.7 $[M+6H]^{6+}$ 5811.7 $[M+5H]^{5+}$ & $[M+4H]^{4+}$	Unlabelled native human insulin
	21.8 (88.7%)	6197.0 (1)	6231.7$[M+MeOH+5H]^{6+}$ 6200.7$[M+5H]^{5+}$ & $[M+4H]^{4+}$	Mono-labelled
	22.6 (8.8%)	6586.3 (2)	6588.7 $[M+5H]^{5+}$	Di-labelled (trace)
	-	6975.7 (3)	-	-
5 hrs	20.5 (PDA)	5807.6 (0)	5812.7 $[M+5H]^{5+}$ 5810.7 $[M+4H]^{4+}$	Unlabelled native human insulin (trace)
	21.8 (77.1%)	6197.0 (1)	6201.7 $[M+6H]^{6+}$ & $[M+5H]^{5+}$ 6200.7 $[M+4H]^{4+}$	Mono-labelled
	22.6 (22.8%)	6586.3 (2)	6591.7 $[M+6H]^{6+}$ 6590.7 $[M+5H]^{5+}$ 6589.7 $[M+4H]^{4+}$	Di-labelled
	-	6975.7 (3)	-	-
45 hrs	-	5807.6 (0)	-	-
	21.8 (6.0%)	6197.0 (1)	6201.7 $[M+5H]^{5+}$ 6199.7 $[M+4H]^{4+}$	Mono-labelled
	22.4 (79.4%)	6586.3 (2)	6591.8 $[M+6H]^{6+}$ 6590.7 $[M+5H]^{5+}$ 6589.7 $[M+4H]^{4+}$	Di-labelled
	23.5 (8.7%)	6975.7 (3)	6979.8 $[M+5H]^{5+}$ 7000.7 $[M+Na+3H]^{4+}$	Tri-labelled

As shown in **Table 4-6**, from the chromatogram peaks and corresponding mass spectra for the reaction times 1 hr, 5 hrs and 45 hrs it was possible to identity the FITC-Insulin conjugate species produced. The chromatogram and mass spectra for the product produced after reaction time of 1 hr shows that predominantly mono-labelled conjugate (89%) was produced with very little di-labelled (9%), it also contained unlabelled native insulin. At a reaction time of 5hrs mono-labelled (77%) and di-labelled (23%) conjugates and trace unlabelled native insulin were present. At 45 hrs reaction time very little mono-labelled (6%), predominantly di-labelled conjugate (79%) and small amount

of tri-labelled conjugate (9%) (absent in the previous reactions) was produced. No unlabelled native insulin was observed. Thus the chromatogram peaks with retention time of Rt 21.8 min shows presence of mono-labelled conjugates, Rt 22.5 min shows presence of di-labelled and retention time of Rt 23.5 min shows presence of tri-labelled FITC-insulin conjugates and PDA peak at Rt 20.5 min shows presence of unlabelled native insulin.

It was observed that it was possible to produce predominantly mono-labelled insulin with short reaction times, however there always was unlabelled native insulin present. Also, from the chromatogram and mass spectra it couldn't be ascertained if the mono-labelled conjugate was A1 or B1 substituted. In order to locate the exact positions where FITC were attached, a *Staphylococcus aureous* digestion of the separated/isolated conjugates as described by Hentz et al would need to be employed. Also, a biological test, an autophosphorylation assay using insulin receptor would aid in confirming the activity of the conjugates produced. These are however outside the remit of the work carried out here.

For the purposes of the *in vitro* experiments it was more important to know the size of the FITC-insulin conjugate produced and the presence of any undesired unlabelled native insulin. Reaction time of 25 hrs was selected for production of FITC-insulin; refer to **Figure 4-16** and **Table 4-7**; here predominantly di-labelled FITC-insulin conjugate (over 75%) was produced with the absence of any unlabelled native insulin. Increasing the reaction time over this period showed no change in the amount of di-labelled conjugate produced as seen in **Table 4-4**.

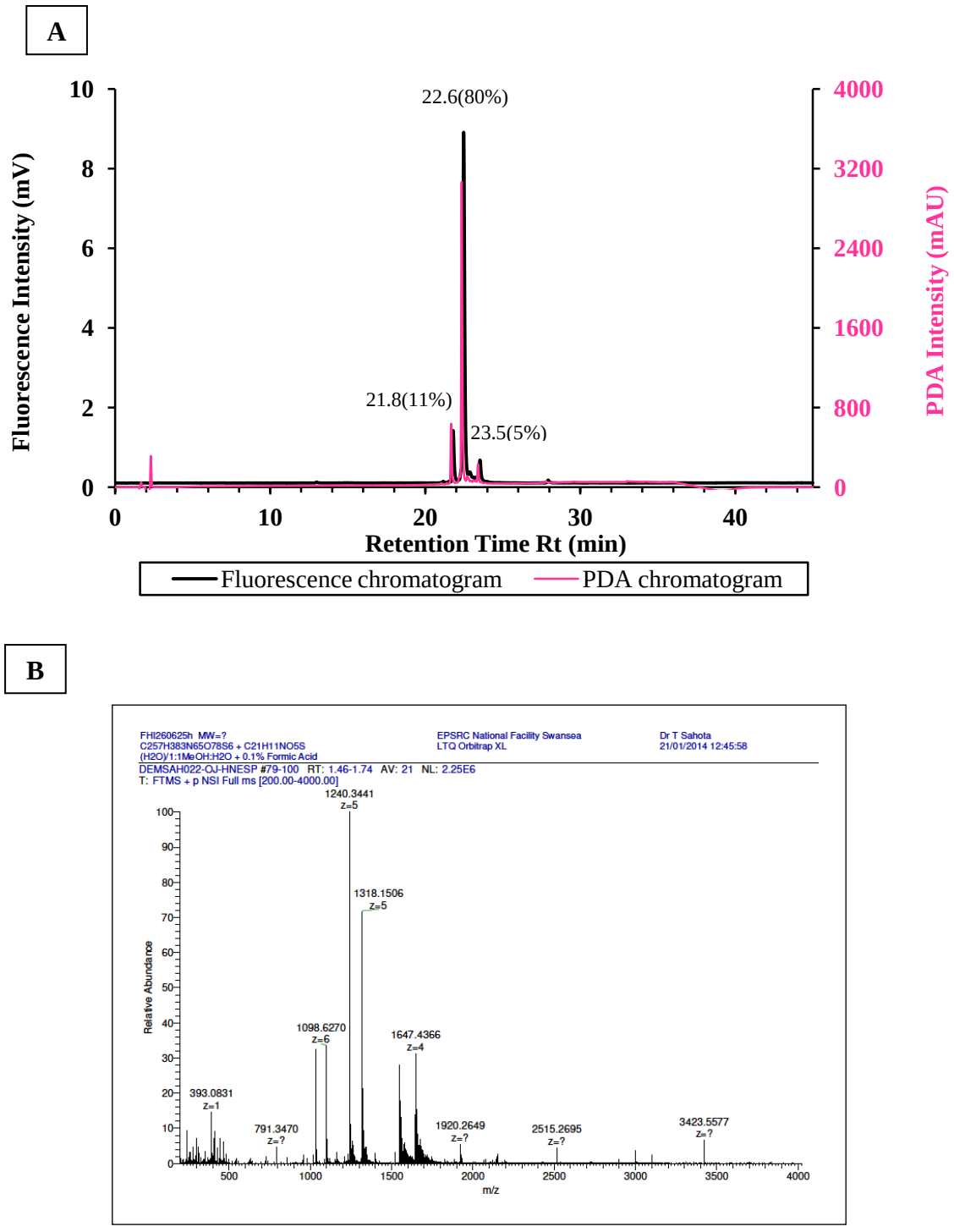

Figure 4-16: A: RP- HPLC fluorescence chromatogram (showing peaks with Rt (%Area) and PDA detector UV chromatogram (no peak at Rt 20.5 min showing absence of unlabelled native insulin) and **B**: mass spectrum of FITC-insulin conjugates produced after a reaction time of 25 hrs (peak present in raw data at m/z 1550.1785 z4 corresponding to mono-labelled conjugate; peak at m/z 1163.4662 z6 corresponding to tri-labelled conjugate not labelled in spectra).

Table 4-7: Fluorescence chromatogram peaks, corresponding mass spectra data and identification of FITC-insulin conjugates produced after a reaction period of 25 hrs.

Chromatogram peaks Rt (min) (area %)	Theoretical mass M(Da) (# FITC)	Molecular mass of conjugate ions produced (Da)	Identity of FITC-insulin conjugates
21.8 (11)	6197.0 (1)	6202.7 $[M+6H]^{6+}$ 6201.7 $[M+5H]^{5+}$ 6200.7 $[M+4H]^{4+}$	Mono-labelled
22.6 (80)	6586.4 (2)	6591.8 $[M+6H]^{6+}$ 6590.8 $[M+5H]^{5+}$ 6589.7$[M+4H]^{4+}$	Di-labelled
23.5 (5)	6975.8 (3)	6980.8 $[M+6H]^{6+}$	Tri-labelled

4.3.1.2 Effect of phenol and *m*-cresol

In order to understand the effect of phenolic compounds on the FITC-insulin conjugates produced in the absence of zinc, phenol or *m*-cresol was included in the reaction solution and the FITC-insulin conjugates produced were investigated. **Table 4-8** presents the FITC-insulin conjugates synthesised with and without phenol or *m*-cresol at reaction time of 2 hrs.

Table 4-8: FITC-insulin conjugates produced with and without phenol or *m*-cresol.

Reaction time (2 hrs)	Without Rt (min) (Area %)	With Rt (min) (Area %)	Identity of conjugates
Phenol	20.5 (PDA)	20.5 (PDA)	Unlabelled native insulin
	21.8 (57)	21.8 (47)	Mono-labelled
	22.5 (36)	22.5 (53)	Di-labelled
	22.7(8%)	-	-
***m*-cresol**	20.5 (PDA)	20.5 (PDA)	Unlabelled native insulin
	21.8 (57)	21.8 (46)	Mono-labelled
	22.5 (36)	22.5 (54)	Di-labelled
	22.7(8%)	-	-

There appears to be a 10% decrease in the amount of mono-labelled conjugate and an increase in di-labelled conjugate produced in presence of phenol or *m*-cresol. The presence of phenolic compounds, which aid the stable R-state of insulin monomer where the B1-B8 segment residues are extended and thus making the B1 residue in an

extended position, seems to have contributed to the increase in the di-labelled conjugate produced.

In the FITC-insulin synthesis method used for synthesising FITC-insulin conjugates, zinc was removed by chelating with EDTA, thus dissociating the hexamer structure and the method does not include any phenolic compounds. These results thus show that in the presence of phenol or *m*-cresol, where the zinc ions have been removed, as would be in the case with all the conjugates produced using commercially available insulin preparations as well, there is an expectation of a small noticeable decrease in mono-labelled FITC-insulin conjugate produced in comparison to if phenol or *m*-cresol were absent.

4.3.2 Synthesis of FITC-insulin conjugates using clinically used insulin injections

A set of commercially available insulin preparations, containing different insulin analogues were fluorescently labelled using the synthesis method described in **Section 4.2.2**. Short-acting human insulin analogues (Humulin®R and Actrapid®), rapid-acting monomeric insulin analogues [NovoRapid® (insulin aspart), Apidra® (insulin glulisine), Humalog® (insulin lispro)], and long-acting hexameric insulin analogues [Levemir® (insulin determir), Lantus® (insulin glargine)] were labelled with FITC and the conjugates produced identified.

Short-acting insulin

The FITC-insulin conjugates synthesised using Humulin® R and Actrapid® after 2 hrs and 20 hrs reaction times are as presented in **Table 4-9**. The corresponding mass spectra are presented in **Appendix 2 Figure A2-1** to **Figure A2-4**. The short-acting insulin analogues in Humulin® R and Actrapid® are structurally similar to natural human insulin (and the human insulin used) hence similar conjugates are expected to be produced, however here the effect of the various formulation excipients present in the commercial preparation (as described in **Table 4-1**) on the FITC-insulin conjugates produced can be examined. As expected, similar FITC-insulin conjugates were

produced using Humulin® R and Actrapid® as with human insulin (refer to **Table 4-4**). For Humulin® R after 2 hrs reaction (no EDTA was added), 82% mono-labelled FITC-insulin conjugate and at 20 hrs similar amounts were produced compared to when human insulin was used, the formulation excipients present namely, glycerine, *m*-cresol and zinc oxide (though EDTA was added) suggest to play a role in aiding more mono-labelled conjugate synthesis at 2 hrs reaction time. Actrapid® however shows increased amounts of mono-labelled conjugate synthesised at 2 hrs (95%) and 20hr (59%) compared to when human insulin was used. The increased amounts of mono-labelled conjugates produced using Actrapid even in comparison to Humulin® R where similar formulation excipients were present suggest that the factor contributing to this could be that the human insulin (rys) in Actrapid is synthesised using a yeast species *Saccharomyces cerevisiae* instead of *Escherichia coli* bacteria as for Humulin R.

Table 4-9: Fluorescence chromatogram peaks, corresponding mass spectra data and identification of FITC-insulin conjugates synthesised using commercially available short-acting insulin preparations.

Reaction Time	RP-HPLC peaks Rt (min) (area %)	Theoretical mass (Da) (#FITC)	Molecular mass of conjugates (Da) [ions]	Identity of conjugates
Humulin® R (human insulin)				
2 hrs*	20.5 (PDA)	5807.6 (0)	5812.7 $[M+6H]^{6+}$ 5811.7 $[M+5H]^{5+}$ 5810.7 $[M+4H]^{4+}$	Unlabelled human insulin
	21.8 (82)	6197 (1)	6226.7$[M+Na+7H]^{7+}$ 6202.7$[M+6H]^{6+}$ 6201.7$[M+5H]^{5+}$ 6200.7$[M+4H]^{4+}$ 6199.7$[M+3H]^{3+}$ 12400.4$[2M+7H]^{7+}$	Mono-labelled
	22.6 (14)	6586.3 (2)	6591.8$[M+6H]^{6+}$ 6590.7$[M+5H]^{5+}$ 6589.7$[M+4H]^{4+}$	Di-labelled
	-	6975.7 (3)	-	-
20 hrs	-	5807.6 (0)	-	-
	21.8 (34)	6197 (1)	6202.7$[M+6H]^{6+}$ 6201.7$[M+5H]^{5+}$ 6200.7$[M+4H]^{4+}$	Mono-labelled
	22.5 (55)	6586.3 (2)	6591.8$[M+6H]^{6+}$ 6590.8$[M+5H]^{5+}$ 6589.7$[M+4H]^{4+}$	Di-labelled
	23.6 (4)	6975.7 (3)	6980.8$[M+6H]^{6+}$ 6979.8$[M+5H]^{5+}$	Tri-labelled
Actrapid® (human insulin(rys))				
2 hrs	20.5 (PDA)	5807.6 (0)	5812.7 $[M+6H]^{6+}$ 5811.7 $[M+5H]^{5+}$ 5810.7 $[M+4H]^{4+}$ 5809.7 $[M+3H]^{3+}$	Unlabelled human insulin
	21.8 (95)	6197 (1)	6202.7$[M+6H]^{6+}$ 6201.7$[M+5H]^{5+}$ 6200.7$[M+4H]^{4+}$ 6198.7 $[M+3H]^{3+}$ 12401.4$[2M+7H]^{7+}$	Mono-labelled
	22.5 (4)	6586.3 (2)	20048.5$[3(4Na+M)+13H]^{10+}$	Di-labelled
	-	6975.7 (3)	-	-
20 hrs	-	5807.6 (0)	-	-
	21.9 (59)	6197 (1)	6201.7$[M+6H]^{6+}$ &$[M+5H]^{5+}$ 6199.7$[M+4H]^{4+}$	Mono-labelled
	22.6 (40)	6586.3 (2)	6592.8$[M+6H]^{6+}$ 6590.8$[M+5H]^{5+}$ 6589.7$[M+4H]^{4+}$	Di-labelled
	23.6 (0.9)	6975.7 (3)	-	Tri-labelled
Note: * No EDTA was added for the 2hr reaction in error.				

Rapid-acting insulin

The rapid-acting insulin, NovoRapid® (insulin aspart), Apidra® (insulin glulisine), Humalog® (insulin lispro) have amino acid replacements at B28, B3 & B29 and B28 & B29 respectively aimed at accelerating hexamer disassembly and thus facilitating rapid absorption. The method used here for fluorescent labelling of insulin produces fluorescent conjugates labelled at amino acid residues at A1, B1 and B29 sites, therefore it was of interest to see which conjugates are produced here especially for insulin glulisine and insulin lispro where the amino acid at B29, lysine has been replaced by glutamic acid and proline respectively. Though, lysine is still present at B3 and B28 for insulin glulisine and insulin lispro, respectively.

The FITC-insulin conjugates synthesised using NovoRapid®, Apidra®, Humalog® after 2 hrs and 20 hrs reaction times are as presented in **Table 4-10**. The corresponding mass spectra are presented in **Appendix 2 Figure A2-5** to **Figure A2-9.** The FITC-insulin conjugates produced using NovoRapid® show that similar conjugates as when human insulin was used were synthesised and the presence of unlabelled insulin aspart (for 2 hr reaction time). However, it shows increased amounts, 77% at 2 hrs and 47% at 20 hrs of mono-labelled FITC-insulin aspart conjugate compared to when human insulin was used. Insulin aspart has B28 proline replaced by aspartic acid, to achieve electrostatic repulsion at the dimer interface to weaken the tendency to associate into dimers and hexamers. Comparison of crystal structures with native insulin have shown a local distortion of the dimer interface associated with absence of B28 proline, thus highlighting the importance of its absence (Berenson et al., 2011). The increased amounts of mono-labelled conjugate observed when insulin aspart was used could be associated with change in conformation of insulin aspart monomer which results in it reduced ability to associate into dimers and hexamers.

Insulin glulisine in Apidra® has decreased zinc-free self-association tendency achieved by B3 asparagine substitution by lysine and B29 lysine substitution by glutamic acid. It shows similar conjugates synthesised as those obtained with human insulin (refer to **Table 4-4**) and the presence of unlabelled insulin glulisine (for 2 hr reaction time). The substitutions seem to promote the synthesis of more mono-labelled FITC-insulin glulisine conjugate at 2 hrs (81%) and at 20hrs (60%).

The FITC-insulin lispro conjugates produced using Humalog® after 2 hr and 20 hr reaction times are same and in similar amounts as those obtained with human insulin (refer to **Table 4-4**), this could be because the amino acid sequence at B28 (lysine) and B29 (proline) for insulin lispro has not been replaced but just swapped.

Table 4-10: Fluorescence chromatogram peaks, corresponding mass spectra data and identification of FITC-insulin conjugates synthesised using commercially available rapid-acting insulin preparations.

Reaction Time	**RP-HPLC peaks Rt(min)(area %)**	**Theoretical mass (Da) (#FITC)**	**Molecular mass of conjugates (Da) [ions]**	**Identity of conjugates**
NovoRapid® (insulin aspart)				
2 hrs	20.5 (PDA)	5825.8 (0)	5829.7 $[M+5H]^{5+}$ 5828.7 $[M+4H]^{4+}$	Unlabelled insulin aspart
	21.7 (77)	6215.2 (1)	6219.7 $[M+5H]^{5+}$ 6218.7 $[M+4H]^{4+}$	Mono-labelled
	22.5 (14)	6604.6 (2)	6608.7 $[M+5H]^{5+}$	Di-labelled
	-	6993.9 (3)	-	-
20 hrs	-	5825.8 (0)	-	-
	21.75 (47)	6215.2 (1)	6220.7 $[M+6H]^{6+}$ 6219.7 $[M+5H]^{5+}$ 6218.7 $[M+4H]^{4+}$	Mono-labelled
	22.5 (53)	6604.6 (2)	6609.7 $[M+6H]^{6+}$ 6608.7 $[M+5H]^{5+}$ 6607.7 $[M+4H]^{4+}$	Di-labelled
	-	6993.9 (3)	-	-
APIDRA® (insulin glulisine)				
2 hrs	20.5 (PDA)	5823 (0)	5828.7 $[M+5H]^{5+}$	Unlabelled insulin glulisine
	21.7 (81)	6212.4 (1)	6216.7 $[M+5H]^{5+}$ 6215.7 $[M+4H]^{4+}$ 12429.4 $[2M+7H]^{7+}$	Mono-labelled
	22.4 (9)	6601.8 (2)	-	Di-labelled*
	-	6991.1 (3)	-	-
20 hrs	-	5823 (0)	-	-
	21.7 (60)	6212.4 (1)	6216.7 $[M+6H]^{6+}$ 6216.7 $[M+5H]^{5+}$ 6215.7 $[M+4H]^{4+}$	Mono-labelled
	22.4 (40)	6601.8 (2)	6606.8 $[M+6H]^{6+}$ 6605.8 $[M+5H]^{5+}$ 6604.7 $[M+4H]^{4+}$	Di-labelled
	Trace	6991.1 (3)	7020.8 $[M+Na+6H]^{6+}$ 6995.8 $[M+5H]^{5+}$	Tri-labelled
HUMALOG® (insulin lispro)				

2 hrs	20.5 (PDA)	5807.6 (0)	5811.7 $[M+5H]^{5+}$	Unlabelled insulin lispro
	21.8 (59)	6197 (1)	6202.7 $[M+6H]^{6+}$ 6201.7 $[M+5H]^{5+}$ 6200.7 $[M+4H]^{4+}$ 6199.7 $[M+3H]^{3+}$ 12399.4 $[2M+7H]^{7+}$	Mono-labelled
	22.6 (34)	6586.4 (2)	6590.8 $[M+5H]^{5+}$ 6589.7 $[M+4H]^{4+}$	Di-labelled
	23.4 (0.5)	6975.8 (3)	None detected	Trace tri-labelled
20 hrs"	-	5807.6 (0)	-	-
	21.8 (27)	6197 (1)	-	Mono-labelled
	22.5 (67)	6586.4 (2)	-	Di-labelled
	-	6975.8 (3)	-	-
Note: * APIDRA® 2hrs reaction time di-labelled conjugate identified based on chromatogram peak Rt. " HUMALOG® 20 hrs reaction time – no mass spectra available, hence conjugates identified based on chromatogram peak Rt.				

Long-acting insulin

The FITC-insulin conjugates synthesised using Levemir® (insulin determir) and Lantus® (insulin glargine) after 20 hrs reaction time are as presented in **Table 4-11**. The corresponding mass spectra for FITC-insulin conjugates synthesised using Levemir® after 20 hrs reaction time is presented in **Appendix 2 Figure A2-10.** Both these insulin analogues have modifications to their B chain B29 and B30 region to impart their long-acting effects and as described earlier this region plays a very important role in receptor binding and hence its biological activity.

Insulin determir contains a fatty acyl group on B29 Lysine which has reversible albumin binding tendency thereby providing a circulating depot and enhances the stability of the modified insulin hexamers (Havelund et al., 2004), (Whittingham et al., 2004). FITC-insulin determir conjugates produced after 20hrs reaction time were mono-labelled (15%) and di-labelled (82%) conjugates species based on their mass spectra results; their retention times seemed to have shifted by 5min. There was no tri-labelled conjugate species produced as expected due to the fatty acyl group substitution at B29.

Insulin glargine molecule differs from human insulin in that the A21 asparagine is replaced with glycine and has 2 arginines attached to the C-terminus of the B-chain that results in the isoelectric point shift of the solution to neutrality thus resulting in formation of microprecipitates at the injection depot aiding protracted absorption. The

Lantus® preparation is at pH 4 and it has very low solubility at neutral pH. It was very difficult to follow the synthesis method where the reaction needed to be carried out at pH 7; hence the reaction was carried out at a higher pH much above its neutral isoelectric point where the reaction solution was clear. The chromatogram results for reaction time of 20 hrs show two peaks which could be mono-labelled conjugate with a combined 92% and very low (2%) of di-labelled conjugate.

Table 4-11: Fluorescence chromatogram peaks, corresponding mass spectra data and identification of FITC-insulin conjugates synthesised using commercially available long-acting insulin preparations.

Reaction Time	RP-HPLC peaks Rt (min) (area %)	Theoretical mass (Da) (#FITC)	Molecular mass of conjugates (Da) [ions]	Identity of conjugates
Levemir® (insulin determir)				
20 hrs	-	5916.9 (0)	-	-
	26.7 (15%) 27.1 (1%)	6306.3 (1)	6310.9 $[M+5H]^{5+}$ 6309.9 $[M+4H]^{4+}$	Mono-labelled
	27.4 (82%)	6695.7 (2)	6699.9 $[M+5H]^{5+}$ 6698.9 $[M+4H]^{4+}$	Di-labelled
	-	7085 (3)	-	-
LANTUS® (insulin glargine)				
20 hrs*	-	6063 (0)	-	-
	21.3 (33%) 21.8 (59%)	6452.4 (1)	-	Mono-labelled
	22.3 (~1%)	6841.8 (2)	-	-
	22.7 (2%)	7231.1 (3)	-	Di-labelled
Note: * LANTUS® 20 hrs reaction time – no mass spectra available, conjugates identified based on chromatogram peak Rt.				

4.3.3 Comparison to FITC-insulin products (synthesised by Sigma Aldrich)

FITC-bovine insulin and FITC-human insulin synthesised by Sigma Aldrich were analysed to determine the conjugates present. Their RP-HPLC chromatograms and mass spectra are as presented in **Figure 4-17** and **Figure 4-18** and their corresponding mass spectra data, chromatogram peaks and conjugate identity are presented in **Table 4-12** .

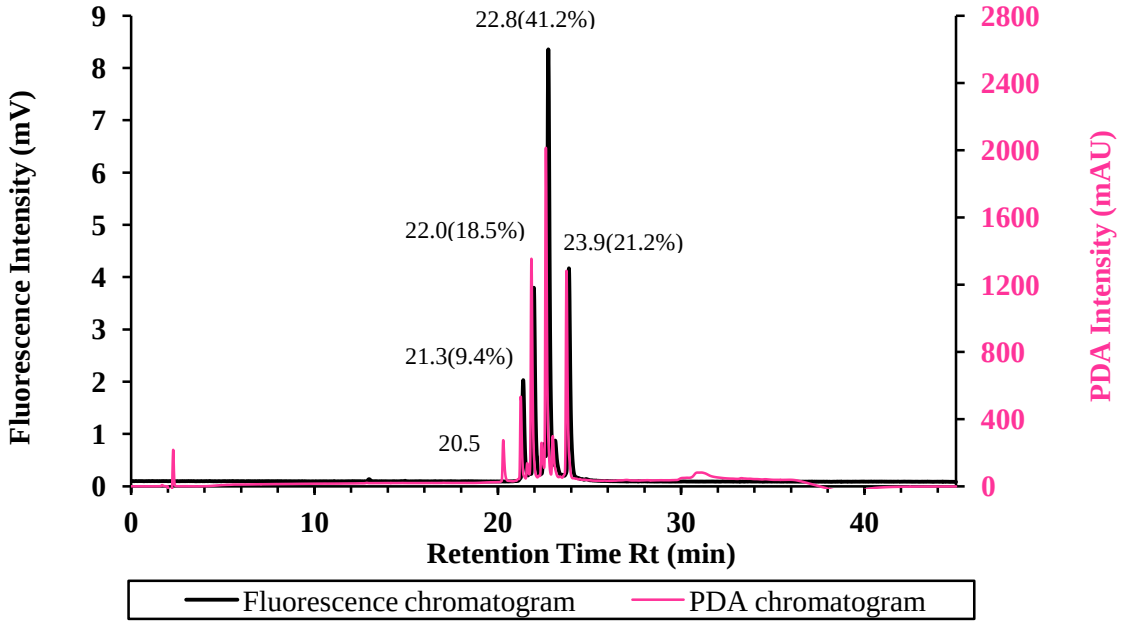

Figure 4-17: RP- HPLC fluorescence chromatogram (showing peaks with Rt(%Area)) and PDA detector UV chromatogram (showing presence of a peak at Rt 20.5 min) for Sigma FITC- bovine insulin.

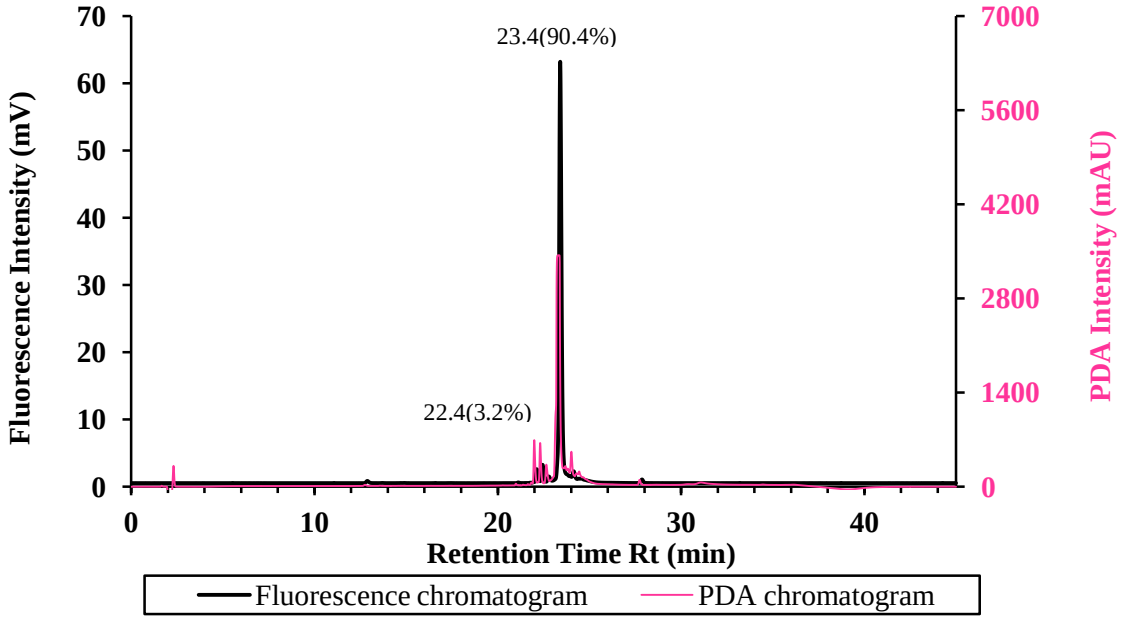

Figure 4-18: RP- HPLC fluorescence chromatogram (showing peaks with Rt(%Area)) and PDA detector UV chromatogram (showing absence of a peak at Rt 20.5 min) for Sigma FITC- human insulin.

Table 4-12: Fluorescence chromatogram peaks, corresponding mass spectra data and identification of FITC-insulin conjugates present in commercially available FITC-insulin products.

Chromatogram peaks Rt (min) (Area %)	Theoretical mass (Da) (# FITC)	Molecular mass of conjugates produced (Da) [ions]	Identity of conjugates formed
FITC-bovine insulin (Sigma)			
20.5 (PDA)	5733.5 (0)	5737.6 $[M+5H]^{5+}$ & $[M+4H]^{4+}$	Bovine insulin
22.0 (18.5)	6122.9 (1)	6126.7 $[M+5H]^{5+}$ 6125.7 $[M+4H]^{4+}$	Mono-labelled
22.8 (41.2)	6512.3 (2)	6516.7 $[M+6H]^{6+}$ & $[M+5H]^{5+}$ 6515.7 $[M+4H]^{4+}$	Di-labelled
-	6901.6 (3)	-	-
FITC-human insulin (Sigma)			
-	5807.6 (0)	-	-
-	6197 (1)	-	-
22.4 (3.2)	6586.4 (2)	6590.8 $[M+6H]^{6+}$ & $[M+5H]^{5+}$ 6589.7 $[M+4H]^{4+}$	Di-labelled
23.4 (90.4)	6975.8 (3)	6980.8 $[M+6H]^{6+}$ & $[M+5H]^{5+}$ 6978.8 $[M+4H]^{4+}$	Tri-labelled

FITC-bovine insulin (synthesised by Sigma Aldrich) show that a number of different conjugates are present. Table with all the chromatographic peaks are presented in **Appendix 2 Table A2-1**. The conjugates present were compared with FITC-bovine insulin conjugates synthesised in-house with a reaction time of 20 hrs. The corresponding chromatogram peaks and mass spectra data are presented in **Figure 4-19**, and **Table 4-13**, respectively. The FITC-bovine insulin (synthesised in-house) showed the usual number of peaks and absence of any unlabelled bovine insulin. The FITC-bovine insulin conjugates (synthesised by Sigma Aldrich) were identified based on their Rt and mass spectra results. The Rt for these peaks were found to be slightly higher than the in-house synthesised conjugates. The product also shows presence of unlabelled bovine insulin and a number of unidentified peaks. Mass spectra for FITC-bovine insulin (synthesised by Sigma Aldrich) and FITC-bovine insulin (synthesised in-house) are presented in **Appendix 2 Figure A2-11** and **Figure A2-13**, respectively.

Chromatogram for FITC-human insulin product (synthesised by Sigma Aldrich) show a number of small peaks, the peaks associated with Rt 12.9 min, 24.1 min and 27.9 min indicate presence of unreacted FITC in the product. The product shows one predominant peak at 23.4 min (90%) which can be confirmed as tri-labelled FITC-insulin conjugate (which is the most biologically inactive species as studied by Hentz et al) based on its corresponding mass spectra data. It shows presence of di-labelled conjugate about 3%. The product did not contain any unlabelled human insulin. Table with all the chromatographic peaks and mass spectra for Sigma FITC-human insulin product are presented in **Appendix 2 Table A2-2 and Figure A2-12**.

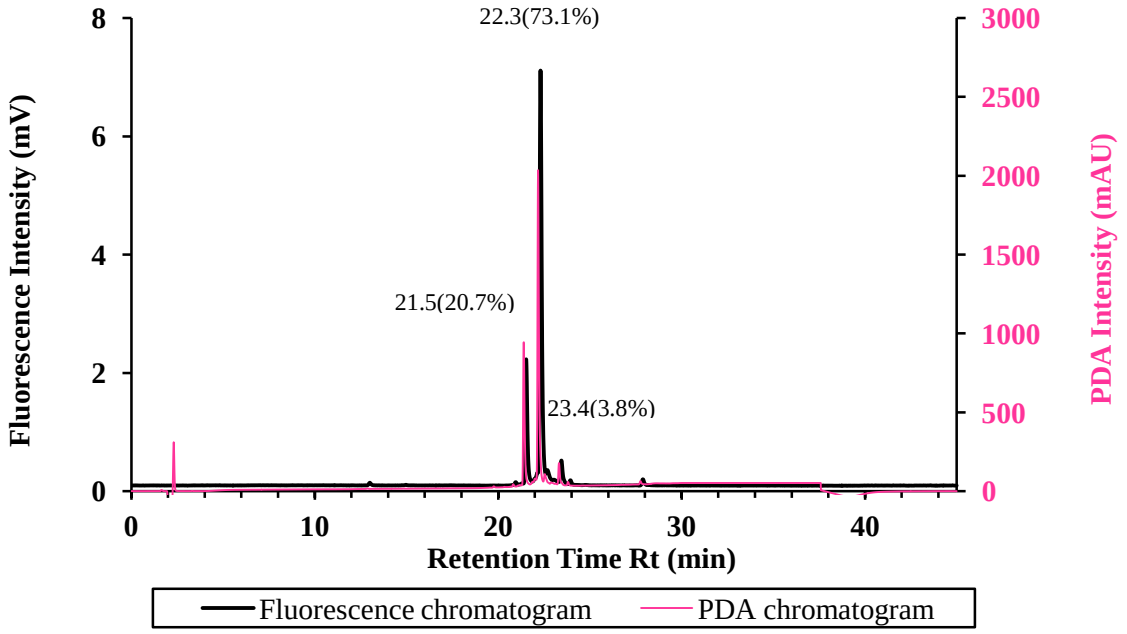

Figure 4-19: RP- HPLC fluorescence chromatogram (showing peaks with Rt (%Area)) and PDA detector UV chromatogram (showing absence of a peak at Rt 20.5 min) for FITC- bovine insulin (synthesised in-house).

Table 4-13: Fluorescence chromatogram peaks, corresponding mass spectra data and identification of FITC-insulin conjugates synthesised using bovine insulin (Note: the small chromatogram peak associated with Rt 23.4 (3.8%) is most probably Tri-labelled conjugate, this was not picked up by the mass spectra).

Chromatogram peaks Rt (min) (Area %)	Theoretical mass (Da) (# FITC)	Molecular mass of conjugates produced (Da) [ions]	Identity of conjugates
-	5733.5 (0)	-	-
21.5 (20.7)	6122.9 (1)	6128.7 $[M+6H]^{6+}$ 6126.7 $[M+5H]^{5+}$ & $[M+4H]^{4+}$	Mono labelled
22.3 (73.1)	6512.3 (2)	6517.7 $[M+6H]^{6+}$ 6516.7 $[M+5H]^{5+}$ 6515.7 $[M+4H]^{4+}$	Di-labelled
23.4 (3.8)	6901.6 (3)	-	-

4.4 Chapter summary

In this project FITC-labelled insulin was used for *in vitro* diffusion experiments as a tool to improve analytical quantification and detection to understand release profiles from the closed loop insulin delivery device. Commercially available FITC-insulin products are very expensive and as substantial amounts were needed for experiments it was synthesized in-house.

The synthesis protocol based on work by Hentz et al was used to produce the B1 mono-labelled FITC-insulin conjugate, which has been shown by them to have equivalent biological activity as native unlabelled insulin. The following are the findings and achievements;

- Mono-labelled FITC-insulin conjugate (A1 or B1) was successfully produced using human insulin at short reaction times (up to 5 hrs) however the product always contained some unlabelled native human insulin. This suggested that 5hrs wasn't long enough for labelling all the insulin molecules.
- As the reaction time was increased over a period of 45 hrs more di-labelled FITC-insulin conjugate (A1B1) was produced than mono-labelled conjugate with the appearance of tri-labelled conjugate (A1B1B29) after 20 hrs reaction time. The quantities switch from mono-labelled to di-labelled FITC-insulin conjugate between reaction times 9 and 20 hrs.

- For the purposes of the in-vitro experiments it was more important to know the size of the FITC-insulin conjugate produced and presence of any unlabelled native insulin was undesirable. Hence, reaction time of 25 hrs was selected for production of FITC-insulin where predominantly di-labelled FITC-insulin conjugate (over 75%) was produced with the absence of any unlabelled native insulin. Increasing the reaction time over this period showed no change in the amount of di-labelled conjugate produced.
- To determine the identity of the mono-labelled FITC-insulin conjugate (A1 or B1 labelled) produced at short reaction times further biological studies to separate and isolate the conjugates and confirm their biological activity would be needed. These are however outside the remit of the work carried out here.
- In the presence of phenol or *m*-cresol, there appears to be a 10% decrease in the amount of mono-labelled conjugate and an increase in di-labelled conjugate produced. This observation could be attributed to the fact that phenolic compounds aid the stable R-state of insulin monomer in which the B1 residue is in an extended form and is more readily available for labelling. Thus in commercially available insulin preparations which usually contain phenolic compounds, there is an expectation of a small noticeable decrease in mono-labelled FITC-insulin conjugate produced in comparison to if phenol or *m*-cresol were absent.
- Clinically used insulin analogues present in commercially available preparations were successfully fluorescently labelled for future biological and *in vitro* applications in tracing and receptor binding studies.
    - The short-acting insulin analogues in Humulin® R and Actrapid®, which are structurally similar to native human insulin after 2 hrs and 20 hrs reaction times produced similar conjugates as with human insulin as expected. Humulin® R after 2 hrs reaction produced higher amount, 82%, mono-labelled FITC-insulin conjugate compared to when human insulin (57%) was used and at 20 hrs similar amounts to human insulin (36%) were produced. The formulation excipients present namely, glycerine, *m*-cresol and zinc oxide (though EDTA was added) suggest to play a role in aiding more mono-labelled conjugate synthesised at the 2 hrs reaction time. Actrapid® however shows increased amounts of mono-labelled conjugate synthesised at 2 hrs (95%) and 20hr

(59%) compared to when human insulin was used, the increased amounts in comparison to Humulin® R where similar formulation excipients are present, suggest that the factor contributing to this could be that the human insulin (rys) in Actrapid® is synthesised using a yeast species *Saccharomyces cerevisiae* instead of Escherichia *coli* bacteria (used for Humulin® R).

- The rapid-acting insulin analogues in NovoRapid® (insulin aspart), Apidra® (insulin glulisine) and Humalog® (insulin lispro) all produced similar conjugates as with human insulin at 2hr and 20hr reaction times and had unlabelled insulin analogues present for 2hr reaction time. At 2hrs and 20hrs reaction times, insulin aspart and insulin glulisine showed increased amounts of mono-labelled FITC-insulin analogue conjugates produced compared to human insulin which could be due to the amino acid replacements at B28 and B3 & B29 respectively. Insulin lispro where the amino acid sequence at B28 and B29 has not been replaced but just swapped, produced similar amounts of conjugates after 2hrs and 20 hrs as those obtained with human insulin.
- The long-acting insulin analogues in Levemir® (insulin determir) and Lantus®(insulin glargine), both having modifications to their B chain B29 and B30 region were fluorescently labelled with 20 hrs reaction time. FITC-insulin determir conjugates synthesised at 20hrs reaction time were mono-labelled (15%) and di-labelled conjugates (82%). No tri-labelled conjugate was produced as expected due to the fatty acyl group substitution at B29. FITC-insulin glargine conjugates synthesised at 20hrs reaction time carried out at a higher pH than 7 produced two peaks which could be mono-labelled conjugates with a combined 92% and very low (2%) di-labelled conjugate.

- FITC-bovine insulin (synthesised by Sigma Aldrich) show that a number of different conjugates were present, including mono-labelled and di-labelled conjugate and also had unlabelled native bovine insulin which was undesirable.
- FITC-human insulin (synthesised by Sigma Aldrich) was found to contain some unreacted FITC, predominantly tri-labelled conjugate (which is biological inactive as studied by Hentz et al) and some di-labelled conjugate. It was thus hugely advantageous to synthesise FITC-insulin in-house with predominantly di-labelled conjugate and absence of unreacted FITC and native human insulin.

Chapter 5 Development of an experimental protocol for measuring diffusion.

5.1 Introduction

The study of molecular transport in solutions and across artificial or biological barriers ranging from simple diffusion and dissolution to complex *in vivo* pharmacokinetic investigations contributes towards understanding drug release mechanisms. This movement of molecules can be mathematically modelled and these descriptions can aid in the design of experiments and interpretation of data. In this chapter concepts of diffusion and drug transport relevant to the INsmart device are presented and the process followed in developing an experimental protocol to ultimately measure diffusion coefficient of insulin through the glucose responsive gel held in the device are discussed.

5.1.1 Diffusion

Movement of molecules in solution or molecular transport across barriers can be caused by migration or diffusion. Migration is caused by an external force, such as gravity, electrical fields or hydrodynamic flow that acts on each of the solute molecules. Diffusion is defined as a process of mass transfer of individual molecules of a solute, from one part of a system to another brought about by random thermal movement in solution in the presence of a concentration gradient. Transport by simple diffusion can be measured as flux (Brodin, Steffansen and Nielsen, 2009). The passage of molecules through a polymeric membrane may occur by simple molecular diffusion involving dissolution of the drug in the matrix of the membrane or also by the process of passage through solvent-filled pores or channels available between polymeric chains of a membrane which is influenced by the size of the permeating molecules and the diameter

of the pores. Molecular diffusion is a particularly convenient way of studying the diffusion process (Martin, 1993).

The study of simple diffusion or passive transport of solute molecules through liquids, solids and membranes is of considerable importance in pharmaceutical sciences and applies to a number of processes that form part of drug delivery such as dissolution of drugs from tablets, powders and granules; release from ointments and suppository bases; lyophilisation; ultra filtration and other mechanical processes. It also applies to passage of water vapour, gases, drugs and dosage form additives through coatings, packaging, films, plastic container walls, seals and caps, and permeation and distribution of drug molecules in living tissues (Martin, 1993). The most common biopharmaceutical use of diffusion flux studies is transport investigations of drug candidates across a barrier tissue, such as intestinal cell culture models or tissue models. It can also be advantageous in determining screening and selection criteria for candidate drug compound or to predict *in vivo* bioavailability of a given drug substance (Brodin, Steffansen and Nielsen, 2009).

5.1.2 The diffusion equations

The mathematical equation of heat conduction derived by Fourier in 1822 was adopted by Fick (1855) to put forward a quantitative basis for diffusion. The mathematical theory of diffusion is based on the hypothesis that the rate of transfer of diffusing molecules through a unit area of a section is proportional to the concentration gradient, as shown in **Equation 5-1**.

$$J = -D\frac{\partial C}{\partial x} \qquad \textbf{Equation 5-1}$$

Where J is the rate of transfer per unit area of section (flux); the units for which are g cm^{-2} sec^{-1}, C is the concentration of a diffusing molecules in g/cm^3, x is the space coordinate measured normal to the section in cm, and D denotes the diffusion coefficient (also called diffusivity) in cm^2/sec. D is defined as a constant that describes the velocity of diffusion and is related to the properties of a given molecule in a given solvent. The SI units of kilogram and meter are sometimes used and time may be given in hours, minutes or seconds. The negative sign in the equation signifies that diffusion

occurs in a direction opposite to that of increasing concentration. **Equation 5-1** is known as Fick's first law (Crank, 1975). In some cases as in dilute solutions, *D* can reasonably be taken as being constant, while in others such as high molecular weight polymers; it depends very markedly on concentration. *D* is also affected by temperature, pressure, solvent properties and the chemical nature of the diffusing solute.

Fick's second law emphasizes the mass transport, change in concentration with time at a definite location rather than the mass diffusing across a unit area of barrier in unit time (Martin, 1993). Fick's second law states that the change in concentration with time in a particular region is proportional to the change in the concentration gradient at that point in the system. Thus Fick's second law can be expressed as;

$$\frac{\partial C}{\partial t} = D\frac{\partial^2 C}{\partial x^2} \qquad \textbf{Equation 5-2}$$

Equation 5-2 represents diffusion only in the *x* direction. Fick's second law of diffusion represents solute concentration changes in three dimensions and can be expressed in the general form as **Equation 5-3**,

$$\frac{\partial C}{\partial t} = D\left(\frac{\partial^2 C}{\partial x^2} + \frac{\partial^2 C}{\partial y^2} + \frac{\partial^2 C}{\partial z^2}\right) \qquad \textbf{Equation 5-3}$$

Where *C* is the concentration of the diffusing solute; *t* denotes time, *D* is the diffusion coefficient and *x*, *y* and *z* are the three spatial (Cartesian) coordinates. This expression is not usually needed in pharmaceutical problems of diffusion, where movement in one direction is sufficient to describe most cases (Martin, 1993).

Steady State is an important condition in diffusion. Fick's first law, **Equation 5-1** gives the rates of diffusion through unit area i.e. flux in the steady state of flow. The second law, **Equation 5-3** on the other hand gives the change in solute concentration with time, at any distance i.e. a steady and nonsteady state of flow.

A number of different experimental methods have been used to measure diffusion coefficients with reasonable accuracy; however it is essential to understand and decide how these measurements will be made. Takeru Higuchi who is considered as the "father of mathematical modelling of drug release" derived his classical equation using the steady state approach. Drug release initially occurs only from the outermost layer(s)

(from one layer, if only one side of the film is exposed to the receptor medium; from two layers, if both sides of the film are exposed to the receptor medium) upon water penetration into the system. Initially the rate controlling membrane is completely free of drug. After an initial period of drug diffusing into the membrane, drug concentration gradients are built up within the membrane during early phase drug release. Based on maximum concentration gradient at the inner and outer membrane surface, steady state is reached where the release rate is constant and the cumulative amount of drug released can be calculated as a function of time. The extrapolation of the steady state straight line on the time-axis at $t =$"$l^2/(6D)$" gives lag-time which depends on the thickness of the release rate controlling barrier membrane and on the mobility of the drug within the membrane. The experimental measurement of these lag-times can be used to experimentally determine the diffusion coefficient of a drug in a specific barrier membrane (knowing the thickness of the membrane) (Siepmann and Peppas, 2011).

The Stokes diaphragm cell developed by Stokes et al in 1950 is considered as one of the best tools to understand diffusion in liquids or across membranes (Cussler, 2009). It consists of two compartments separated by either a glass frit or a porous membrane and is similar to the diffusion cell as shown in **Figure 5-1**. **Figure 5-1** shows a simple diffusion cell where the solute dissolved in solvent is present in left hand compartment of the cell i.e. donor compartment and solvent alone is placed on the right hand side of the barrier i.e. receptor compartment and the solute diffuses from the donor compartment through the central barrier or membrane to the receptor compartment. This is shown schematically in

Figure 5-2. In diffusion experiments, sink conditions i.e. very low solute concentration is maintained in the receptor compartment so that the concentration gradient driving diffusion remains constant.

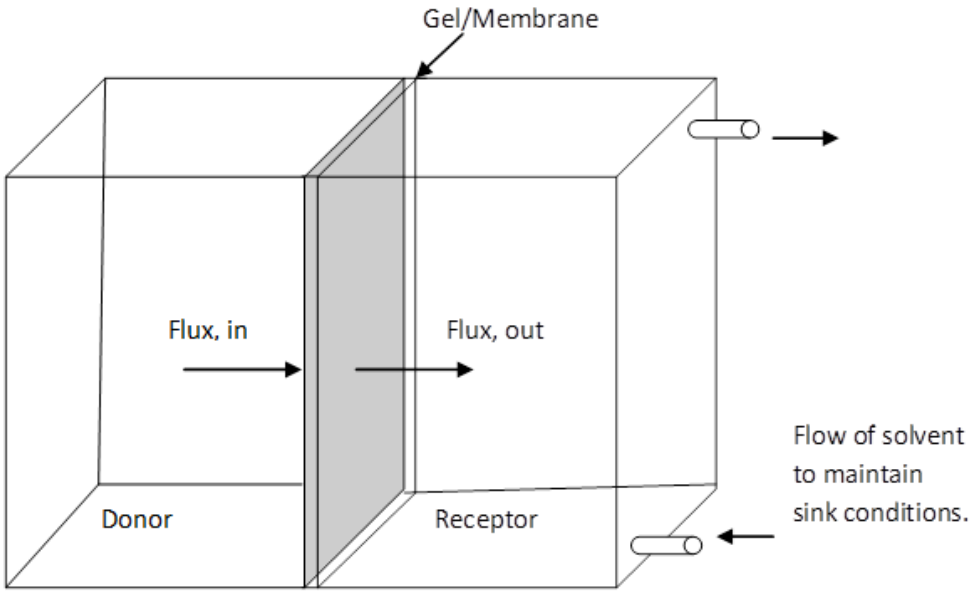

Figure 5-1: Typical set-up of a diffusion cell, donor compartment contains solute at concentration *C*.

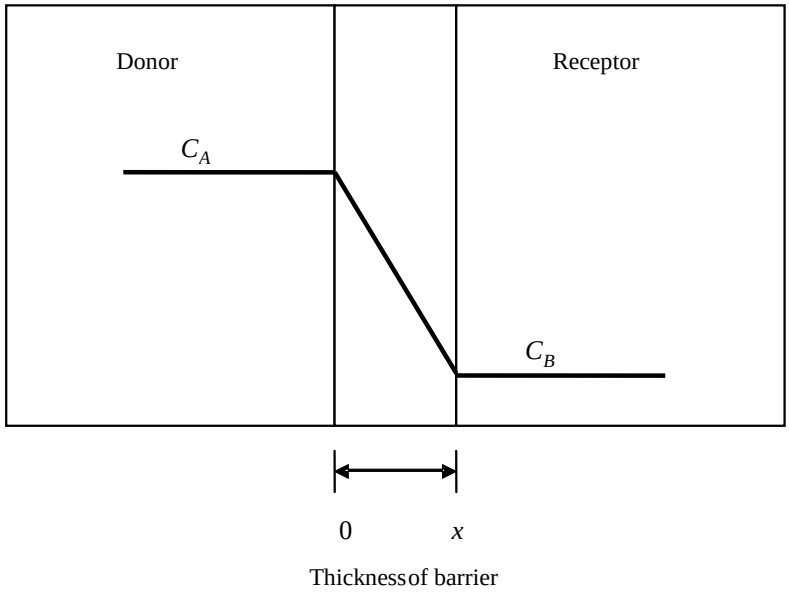

Figure 5-2: Schematic diagram showing concentration gradient of diffusing solute molecules across the diaphragm/gel of a diffusion cell.

The solute concentration will fall in the donor compartment of **Figure 5-1** and rise in the receptor compartment until the system comes to an equilibrium, based on the rate of removal of solute molecules from the sink and the nature of the barrier. If sink conditions are maintained wherein the solute concentration in the donor compartment is so high that the concentration gradient is equivalent to the solute concentration, then the concentration gradient across the two compartments remains constant over long periods of time sufficient to cover experimental measurements. Then within each diffusional slice perpendicular to the direction of flow, the rate of change of concentration, $\partial C/\partial t$, will be zero, therefore the second law is as shown in **Equation 5-4**;

$$\frac{\partial C}{\partial t} = D\frac{\partial^2 C}{\partial x^2} = 0 \qquad \textbf{Equation 5-4}$$

Here, C is the solute concentration in the barrier and as D cannot equal zero, $\partial^2 C/\partial x^2 = 0$. This means that the concentration gradient across barrier is constant, signifying a linear relationship between concentration and distance as shown by **Figure 5-2**. The concentration will not be rigidly constant but rather is likely to vary slightly with time i.e. when $\partial C/\partial t$ is not equal to 0. The conditions are referred to as "quasi-stationary" or **"quasi-steady state"** (QSS) with little error introduced by assuming steady state.

Calculating diffusion coefficient using a diffusion cell requires an accurate chemical analysis method, total area available for diffusion, type and thickness of diaphragm used (Cussler, 1997). Taking into account the cross-sectional area available for diffusion, Fick's first law for a simple diffusional cell set-up in which a polymer membrane of cross-sectional area A and thickness x separates the two compartments may be written as **Equation 5-5**, where the concentrations on the donor and receptor sides are C_A and C_B,

$$J = \frac{dM}{Adt} = D\left(\frac{C_A - C_B}{x}\right) \qquad \textbf{Equation 5-5}$$

Where $(C_A - C_B)/x$ approximates dC/dx, this gradient within the polymer membrane must be assumed to be constant for the quasi-steady state to exist. **Equation 5-5** assumes that the aqueous boundary layer, which is the unstirred and static aqueous layers on both sides of the membrane do not significantly affect the total transport process. Unit activity ensures constant release of the drug at a rate that depends on the membrane permeability and the geometry of the dosage form (Martin, 1993).

5.1.3 Mathematical models for diffusion

General solutions for the diffusion equation can be obtained by means of mathematical modelling for a variety of initial and boundary conditions provided the diffusion coefficient is constant. The importance of *in silico* optimization of advanced drug delivery systems is expected to significantly increase in the future due to the advances in information technology (Siepmann and Siepmann, 2012). Mathematical modelling of drug release which uses mechanistic realistic mathematical description of mass transport (Siepmann and Siepmann, 2008; Siepmann and Peppas, 2001; Siepmann and Göpferich, 2001; Siepmann, Siepmann and Florence, 2006), can be highly beneficial in understanding the mechanisms controlling drug release (Glaessl et al., 2010; Marucci et al., 2008; Brandl et al., 2010) and for quantitative predictions of the effects of formulation and design parameters on the resulting drug release kinetics (Siepmann et al., 1998; Siepmann, Lecomte and Bodmeier, 1999; Siepmann et al., 2010)(Siepmann and Siepmann, 2012). Relatively simple mathematical equations can be used to quantitatively describe drug release from predominantly diffusion controlled delivery systems (Siepmann and Siepmann, 2012). Drug product development could be accelerated and experimentation time and cost reduced by using *in silico* simulations to optimise composition and design of drug delivery systems in order to provide the desired drug release profiles. In addition, they can provide deeper insight into the underlying drug release mechanisms.

Drug release from dosage forms can be controlled by different types of mass transport processes (Marucci et al., 2011; Yin and Li, 2011; Herrmann et al., 2007a; Kreye, Siepmann and Siepmann, 2011a; Kreye et al., 2011b). Processes involved could be diffusion of water into the system, drug diffusion out of the device, drug dissolution,

polymer swelling, matrix former erosion, osmotic effects and various other phenomena (Lee, 2011; Lao et al., 2011; Sackett and Narasimhan, 2011; Frenning and Strømme, 2003; Narasimhan, 2001). If several of these processes occur in sequence, the slowest process can be considered as the rate-limiting step for the entire sequence for a simplified mathematical description of drug release from the system (Siepmann and Peppas, 2012). Diffusional mass transport is the most common process involved in controlling drug release from a dosage form (Herrmann et al., 2007b; Zhou et al., 2005; Helbling et al., 2010b; Helbling et al., 2010a). In numerous cases drug diffusion is the predominant step (Seidenberger et al., 2011; D'Aurizio et al., 2011; Siepmann and Siepmann, 2011). In some cases drug diffusion could play a major role in combination with polymer swelling (Siepmann and Peppas, 2000; Siepmann, Streubel and Peppas, 2002; Faisant, Siepmann and Benoit, 2002) or in combination with polymer degradation/matrix erosion. Also, in certain cases drug diffusion could even play a minor role (Siepmann and Göpferich, 2001). Diffusional mass transport is generally quantified by Fick's law as described by **Equation 5-1** and **Equation 5-2**.

For the type of drug delivery system and type of release conditions, the following conditions including the so-called "initial and boundary" conditions need to be considered.

- The **"initial conditions"** concern the initial distribution of the diffusing solute molecules in the system. The mathematical treatment is much simpler if this distribution is homogeneous.

- The **"boundary conditions"** concern the conditions for diffusion at the boundaries of the drug delivery system. The boundary conditions are called "stationary" if the device dimensions are constant with time (no significant swelling or dissolution/erosion), are called "moving" in case of time-dependent device dimensions. If the device swells significantly, the boundaries are moving outwards; if the system dissolves/erodes significantly, they move inwards.

- In case of **"perfect sink conditions"** the drug concentration in the surrounding bulk fluid can be considered negligible. Furthermore, if the receptor medium is well stirred, the liquid unstirred boundary layer surrounding the device is generally thin. If the mass transfer resistance within the drug delivery system for drug diffusion is

much higher than the mass transfer resistance in this liquid boundary layer, the latter can generally be neglected.

- Whether or not the **diffusion coefficient *(D)*** of the diffusing species is constant is a very important aspect when solving Fick's law of diffusion. The mathematical treatment is much simpler if *D* is constant which is the case in a purely diffusion controlled drug release system where matrix erosion or polymer swelling is not an issue and hence mathematical modelling is very simple. Reasons for time and position dependent diffusion coefficients might include matrix erosion, polymer swelling and/or degradation (Verhoeven et al., 2009; Lin and Metters, 2006), where generally no " exact analytical solutions" of Fick's law can be derived (solutions quantifying the amount of drug released as a function of time), but " approximate numerical solutions" can be used (Frenning, 2011; Perale et al., 2009).

General solutions for the diffusion equation can be obtained by means of mathematical modelling for a variety of initial and boundary conditions provided the diffusion coefficient is constant. For the appropriate selection of the mathematical equation, that is valid for a particular type of diffusion controlled dosage form, the following information is crucial;

1. Type of the system – in a reservoir system the drug and the release rate controlling barrier material (polymers) are physically separated (here the drug may be located at the centre of the dosage form whereas the polymer forms a membrane surrounding this drug depot). In a matrix system, also called "monolithic system" the drug and the release rate controlling material (polymers or lipids) are homogeneously distributed throughout the device.

2. Drug concentration – A high initial drug concentration in the reservoir medium is preferred to maintain steady state for a longer time. The exact solubility of the drug in the wetted device might be difficult to ascertain. Here a rough estimate of the drug solubility in the receptor medium at 37 °C might be used, taking into account presence of other dissolved compounds which might significantly affect drug solubility.

3. Geometry of the drug delivery system – diffusional mass transport determinations through thin films are simpler compared to other geometries (Siegel, 2000; Helbling, Luna and Cabrera, 2011).

Understanding the mass transfer behaviour of insulin through the gel is essential for the modelling, design, optimisation and application of the closed loop implantable INsmart device, a reservoir system. Measuring the diffusion coefficients of drug molecules is important for theoretical predictions of the drug bioavailability in terms of drug release. Determination of diffusion of drug molecules in aqueous media can be complicated where avoiding disturbance is not easy. Diffusion coefficient measurements can be done in a variety of ways and estimates made in many systems for a range of drugs from small to large molecules. The approach presented here shows progression adopted in selecting a suitable method and mathematical model with the use of a model dye (tartrazine) in a model gel (agarose) media initially for determining diffusivity.

Based on the type, geometry and design of the closed loop insulin delivery device, INsmart the following mathematical models and methods were considered for measurement of diffusion coefficient. The mathematical methods presented in detail below are based on general solution for the diffusion equation, Fick's law, taking into account the initial and boundary conditions and assuming that the diffusion coefficient is constant.

- The Laplace transform method
- The diffusion cell quasi-steady state (QSS) method
- The diffusion cell time-lag (TL) method
    - -The TL Intercept method (TL intercept)
    - -The TL Slope method (TL slope)

These have been discussed individually in detail below.

5.1.3.1 The Laplace transform method

The solutions for diffusion usually take two standard forms. It comprises a series of error functions which are suitable for numerical evaluations at early stages of diffusion or is in the form of trigonometrically derived series which cover large values of time. However when diffusion occurs in a cylinder, the trigonometrically derived series are

replaced by a series of Bessel functions which are used in the Laplace transform equation which is essentially an operator method and is most powerful for complicated problems. Application of the Laplace transform to the diffusion equation removes the time variable, leaving an ordinary differential equation; the solution of which yields the transform of the concentration in terms of *x*, *y*, *z* and time, satisfying the initial and boundary condition.

Consider the problem of diffusion in a semi-infinite medium, $x > 0$, when the boundary is kept at a constant concentration C_0, the initial concentration being zero throughout the medium.

By applying Laplace transform, a solution for Fick's second law **Equation 5-6** can be derived;

$$\frac{\partial C}{\partial t} = D\frac{\partial^2 C}{\partial x^2} \qquad \textbf{Equation 5-6}$$

Satisfying the boundary condition;

$$C = C_{0,}\ \mathrm{x} = 0,\ t > 0$$

And the initial condition;

$$C = 0_{,}\ x > 0,\ t = 0$$

And is given by;

$$C = C_0\ erfc\ \frac{x}{2\sqrt{(Dt)}} \qquad \textbf{Equation 5-7}$$

Where, erfc z = 1 – erf z

Equation 5-7 can be used as a solution for a diffusion problem, provided **Equation 5-6** and the boundary and initial conditions are satisfied (Sebti et al., 2004).

The cylinder experimental setup is such that the two solutions, one with diffusing dye and the other without are separated by a membrane or gel (in this case). The concentration profile with distance in this setup over time changes at the junction and assumes a half Gaussian curve (or one half of a normal distribution). At this time the concentrations at the two ends of the cylinder are assumed to be as they were at the start (i.e. full solute concentration at the lower end and zero concentration at the upper end). Eventually the dye reaches the same concentration throughout. The integral for the Gaussian curve is also known as the *complementary error function* (erfc) and it is equal to (1-error function) or (1-erf). The error function is actually the inverse curve and values can be found tabulated like log tables.

5.1.3.2 The diffusion cell technique – Quassi steady state (QSS) method

The measurement of effective diffusivities (D_e) for substrates within gel matrices in the form of beads or large membranes has been reported extensively, Klein,J (1985), Vanancio,A (1997), Tanaka,H (1984), Bassi,A.S. (1987), Axelsson,A (1988) and Teixeira,J.A. (1994)) as cited by (Zhang and Furusaki, 2001). The most common techniques for determining diffusivities are the non-steady state technique (Tanaka, Matsumura and Veliky, 1984) and the diaphragm diffusion cell technique (Axelsson and Persson, 1988). The diffusion cell technique, modified particularly for determining D_e within the gel, is recognized as reliable, rapid and accurate technique (Axelsson and Persson, 1988).

The diffusion cell technique uses a diaphragm diffusion cell that consists of two identical chambers separated by a gel membrane in which the diffusivity will be measured. In both chambers, sufficient mixing will ensure negligible external mass transfer resistance. Initially, one chamber (A) is filled with a solution that contains the solute and the other (B) with pure solvent. As the solute diffuse through the membrane, the concentrations in both chambers are measured as a function of time. After an initial period of time (time-lag), a quasi steady state of solute flux is attained. The diffusivity can be estimated by either the QSS or TL method that has been treated mathematically previously (Crank, 1975; Cussler, 1997).

The diffusion coefficient *D* as defined by Fick's first law is based on the average concentration of solute in the whole gel. The effective diffusion coefficient, D_e, is based on the average concentration of solute in liquid phase in equilibrium with the average concentration of solute in the whole gel (C_L) and is represented by,

$$J = -D_e \frac{\partial C_L}{\partial x}$$ **Equation 5-8**

The relationship between diffusion coefficient, *D*, and the effective diffusion coefficient, D_e in gels has been discussed by Zhang (Zhang and Franco, 1999; Zhang and Furusaki, 2001) and is represented by **Equation 5-9**

$$D_e = KD$$ **Equation 5-9**

Where, *K* is the equilibrium partition coefficient.

The QSS method assumes that a QSS is attained, resulting in a linear concentration profile of the solute in the gel membrane after an initial period of time (t_0).

The molar flow, *N* can be obtained by integrating **Equation 5-8** to obtain **Equation 5-10**;

$$N = -D_e A_g \frac{C_{L,A\,(t)} - C_{L,B(t)}}{l}$$ **Equation 5-10**

Under QSS, the flux of the solute leaving chamber A equals the flux of the solute entering chamber B which can be written as **Equation 5-11**;

$$\frac{d(C_{L,A}(t)V_A)}{dt} = -\frac{d(C_{L,B}(t)V_B)}{dt}$$ **Equation 5-11**

Another condition that needs to be satisfied is that the volumes V_A and V_B of the two chambers separated by the gel are constant.

By combining **Equation 5-10** and **Equation 5-11**, D_e can be calculated from the slope of the line obtained by plotting the left-hand side of **Equation 5-12** against time *t*:

$$In\frac{C_{L,A\,(t)} - C_{L,B(t)}}{C_{L,A0} - C_{L,B0}} = -\frac{D_e}{l}A_g\left(\frac{1}{V_A} + \frac{1}{V_B}\right)(t - t_0)$$ **Equation 5-12**

The essential condition to apply **Equation 5-12** is that the QSS must be fulfilled, i.e. 'the solute flux in' has to equal 'the solute flux out' of the gel, mathematically checking whether **Equation 5-11** is satisfied.

5.1.3.3 The diffusion cell technique - The time lag (TL) method

The diffusion cell technique, where the diffusion mass transfer process occurs through the gel membrane, has been used to estimate diffusivity using the TL method that has been treated mathematically previously (Crank, 1975; Cussler, 1997).

Here, the basic conditions assumed are the two chambers are well mixed, that both chambers are large enough so that changes in concentration are negligible and that initially solute is only present in chamber A. Upon satisfaction of these conditions, Fick's law can be solved to give the total amount of solute transferred through the membrane (Q_t), **Equation 5-13**:

$$Q_t = V_{B0}C_{L,B(t)} = \frac{A_g D C_{L,A0}}{l}\left(t - \frac{l^2}{6D}\right)$$ **Equation 5-13**

To estimate the diffusivity, the TL method uses a plot of the total amount of solute transferred through the gel membrane (Q_t), the left-hand side of **Equation 5-13** vs. time (t) as represented in **Figure 5-3**.

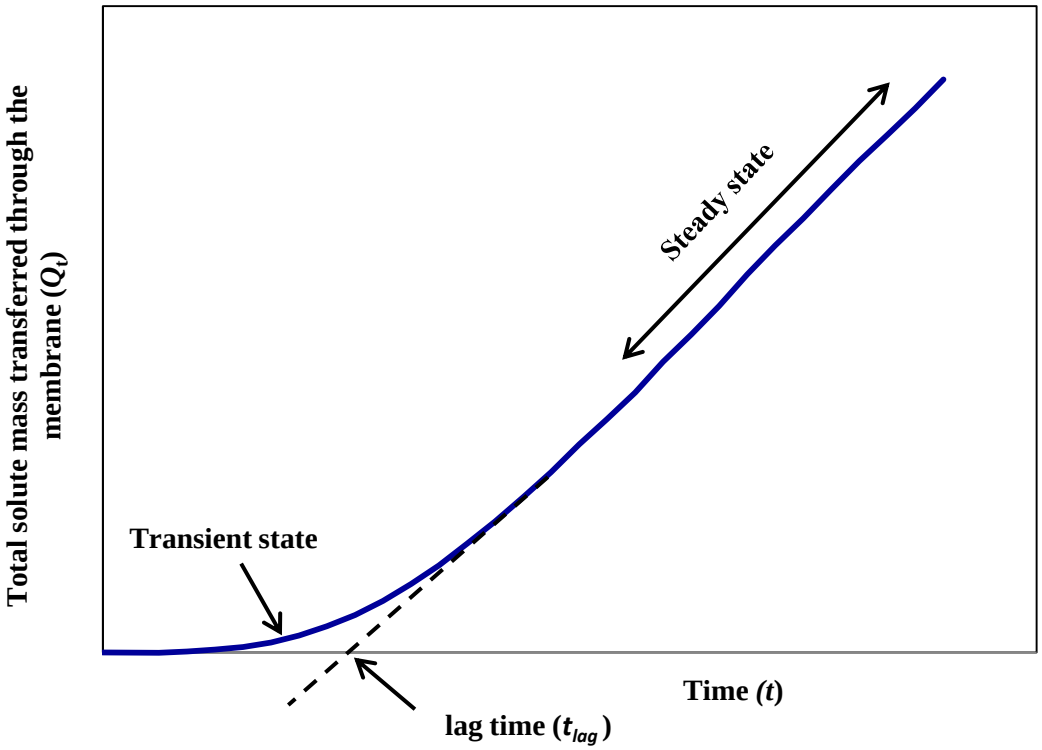

Figure 5-3 : Total solute mass transferred through the gel membrane (Q_t) as function of time in through-diffusion tests. The slope of linear part (steady state) gives D and its intercept gives lag time.

The TL Intercept method

The intercept of the linear part of the curve is known as the 'lag time', that physically corresponds to the time point when the solute appears in downstream chamber B and is given by **Equation 5-14**,

$$t_{lag} = \frac{l^2}{6D} \qquad \textbf{Equation 5-14}$$

In literature, the diffusion coefficients (D) for solute molecules have been calculated exclusively from the lag time using the TL method (Frisch and Prager, 2003; Venâncio and Teixeira, 1997; Chen, Loo and Wang, 2012; Oztan and Mutlu, 2005).

The TL Slope method

Alternatively, D can also be estimated from the plot slope. It, however, remains unresolved as to which of the two estimations produces the correct result. Zhang and Furusaki (2001) have discussed and compared the QSS method with widely used methods, the TL method and the variant-quasi- steady- state (VQSS) method in order to assess their applicability. The VQSS method as developed by Converti et al (Converti et al., 1996) evaluates D_e from a diffusion cell experiment by rearranging the QSS **Equation 5-12** for mass balance for the receptor chamber and by estimated point by point and then averaging to give a global D_e value. They concluded that in their experiments it was observed consistently that diffusivities estimated by the TL intercept method were substantially lower than those estimated by the TL slope method. However, the estimation by the TL slope method produced similar value as that by the QSS and VQSS method when a QSS is established. They concluded that the TL method using the intercept, which has been extensively used in literature, generates erroneous estimations of diffusivity in most cases and should not be relied upon.

5.2 Outline of experiments

Diffusion coefficient measurements were performed using a custom made experimental test rig which mimics the peritoneal cavity and data was recorded using UV or fluorescence spectroscopy. Initially model dyes such as tartrazine and fluorescein sodium and model gel such as agarose were used for technique development and mathematical model selection. The primary aim for using model dyes and gels was for understanding the diffusion kinetics of small solute molecules, to develop an appropriate experimental technique and for selecting appropriate mathematical models for measuring diffusion coefficient.

The experimental results presented here provide a good platform for understanding the drug release mechanism of insulin from the formulation held within the device and the performance window for the device, which are discussed in **Chapter 7** and **Chapter 8**.

The following assumptions and consideration were made for the INsmart device set-up used later on in the experiments (conditions considered for applicability of the diffusional equations) for determining insulin diffusivity;

• The INsmart device set-up is considered to have "perfect sink conditions" during the entire experimental time period, here the drug concentration in the donor compartment is high and in the surrounding bulk receptor compartment fluid is considered negligible.

• Diffusional drug mass transport is release-rate limiting in the gel.

• The diffusion coefficient of the drug (within the gel 'film') is constant and does not depend on its time or position within the device.

• The device (gel) is not significantly swelling (or swells very rapidly upon contact with receptor medium and then reaches an equilibrium state) or dissolve during drug release.

• The device (gel) is not significantly eroding during drug release or losing its constituents by some other process.

• Mass transfer resistance due to liquid unstirred boundary layers on the surface of the system is negligible. As the receptor medium is well stirred, the liquid unstirred boundary layer surrounding the device is generally thin. The mass transfer resistance in this liquid boundary layer is much lower than that within the drug delivery system for drug diffusion and hence the former can be neglected.

• The initial drug concentration in the gel film/slab is much higher than the solubility of the drug in the (wetted) system.

• Gel placed in the device can be considered as a thin film with negligible edge effects, which means that diffusional mass transport through the edges of the film is negligible compared to diffusional mass transport through the film's main surface. The mathematical description of drug diffusion can be restricted to one dimension

The development of an experimental model and selection of an appropriate mathematical model with an aim of determining the diffusivity of insulin through the glucose-responsive gel in the INsmart device was performed in a sequential manner as shown in **Figure 5-4**. The left hand arrow describes each experimental stage with dye, gel and system used and the corresponding right hand tab describes the aim and desired outcome.

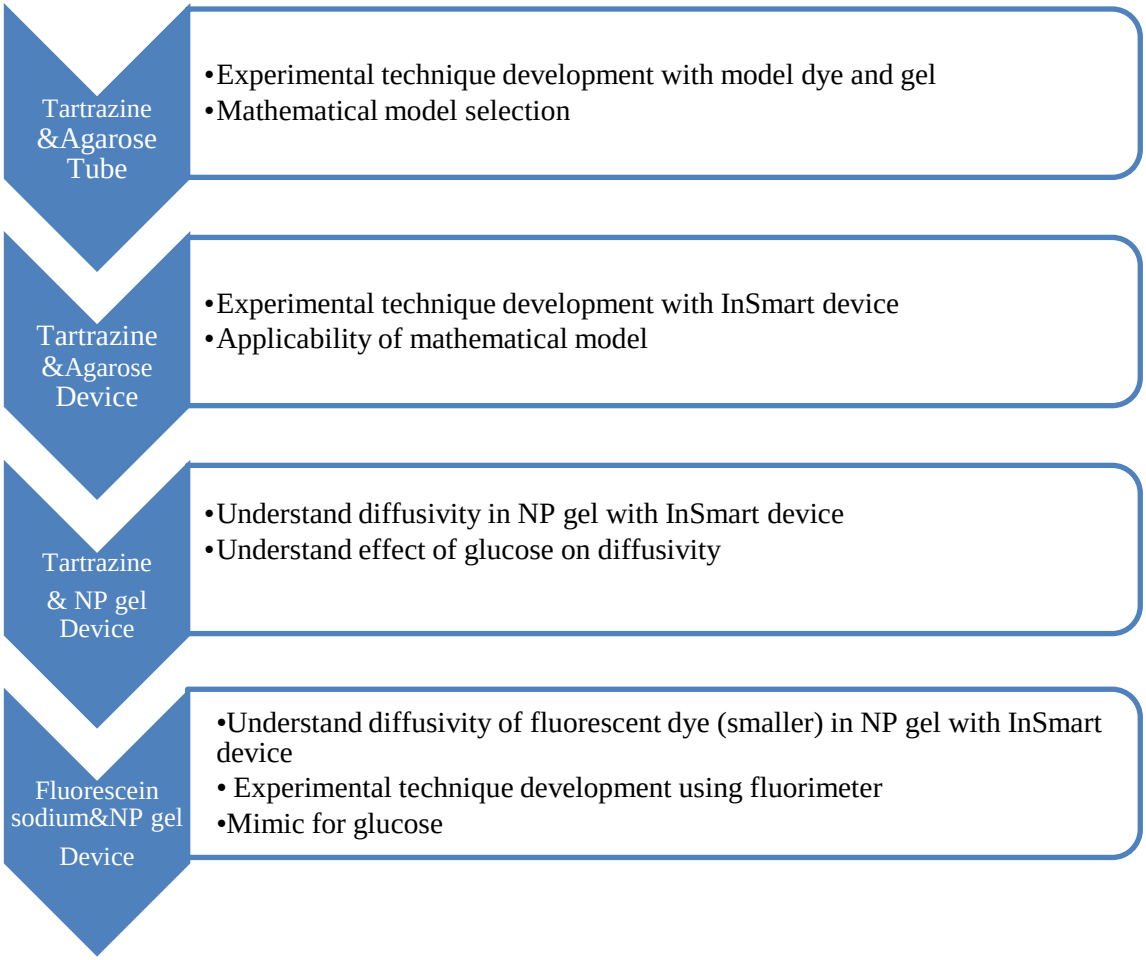

Figure 5-4: Development of mathematical model for diffusion study

A simple diffusion model (tube) was initially investigated to develop the experimental technique and to understand the diffusivity of a model dye, tartrazine through a model gel, agarose. This experimental model allowed a quick, easy and efficient system to test feasibility of the system to determine diffusion coefficient.

Tartrazine, molar mass: 534.36 Da was selected as a model dye because of its small size, availability, stability, compatibility with gels, its non-staining properties as well as strong absorbance at 427 nm aiding easy UV/Vis assay. Tartrazine diffusivity in agarose gel was checked, taking into account factors possibly influencing the diffusion rates such as tartrazine concentration, gel thickness and agarose concentration. From various possible gels agarose was chosen because of its neutral structure (Foord and Atkins, 1989). Diffusion in agarose, similar to diffusion in polymers, is regarded as diffusion in a porous solid matrix where pores are connected and filled with the solvent. Agarose forms a gel at very low concentrations and has been used to find the aqueous diffusion coefficient of small molecules in water as the water in these gels exists mainly as "free" water through which the solutes move unhindered –i.e. the *micro*-environment is not viscous whereas the *macro*-environment is.

The four mathematical methods for determining the diffusion coefficient described in **Section 5.1.3**, namely: Laplace transform, diffusion cell-QSS, TL, slope and intercept analysis were assessed and compared for their applicability using the tube model and model dye and gel.

Following tube diffusion, experiments were undertaken with the INsmart device using the model dye, tartrazine and gel, agarose held within the device. Experimental technique improvement learnt from the tube set-up was applied to the device set-up. Selected agarose gels were used in these experiments. Further the applicability of the four mathematical models for determination of diffusion coefficient was assessed and suitable models selected for further experiments.

The selected mathematical models were then taken forward to determine diffusivity of tartrazine in the non-polymerised dex2M-conA gel (NP gel) prepared using dextran (molecular weight 2 million daltons) and concanavalin A (conA) housed in the INsmart device. The NP gels were used instead of the cross-linked dex500MA-conAMA gels (CL gel) in order to study the underlying drug release mechanism. Refer to **Chapter 2** for the function of the gels and **Section 5.3.3** and **Chapter 6, Section 6.2.1** for preparation of the gels. Tartrazine diffusivity through NP gel was also determined in presence of physiologically relevant glucose concentrations. Where, glucose

concentration of 0.1% w/w as used in the experiments corresponds to ~5.5 $mmolL^{-1}$ the basal normal limit of fasting plasma glucose for most individuals, 0.2% w/w corresponds to ≥ 11.1 $mmolL^{-1}$ which indicates diagnosis of diabetes and higher concentrations of 0.5% w/w (27.75 $mmolL^{-1}$) and 1% w/w (54 $mmolL^{-1}$) are levels that might be reached or threatened after food or glucose challenges.

The next step in the experimental plan was to understand the diffusivity of glucose molecule itself in the NP gel to gain some idea of the responsiveness of the gel to glucose levels. However, it is difficult to determine the diffusion properties of glucose molecule itself in the NP gel as free glucose dismantles the gelatinous three-dimensional network of the gel by competitive displacement resulting in a fall in its viscosity. Fluorescein sodium was chosen as a glucose mimic as its molecular weight (376.28 Da) lies midway between glucose (180.2 Da) and tartrazine (534.3 Da). There were two advantages for using fluorescein sodium, firstly to provide some estimation of glucose diffusivity in the NP gel and secondly to aid with experimental technique development using the fluorimeter, which is required for diffusivity determination of fluorescently labelled insulin through the NP gel and CL gel as discussed in **Chapter 7**.

Fluorescein sodium salt (Acid Yellow 73), $C_{20}H_{10}Na_2O5$, molecular weight 376.28 Da has been extensively used as fluorescent tracer to study blood brain barrier (Oishi et al., 1989), in permeability and perfusion studies due to its small molecular radius (De Bruyn et al., 2011; Kozler and Pokorny, 2003). Its excitation wavelength of 485 nm and emission wavelength of 515nm makes it suitable for fluorescent measurements.

Each experimental stage has been discussed separately below along with details of the experiment system set-up and diffusivity results determined using the different mathematical models.

5.3 Materials and methods

5.3.1 Materials /Chemicals and reagents

Agarose, batch no: 19843, gelation temperature (1.5% Gel) 32-40°C was purchased from Fisher Bioreagents, UK. Tartrazine No T-0388 (C.I.1914, Acid Yellow 23) Lot: 45F-0127, and sodium azide were purchased from Sigma-Aldrich Chemical Company

Ltd. (Poole, Dorset, UK). Concanavalin A, from *Canavalia ensiformis*, lyophilised powder (Type VI) (conA) and dextran (produced by *Leuconostoc mesenteroides*, strain no. B512; average molecular weight 2000 kDa) (dex2m) were purchased from Sigma Aldrich Co. 3050, St Louis, M.O. 63103, USA 314-771-5765. Fluorescein sodium salt, molecular weight 376.28 Da, was obtained from BDH. 0.2 μm cellulose nitrate membrane filter was purchased from Whatman International Ltd, England. Dialysis membranes (molecular weight cut off: 100 kDa) were obtained from Spectrum Europe B. V. (4800 DG Breda, Netherlands). Metric 180 PVC tubing-FDA/USPVI (1mmID, 2mmOD, 5mmWall) was purchased from Nalgene® Brand products,USA. All other chemicals were of analytical grade and distilled water was used throughout.

5.3.2 Preparation of agarose gel

Agarose gels, 0.5%, 0.7%, 1%, 1.5% and 2% w/w were prepared in glass beakers. Gels were prepared by dispersing agarose powder in distilled water using a magnetic stirrer and left for about 10 min to ensure sufficient hydration. The mixture was then heated to 80°C with continuous stirring for approximately 10 minutes and cooled to 60°C prior to casting. For storage, it was mixed thoroughly and cooled at room temperature for 2-3 hours and stored at 4°C until use. For casting purposes the stored gel was brought to a boil with continuous stirring and the solution was cooled to 60°C prior to casting.

5.3.3 Preparation of NP gel

1 g of conA was dissolved in 8 mL of distilled water containing 0.3% w/w sodium azide. 1g of dex2M was then added to the solution and stirred to form a viscous mixture. The mixture was stored at 4°C for at least 24 hours before use.

For experiments with glucose, the relevant amount of glucose was added to the prepared NP gel and mixed and stored at 4°C for at least 24 hours before use. Prior to use the gels were allowed to equilibrate at room temperature for at least 2 hours.

5.3.4 Data analysis method for determination of *D*

The absorbance data from diffusion experiments was first converted into concentration of tartrazine using a calibration curve. The data was then plotted as described below based on the mathematical methods for calculating diffusion coefficient;

The Laplace transform method

Here the solution for the diffusion problem as described in **Section 5.1.3.1, Equation 5-7** was used.

$$C = C_0 \, erfc \, \frac{x}{2\sqrt{(Dt)}}$$

(**Equation 5-7** repeated here for reference)

The data was plotted as Cx/C_0 over time as shown in **Figure 5-5**;

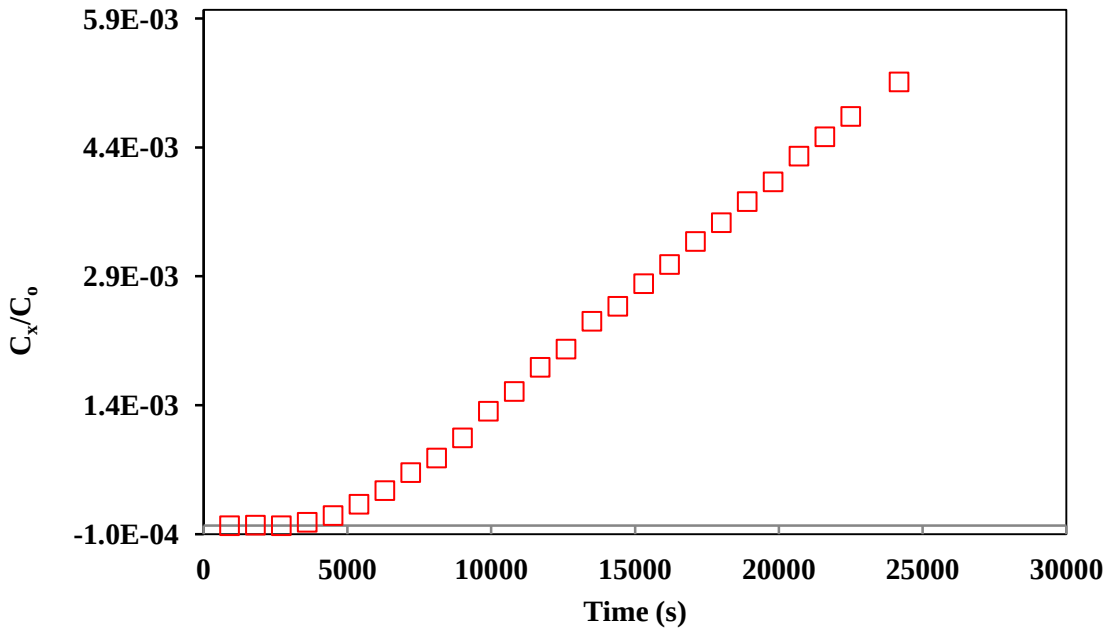

Figure 5-5: Representative plot of the Laplace transform method: Evaluation of diffusivity *D* for tartrazine in 0.7% w/w agarose gel using tube experiment.

Using the following solution for the equation, the erf function was calculated by reading the C_x/C_o values at five different time points and solving for *D* at that particular time. The reported *D* was an average calculated at five different time points.

$$1 - \frac{C_x}{C_0} = \text{erf}\left[\frac{x}{2\sqrt{(Dt)}}\right] \qquad \textbf{Equation 5-15}$$

$$D = \frac{\left[\frac{x}{erf\left(1\text{-}\frac{C_x}{C_0}\right)*2}\right]^2}{t} \qquad \textbf{Equation 5-16}$$

QSS Method

Here the solution for diffusion problem as described in **Section 5.1.3.2, Equation 5-12** was used.

$$In\frac{C_{L,A\,(t)} - C_{L,B(t)}}{C_{L,A0} - C_{L,B0}} = -\frac{D_e}{l}A_g\left(\frac{1}{V_A} + \frac{1}{V_B}\right)(t - t_0) \qquad \textbf{(Equation 5-12} \text{ repeated here for reference)}$$

D_e was calculated from the slope of the line obtained by plotting the left-hand side of **Equation 5-12** against time *t*:

The data was plotted as ln ($C_{A(t)}$-$C_{B(t)}$/$C_{A(t0)}$-$C_{B(t0)}$) over time as show in **Figure 5-6**;

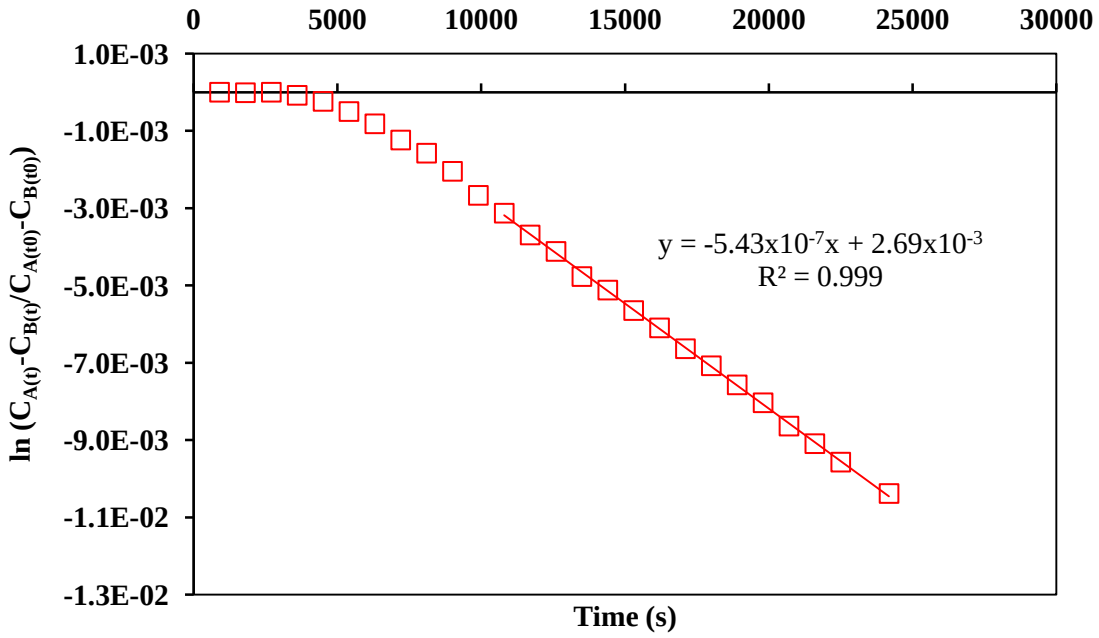

Figure 5-6: Representative plot of the QSS method: Evaluation of diffusivities, D_e for tartrazine in 0.7% w/w agarose gel using the tube experiment.

Using the slope of the curve at the QSS the **Equation 5-12** was solved for D_e as shown in **Equation 5-17**,

$$D_e = Slope \frac{l}{A_g\left(\frac{1}{V_A}+\frac{1}{V_B}\right)} \qquad \textbf{Equation 5-17}$$

TL slope and TL intercept methods

Here the solution for the diffusion problem as described in **Section 5.1.3.3, Equation 5-13** was used.

$$Q_t = V_{B0}C_{L,B(t)} = \frac{A_g D C_{L,A0}}{l}\left(t - \frac{l^2}{6D}\right) \qquad \textbf{(Equation 5-13} \text{ repeated here for reference)}$$

To estimate the diffusivity, the TL method uses a plot of the total amount of solute transferred through the gel membrane (Q_t) vs. time (t) as shown in **Figure 5-7**;

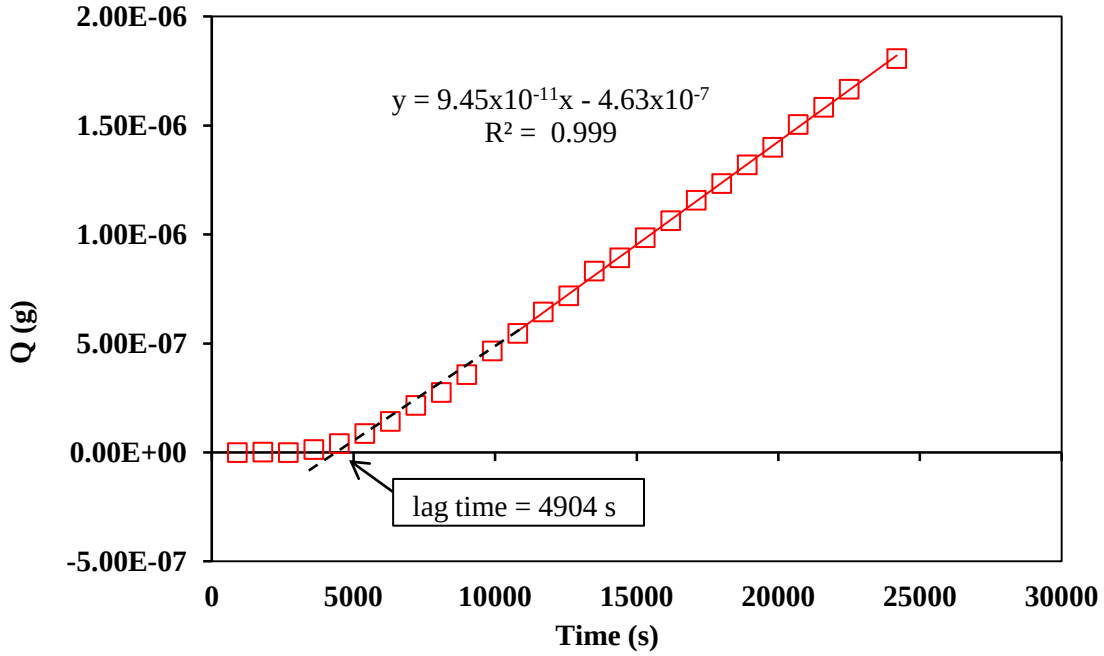

Figure 5-7: Representative plot of the total amount of tartrazine transferred through the gel, Q vs. time by the TL method: Evaluation of diffusivity, D for tartrazine in 0.7% w/w agarose gel using the tube experiment.

For the TL slope method, D was estimated from the plot slope by solving **Equation 5-19**.

$$Slope = \frac{A_g D C_{L,A0}}{l} \qquad \textbf{Equation 5-18}$$

$$D = \frac{Slope * l}{A_g C_{L,A0}} \qquad \textbf{Equation 5-19}$$

For the TL intercept method, the intercept of the linear part of the curve which is known as the 'lag time', is determined from the plot and *D* is determined by solving **Equation 5-20**.

$$t_{lag} = \frac{l^2}{6D}$$ (**Equation 5-14** repeated here for reference)

$$D = \frac{l^2}{6t_{lag}}$$ **Equation 5-20**

5.4 Determination of diffusion coefficient of tartrazine in agarose using tube set-up

A simple system using model dye, tartrazine and gel, agarose was investigated as a diffusion model with the ultimate aim to model insulin release through the glucose-responsive gel in the INsmart. Here a tube set-up was used to test the feasibility of the system, to develop the experimental technique and to understand the diffusivity of a small molecule.

The four mathematical methods for determining the diffusion coefficient described in **Section 5.1.3**, namely: Laplace transform, diffusion cell-QSS, TL, slope and intercept analysis were assessed and compared for their applicability using the tube set-up and model dye and gel.

5.4.1 Experimental set-up and procedure of diffusion

Polyethylene tubes (dimensions: ranging from 11 to 20 mm diameter) were used. The casting of agarose gel was performed by placing the cylindrical tube on a clean glass plate and agarose solution maintained at 60°C was decanted into the tube to produce hydrogels ranging from approximately 3 to 9 mm thick. During this it was ensured that the tube was held clamped tight against the glass plate to prevent leaks. The agarose

solution was allowed to cool and gel at room temperature for approximately 15 min. The tube was lifted slowly and gently from the glass plate and these agarose containing tubes were used immediately for experiments.

The experimental set up is as shown in **Figure 5-8** and **Figure 5-9**;

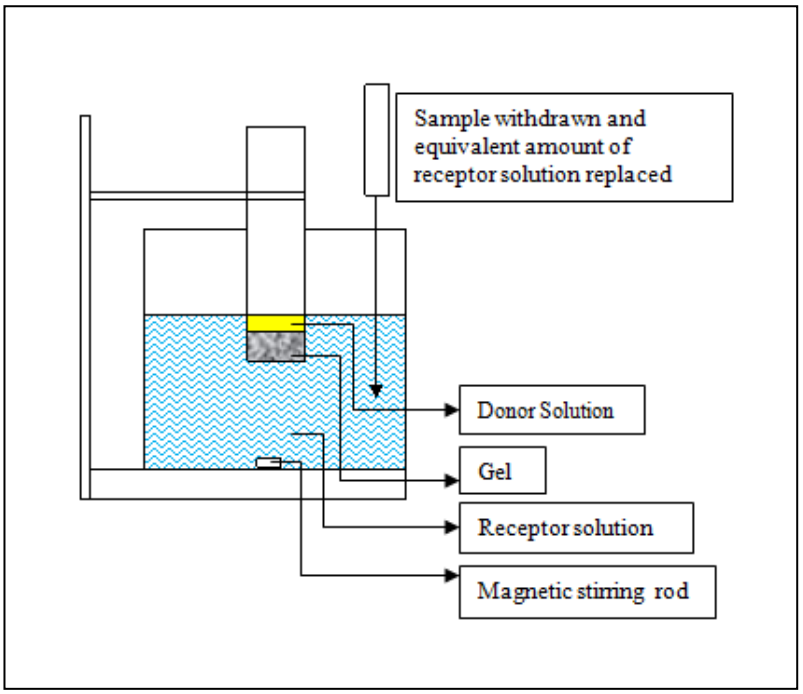

Figure 5-8: Experimental set-up for diffusion in tube experiment.

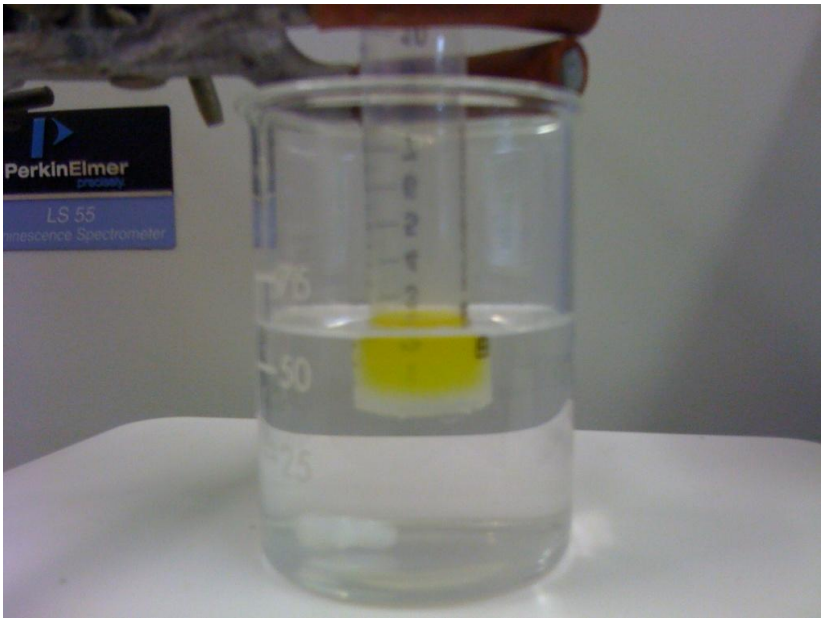

Figure 5-9: Photograph of set-up for tube measurements.

Agarose gels – 0.5%, 0.7%, 1% and 2% w/w were prepared as described in **Section 5.3.2**. Once the gel was cast within the tube the following steps were followed;

1) The thickness of the cast agarose gel in the tube was measured.

2) The receptor beaker containing distilled water (approximately 25 to 35 mL) was stirred using a magnetic rod to ensure uniform concentration in the receptor and to reduce sampling errors.

3) The tube cast with agarose gel was placed in a receptor beaker containing distilled water using a stand and clamp. The height of the tube in the beaker was adjusted so the level of water in the beaker matched the donor solution level to ensure no pressure differences.

4) The donor tartrazine solution (approximately 1 mL of 1% w/w solution) carefully added onto the top of the gel in the tube and the exact volume was noted.

5) 0.1 mL of sample was withdrawn every 15 min and diluted to 3 mL with distilled water to ensure measurement in the detection range and analysed using Perkin Elmer UV/Vis Spectrometer Lambda 40 at 427 nm.

6) After each sampling, equivalent volume (0.1 mL) of water was added to the receptor to eliminate any errors due to volume difference.

Sampling was performed over a period of minimum 5 hours. All experiments were performed at 20°C and in triplicate. The UV Winlab wavelength program software application provided by PerkinElmer, UK was used to measure the sample absorbance at 427 nm. Tartrazine shows strong absorbance at 427 nm as shown in **Figure 5-10**. The absorbance data was imported into Excel for the concentration time plots. The tartrazine absorbance intensity at 427nm wavelength was linear with respect to concentration thus enabling simple conversion of intensity data into concentration values observed for tartrazine using the calibration curve shown below in **Figure 5-11**.

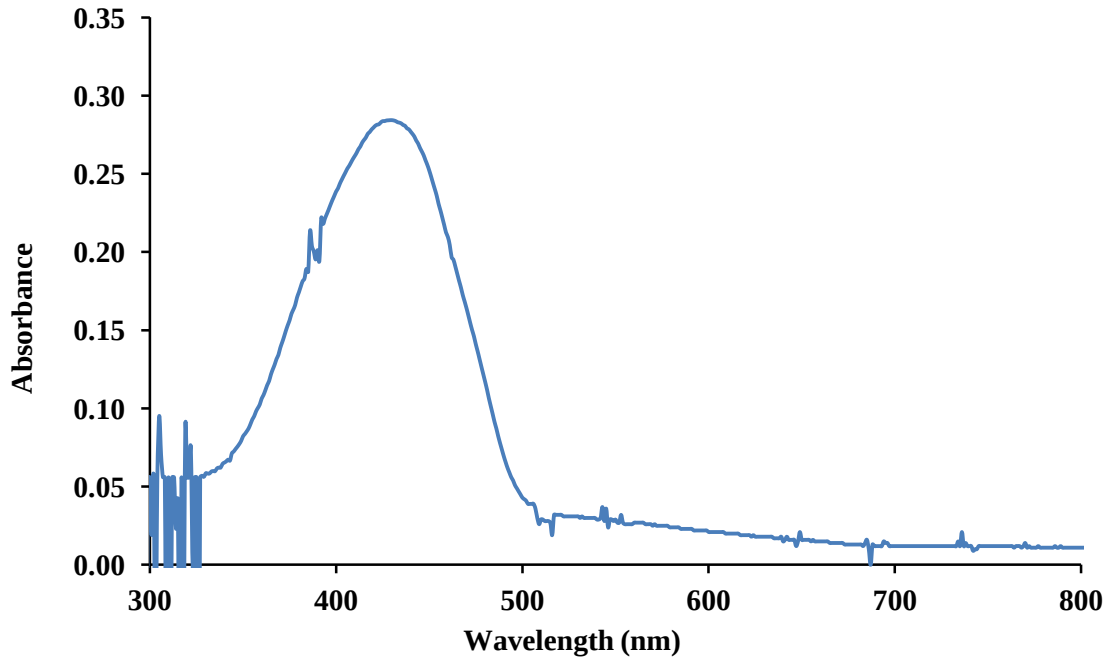

Figure 5-10: UV spectrum for tartrazine showing strong absorbance at 427 nm.

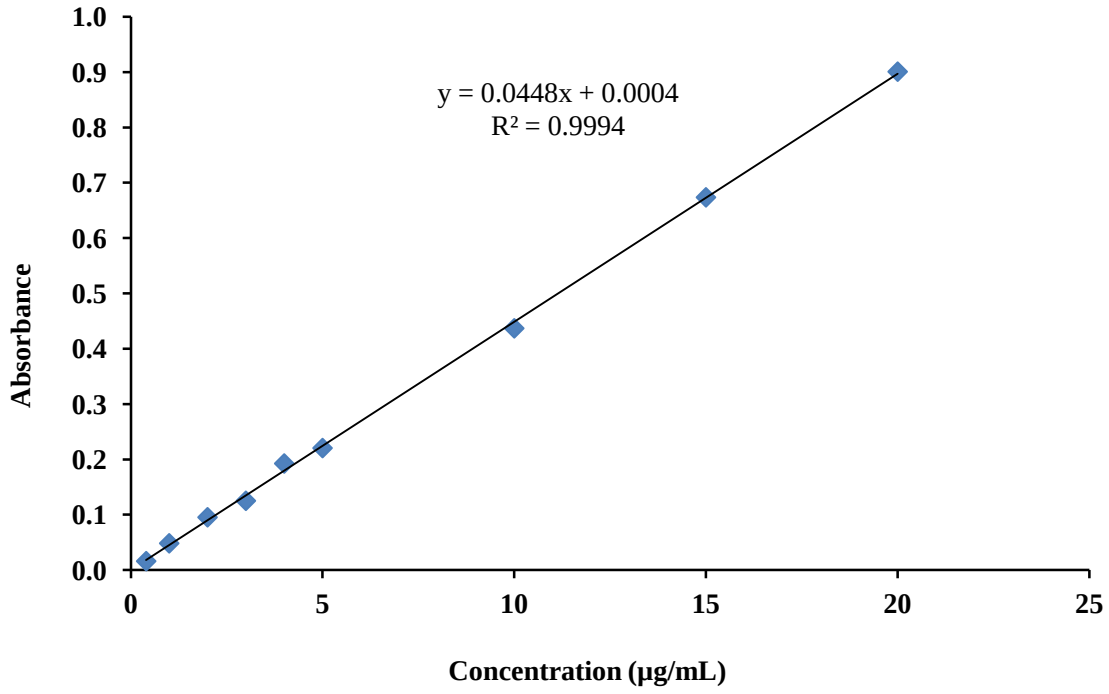

Figure 5-11: Calibration graph for tartrazine (0 – 20 µg/mL) (using disposable cuvette). (Data represent mean±SD of six measurements, error bars present but may not be visible as smaller than marker size).

5.4.2 Results and Discussion

The diffusivities of tartrazine in increasing agarose gel concentrations from 0.5% to 2% w/w were determined using the Laplace transform; QSS, TL slope and TL intercept methods. The results are as presented in **Table 5-1**.

Table 5-1: Diffusion coefficient values (D and D_e) for tartrazine in increasing agarose gel concentration determined using different methods. The number of replicates for each experiment was 3. Where V_A – volume of tartrazine solution above the gel, V_B – volume of water in the beaker.

Agarose gel concentration	**Laplace transform**	**QSS**	**TL slope**	**TL intercept**
(%w/w)	$\boldsymbol{D \times 10^{-10}}$ **(m^2/s)**	$\boldsymbol{De \times 10^{-10}}$ **(m^2/s)**	$\boldsymbol{D \times 10^{-10}}$ **(m^2/s)**	$\boldsymbol{D \times 10^{-10}}$ **(m^2/s)**
0.5	1.04 ± 0.30	0.22 ± 0.07	4.13 ± 0.42	10.57 ± 2.50
0.7	0.82 ± 0.24	0.24 ± 0.07	4.46 ± 0.47	8.37 ± 2.25
1	0.75 ± 0.11	0.32 ± 0.11	5.47 ± 1.58	5.45 ± 3.37
2	0.70 ± 0.07	0.20 ± 0.06	3.38 ± 0.68	6.34 ± 2.30
2 (where $V_A \sim V_B$)	2.00 ± 0.74	3.40 ± 0.36	6.14 ± 2.20	11.92 ± 2.79

Table 5-1 shows the D values determined using the Laplace transform and QSS methods for diffusion in tube are significantly different from the values determined using the TL slope and TL intercept methods for all agarose gel concentration. The data thus suggested that either the QSS state was not achieved or because V_A and V_B were not same (the second requirement for QSS method). By keeping V_A and V_B as close to each other as possible the tube set-up can be considered to be same as a diffusion cell. The results for 2% w/w where $V_A \sim V_B$ (the tartrazine solution placed above the gel being V_A and water in the beaker being V_B) are as shown in the table, here the D values for the Laplace transform, QSS and TL slope method match, however the D obtained using the TL intercept method is faster.

The experimental data are graphically presented in **Appendix 3** the Laplace transform method data has been presented as C_x/C_0 vs. Time (s), QSS method $ln\ (C_{A(t)}\text{-}C_{B(t)}/C_{A(t0)}\text{-}C_{B(t0)})$ vs. Time (s) and the TL slope and TL intercept method Q(g) vs. Time (s). Representative data for 0.5% w/w, 0.7% w/w, 1.0% w/w , 2.0% w/w agarose gel and 2.0%w/w agarose gel with matched donor and receptor volumes are presented in **Figure A3-1**, **Figure A3-2**, **Figure A3-3**, **Figure A3-4** and **Figure A3-5**, respectively.

Constraints and factors affecting the design of experimental protocol

The simple tube experiments enabled to identify a number of key factors that need to be controlled and defined to progress with the experimental protocol for the next stage. For further experiments the test rig was changed to be very like the actual conditions for the INsmart device. Diffusivity was measured using the four mathematical methods in a glucose sensitive gel held within the INsmart device.

The following constraints and factors that need consideration were identified for refining the experimental protocol;

- The "boundary conditions" needs to be constant which means that the glucose-responsive gel should show no swelling or erosion. This was achieved by the INsmart design itself in which the glucose-responsive gel is housed within the device between two cellulose nitrate membranes supported by stainless steel mesh in such a way which restricts the gel from swelling or eroding.
- "Perfect sink conditions" was achieved by using a high concentration of drug/dye in the donor compartment and ensuring that the receptor fluid is well stirred.
- Understanding the geometry of the system is essential to design the experiment around the constraints imposed by the model used to interpret the data and ensure its suitability. The gel placed in the device can be considered as a thin film with negligible edge effects, the gel is contained within a stainless steel housing with the gel spacer surrounding the gel film, as the surface of the film exposed to the receptor medium is large compared to its thickness which means that diffusional mass transport through the edges of the film is negligible compared to the film's

main surface. The mathematical description of drug diffusion here can thus be restricted to one dimension.

- Osmotic effects – Osmotic effects within the whole system can be kept constant if the boundary conditions as discussed above are kept stationary. For diffusivity experiments in presence of glucose, the osmotic effects due to presence of glucose are avoided by maintaining same glucose concentration throughout the system; donor side, in the gel and receptor side.
- Detection limit – The detection limit for the detector used should be taken into account as very high drug/dye concentration on donor side coupled with low volumes on receptor side could lead to the detector getting saturated very quickly. This could result in inability to detect the lag time as well as the steady state.
- Gel area and thickness – The diffusion rate of the drug depends on the gel permeability and the gel area and thickness (geometry of the device). Depending on the size and shape of the diffusing molecules, the gel pore sizes affect their simple diffusion. The total amount of the drug delivered from the device however depends on the surface area available to diffuse through, which in turn depends on the geometry of the device. The gel thickness affects the rate at which the diffusing drug is delivered; the flux is inversely proportional to the gel thickness, the thinner the gel quicker the drug is delivered.
- Volume of receptor fluid – As was an outcome from the tube experiments in order to attain a QSS state in a diffusion cell type system, it is essential to maintain the donor and receptor volume same. Furthermore for detection purposes it is paramount to maintain an appropriate volume, if the volume is too high the diffused species will be detected after a considerably long time thereby increasing the overall experimentation time.
- Gel concentration: The homogeneity of the gel affects the diffusivity of the diffusing species, unwetted areas lead to inconsistent diffusion coefficient values. A non-uniform gel will have uneven thickness across the surface of a thin film/ slab. Therefore special care is required in preparation of the gel. The presence of a significant meniscus could also affect the *D* value calculated especially when using the TL intercept method. Extra care needs to be taken when casting the gel, for the

INsmart device this should be less of a concern as a gel spacer is used and the weight of gel placed in it is always kept constant.

5.5 Determination of diffusion coefficient of tartrazine in agarose in the INsmart device

Following the tube diffusion measurements further experiments were untaken with the INsmart device using tartrazine and agarose gel held within the device. From the tube experiments, it was understood that the models can be applied only when the volumes in the donor and receptor compartments are kept the same and that the TL intercept method might not give consistent results. The experimental set-up was designed to incorporate the learning from tube diffusion experiments. Diffusion of tartrazine was assessed in 2 and 1.5% w/w agarose gels, selected as model gel concentrations for use with the INsmart device. Here the applicability of the four mathematical models for diffusion coefficient determination was assessed for tartrazine in agarose gel held within the INsmart device.

5.5.1 Experimental set-up and procedure of diffusion

The design of the INsmart device has been explained in **Chapter 2, Section 2.1.** Assembling the device was crucial for the success of the experiment and its performance. A detailed list of its components is shown in **Figure 5-12**.

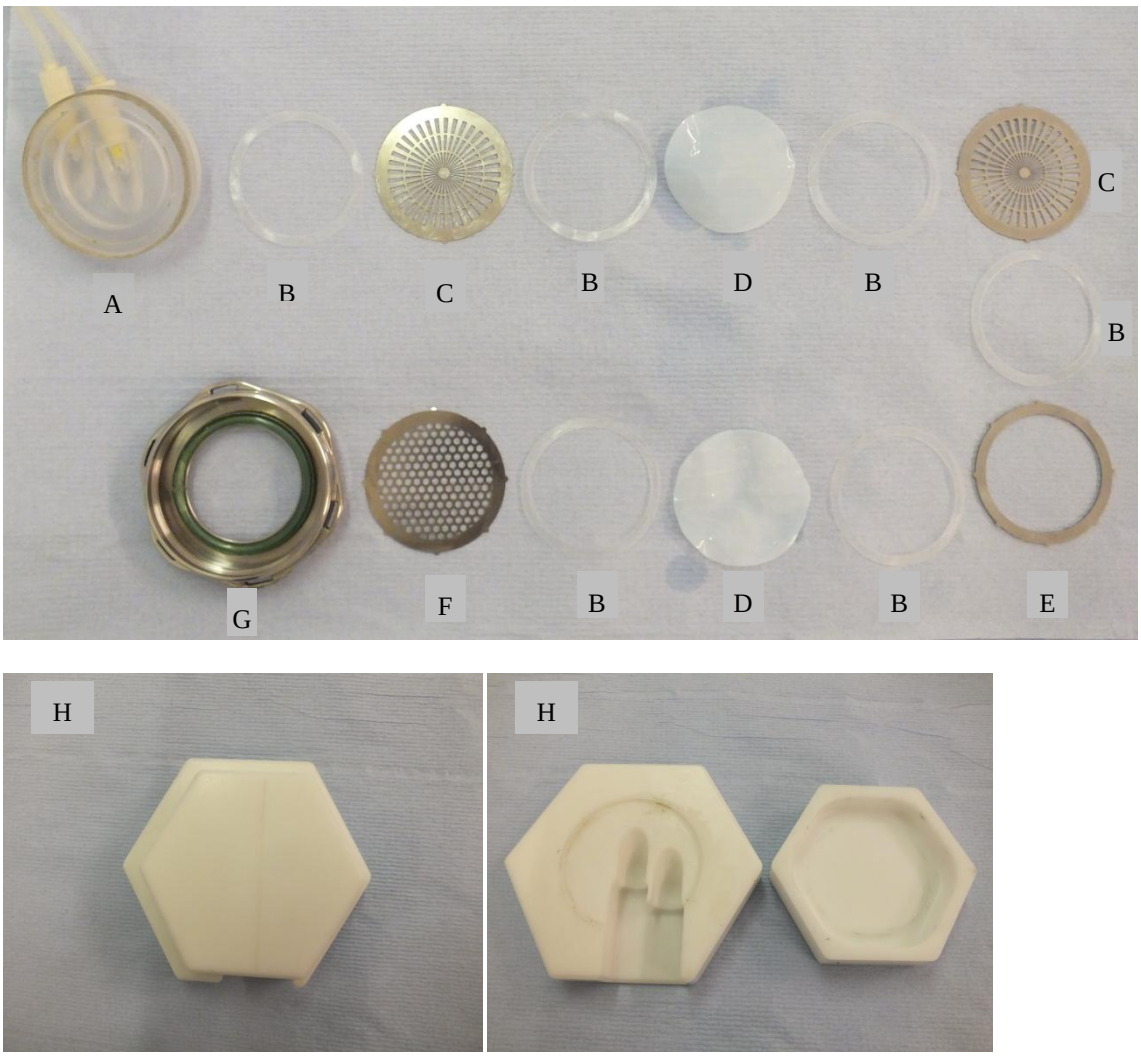

Figure 5-12: Figure showing the various components of the INsmart device. Key: A-polycarbonate base, B- parafilm, C-stainless steel screen, D- membrane (specific MWCO), E-stainless steel gel spacer, F- stainless steel mesh, G-stainless steel top with O-ring, H-mould for holding device whilst assembly.

The device was assembled, ensuring that components were placed sequentially as shown in **Figure 5-12** and PTFE (Polytetrafluoroethylene) grease, (Magnalube®-G) applied between metal components. The polycarbonate base which has the luer connections was placed on a specially designed mould to keep it flat. A 0.2 µm cellulose nitrate membrane was placed in between two stainless steel screens with parafilm rings in between for a tight seal, ensuring that they are placed flush. The stainless steel gel spacer was placed with a parafilm ring over the screen. The agarose gel solution at 60°C

was poured into the gel spacer, 3 mm thick and left to set at room temperature for approximately 15 minutes. After the agarose gel had formed a 0.2 μm cellulose nitrate membrane and stainless steel mesh were placed on top with parafilm rings in between to ensure a good seal is formed. The stainless steel top which holds the O-ring was screwed on and tightened, initially by hand and then using a specially designed wrench. This was to ensure that there were no gaps in between components which could lead to leak in the device.

After the device was assembled as described above, the experiment test rig was set up as shown in **Figure 5-13**. The receptor compartment circuit is a closed circuit; with receptor reservoir to ensure equal volumes in both receptor and donor sides and to eliminate any air bubbles generated. As shown in **Figure 5-13** and **Figure 5-14**, the polycarbonate base (donor compartment) of INsmart device was used as part of the receptor in this setting while the donor compartment was on the outside. This receptor compartment plumbed with tubing was made closed circuit by emptying and drawing from a receptor reservoir. The circuit passes through the UV spectrometer to enable continuous monitoring of changes in solute concentration.

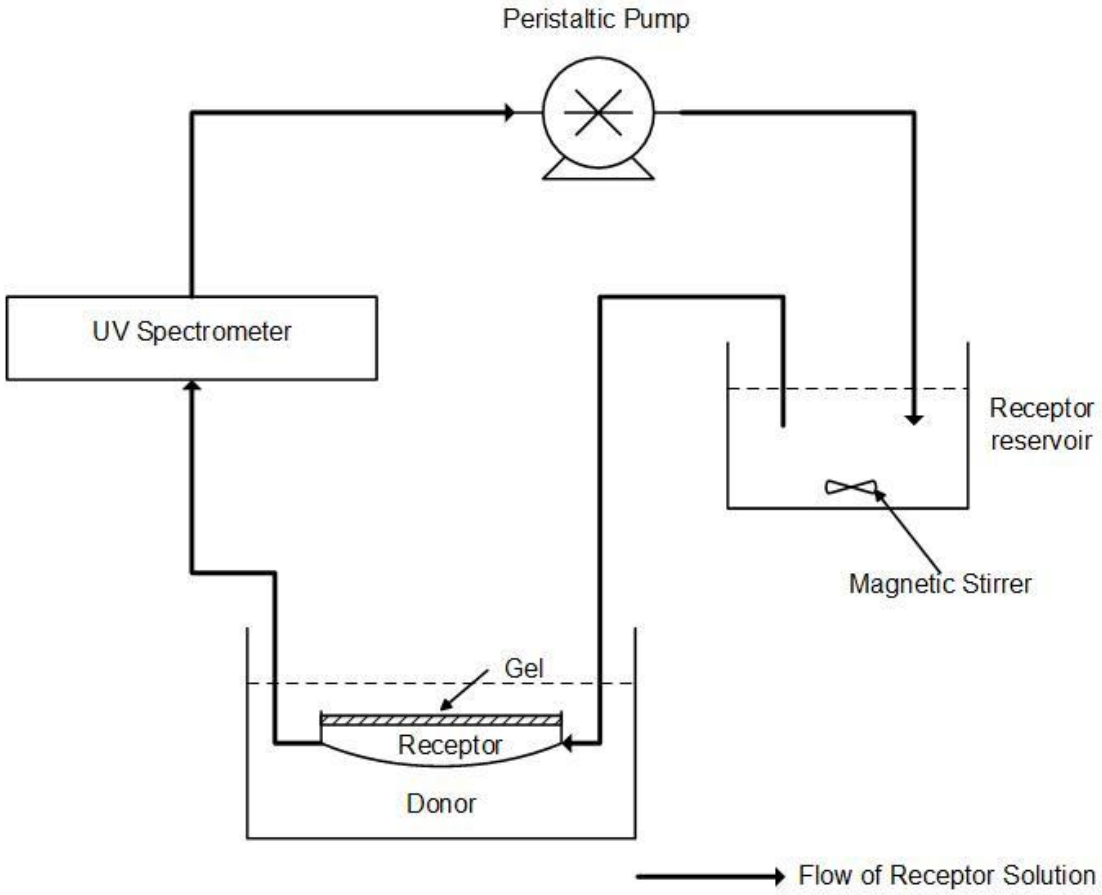

Figure 5-13: Schematic of the experimental set-up for diffusion of tartrazine in agarose gel housed within an adapted INsmart device.

Figure 5-14: Photographs of the experimental set-up for diffusion of tartrazine in agarose gel housed within the INsmart device.

After the INsmart device was assembled as described above the following steps were followed;

1) The assembled device with tubing was placed in the empty donor beaker.
2) The receptor reservoir with tubing from the device was placed on a magnetic stirrer, Electronic Stirrer Model 300 Rank Brothers Ltd, Cambridge, England.
3) The circuit was completed by placing a quartz flow cell in the Perkin Elmer UV/Vis Spectrometer Lambda 40
4) The Watson-Marlow 101U peristaltic pump and the UV spectrometer were switched on. The pump speed was kept constant with tubing volume output of 7.4 mL/min.
5) A known volume of water was placed in the receptor reservoir and passed through the entire circuit filling the device receptor compartment and ensuring no air bubbles were present in the circuit.
6) Magnetic stirrer was set to stir the receptor reservoir.

7) As soon as the blank reading was taken on the spectrophotometer, the tartrazine solution was placed in the donor beaker and the experiment was started to record readings at 1min interval.

8) The UV spectrophotometer monitored the amount of tartrazine dye diffusing through the gel from the donor side by recording the absorbance of the solution in the receptor side passing through the flow cell at 427 nm wavelength.

Measurements were taken at 1min intervals over time (minimum 5 hours). All experiments were performed at 20°C and in triplicate. The UV Winlab wavelength program application provided by PerkinElmer, UK enabled time dependent absorbance measurements at fixed wavelengths at defined time intervals over a specified period of time. The UV Winlab software in wavelength mode was set to the above wavelength to record absorbance measurements per minute. A macro, Waveprog was used to group data for import into Excel for concentration time plots. The absorbance at 427 nm wavelength was found to be linear to tartrazine concentration (0-20 μg/mL) thus enabling simple conversion of absorbance data into concentration values observed for tartrazine as shown in the calibration curve **Figure 5-15**.

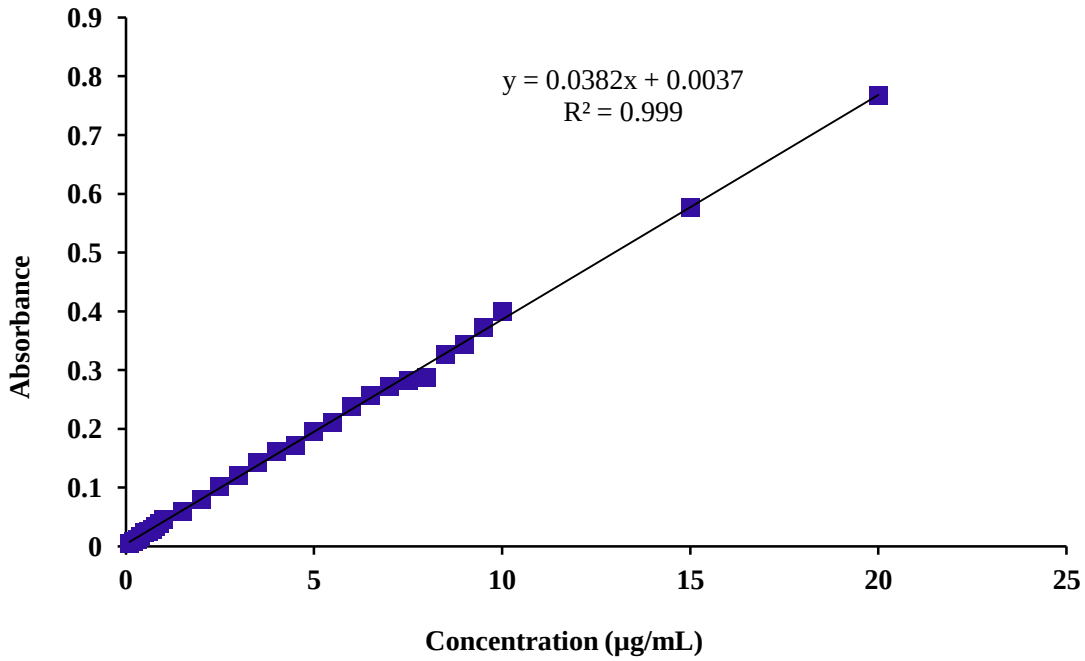

Figure 5-15: Calibration graph for tartrazine (0-20 µg/mL) (using quartz flow cell). (Data represent mean±SD of ten measurements, error bars present but may not be visible as smaller than marker size).

Absorbance data was converted into tartrazine concentration using the calibration curve, **Figure 5-15**. The data was plotted based on the mathematical methods; Laplace transform, QSS, TL slope and TL intercept methods for calculating diffusion coefficient as discussed in **Section 5.3.4**.

5.5.2 Results and discussion

The diffusivities of tartrazine in agarose gel concentrations 2% and 1.5% w/w were determined using the Laplace transform, QSS, TL slope and TL intercept methods and are presented in **Table 5-2**.

Table 5-2: Diffusion coefficient values (D and D_e) for tartrazine in agarose gel using INsmart device determined using Laplace transform, QSS, TL slope and TL intercept methods. The number of replicate measurements is shown by n=x.

Agarose gel concentration	**Laplace transform**	**QSS**	**TL slope**	**TL intercept**
(% w/w)	$\boldsymbol{D \times 10^{-10}}$ **(m^2/s)**	$\boldsymbol{De \times 10^{-10}}$ **(m^2/s)**	$\boldsymbol{D \times 10^{-10}}$ **(m^2/s)**	$\boldsymbol{D \times 10^{-10}}$ **(m^2/s)**
2 (n=4)	0.34 ± 0.05	2.47 ± 0.44	1.72 ± 0.30	2.11 ± 0.23
1.5 (n=1)	0.38	2.38	1.66	2.56

It can be seen in **Table 5-2** that the diffusivities estimated using the Laplace transform method for tartrazine diffusion in device are a decade slower than the values determined using QSS, TL slope and TL intercept methods. Diffusion coefficient values (D or D_e) for tartrazine determined using QSS, TL slope and TL intercept methods were found to be similar (D: 1.72-2.47x10^{-10} and 1.66-2.56x10^{-10} m^2/s for 2 and 1.5 %w/w agarose gel respectively). The diffusivity of tartrazine in 2% w/w agarose gel determined in the INsmart device was also comparable to D values obtained when determined using tube where the D values in 2% w/w agarose with equal donor and receptor side volumes using the Laplace transform, QSS and TL slope method was 2.0 – 6.14x10^{-10} m^2/s.

Using the experimental set-up with the INsmart device a QSS state was achieved and the QSS and TL methods gave reliable results. Hence these mathematical models can be taken forward for future diffusivity estimations.

The experimental data are graphically presented for the Laplace transform method the data has been presented as C_x/C_0 vs. Time(s), for QSS method ln ($C_{A(t)}$-$C_{B(t)}$ /$C_{A(t0)}$-$C_{B(t0)}$) vs. Time(s) and for TL slope and TL intercept method Q(g) vs. Time(s), representative data for 2.0 %w/w and 1.5 %w/w agarose gels are presented in **Appendix 3**, **Figure A3-6** and **Figure A3-7**, respectively.

5.6 Determination of diffusion coefficient of tartrazine in non-polymerised dex2M-conA mixture in INsmart device

Mixtures of dextran, molecular weight 2 million daltons (dex2M) and concanavalin A (conA) will be referred to as non-polymerised dex2M-conA gel (NP gel) hereafter.

In the previous section it was understood that the Laplace transform method for tartrazine diffusion in device did not give comparable diffusion coefficient values to those determined using QSS, TL slope and TL intercept method which were all found to be similar. Therefore these three mathematical models are being taken forward for diffusivity estimations of tartrazine in NP gel in device.

Diffusivity of tartrazine was determined in presence of physiologically relevant glucose concentrations. As glucose responsiveness forms the basis for the closed-loop drug delivery mechanism of the INsmart device, the effect of this response on the diffusivity of tartrazine was determined. Here, glucose concentration of 0.1% w/w as used in the experiments corresponds to ~5.5 $mmolL^{-1}$ the basal normal limit of fasting plasma glucose for most individuals, 0.2% w/w corresponds to ≥ 11.1 $mmolL^{-1}$ which is indicative of diagnosis of diabetes and higher concentrations of 0.5% w/w (27.75 $mmolL^{-1}$) and 1% w/w (54 $mmolL^{-1}$) are instances of glucose challenges following a very high sugary meal.

5.6.1 Experimental set-up and procedure for diffusion

The experimental set-up and data analysis procedures followed were exactly the same as described in **Section 5.5.1**, the only difference being that NP gel was used instead of agarose. A 3 mm gel spacer was filled with weighed amount of NP gel and dialysis membrane with a molecular weight cut-off of 100 kDa was used. All experiments were performed at 20°C.

For experiments investigating the impact of reduced gel viscosity which occurs in the presence of glucose, a relevant amount of glucose was added to the donor tartrazine solution, mixed with the gel and in the receptor solution to keep the concentration of glucose the same throughout in order to eliminate any osmotic interference and possibly

density interference and to determine the true diffusivity of tartrazine in presence of a range of different relevant glucose concentrations.

For diffusivity estimation experiments of tartrazine in presence of glucose, calibration curves for tartrazine containing the relevant glucose concentrations were generated each time.

5.6.2 Results and discussion

The diffusivities of tartrazine in NP gel in the presence of different glucose concentrations were determined using QSS, TL slope and TL intercept methods. The results are as presented in **Table 5-3**.

Table 5-3: Diffusion coefficient values (D and D_e) for tartrazine in NP gel in presence of glucose determined using QSS, TL slope and TL intercept methods. The number of replicate measurements is shown by n=x.

Glucose concentration in NP gel	**QSS**	**TL slope**	**TL intercept**
(% w/w)	***De* × 10^{-10} (m^2/s)**	***D* × 10^{-10} (m^2/s)**	***D* × 10^{-10} (m^2/s)**
0 (n=2)	0.54 ± 0.06	0.38 ± 0.04	0.73 ± 0.02
0.1 (n=1)	0.87	0.61	0.85
0.5 (n=1)	0.93	0.65	1.00

It can be seen in **Table 5-3** that the diffusion coefficient values (D or D_e) for tartrazine determined using QSS, TL slope and TL intercept methods are in close agreement based on the limited data set available. Higher diffusion coefficient values for tartrazine with increasing glucose concentration were observed in a graded manner as shown in **Figure 5-16**.

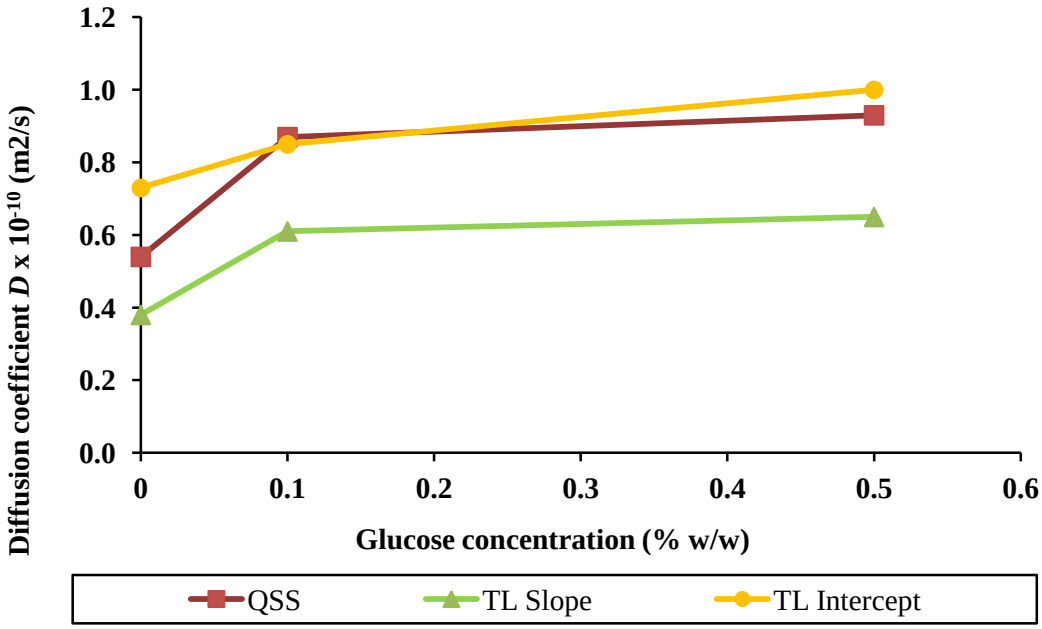

Figure 5-16: Increasing diffusion coefficient values for tartrazine in NP gel in presence of glucose determined using QSS, TL slope and TL intercept methods.

The diffusion coefficient for tartrazine increases with increasing glucose concentration. The diffusivity of tartrazine increased in the gel containing 5.4 mmol/L (0.1 %w/w) as the viscosity of the gel decreased to aid free movement of tartrazine molecules, further fall in viscosity in gel containing 27.75 mmol/L (0.5 % w/w)of glucose did not make much difference to the diffusivity of tartrazine. This could be due to the fact that tartrazine being a small molecule, its free movement is impeded by the micro viscosity created by increased glucose molecules.

Representative experimental data are graphically presented in **Appendix 3**; data for NP gel with no glucose is presented in **Figure A3-8**, with 0.1 %w/w glucose in **Figure A3-9** and with 0.5 %w/w glucose is presented in **Figure A3-10**.

5.7 Determination of diffusion coefficient of fluorescein sodium in NP gel in INsmart device

The diffusivity of fluorescein sodium, which has a smaller size than tartrazine, was determined to gain some estimation for diffusivity of glucose in NP gel and to aid with

experimental technique development using a fluorimeter, which is required later for determination of fluorescently labelled insulin diffusion through the gel as presented in **Chapter 7**.

Here effect of gel thickness (pathlengths) and two batches of conA used to prepare NP gel on diffusivity were also investigated.

5.7.1 Experimental set-up and procedure for diffusion

The device was assembled as described in **Section 5.5.1**. Experiments were performed using 2.50 mm gel spacer and then with a 1.17mm gel spacer with an aim to reduce the amount of gel used. Dialysis membrane with molecular weight cut off of 100 kDa was used. All experiments were performed at 20°C.

One major modification to the experimental device set-up was to mimic the diffusion cell design, to this effect; the INsmart device was coupled with a receptor compartment. They were held together by an in-house developed system made of perspex which could be tightened to ensure a perfect seal as shown in **Figure 5-17**. Parafilm and silicone gel was applied at the point of contact to further ensure the seal. The receptor compartment also had luer connections for plumbing tubing.

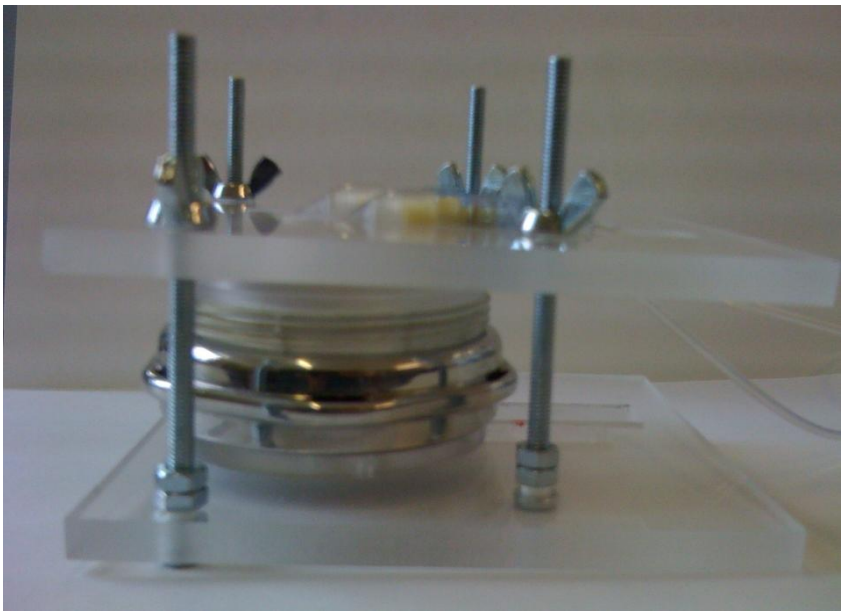

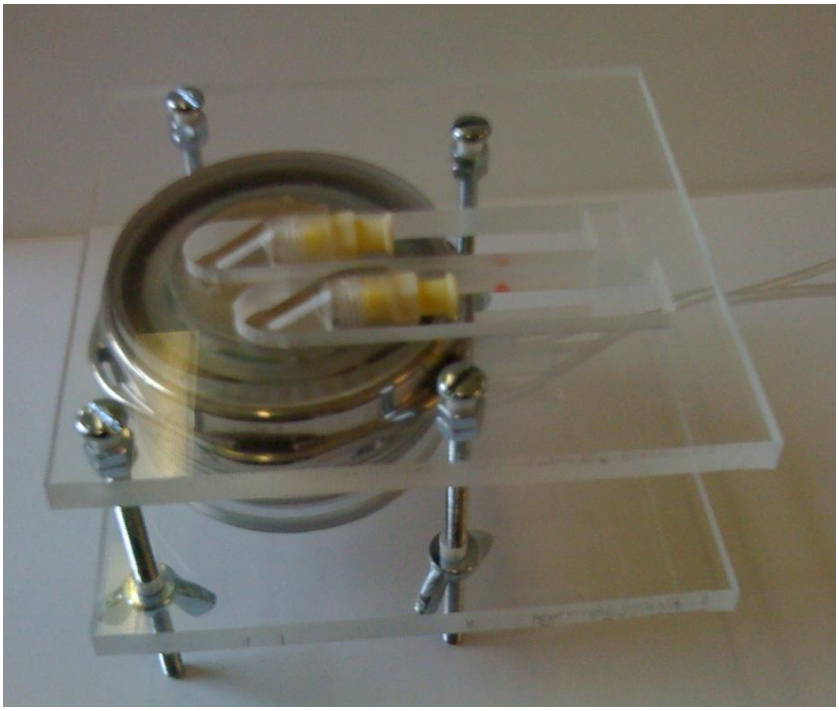

Figure 5-17: Diffusion cell design using the INsmart device**.**

The schematic of the experimental set up is as presented in **Figure 5-18** and as shown in **Figure 5-19**;

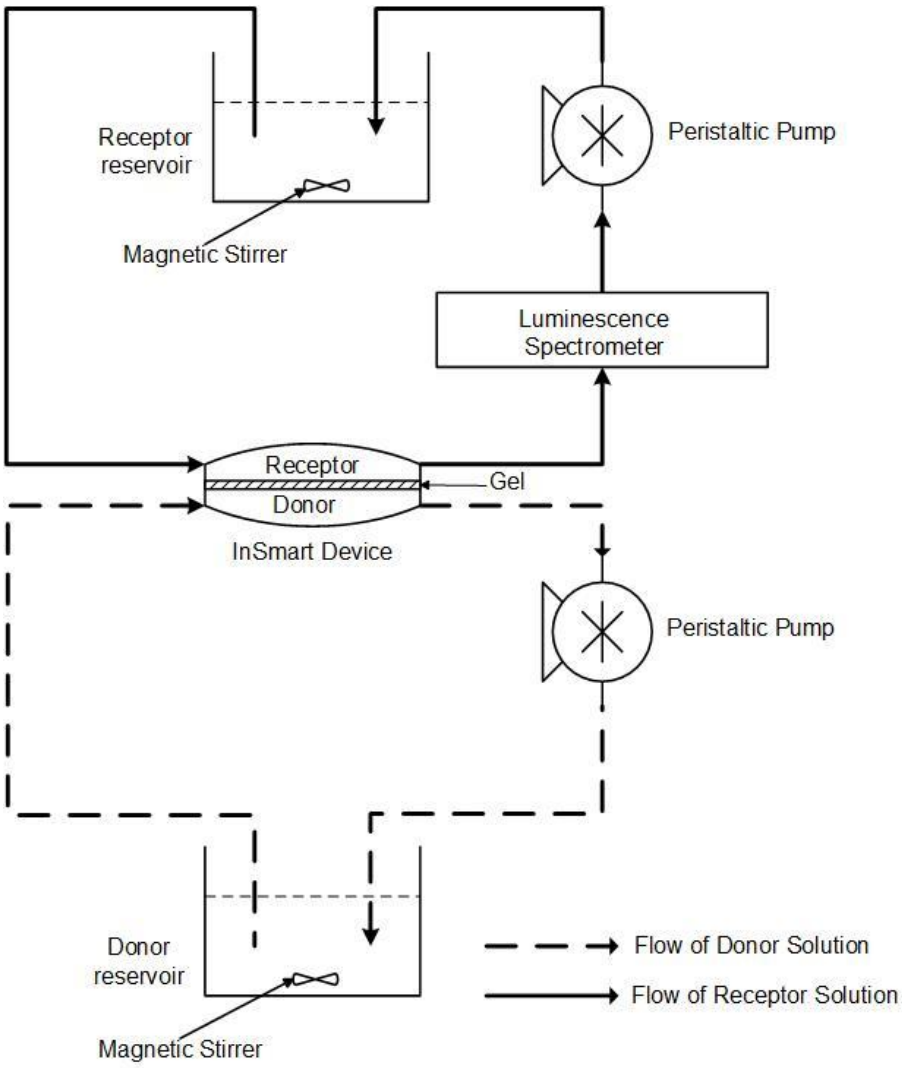

Figure 5-18: Schematic of the experimental set-up for diffusion of fluorescein sodium in NP gel housed within the INsmart device.

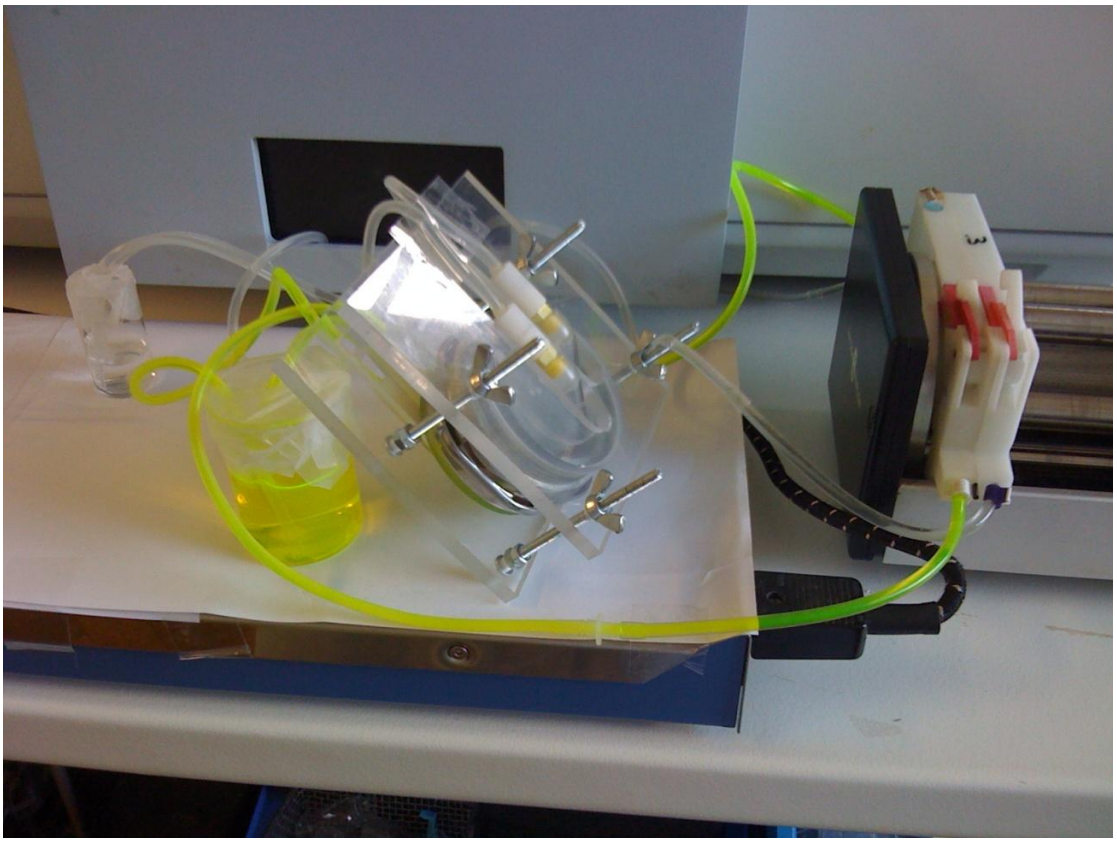

Figure 5-19: Photograph of the experimental set-up for diffusion of fluorescein sodium in NP gel housed within the INsmart device.

The test rig comprised of the receptor and donor compartment circuits forming a closed circuit system; both sides have a reservoir in the circuit in order to maintain same volumes.

For experiments investigating the impact of reduced gel viscosity in the presence of glucose, relevant amount of glucose was added to the donor fluorescein sodium solution, the gel and the receptor solution to eliminate any osmotic interference and to determine the true diffusivity of fluorescein sodium in the presence of a range of different relevant glucose concentrations.

The NP gel was prepared as described in **Section 5.3.3**. After the INsmart device was assembled the following steps were followed;

1) The donor reservoir containing fluorescein sodium solution of known concentration and volume and the receptor reservoir containing distilled water with glucose of same volume were placed on a magnetic stirrer.

2) The fluorimeter, PerkinElmer LS55 Luminescence Spectrometer was switched on at least 15 min before the start of the experiment. The method was set-up using the FLWinlab wavelength program, with fluorescence intensity measurements recorded at every 1 min interval.

3) The circuit was set-up using tubing as shown in **Figure 5-18**.

4) The peristaltic pump (Watson-Marlow 101U) speed was kept constant, with tubing volume output of 9.8 mL/min, to draw only the receptor solution first into the device receptor compartment ensuring the compartment was full with no air bubbles. The receptor side was made closed circuit by emptying into and drawing from the same receptor reservoir. All the tubing was checked to ensure there were no air bubbles. The receptor solution passed through a special fluorimeter quartz flow cell (with 3 sides clear) which was placed in the fluorimeter.

5) The background reading was taken which the software subtracts from the measurements. As soon as the blank reading was taken, the device donor compartment was filled with fluorescein sodium solution by placing the tubing in the donor reservoir. Measurements were started when the device donor compartment was filled with the donor fluorescein sodium solution.

6) The Fluorimeter monitored the amount of dye diffusing through the gel from the donor side by recording the absorbance of the solution in the receptor side passing through the flow cell at 515 nm wavelength.

7) As fluorescein sodium is photosensitive, the entire set-up was protected from light by covering with a black paper.

Fluorescein sodium shows strong fluorescence at excitation wavelength 485nm and emission wavelength 515 nm as shown in **Figure 5-20**. The FL Winlab software in wavelength mode was set to the above excitation and emission wavelengths to record fluorescence measurements per minute. Sampling was performed over a period of minimum of 5 hours.

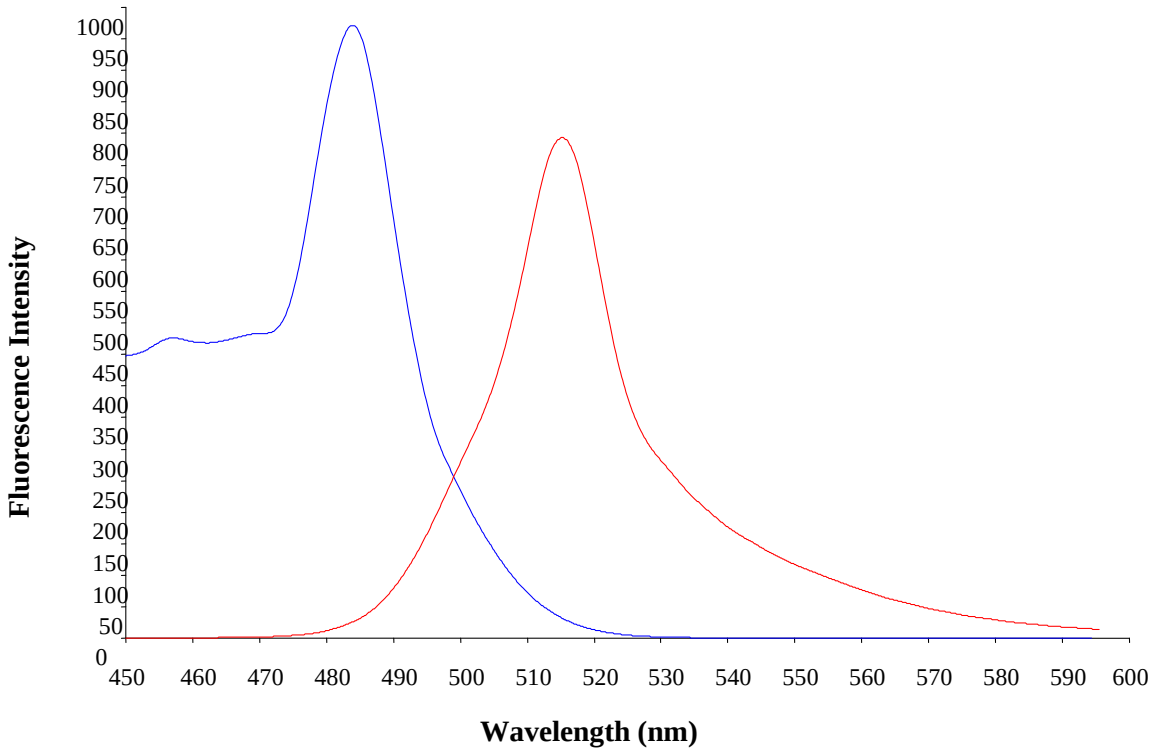

Figure 5-20: Fluorescence spectrum for fluorescein sodium showing strong fluorescence intensity at excitation wavelength 485 nm and emission wavelength 515 nm.

The fluorescence data was imported into Excel to produce concentration versus time plots. The fluorescence intensity at 515 nm wavelength was linear with respect to fluorescein sodium concentration thus enabling simple conversion of intensity data into concentration values observed for fluorescein sodium using the calibration curve shown below in **Figure 5-21**.

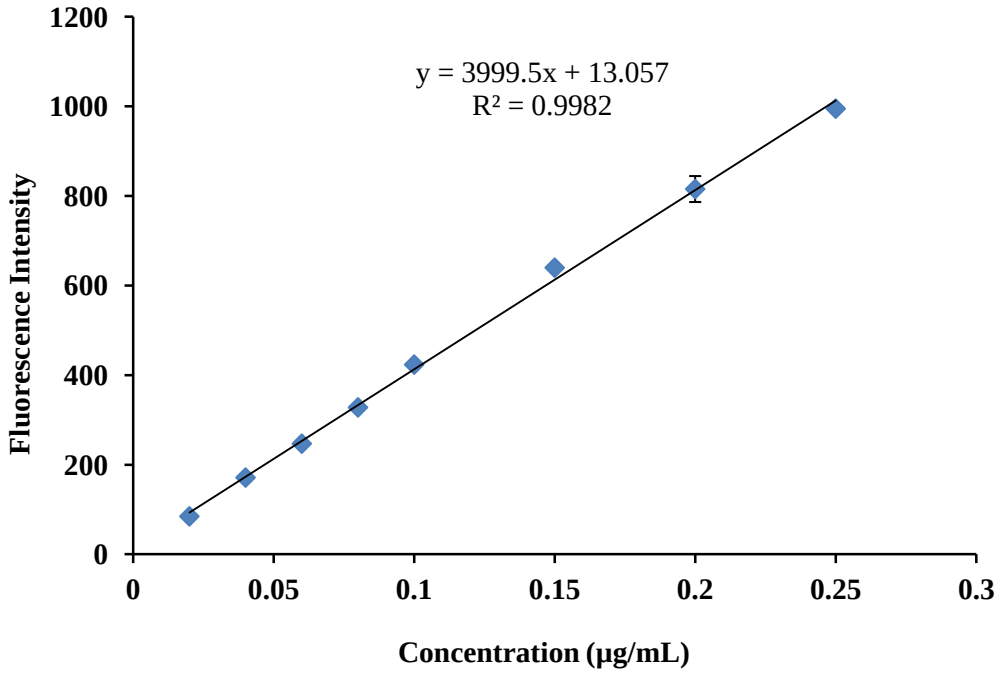

Figure 5-21: Calibration graph for fluorescein sodium (0-0.25 µg/mL) ((using fluorimeter quartz flow cell). (Data represent mean±SD of four measurements, error bars present but may not be visible as smaller than marker size).

For diffusivity experiments of fluorescein sodium in presence of glucose, a calibration curve for fluorescein sodium containing the relevant concentration of glucose was generated each time.

For experiments investigating the impact of reduced gel viscosity in the presence of glucose, a calibration curve for fluorescein sodium containing the relevant concentration of glucose was generated.

Data Analysis

The fluorescence intensity data was first converted into fluorescein sodium concentration using the calibration curve as shown in **Figure 5-21**. The data was plotted based on the mathematical methods; QSS, TL slope and TL intercept method for calculating diffusion coefficient as described in **Section 5.3.4.**

5.7.2 Results and Discussion

The diffusivities of fluorescein sodium in NP gel with 0 and 0.1% w/w glucose concentration were determined using QSS; TL slope and TL intercept methods. The results are as presented in **Table 5-4**;

Table 5-4: Diffusion coefficient values (D and D_e) for fluorescein sodium in NP gel in absence and presence of 0.1% w/w glucose determined using the QSS, TL slope and TL intercept methods. The number of replicates for each experiment was 2.

Glucose concentration in NP gel	**QSS**	**TL slope**	**TL intercept**
(% w/w)	$\boldsymbol{De \times 10^{-10}}$ **(m^2/s)**	$\boldsymbol{D \times 10^{-10}}$ **(m^2/s)**	$\boldsymbol{D \times 10^{-10}}$ **(m^2/s)**
0	0.82 ± 0.03	0.81 ± 0.03	0.91 ± 0.04
0.1	0.85 ± 0.02	0.85 ± 0.01	0.84 ± 0.14

As shown in **Table 5-4** the diffusion coefficient values (D or D_e) for fluorescein sodium determined using the QSS, TL slope and TL intercept methods were in close agreement. Higher diffusion coefficient values for fluorescein sodium in the presence of glucose are due to drop in viscosity of the gel which aids higher diffusivity. Representative experimental data using the three methods are graphically presented in **Appendix 3**, **Figure A3-11** for NP gel with no glucose and **Figure A3-12** for NP gel with 0.1% w/w glucose.

Effect of gel thickness on fluorescein sodium diffusion coefficient values

With an aim to reduce the amount of gel used, reduced gel thickness (pathlength) was investigated. The impact of a reduced gel thickness of 1.17 mm over 2.50 mm on the diffusivity of fluorescein sodium was assessed. The gel spacer thickness should not affect the diffusivity D values for fluorescein sodium, though the profile of flux might be different.

The experiments for estimating diffusivities of fluorescein sodium in NP gel using 2.50 mm and 1.17 mm gel spacer were performed using gel with 0.1% w/w glucose. The diffusivities were determined using QSS, TL slope and the TL intercept methods. The results are as presented in **Table 5-5**.

Table 5-5: Diffusion coefficient values (D and D_e) for fluorescein sodium in NP gel with 0.1% w/w glucose determined for 2.50 mm and 1.17 mm gel thickness using QSS, TL slope and TL intercept methods (limited number of repeats due to shortage of conA).

NP gel thickness	**QSS**	**TL slope**	**TL intercept**
(mm)	$\boldsymbol{De \times 10^{-10}}$ **(m^2/s)**	$\boldsymbol{D \times 10^{-10}}$ **(m^2/s)**	$\boldsymbol{D \times 10^{-10}}$ **(m^2/s)**
2.50	0.78	0.78	0.86
1.17	0.79	0.78	1.88

The diffusion coefficient values (D or D_e) for fluorescein sodium determined using the QSS and TL slope methods for the two gel thickness were in close agreement based on the limited data set available; however the TL intercept method gave higher value for 1.17 mm gel thickness compared to the 2.50 mm gel thickness, as the time lag has been reduced due to reduced pathlength. This attribute is useful if a faster delivery is required when the device is first placed in the receptor environment. The data (limited) also suggests the unreliability of the TL intercept method for determination of diffusion coefficient.

Representative experimental data are graphically presented in **Appendix 3**; **Figure A3-13** for NP gel with 0.1% w/w glucose with 2.50 mm and 1.17 mm gel thickness.

Comparison of effect of two different batches of conA on fluorescein sodium diffusivity in NP gel with no glucose in device

Batch to batch consistency of available conA was investigated to assess its impact on diffusivity of fluorescein sodium. The reason for this being that one of the batches of conA was found to be slightly different from previous conA batch that was used in

previous experiments in terms of both the appearance of the gel formed and its gelling properties; the gel formed was very opaque and sloppy; when the same procedure for gel preparation as described in **Section 5.3.3** was followed. It was eventually found that the gel formed had a pH below 6 and on adjusting the pH above 7, it displayed similar gelling and glucose responsiveness as the gel prepared using the first conA batch. The pH of the gel prepared using the new conA batch was adjusted to physiological pH7.6 and it appeared clear after storage at 4°C for 24 hours. Hereafter, the gel formed using the first conA batch will be referred to as NP1 and one prepared using the second conA batch will be referred to as NP2. Some preliminary assessments were performed to compare the results obtained using the two conA batches. Rheological assessments of the gels formed using the two conA batches showed that the NP2 gel produced higher viscosity profiles with time compared to NP1 gel however both show graded response to increasing glucose concentrations. The comparison of the viscosity profiles for the two NP gels highlighted the batch to batch variation of conA that should be considered when preparing and using these gels, refer to **Chapter 6, Section 6.3.1** for the rheological assessments.

Diffusivity experiments were performed on NP gels prepared using the two batches of conA in the absence of glucose to compare the effect on fluorescein sodium diffusivity. The diffusivities were determined using QSS, TL slope and TL intercept methods. The results are as presented in **Table 5-6**.

Table 5-6: Diffusion coefficient values (D and D_e) for fluorescein sodium in NP gel prepared using two different conA batches determined using QSS, TL slope and TL intercept methods (**Note:** the data for first conA batch is using 2.50 mm gel spacer and for the second conA batch is using 1.17 mm gel spacer). The number of replicates for each experiment was 2.

NP gel with no Glucose	**QSS**	**TL slope**	**TL intercept**
	$\boldsymbol{De \times 10^{-10}}$ **(m^2/s)**	$\boldsymbol{D \times 10^{-10}}$ **(m^2/s)**	$\boldsymbol{D \times 10^{-10}}$ **(m^2/s)**
NP1 gel (first conA)	0.82 ± 0.03	0.81 ± 0.03	0.91 ± 0.04
NP2 gel (second conA)	0.79 ± 0.04	0.79 ± 0.04	0.49 ± 0.00

The diffusivity of fluorescein sodium in NP1 gel was determined through a gel thickness of 2.50 mm compared to 1.17 mm for NP2 gel, this should not affect the diffusion coefficient value calculated but does affect the lag time (time when fluorescein sodium starts appearing in the receptor compartment). The diffusion coefficient values (D or D_e) for fluorescein sodium determined using QSS and TL slope methods for the two conA batches were in close agreement; however the TL intercept method showed that using the second conA a slower value compared to the first conA batch as expected due to the difference in pathlength (gel thickness).

Representative experimental data are graphically presented in **Appendix3**; **Figure A3-14** for NP gel with two different batches on conA.

5.8 Chapter summary

An experimental protocol was developed and suitable mathematical models were applied with an aim to determine the insulin diffusivity through the glucose-responsive gel in the INsmart device. A sequential approach adopted here has enabled to select a suitable system and mathematical model using a model dye (tartrazine) in a model gel (agarose) initially for determining diffusivity of a solute molecule.

A simple diffusion cell (using a tube) investigated initially using model dye, tartrazine through a model gel, agarose allowed a quick, easy and efficient system to test feasibility of the system to determine diffusion properties of a molecule with a small size through a hydrophilic gel. The four mathematical methods for determining the diffusion coefficient namely: Laplace transform, diffusion cell-QSS, TL, slope and intercept analysis were assessed and compared for their applicability using the tube model and model dye and gel. The diffusivities of tartrazine determined in increasing agarose gel concentrations from 0.5% to 2% w/w using the four methods showed that the D values determined using the Laplace transform and QSS methods (D:0.70-1.04x10^{-10} to 0.2-0.32x10^{-10} m^2/s respectively) were significantly different from the values determined using the TL slope and TL intercept methods (D: 3.38 – 10.57x10^{-10} m^2/s). By ensuring that the volume in donor and receptor side were kept as close to each

other and that QSS was achieved, the *D* values for the Laplace transform, QSS and TL slope method matched (D= 2.0 – 6.14x10^{-10} m^2/s), however the *D* using the TL intercept method was found to be a decade faster (D=1.19x10^{-9} m^2/s). The *D* values for tartrazine (molecular weight 534.3 Da) in agarose gel was observed to be in the correct range in comparison to similar molecular weight solute, raffinose *D* value in aqueous solution as shown in **Table 5-7**. From the tube experiments, it was understood that it was paramount that the volumes in the donor and receptor compartments need to be kept the same and that the TL intercept method might not give consistent results.

Table 5-7: Reported diffusion coefficient values in aqueous solution and corresponding molecular weight of solutes from literature.

Solute	Molecular weight (Da)	Reported diffusion coefficient, *D* in aqueous solution (m^2/s)	Reference
Methanol	32	1.3×10^{-09} (25ºC)	(Friedman, 2008)
Urea	60	1.2×10^{-09} (25ºC)	(Friedman, 2008)
Glycerol	92	8.3×10^{-10} (25ºC)	(Friedman, 2008)
2-Deoxyglucose*	164	5.3×10^{-10}	(Hazel and Sidell, 1987)
Glucose	180	6.8×10^{-10} (25ºC)	(Friedman, 2008; RENKIN, 1954)
Antipyrine	188	6.8×10^{-10} (25ºC)	(Snyder et al., 2001)
Sucrose	342	5.5×10^{-10} (25ºC)	(Friedman, 2008)
Dexamethasone	392	$4.0 \pm 2.0 \times 10^{-10}$ (25ºC)	(Moussy, Dungel and Hersh, 2006)
Raffinose	504	4.2×10^{-10} (25ºC)	(Friedman, 2008)
Vitamin B12*	1355	4.1×10^{-10}	(Kanamori et al., 1994)
Insulin	5700	2.16×10^{-10} (37ºC)"	(WEBER, LOPEZ and ANSETH, 2009; Lin-Gibson et al., 2005)
Myoglobin	17000	1.5×10^{-10} (37ºC)"	(WEBER, LOPEZ and ANSETH, 2009; Lin-Gibson et al., 2005)
Trypsin Inhibitor	20000	1.45×10^{-10} (37ºC)"	(WEBER, LOPEZ and ANSETH, 2009; Lin-Gibson et al., 2005)
Carbonic Anhydrase	29000	1.35×10^{-10} (37ºC)"	(WEBER, LOPEZ and ANSETH, 2009; Lin-Gibson et al., 2005)
Ovalbumin	43000	1.07×10^{-10} (37ºC)"	(WEBER, LOPEZ and ANSETH, 2009; Lin-Gibson et al., 2005)
Bovine Serum Albumin	67000	0.89×10^{-10} (37ºC)"	(WEBER, LOPEZ and ANSETH, 2009; Lin-Gibson et al., 2005)

* Temperature for diffusion coefficient measurement not reported.

" *D* calculated by the Stokes-Einstein equation.

Following the tube diffusion experiments, experiments undertaken with the INsmart device using tartrazine and agarose gel held within the device, further aided in assessing the applicability of the four mathematical models for determination of diffusion coefficient with the device. Here the learning from the tube experiments in terms of maintaining similar volumes in donor and receptor side was incorporated in the experimental set-up. It was found that the Laplace transform method for tartrazine

diffusion in device (*D*: 0.34x10^{-10} and 0.38x10^{-10} m^2/s for 2 and 1.5 %w/w agarose gel respectively) did not give comparable diffusion coefficient values to those determined using QSS, TL slope and TL intercept method (*D*: 1.72-2.47x10^{-10} and 1.66-2.56x10^{-10} m^2/s for 2 and 1.5 %w/w agarose gel respectively), which were all found to be similar. This further suggested that using the experimental set-up a QSS state was achieved and the three mathematical models could be taken forward for diffusivity estimations of tartrazine in NP gel housed in the INsmart device.

It was observed that the diffusion coefficient values (*D*: 0.38-0.78x10^{-10} m^2/s) for tartrazine in NP gel in the device determined using QSS, TL slope and TL intercept methods were in close agreement. The higher diffusion coefficient values for tartrazine observed with increasing physiologically relevant glucose concentrations were as expected. The diffusivity of tartrazine increased in the gel containing 0.1 %w/w glucose (*D*: 0.61-0.87x10^{-10} m^2/s) as the viscosity of the gel decreased to aid free movement of tartrazine molecules, further fall in viscosity in gel containing 0.5 % w/w glucose (*D*: 0.65-1.0x10^{-10} m^2/s)did not make much difference to the diffusivity of tartrazine which could be due to the fact that tartrazine being a small molecule, its free movement is impeded by the micro viscosity created by increased glucose molecules.

The diffusivity of fluorescein sodium salt, a common fluorescent tracer of relatively small size was determined in order to develop the experimental method using the Luminescence spectrometer and to understand the diffusional properties of glucose through the NP gel due to the difficulty in determining its diffusivity in the NP gel as free glucose dismantles the gelatinous three- dimensional complex of the gel by competitive displacement thus dropping its viscosity which forms the basis for the responsiveness of the gel. The diffusivities of fluorescein sodium in NP gel with 0 and 0.1% w/w glucose concentration determined using QSS; TL slope and TL intercept methods show diffusion coefficient values (*D*: 0.81-0.91x10^{-10} and 0.84-0.85x10^{-10} m^2/s for 0 and 0.1 %w/w glucose respectively) for fluorescein sodium determined using the QSS, TL slope and TL intercept methods were in close agreement.

Diffusivity of fluorescein sodium determined for two different path lengths, 2.50 mm and 1.17mm (gel thickness) using QSS and TL slope methods were in close agreement

(D: $0.78x10^{-10}$ and $0.78\text{-}0.79x10^{-10}$ m^2/s for 2.50 and 1.17mm gel thickness respectively); however the TL intercept method gave higher value for 1.17mm gel thickness compared to the 2.50 mm gel thickness, due to reduced lag time *(D*: $0.86x10^{-10}$ and $1.88x10^{-10}$ m^2/s for 2.50 and 1.17mm gel thickness respectively). This attribute is useful if a faster delivery is required when the device is first placed in the receptor environment. However this also highlighted the unreliability of using only the TL intercept method for determination of diffusion coefficient.

Batch to batch variability in conA was highlighted during experimental work, as a second batch of conA formed a gel which differed in consistency, which on adjusting to pH 7.6 displayed similar gelling properties. Rheological assessments of the gels formed using the two conA batches highlighted the batch to batch variation of conA that must be considered when preparing and using these gels. Diffusivity experiments performed on NP gels prepared using the two batches of conA in the absence of glucose to compare the effect on fluorescein sodium diffusivity showed that diffusion coefficient values (*D*: $0.79\text{-}0.8x10^{-10}$ and $0.79x10^{-10}$ m^2/s for NP1 gel and NP2 gel respectively) for fluorescein sodium determined using QSS and TL slope methods for the two conA batches were in close agreement. The difference in values due to the TL intercept method (*D*: $0.89x10^{-10}$ and $0.49x10^{-10}$ m^2/s for NP1 gel and NP2 gel respectively) was attributed to the different gel thickness (pathlengths) used in the two experiments.

Chapter 6 Rheological testing of gels

6.1 Introduction

The design of the INsmart device for the management of diabetes is based on the small changes occurring in the glucose responsive gel in response to the diabetic physiological glucose levels and its corresponding ability to modulate the diffusion of insulin through the material. The viscoelastic properties of the material should be such as to allow the relevant degree of relaxation required to produce a change in state upon glucose triggering. The gels are actually mixtures as shown by their rheological tan delta values (which will be discussed later in this chapter), however throughout the thesis the mixtures are referred to as gels for simplicity.

The NICE recommended target fasting plasma glucose level ranges for most individuals is 4.0 to 5.9 $mmolL^{-1}$ (70 to 107$mgdL^{-1}$). Fasting plasma glucose concentration of >7.0 $mmolL^{-1}$ (126 $mgdL^{-1}$) or a 2 h postprandial plasma glucose concentration of >11.1 $mmolL^{-1}$ (200$mgdL^{-1}$) are reliably diagnosed as diabetes (NICE, 2004; World Health Organization Expert Committee, 1999; World Health Organization, 2011b). The device must always be able to deliver basal insulin amounts to cope with the continuous physiological release of glucose (glucose range from 4.0 to 5.9 $mmolL^{-}1$) from glycogen from the liver. The device also needs to deliver appropriate doses of insulin in response to post-prandial glucose levels above 5.9 $mmolL^{-1}$. A glucose concentration of 0.1% w/w as used in the experiments corresponds to a ~5.5 $mmolL^{-1}$. Therefore the glucose responsive gel needs to show a small change in viscosity between 0% and 0.1% w/w glucose and a major change between 0.1-1% w/w glucose, which is an upper glucose limit of ~55 $mmolL^{-1}$. The rheological characteristics of various dextran-concanavalin A mixtures have been extensively studied within the INsmart group over the last decade (Tanna et al., 2006a; Tanna et al., 2006b; Taylor et al., 2006). Learning from these was used to understand the behaviour of the glucose responsive gel used here.

The rheological properties of non-polymerised dex2M-conA mixture (NP mixture) prepared using two different batches of conA and the cross linked dexMA-conAMA mixture (CL mixture) used in *in vitro* diffusion studies in the presence of glucose were determined and compared. The mixtures were examined in the presence of glucose in oscillatory mode to yield viscoelastic properties of the mixtures and to gauge their glucose sensitivity and glucose responsiveness with respect to differential delivery of insulin from the device.

The rheological characteristics of glucose sensitive mixtures containing dextran and concanavalin A (conA) with and without glucose were studied using oscillatory rheometry at 20 and 37°C. The rheological data gathered in the linear viscoelastic (LVE) range were used to compare the mixtures used in *in vitro* diffusion studies.

A rheometer measures two independent variables namely the deflection angle and the phase shift angle in the constant torque, controlled shear stress oscillatory mode.

From this raw data, *G'* (storage modulus which is a measure of the stored energy, the elastic part), and *G"* (loss modulus which is a measure of the energy lost as heat, the viscous part), η^*, the complex viscosity and tan delta (the ratio of *G"/ G'*) of the viscoelastic mixtures were obtained.

6.2 Experimental

6.2.1 Preparation of NP mixture and CL mixture

The preparation of the non-polymerised dex2M-conA mixture (NP mixture) containing underivatised conA and dextran (RMM 2000 kDa) has been described in **Chapter5**, **Section 5.3.3.**

The cross-linked dex500MA-conAMA mixture (CL mixture) was prepared using methacrylated dextran 500 kDa, DS 3% (dex500MA) and methacrylated concanavalin A (conAMA), crosslinking them by irradiation for 5mins, which was enough to retain the gel behind a 100k dialysis membrane. Similar mixture was used in the previous *in vivo* pig studies. The preparation of the mixture has been described previously

(Taylor and Sahota, 2012). Briefly, conAMA (100 mg) was dissolved in distilled water (800 mg) and photoinitiator Irgacure® (0.178 µmoles) was added. Dex-MA (RMM 500Da) (100 mg) was added to the mixture and stirred to form a viscous solution, covered in foil and allowed to stand for 2 hours at room temperature; the mixture was then placed between two glass plates separated by a 60 µm thick gasket and was irradiated under UV-light (365 nm, 10 mJ cm^{-2}) for 5 minutes. The CL mixture formed was stored aseptically at 4° C for at least 24 hours prior to use.

For experiments with glucose, weighed amounts of glucose were added to the NP mixture or the CL mixture, mixed well and stored overnight at 4°C before use.

6.2.2 Rheological testing of mixtures

The rheological testing of the mixtures was conducted on a Physica MCR 300 rheometer (Anton Paar, Germany) with cone and plate geometry (CP 25-1) and Peltier temperature control. The tests were conducted in the non-destructive oscillation mode using controlled strain. NP mixtures (NP1 and NP2) formulated with dextran and two different batches of conA and CL mixture formulated with dexMA and conA MA, in the presence of glucose from 0 to 1% w/w have been compared at 20 and 37 ± 0.1°C using frequency sweeps. Firstly, a strain sweep between 0.1% and 10% was conducted at a frequency of 1Hz for all the mixtures containing no glucose and 1% w/w glucose respectively and a 1% strain value, which was within the LVE region for both samples, was selected for the subsequent frequency sweeps. The strain profile for all mixtures was linear - representative data for NP mixtures are presented in **Figure 6-1** and **Figure 6-2**. Frequency sweeps at this constant strain was then conducted between 0.01 and 50 Hz and a solvent trap was used to prevent sample dehydration during the test. All tests were done in triplicate using fresh sample for each test. Constant sample mass was used and care was taken to ensure that the sample geometry remained unchanged throughout the testing period. The rheological data generated in controlled strain across varying frequency range within the LVE ensured that any deformation applied to the sample did not destroy its structure and that no slippage occurred between the cone and plate. All rheological parameters examined were processed using the Anton Paar software.

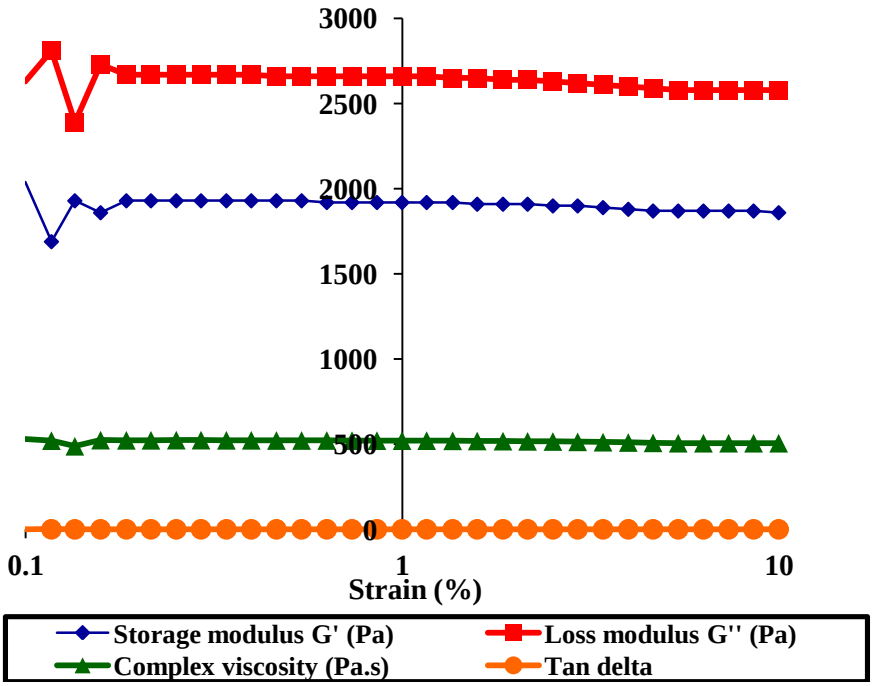

Figure 6-1: Storage modulus, loss modulus, complex viscosity and tan delta profiles across a strain sweep range of 0.1-10% at 20°C for NP2 mixture with no glucose.

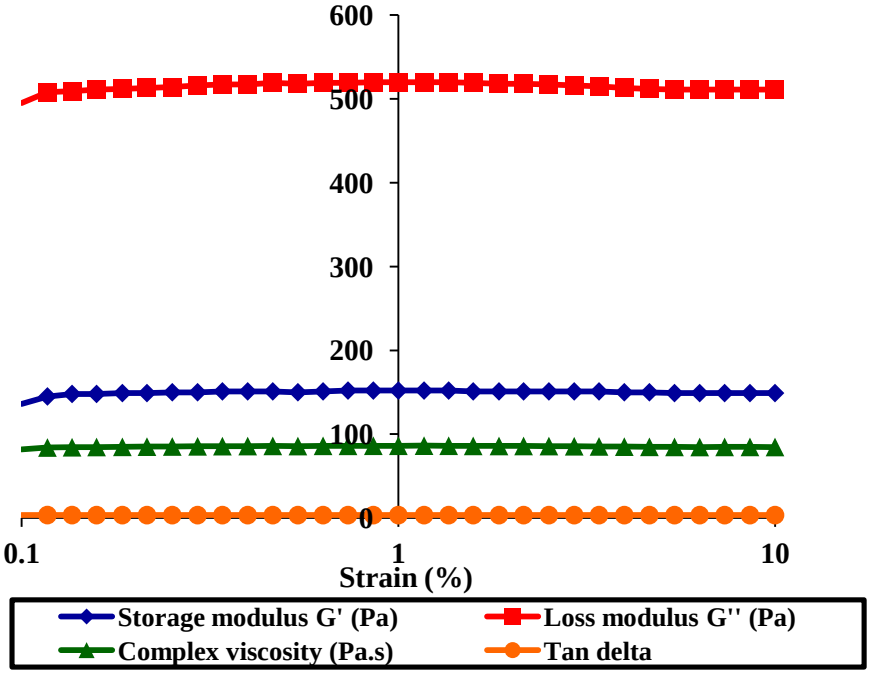

Figure 6-2: Storage modulus, loss modulus, complex viscosity and tan delta profiles across a strain sweep range of 0.1-10% at 20°C for NP2 mixture with 1% w/w glucose.

6.3 Results and Discussion

Dynamic rheological data was generated for the mixtures to compare and monitor their glucose sensitivities. **Figure 6-3 a-d** show the viscoelastic behaviour components *G'* (storage modulus), *G"* (loss modulus), η* (complex viscosity) and tan delta (the ratio of *G"/ G'*) throughout the chosen frequency range at 20°C for CL dexMA-conAMA mixture. **Figure 6-3 a and b** show an increase in both *G'* and *G"* as the frequency increased and there was a graded gradual decrease in the respective frequency sweep profiles with increasing glucose concentration. **Figure 6-3 c** shows complex viscosity decreasing across the frequency range suggesting pseudoplastic behaviour and a graded decrease in the frequency sweep profiles with increasing glucose concentration. These results confirm the ability of the cross linked mixture to interact reversibly with glucose, by dismantling the temporary three-dimensional network and forming a less viscous sol state by competitive displacement between free glucose and dextran. As the results show the viscoelastic changes (transformation from high viscosity gel-like to low viscosity sol-like state) occur in response to increasing glucose concentration it further confirms that the underlying mechanism of the smart glucose responsive gel is functioning and the lectin sites remain freely accessible and are not impeded by glucose ingress.

The complex viscosity profiles showing a graded gradual drop through the physiologically relevant glucose levels confirms the response criterion of the INsmart device in the control of diabetes. Tan delta frequency sweep profiles for the mixture show a decrease as the frequency is increased, however in the presence of glucose, the profiles show a graded increase with increasing glucose concentration. Tan delta which is a ratio of the loss modulus to the storage modulus and a value above 1 indicates a material with dominant liquid-like behaviour and a value below 1 show a material with dominant elastic (solid-like) behaviour. As all values at 1Hz are above 1, it would indicate that the glucose responsive gels exhibit predominantly liquid-like behaviour and hence are referred to as mixtures. The tan delta profiles suggest with increasing physiologically relevant glucose concentration the mixture shows increasing liquid-like behaviour.

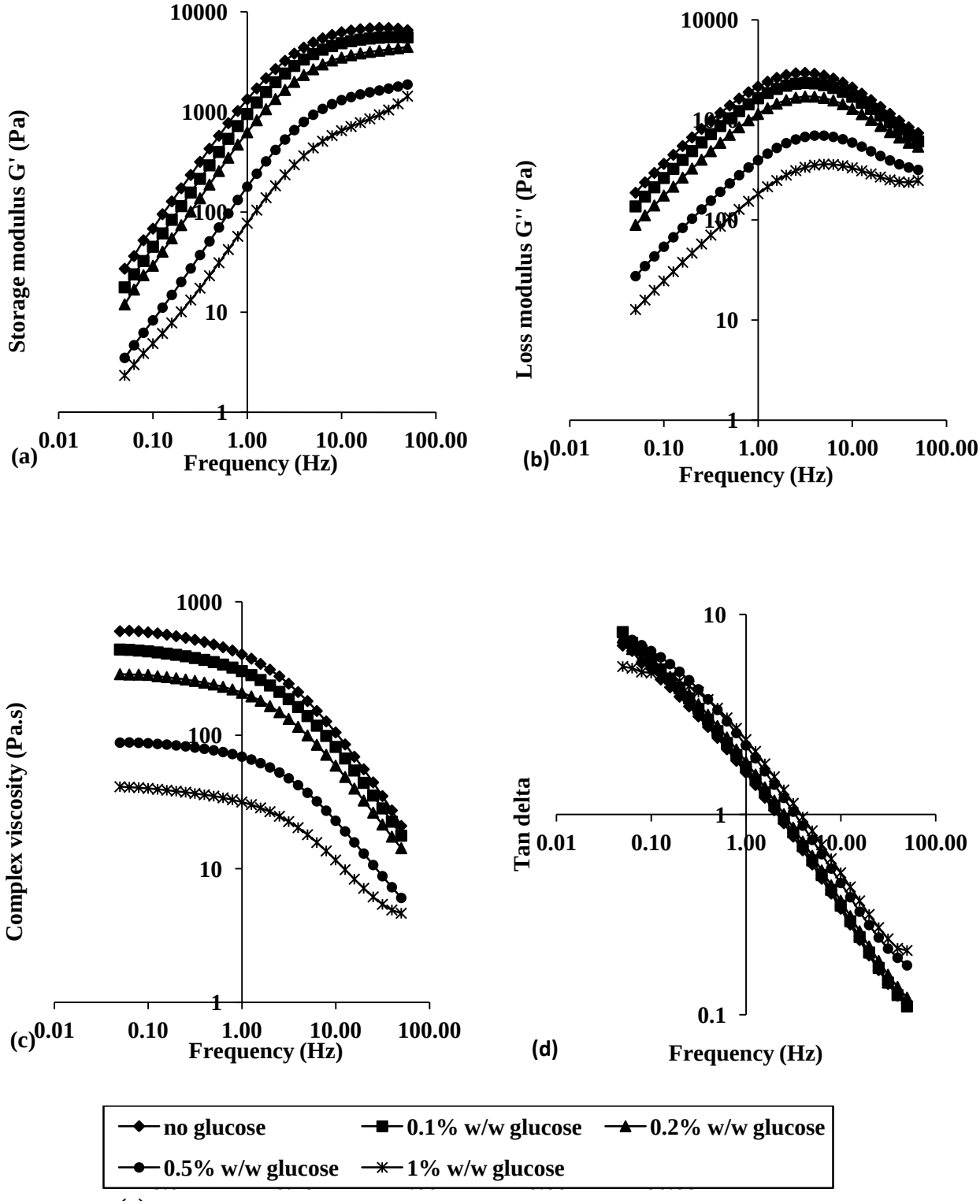

Figure 6-3: (a) Storage modulus, **(b)** loss modulus, **(c)** complex viscosity and **(d)** tan delta profiles across a frequency range of 0.05-50Hz at 20°C for CL mixture with increasing glucose concentrations.

For all the mixtures studied, the general trends of *G'*, *G"*, complex viscosity and tan delta from frequency sweep profiles with increasing glucose was similar to that described in **Figure 6-3 a-d**. For purposes of comparison of mixtures with different levels of glucose, indicating their glucose responsiveness, further data were compared at a single frequency of 1 Hz (mid-way through the frequency sweeps).

A comparison for the viscoelastic behaviour components *G'*, *G"*, complex viscosity and tan delta for the NP mixtures prepared using two different batches of conA (NP1 and NP2) and CL mixture at 20°C and 37°C with increasing glucose concentrations are presented in **Figure 6-4** to **Figure 6-7**.

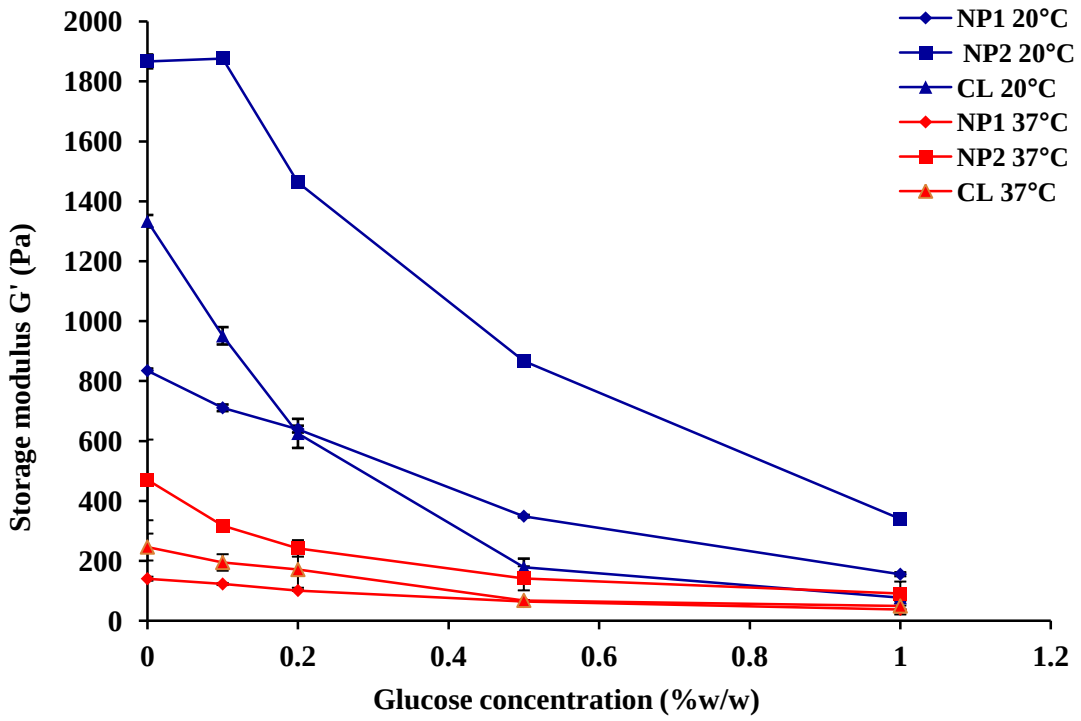

Figure 6-4: Storage modulus values at different glucose concentrations for the three mixtures at 20 and 37°C. Data were taken at a frequency of 1 Hz from frequency sweeps conducted in the range 0.01-50 Hz. (Data represent mean±SD of three measurements)

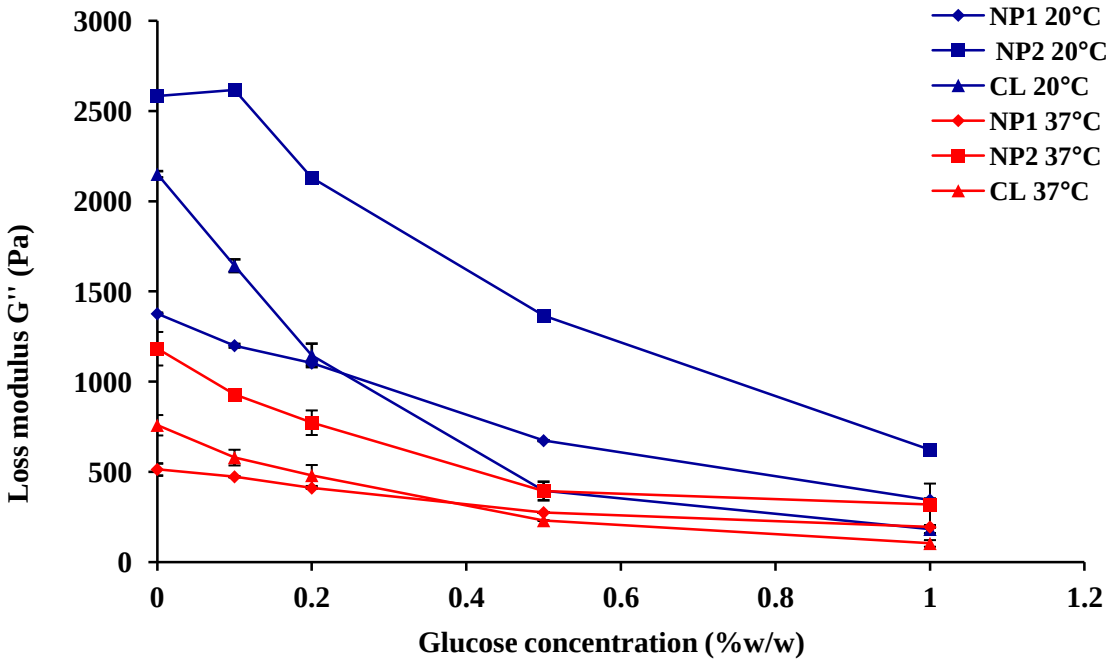

Figure 6-5: Loss modulus values at different glucose concentrations for the three mixtures at 20 and 37°C. Data were taken at a frequency of 1 Hz from frequency sweeps conducted in the range 0.01-50 Hz. (Data represent mean±SD of three measurements)

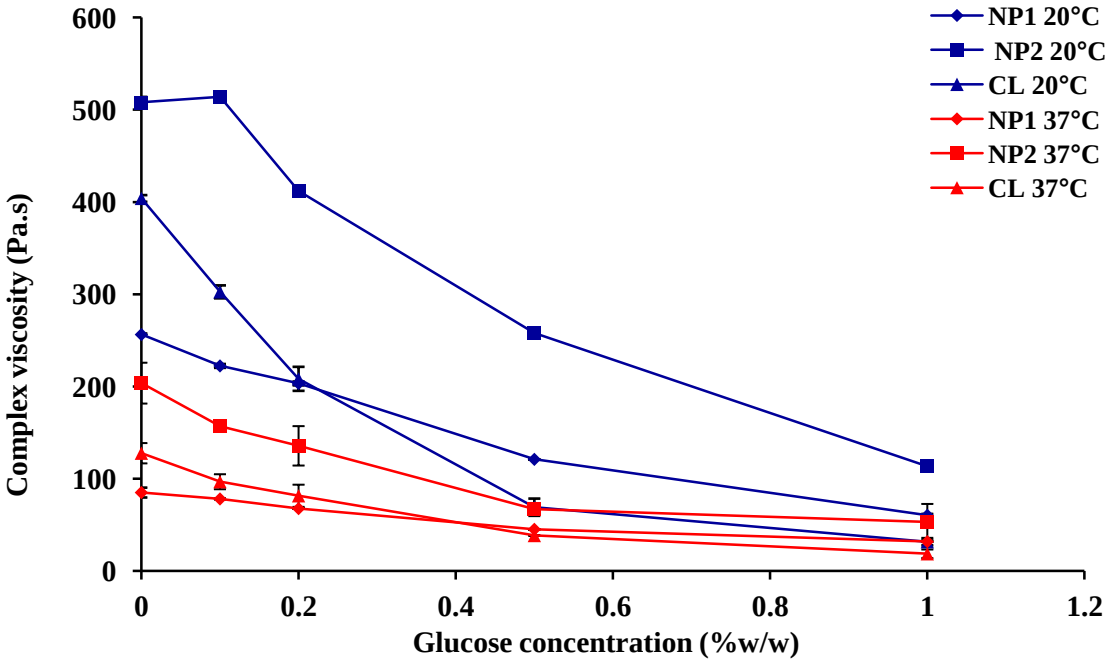

Figure 6-6: Complex viscosity values at different glucose concentrations for the three mixtures at 20 and 37°C. Data were taken at a frequency of 1 Hz from frequency sweeps conducted in the range 0.01-50 Hz. (Data represent mean±SD of three measurements)

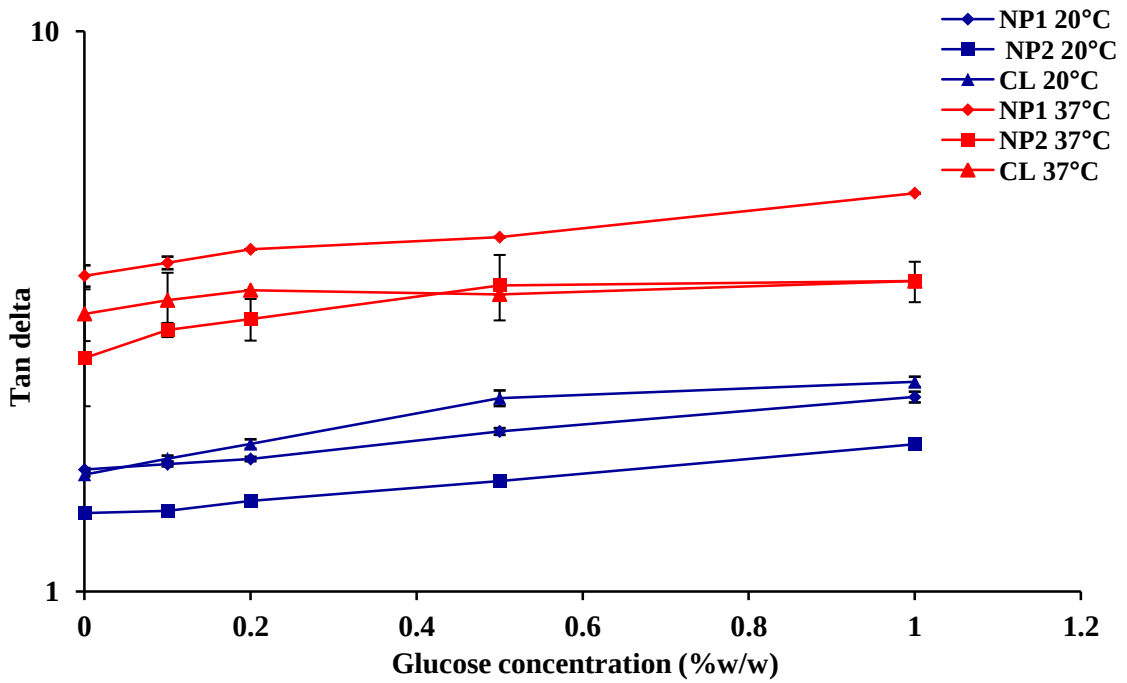

Figure 6-7: Tan delta values at different glucose concentrations for the three mixtures at 20 and 37°C. Data were taken at a frequency of 1 Hz from frequency sweeps conducted in the range 0.01-50 Hz. (Data represent mean±SD of three measurements)

6.3.1 Comparison of the mixtures

The NP2 mixture produced higher viscosity profiles with time compared to NP1and CL mixtures. The comparison of the viscosity profiles for the two NP mixtures highlight the batch to batch variation of conA that need to take into account when preparing and using these mixtures. The NP mixtures were used in the *in vitro* diffusion studies initially for technique and experimental model development. These mixtures were non-polymerised mixtures and used a higher molecular weight dextran(average molecular weight 2,000,000 Da) compared to the cross linked mixture which used the methacrylated dextran (dextran average molecular weight 473,000 Da) and methacrylated conA and were UV irradiated for 5 min. It is interesting to see that the complex viscosity profile for the CL mixture shows more graded response to increasing glucose concentration compared to the NP2 mixture. The CL mixture shows ~90% drop

in complex viscosity between the physiologically useful glucose concentration range (0.1-1% w/w) compared to the NP mixtures which showed ~75% drop at 20 °C.

6.3.2 Effect of temperature

In many polymeric systems, a rise is temperature results in a drop in viscosity of the material due to fewer polymer chain entanglements (Mezger, 2002). Dispersions with a gel or paste like character become more flexible at higher temperatures. At low temperatures, $G' > G''$, this relation can reverse at high temperatures and the value of tan delta may increase (Mezger, 2002). As seen in **Figure 6-4** to **Figure 6-7**, at 37°C lower viscosity profiles were obtained throughout the glucose range for all three mixtures. Their loss modulus, was $G'' > G'$ at 37°C and the higher viscosity mixtures with 0% glucose show greater temperature-dependence than those with 1% w/w glucose. The CL mixture shows ~80% drop in complex viscosity between the physiologically useful glucose concentration ranges (0.1-1% w/w) compared to the NP mixtures which showed ~63% drop. The viscosity profiles suggest that the viscoelastic behaviours of the different mixtures are suitable for the intended use in the implantable device.

6.4 Chapter summary

Rheological studies on the mixtures have shown that they are glucose responsive and their glucose sensitivity was shown by graded lowering of their viscosity due to change in the physical cross-linking in response to increasing glucose concentration.

The viscoelastic components; namely storage modulus, loss modulus, complex viscosity and tan delta for the non-polymerised dex2M-conA (NP) mixtures and the cross-linked dexMA-conAMA (CL) mixture examined using oscillatory rheometry within the linear viscoelastic range across a frequency range of 0.05-50 Hz confirm their ideal elastic and viscous responses. The storage modulus, loss modulus, complex viscosity profiles for the mixtures show a graded decrease in viscosity with increasing glucose concentration when compared at 1 Hz. These results confirm the ability of the polymerised mixtures to interact reversibly with glucose, by dismantling the temporary three-dimensional

network and forming a less viscous sol state by competitive displacement between free glucose and dextran. The results show that the viscoelastic changes (transformation from high viscosity gel-like to low viscosity sol-like state) occur in response to increasing glucose concentration further confirming that the underlying mechanism of the smart glucose responsive gel is functioning. The results for the NP mixtures suggest their suitability for *in vitro* diffusion studies, however it also highlighted the batch to batch variation of conA that should be taken into account when preparing and using these mixtures.

The comparison of the mixtures at 20 and 37°C suggest that the viscoelastic behaviours of the different mixtures are suitable for the intended use in the device. The CL mixture shows ~90% drop in complex viscosity between the physiologically useful glucose concentration range (0.1-1% w/w) at 20°C and ~80% drop at 37°C thus confirming its suitability for use in the closed-loop insulin delivery device for the management of diabetes.

Chapter 7 Drug delivery mechanism and diffusion kinetics of FITC-insulin

7.1 Introduction

Mathematical modelling of drug delivery and predictability of drug release kinetics is a field of steadily increasing academic and industrial importance with enormous potential. Mathematical predictions allow good estimates of the required composition, geometry, dimensions and preparations of the required dosage taking into account the route of administration, drug dose to be incorporated and the targeted drug release profiles (Siepmann and Siepmann, 2012; Siepmann and Peppas, 2012).

The classical mathematical equation, **Equation 7-1**, for drug delivery was proposed by Higuchi in 1961 where he described drug release from an ointment base exhibiting a considerable initial excess of non dissolved drug within an inert matrix with film geometry.

$$\frac{M_t}{A} = \sqrt{D(2C_0 t - C_s t_0)C_s t} \qquad \textbf{Equation 7-1}$$

Where, M_t is the cumulative absolute amount of drug released at time t, A is the surface area of film exposed to the release medium, D is the drug diffusivity in the carrier material, C_0 and C_s represent the initial drug concentration and the solubility of the drug in the carrier material, respectively.

Apparently numerous mathematical theories for drug delivery since then described in literature still lack in accuracy and/or ease in application according to Siepmann (Siepmann and Siepmann, 2008). The mathematical models generally used are either empirical/semi-empirical or mechanistic realistic types. A number of factors need to be considered when trying to understand drug release from a dosage form or system such as type of drug, formulation, preparation technique, environmental conditions during drug release as well geometry and dimensions of the drug delivery system. Furthermore

the release is influenced by a number of factors such as wetting of the system's surface with water, water penetration into the device, creation of water-filled pores, changes in the drug and/or excipient solubility due to altered micro environmental conditions and many more potentially involved phenomena, among which is the diffusion of drugs and/or excipients out of the dosage form or device with potentially time and/or position-dependent diffusion coefficients (Siepmann and Siepmann, 2008).

7.1.1 Determining the drug delivery mechanism - the Power law (Peppas equation)

One of the most frequently used and easy to apply semi-empirical mathematical models used to describe drug release is the power law or the so-called Peppas equation, **Equation 7-2** (Peppas, 1985). This model helps to determine the drug release mechanism from polymeric systems.

$$\frac{M_t}{M_\infty} = k\mathrm{t}^{\mathrm{n}} \qquad \textbf{Equation 7-2}$$

Where, M_t and M_∞ are the absolute cumulative amount of drug released at time t and infinite time, respectively; k is a constant incorporating structural and geometric characteristics of the system and n is the diffusional exponent, which is indicative of the mechanism of drug release. The classical Higuchi equation and Peppas equation (**Equation 7-2**) are an approximation of Fick's second law for thin films and represents a special case of the power law where n=0.5. The power law can be seen as a generalisation of two independent mechanisms of drug transport, Fickian diffusion and a case-II transport (non-Fickian transport mechanism with effects of polymer swelling, stresses, structural changes and influence of polymer relaxation on movement of molecules in the matrix (Kosmidis et al., 2003)). Thus the power law has two distinct physical realistic meanings in the two special cases, where n=0.5 indicates diffusion controlled drug release and n=1 indicating swelling controlled drug release. Values of n between 0.5 and 1.0 can be regarded as an indicator of potential overlapping of both

phenomena (anomalous transport). However the above values for n are only valid for a slab/thin film geometry. For spheres and cylinders different values have been derived as listed in the **Table 7-1.**

Table 7-1: Drug release exponent *n* of the power law and corresponding drug release mechanism from polymeric controlled delivery systems of different geometry (Siepmann and Siepmann, 2008).

Exponent, *n*			**Drug release mechanism**
Thin Film	**Cylinder**	**Sphere**	
0.5	0.45	0.43	Fickian diffusion
$0.5<n<1.0$	$0.45<n<0.89$	$0.43<n<0.85$	Anomalous transport
1.0	0.89	0.85	Case-II transport

7.1.2 Determination of diffusion coefficient using mathematical models

The mechanistic mathematical models describe real phenomena such as mass transfer by diffusion, dissolution of drug and/or excipient, transition of a polymer from the glassy to the rubbery state. The drug releases that are purely diffusion controlled with constant diffusion coefficients are commonly based on Fick's law of diffusion. Various modifications and variations are applied to the Fick's law of diffusion equation for mathematical modelling purposes depending on the system, shape and boundary conditions. As discussed in **Chapter 5**, the experimental protocol developed to determine diffusion coefficient was used. The mathematical models, the diffusion cell technique – Quasi steady state (QSS), the Time lag (TL) slope and the TL intercept methods based on Fick's law as discussed in **Chapter 5** were used for determination of diffusion coefficient of FITC-Insulin.

7.1.3 Glucose responsiveness

Glucose responsiveness forms the basis for the closed-loop drug delivery mechanism of the INsmart device. The device encases a glucose-sensitive gel of co-polymerised dextran methacrylate (dexMA) and concanavalin A methacrylamide (conAMA), which produces a reversible change in consistency on contact with glucose to modulate insulin transport and thus acts as a self adjusting system. The design of the closed loop self regulating implantable insulin delivery device for the management of diabetes is based on the small changes occurring in the glucose sensitive gel in response to the diabetic physiological glucose levels and its corresponding ability to modulate diffusion of insulin through the material. The device implanted in the peritoneal cavity, works on a very fast feedback mechanism for controlling insulin release. This mimics a normal pancreas and may overcome inherent problems encountered in maintaining normoglycaemia with current electronically or biologically based closed loop systems. For the responsive drug delivery system to operate effectively for the management of diabetes, changes in viscosity need to be in the clinically useful glucose range and need to occur in a physiologically relevant timescale. **Figure 7-1** shows the well known sigmoid relationship between tissue glucose concentration (dashed line) and beta cell insulin release (solid line) (Taylor et al., 2006). Either differential beta cell sensitivity or cellular insulin granule content has been argued to be responsible for this sliding scale physiological sensitivity (Nesher and Cerasi, 2002).

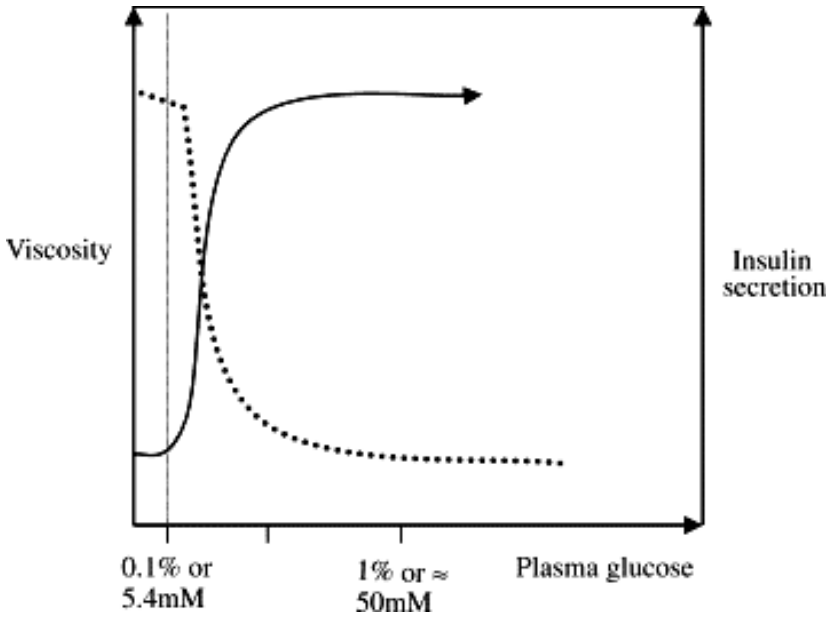

Figure 7-1: Profile of viscosity and insulin secretion (bold line) as a function of glucose plasma concentration (dotted line) (Taylor et al., 2006).

Insulin secretion is quite low under normal conditions (with basal glucose levels) and is required to control post-prandial glucose levels from absorbed food by raising secretion appropriately. A normal pancreas responds to post-prandial glucose levels by gradual ramping up of insulin secretion and is capable of high output if glucose reaches abnormal levels. At the same time, a normal pancreas is capable of responding to falling glucose levels if there is a risk of hypoglycaemia for any reason (although counter regulatory systems also contribute to restoring normality). The gel held within the INsmart device should also respond in a similar manner to increasing physiologically relevant concentrations of glucose (0.1% to 1% w/w glucose).

7.2 Experimental outline

In order to determine if the drug delivery mechanism from the INsmart device was "Fickian diffusion", the release of fluorescein sodium from the non-polymerised dex2M-conA gel (NP gel) was recorded over time and the power law applied to the data. Following this fluorescently labelled insulin synthesised in-house, as discussed in **Chapter 4,** was used in the experiments to determine its diffusion coefficient in the NP

gel and the cross-linked dex500MA-conAMA gel (CL gel). The experimental protocol developed, as discussed in **Chapter 5** and selected mathematical models were applied to the INsmart device to determine the diffusion coefficient of FITC- insulin. Glucose sensitivity of the NP gel was assessed by challenging the system with increasing physiologically relevant concentrations of glucose (0.1% to 1% w/w glucose).

7.3 Experimental conditions and data analysis for INsmart device experiment

7.3.1 Chemicals and reagents

Concanavalin A, from Canavalia ensiformis, Type VI lyophilised powder (Type VI) (conA) and dextran (produced by *Leuconostoc mesenteroides*, strain no. B512; average molecular weight 2000 kDa) (dex2m) were purchased from Sigma-Aldrich Chemical Company Ltd. (Poole, Dorset, UK). Dialysis membranes (MWCO.100 kDa) were obtained from Medicell International Ltd (Liverpool,UK). Radical photoinitiator 1-[4-(2-hydroxyethoxy)-phenyl]-2-hydroxy-2-methyl-1-propane-1-one (Irgacure® 2959) (IRG) from Ciba Speciality Chemicals (Cheshire,UK). Metric 180 PVC tubing-FDA/USPVI (1mmID, 2mmOD, 5mmWall) was purchased from Nalgene® Brand products,USA. All other chemicals were of analytical grade and distilled water was used throughout. FITC-insulin synthesised in-house and characterised as discussed in **Chapter 4** was used.

7.3.2 Preparation of NP gel and CL gel

The preparation of the non-polymerised dex2M-conA gel (NP gel) containing underivatised conA and dextran (RMM 2000 kDa) has been described in **Chapter5**, **Section 5.3.3.** The preparation of the cross-linked dex500MA-conAMA gel (CL gel) prepared using methacrylated dextran 500 kDa, DS 3% (dex500MA) and methacrylated concanavalin A (conAMA) and crosslinking them by irradiation for 5mins has been described in **Chapter 6, Section 6.2.1.** For experiments with glucose, weighed amount

of glucose was added to the NP gel or the CL gel, mixed well and stored overnight at 4°C before use.

7.3.4 Experimental set-up

The device was assembled as described in **Chapter 5, Section 5.5.1**. All experiments were performed at 20°C, using 1.17 mm gel spacer and dialysis membrane with molecular weight cut off 100 kDa.

The experimental set-up was the same as described in **Chapter 5, Section 5.7.1**. Here the donor compartment had FITC-insulin solution. Also, for these experiments the pH of the donor FITC-insulin solution, the receptor distilled water and the gel was always adjusted to approximately pH 7.6 with either 0.1M HCl or 0.1 M NaOH. This was to keep the FITC-insulin in dissolved state as any drop in pH compromises its solubility and leads to precipitation in the gel. Peritoneal fluid similar to serum fluids contains phosphorus, uric acid, blood urea nitrogen, creatinine, potassium, bicarbonate, sodium and lower concentrations of calcium and albumin. Because the peritoneal fluid is in equilibrium with the serum, it also contains other low molecular-weight substances *in vivo* that cross the peritoneal membrane (Kelton et al., 1978). However for the diffusion experiments in order to determine the diffusion coefficient for FITC-insulin, these components of the peritoneal cavity were not included as these could interfere with the measured diffusion rate. The schematic of the experimental set up is as presented in **Figure 7-2** and as shown in **Figure 7-3**;

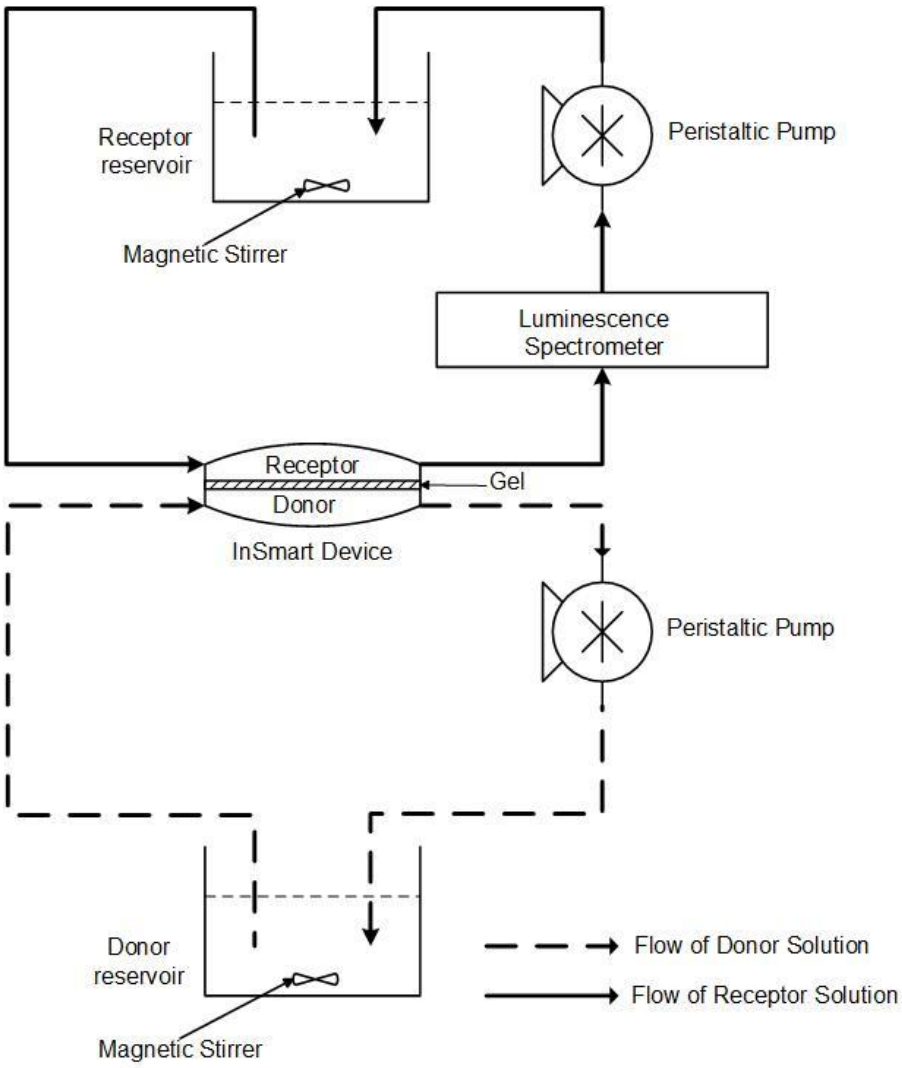

Figure 7-2: Schematic of the experimental set-up for diffusion of FITC-insulin in NP gel or CL gel housed within the INsmart device.

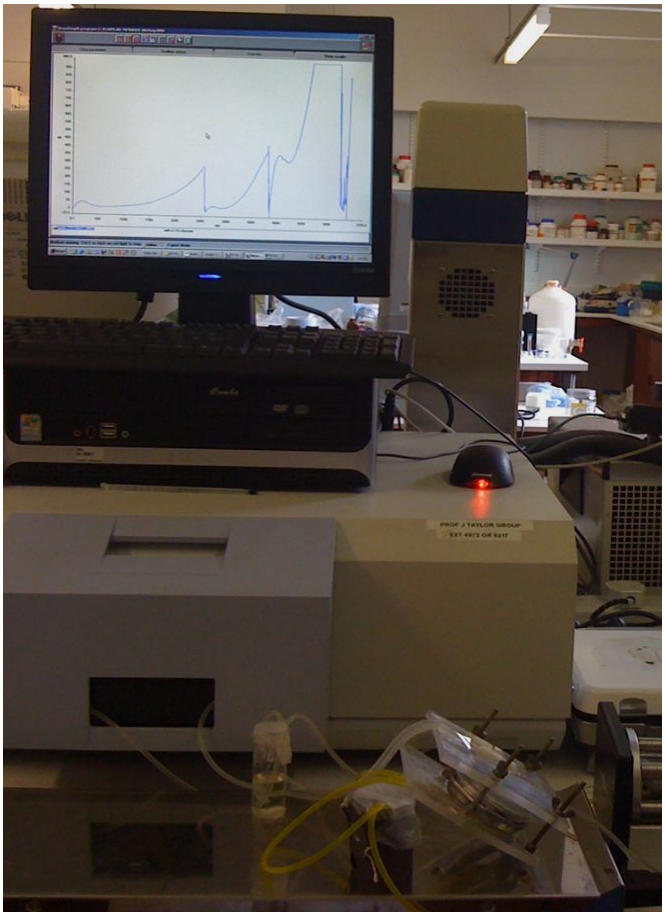

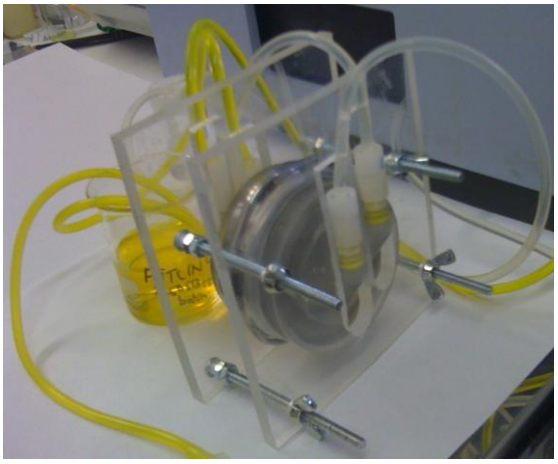

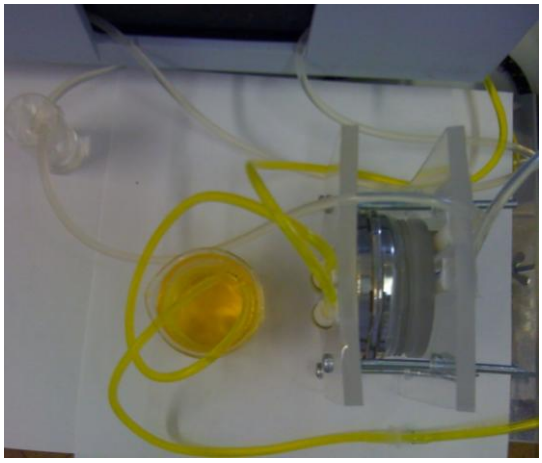

Figure 7-3: Photographs of the experimental set-up for diffusion of FITC-insulin in NP gel or CL gel housed within the INsmart device.

The receptor and donor compartment circuits were closed circuit; with reservoirs in the circuit to maintain equal volumes on both sides. For determination of FITC-insulin diffusivity in the presence of a range of different physiologically relevant glucose

concentrations i.e. the diffusivity due to reduced gel viscosity in the presence of glucose, physiologically relevant amount of glucose was added to the donor FITC-insulin solution, the gel and the receptor solution to eliminate any osmotic interference and density interferences.

For glucose responsiveness experiments, to determine FITC-insulin diffusivity due to reduced gel viscosity that occur real time in presence of glucose triggers, glucose was present only in the receptor solution.

The NP gel was prepared as described in **Chapter 5, Section 5.3.3** and CL gel as described in **Chapter 6, Section 6.2.1**. Once the INsmart device was put together the steps as described in **Chapter 5, Section 5.7.1** were followed.

FITC-insulin shows strong fluorescence at excitation wavelength 494 nm and emission wavelength 518 nm as shown in **Figure 7-4**. FITC-insulin diffusing through the gel from the donor side to the receptor side was monitored over time, using the FLWinlab wavelength program application, by conversion of fluorescence intensity recordings at 518 nm into concentration values using calibration curves. Sampling was performed over a period of minimum 5 hours.

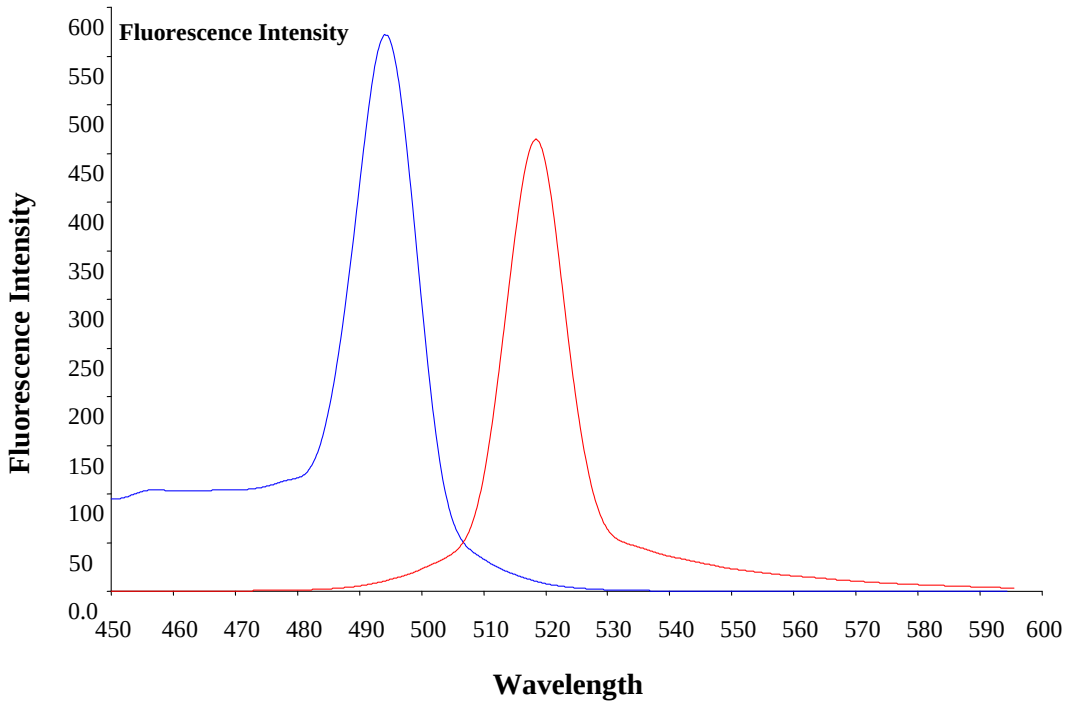

Figure 7-4: Fluorescence spectrum of FITC-insulin showing strong fluorescence intensity at excitation wavelength 494 nm and emission wavelength 518 nm.

The FL Winlab software in wavelength mode was set to plot the data per minute. The data was imported into Excel for generation of concentration versus time plots. The fluorescence intensity at 518 nm showed a second degree polynomial fit with respect to concentration for FITC-insulin as shown in **Figure 7-5**, thus enabling simple conversion of fluorescence intensity data into concentration values observed for FITC-insulin.

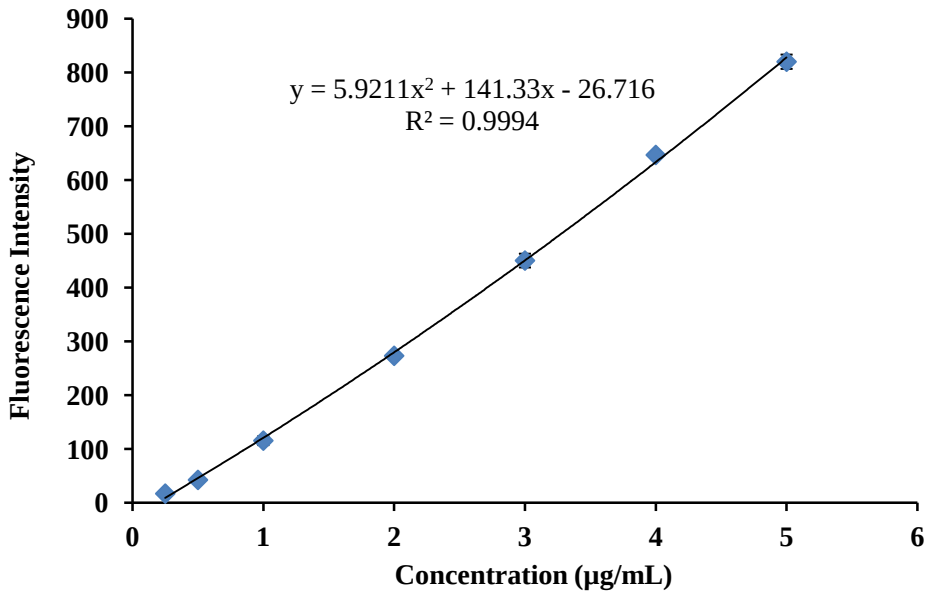

Figure 7-5: Calibration graph of various concentrations of FITC-insulin (using fluorimeter quartz flow cell). (Data represent mean±SD of six measurements, error bars present but may not be visible as smaller than marker size).

For diffusivity estimation experiments of FITC-insulin in presence of glucose, calibration curves for FITC-insulin containing the relevant concentrations of glucose were generated each time.

7.3.5 Data analysis

The fluorescence intensity data was first converted into FITC-insulin concentration using the calibration curve as shown in **Figure 7-5**. The data was plotted based on the requirements of the mathematical methods; QSS, TL slope and TL intercept method for calculating diffusion coefficient as described in **Section 5.3.4**.

7.4 Results and Discussion

7.4.1 Determining the drug delivery mechanism - The Power Law (Peppas equation)

The release of fluorescein sodium from the NP gel was recorded over time and applied to the power law as discussed in **Section 7.1.1** to determine if the drug delivery mechanism from the INsmart device was Fickian diffusion.

The gel (thickness 1.17 mm) housed in the INsmart device can be considered as a thin film or slab with no edge effects and the power law fit, for n=0.5 for the release of fluorescein sodium through the gel is as shown in **Figure 7-6:**;

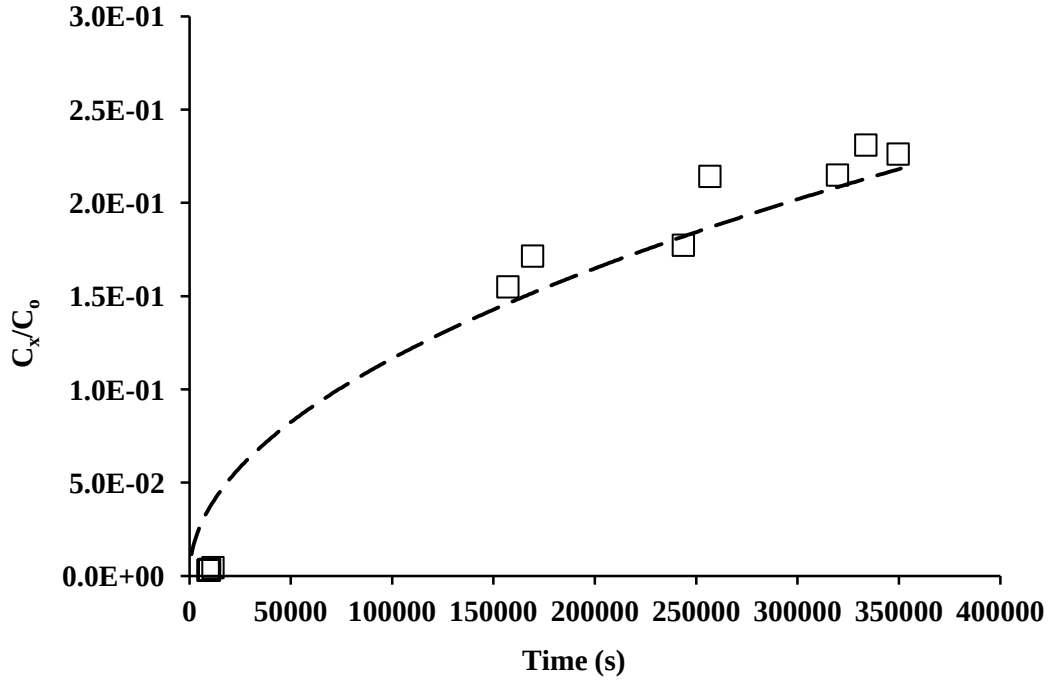

Figure 7-6: Power law fit for fluorescein sodium release through NP gel. Dotted line represents the power law fit for n=0.5, indicating diffusion controlled release.

The power law fit, for n=0.5 for the release of fluorescein sodium through the gel indicates diffusion controlled release mechanism, Fickian diffusion.

7.4.2 Determination of diffusion coefficient using mathematical models

The diffusivities of FITC-insulin in NP gel and in the presence of 0.1, 0.2, 0.5 and 1% w/w glucose are as presented in **Table 7-2**;

Table 7-2: Diffusion coefficient values (D and D_e) for FITC-insulin in NP gel and in presence of glucose determined using different methods. The number of replicate measurements is shown by n=x.

Glucose concentration in NP gel	**QSS**	**TL slope**	**TL intercept**
(% w/w)	$\boldsymbol{D_e \times 10^{-11}}$ **(m^2/s)**	$\boldsymbol{D \times 10^{-11}}$ **(m^2/s)**	$\boldsymbol{D \times 10^{-11}}$ **(m^2/s)**
0 (n=2)	1.05 ± 0.02	1.04 ± 0.02	1.12 ± 0.11
0.1 (n=1)	0.46	0.46	2.24
0.2 (n=1)	0.57	0.57	2.11
0.5 (n=1)	0.43	0.43	3.76
1.0 (n=1)	0.90	0.89	3.59

Based on the limited data set the diffusion coefficient values for FITC-insulin using the QSS method, the TL slope and intercept method are in agreement for the NP gel; however for experiments in presence of glucose the D calculated using the TL intercept method were higher than D calculated using the QSS and the TL slope method.

In presence of glucose the D for FITC-insulin seems to be lower than in absence of glucose, the reason for which could be the micro viscosity created by glucose within the gel structure contributing towards interference in the diffusion of FITC-insulin. The D values show an increase with increasing glucose concentration as the viscosity of the gel (it's macroviscosity) drops with increasing glucose concentration.

The diffusivities of FITC-insulin in CL gel and in presence of 0.1, 0.2, 0.5 and 1% w/w glucose were determined using the mathematical models. The results are as presented in **Table 7-3**;

Table 7-3: Diffusion coefficient values (D and D_e) for FITC-insulin in CL gel and in presence of glucose determined using different methods. The number of replicate measurements is shown by n=x.

Glucose concentration in CL gel	**QSS**	**TL slope**	**TL intercept**
(% w/w)	$\boldsymbol{D_e \times 10^{-11}}$ **(m^2/s)**	$\boldsymbol{D \times 10^{-11}}$ **(m^2/s)**	$\boldsymbol{D \times 10^{-11}}$ **(m^2/s)**
0 (n=2)	0.75 ± 0.06	0.75 ± 0.06	1.44 ± 0.57
0.1 (n=2)	0.98 ± 0.55	0.97 ± 0.55	6.10 ± 5.40
0.2 (n=1)	0.34	0.34	1.93
0.5 (n=1)	0.39	0.39	15.67
1.0 (n=1)	0.44	0.44	4.47

The diffusion coefficient values for FITC-insulin using the QSS and the TL slope methods are not in agreement with their corresponding TL intercept method values for CL gel, both in absence and presence of glucose. This highlights the unreliability of the TL intercept method in determining diffusion coefficient as discussed in **Chapter 5, Section 5.1.3.3**.

In presence of 0.1% glucose the D for FITC-insulin in CL gel was slightly higher than in absence of glucose, however the FITC-insulin D values in CL gel with 0.2 to 1% glucose are lower than in the absence of glucose. For CL gel, microviscosity created by higher concentration, 0.2% glucose seems to contribute towards interference in the diffusion of FITC-insulin. The D values do show an increase with increasing glucose concentration as the viscosity of the gel (macroviscosity) drops with increasing glucose concentration, observed only from 0.2% to 1% w/w glucose.

The QSS and TL methods gave reliable correlations in diffusion coefficient values for FITC-insulin in NP gel and CL gel. The TL intercept method gave different values, approximately a decade faster in some instances, which is consistent with the findings of others (Zhang and Furusaki, 2001). Representative experimental data are graphically presented in **Appendix 4**; **Figure A4-1** to **Figure A4-5** for NP gel with no glucose, 0.1, 0.2, 0.5 and 1.0% w/w glucose and in **Appendix 4**; **Figure A4-6** to **Figure A4-10** for CL gel with no glucose, 0.1, 0.2, 0.5 and 1.0% w/w glucose.

7.4.3 Glucose responsiveness

The response to physiologically relevant glucose triggers was determined in the NP gel. The diffusivity of FITC-insulin in response to triggers of physiologically relevant glucose concentrations was determined using the test rig by challenging the NPgel in the device with glucose added to the receptor side. In **Figure 7-7**, the total mass of FITC-insulin released from the device in response to 0.1 to 1.0% w/w glucose triggers are presented. For glucose triggers from 0.1 to 0.5% w/w an initial FITC-insulin release is observed followed by a period of slight drop in release rate and then a second steady state release. A possible explanation for this could be that on glucose trigger, the FITC-insulin present in the gel layers close to the receptor side drop in viscosity due to glucose diffusing into these layers and hence release the amount of FITC-insulin present in these layers, then there is a short period where the FITC-insulin diffusing from the donor side reaches these outermost layers and which then achieves a steady state release. In real time scenario however, the feedback loop is quick, less than 10 min and hence only the initial release as seen in **Figure 7-7** will be observed.

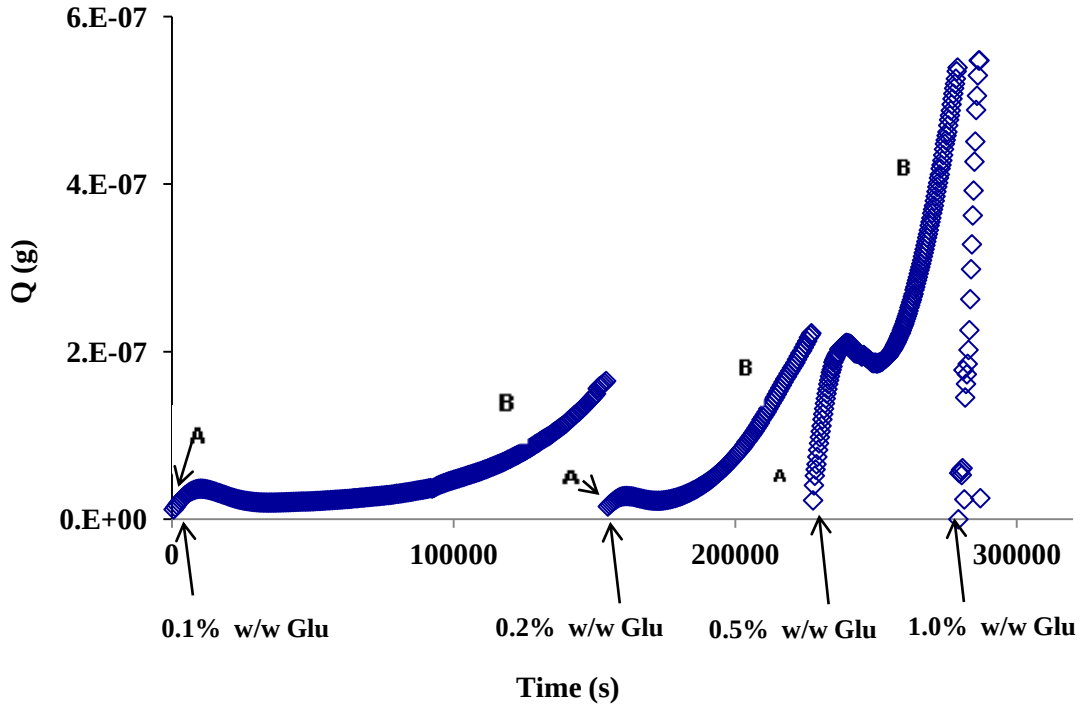

Figure 7-7: FITC-insulin total mass delivered with increasing glucose concentration triggers in NP gel. The data set presented here has been reduced to every 10th data point for 0.1 and 0.2% w/w glucose triggers and 5th data point for 0.5 and 1% w/w glucose triggers to aid visual clarity (**A**: first slope, **B**: second slope).

The diffusion coefficient of FITC-insulin in NP gel in response to the glucose triggers, 0.1, 0.2, 0.5 and 1% w/w was estimated. The diffusion coefficients were calculated using the first and second slopes (A and B) as shown in **Figure 7-7**. When the values of *D* found in this way were plotted against glucose concentration, FITC-insulin diffusivity showed a second and third order polynomial fit to increasing glucose concentration showing its sensitivity and graded response to increasing glucose concentration. The FITC-insulin *D* values increase with increasing glucose concentration in NP gel. The diffusion coefficient values calculated using the first slopes (initial drug release following the trigger) were found to be comparable to the values calculated using second slopes. In real-time scenario, the trigger response and sol to gel transformation following a drop in glucose levels is assumed to be much quicker and hence only the first release will be observed.

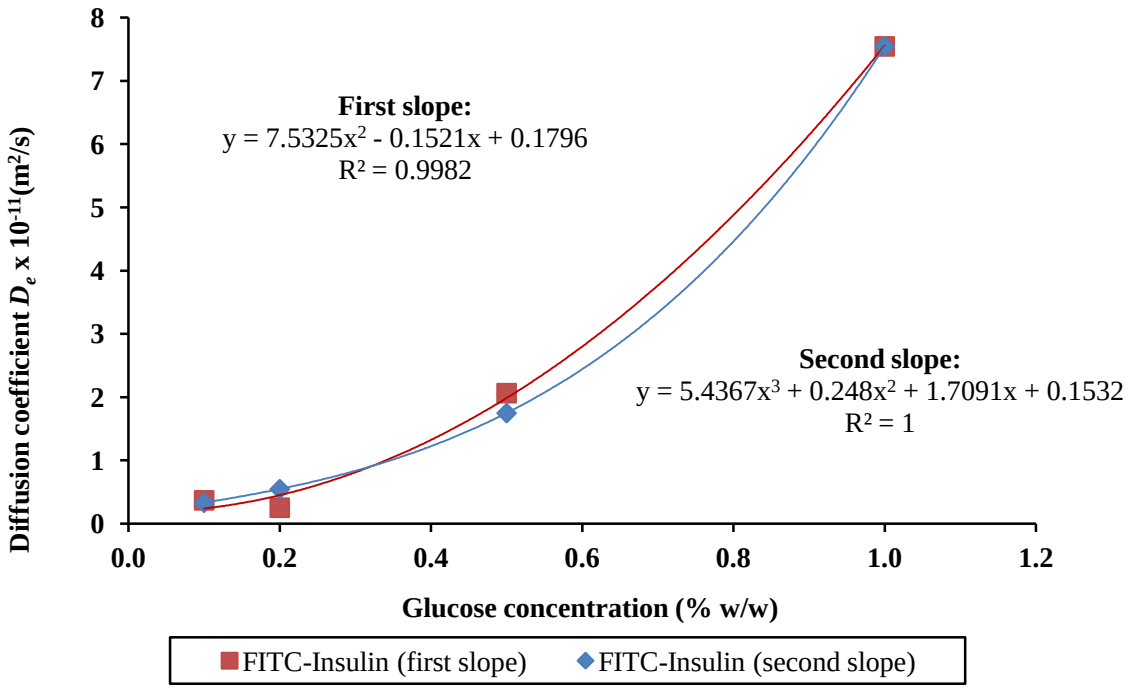

Figure 7-8: Figure showing FITC-insulin diffusion coefficient values with increasing glucose concentration triggers in NP gel from first and second slopes showing polynomial fit.

Rheological studies on the NP and CL gels (mixtures) as discussed in **Chapter 6** have shown that they are glucose responsive and their glucose sensitivity was shown by graded lowering of their viscosity due to change in the physical cross-linking in response to increasing glucose concentration. The storage modulus, loss modulus, complex viscosity profiles for the gels which showed a graded decrease with increasing glucose concentration when compared at 1 Hz confirm the viscoelastic changes (transformation from high viscosity gel-like to low viscosity sol-like state) occurring in response to increasing glucose concentration. This confirmed that the underlying mechanism of the smart glucose responsive gel was functioning. This was further demonstrated by the relationship (third order polynomial fit) between diffusion coefficient values for FITC-insulin in NP gel (using second slope) and the complex viscosity of the gel measured in response to increasing glucose concentration as shown in **Figure 7-9**.

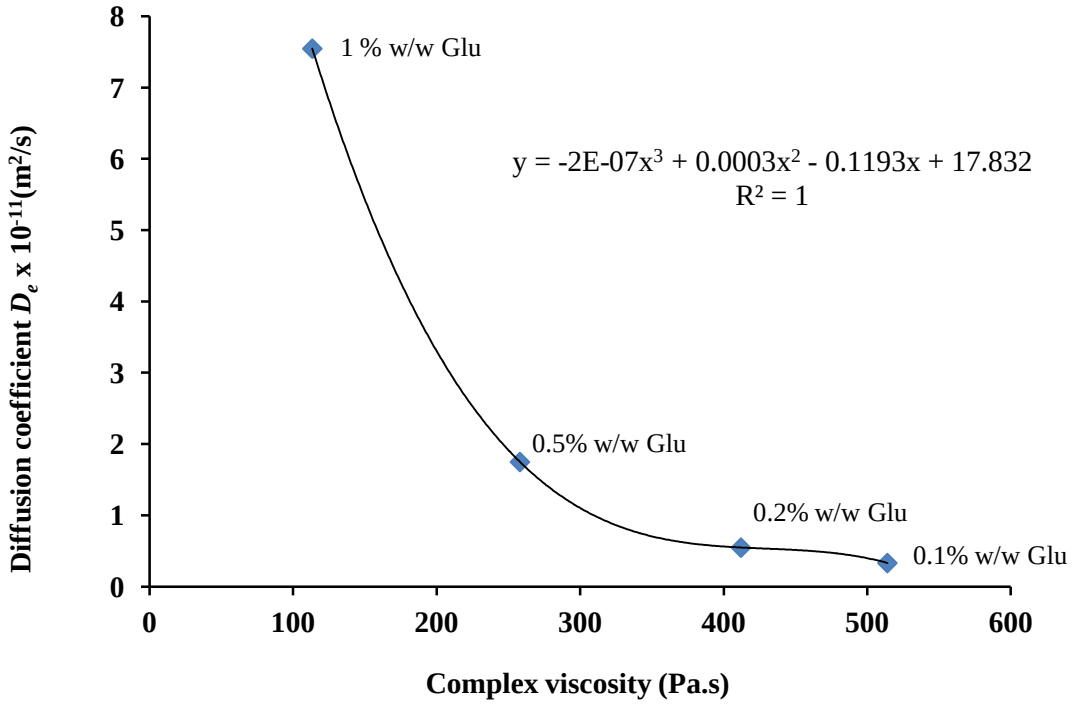

Figure 7-9: Relationship between FITC-insulin diffusion coefficient values in NP gel and complex viscosity of the gel measured in response to increasing glucose concentration at 20°C.

The FITC-insulin *D* values calculated following glucose challenges to the NP gel were compared to the *D* value in NP gel and CL gel in the presence of the relevant glucose concentration (where the system had glucose present throughout to avoid osmotic interferences) (refer to *D* values in **Table 7-2**and **Table 7-3**). As shown in **Figure 7-10**, the FITC-insulin *D* values determined in NP gel following glucose challenges and actual *D* values in NP and CL gel in presence of different glucose concentrations were plotted graphically for comparison. The FITC-insulin *D* values calculated in NP gel and CL gel in presence of relevant glucose concentrations show only a slight graded response to increasing glucose concentration; however the D values in NP gel show a much more graded response to glucose challenges, which is more representative of a real-time trigger scenario.

The *in vitro* diffusivity experiments have aided in determining the actual diffusivity of FITC-insulin in presence of different glucose concentrations, however the potential limitation for using these values to calculate drug release is that these may not be the

actual diffusivities observed in real-time *in vivo* situation. This highlights the importance of understanding the device design-specific parameters to achieve greater understanding of the underlying drug release mechanism. The glucose trigger experiment is a much better approximation of what is really happening when the gel is challenged with glucose.

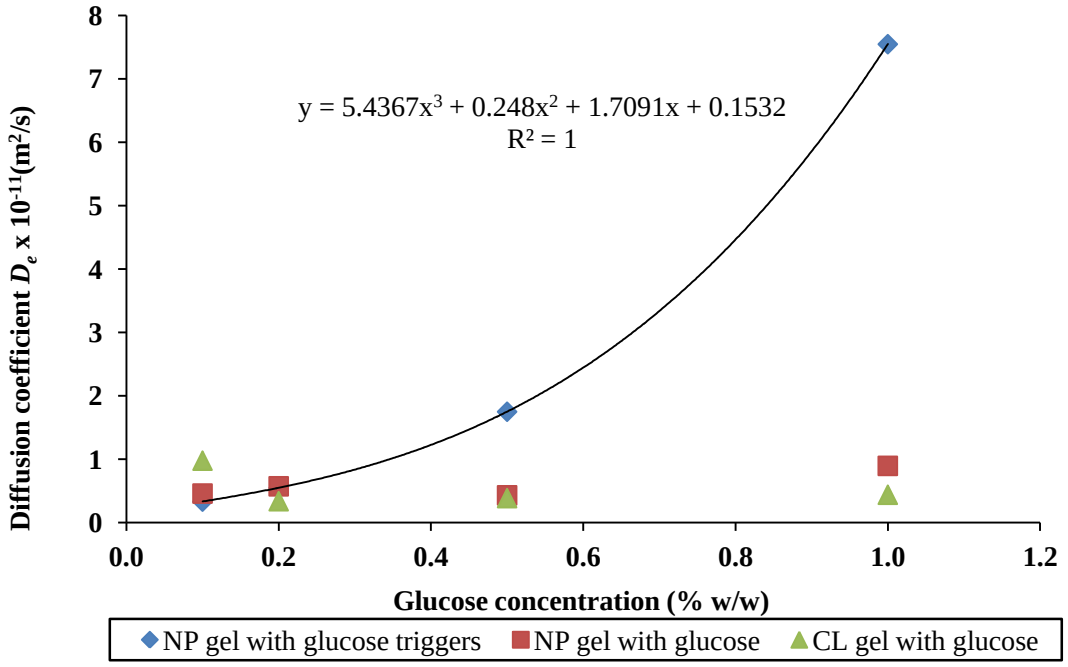

Figure 7-10: FITC-insulin diffusion coefficient values with increasing glucose concentration triggers in NP gel in comparison to values determined using NP gel and CL gel with relevant glucose concentration present throughout the system.

7.5 Chapter summary

The drug release mechanism of FITC-insulin from the glucose sensitive gel held in the INsmart device, studied using fluorescein sodium was found to be diffusion controlled. Fluorescein sodium release from the NP gel over time demonstrated the Peppas equation (power law) fit, for n=0.5 thus indicating a Fickian diffusion controlled release mechanism.

The diffusion coefficient (*D*) for FITC-insulin in the NP gel determined using mathematical models, QSS and TL slope methods was $1.05 \pm 0.02 \times 10^{-11}$ m^2/s. The diffusion coefficient (*D*) for FITC-insulin in the CL gel determined using mathematical models, QSS and TL slope methods was $0.75 \pm 0.06 \times 10^{-11}$ m^2/s.

In presence of glucose the *D* values determined using the mathematical models for FITC-insulin seems to be lower than in its absence, the reason for which could be the micro viscosity created by glucose within the gel structure contributing towards interference in the diffusion of FITC-insulin. However, the *D* values do show an increase with increasing glucose concentration, approximately 48% from 0.1 to 1% w/w for NP gel and approximately 23% from 0.2 to 1% w/w for CL gel. Here, the increase in glucose having a greater effect on the macroviscosity of the gel.

In response to physiologically relevant glucose triggers in the NP gel, the diffusivity of FITC-insulin increases (from 0.33 to 7.55×10^{-11} m^2/s) with increasing glucose concentrations (from 0.1% to 1% w/w), showing a polynomial fit, device thus showing glucose sensitivity and graded response, mimicking pancreas. It also shows that the diffused glucose molecules in the gel drop the viscosity of the gel but do not hinder the diffusivity of FITC-insulin in the gel thus the release kinetics is controlled entirely by the diffusivity of FITC-insulin in the gel.

Chapter 8 Predicting the performance of the INsmart device

8.1 Introduction

Using the available information and assumptions and the set initial and boundary conditions, mathematical equations were selected for the type of system used (as has been shown in the model selection **Chapter 5**). Using the diffusion coefficient values calculated by fitting the respective equation to sets of experimental data it is possible to minimize the difference between experimental and theoretical data. Also, using these diffusion coefficient values, the model can be used to quantitatively predict the impact of a certain parameter (e.g., area or thickness of gel) on the resulting drug release kinetics. Such theoretical predictions can be then compared with independent experimental results (Siepmann and Siepmann, 2008).

As discussed in **Chapter 7**, the INsmart device can be considered as a reservoir system with constant activity source where the drug is physically completely separated from the barrier gel. The gel is housed within the device in such a way that there is minimum likelihood of gel swelling. Importantly, the water uptake is minimal, very rapid and complete upon exposure to the release medium. Thus, during the drug release period, constant device dimensions (stationary boundary conditions) are maintained and the drug diffuses out of the system through the gel. The drug release mechanism from the device has been confirmed as Fickian diffusion; refer to **Chapter 7.**

8.2 Theoretical estimations

An idealised artificial pancreas should be able to maintain normal glucose control by an automated continuous negative feedback (closed-loop) causing appropriate response to losses and gain in glucose levels akin to normal pancreatic flux of insulin. Such dose targeting which mimics the natural pattern of insulin release in the human body could be

achieved by the INsmart device containing the glucose responsive gel which is the sensor and insulin delivery port.

Daly et al have presented the profiles for blood glucose and serum insulin, as shown in **Figure 8-1** and **Figure 8-2**, for eight healthy adults from a randomised, crossover trial which reveal higher peaks and lower troughs with the high-sucrose diet whereas higher area under the curve for the high starch diet (Daly et al., 1998; Daly, 2003).

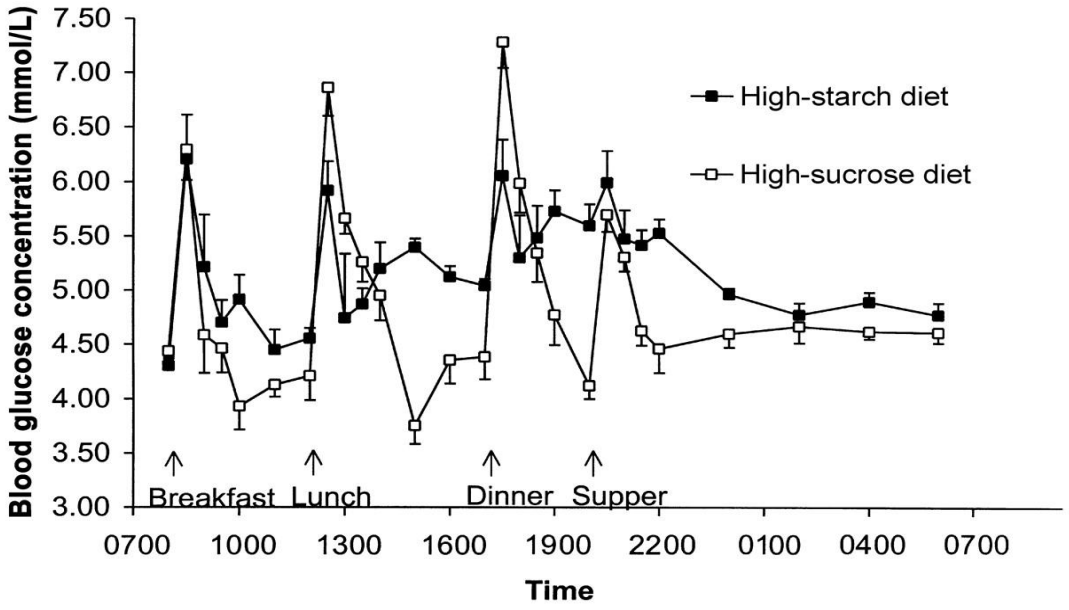

Figure 8-1: Glucose responses to high-sucrose and high-starch diets (from Ref (Daly, 2003)).

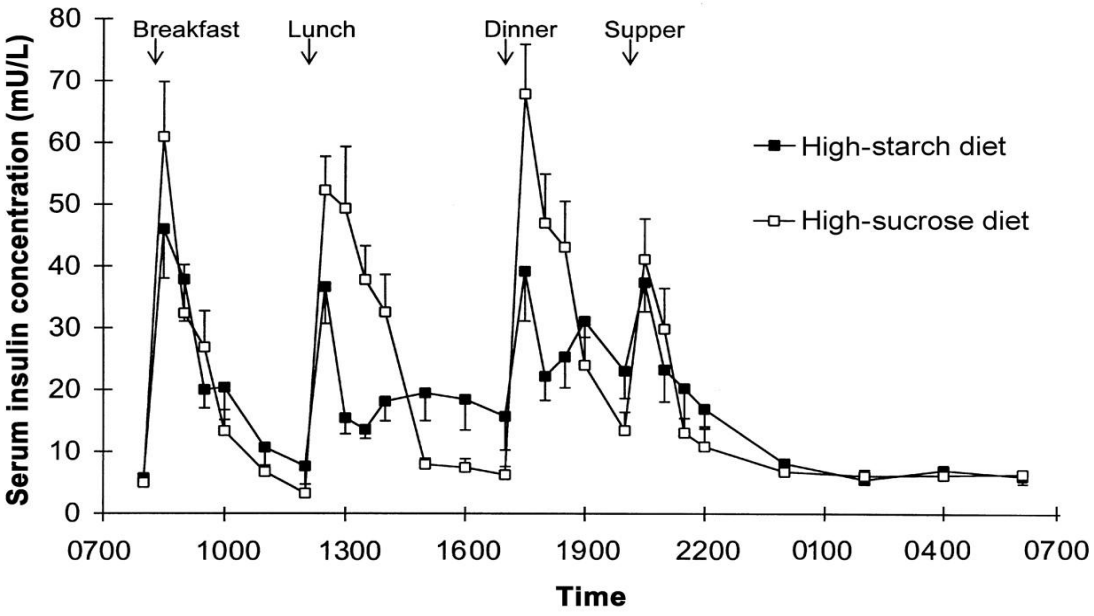

Figure 8-2: Insulin responses to high-sucrose and high-starch diets (from Ref (Daly, 2003)).

The capability of the INsmart device relies on it being efficient, consistent and reproducible in maintaining the automated continuous negative feedback and being able to achieve real-time serum insulin profile as shown in **Figure 8-2**. Based on the *in vitro* diffusion kinetics measured for FITC-insulin through the glucose-responsive gel held within the device some theoretical calculations and design improvements could be suggested to achieve this real-time insulin response clinically.

Insulin release rates from the device in response to real-time glucose in mammal/human as discussed in **Chapter 2** depend on the device design; gel thickness and surface area available for release. The concentration gradient achieved may vary with decreasing insulin on the donor side. And the glucose responsiveness of the gel and diffusion coefficient of insulin could be affected by gel polymer content, gel thickness or the site of implant of the device.

8.2.1 Predictive capability of the device

Can the device deliver the daily insulin requirement?

Most patients with T1DM require an insulin dosage of 0.5 to 1.0 IU per kg per day (Hirsch, 1999). The average adult male body mass by world region in 2005 published by Walpole et al in 2012 for Europe was reported as 70.8 kg and for the world (excluding some countries and territories due to insufficient data) as 62 kg (Walpole et al., 2012). Considering the body weight as 70.8 kg the daily insulin requirement for a patient with T1DM diabetes would be 2.14 x 10^{-4} to 4.25 x 10^{-4} mmol per day.

Daily insulin requirement for T1DM = 0.5 – 1 IU per kg per day
1IU = 0.0349 mg = 3.49x10-5 g
Daily insulin requirement = 1.745x10^{-5} to 3.49x10^{-5}g per kg per day
For a 70.8Kg adult = 0.124 x 10^{-2} to 0.247 x10^{-2} g per day
= 2.14x10^{-7} to 4.25x10^{-7} mols per day
= 2.14x10^{-4} to 4.25x10^{-4} mmols per day

Here an assessment is made into whether the device is capable of delivering the daily insulin requirement for an average body weight of 70.8 kg. Using Fick's law, **Equation** 8-1 and the calculated diffusion coefficient values for FITC-insulin in the NP gel in response to glucose triggers, estimations were made of whether the device can deliver the daily requirement. These were made when in the gel state with basal glucose present and with elevated glucose levels, 0.2% w/w (equivalent to 11 mmol/mL, which is diagnosed as diabetes). Here it was assumed that a maximum insulin concentration of 10ml of 500 IU/mL was included in the donor compartment and gel thickness was 0.117 cm.

Fick's Law:

$$J = -D\frac{\partial C}{\partial x} \qquad \textbf{Equation 8-1}$$

The delivery rates from the device are dependent on the diffusion in gel state and sol state (which define the performance window).

Using the following criteria, the insulin delivered from the device was calculated and is presented in **Table 8-1**;

D gel state with basal glucose - 3.32×10^{-8} cm^2s^{-1} (3.32×10^{-12} m^2s^{-1})

D sol state with 0.2% w/w glucose - 5.48×10^{-8} cm^2s^{-1} (5.48×10^{-12} m^2s^{-1})

These were made under the conditions;

C_D = 10ml of 500 IU/mL (3×10^{-5} mol).

C_R = 0 (assuming rapid elimination of insulin in the body)

Surface area - 6.2 cm^2

Gel thickness – 0.117 cm

Table 8-1: Insulin delivered from device in presence of different glucose concentrations.

	Flux *J*(mmol/cm^{2}s)	**Insulin (mmol/s)**	**Insulin (mmol/day)**
Daily requirement for an average body weight (max)	-	-	4.25×10^{-04}
Device delivery in presence of basal glucose	8.52×10^{-09}	5.28×10^{-08}	4.56×10^{-03}
Device delivery with presence of 0.2% w/w glucose	1.41×10^{-08}	8.75×10^{-08}	7.56×10^{-03}
Device delivery with presence of 0.5% w/w glucose	4.49×10^{-08}	2.78×10^{-07}	2.41×10^{-02}
Device delivery with presence of 1% w/w glucose	1.94×10^{-07}	1.20×10^{-06}	1.04×10^{-01}

As shown in **Table 8-1** the device is capable of delivering the daily required insulin amount in sol state (in response to different glucose challenges) and also under basal glucose conditions using the current experimental design comprising of gel thickness 0.117 cm and surface area 6.2 cm^2. The calculations shown here is using the assumption is that the value of *D* changes throughout the gel thickness in a relevant time period. In real-time the value of *D* changes for the exposed layers of the gel which allows for the quick gel to sol and again to gel state based on the level of glucose present.

Another main requirement that needs to be satisfied is whether the device is capable of matching the basal insulin concentration requirement. The distribution volume of insulin in the body as determined by Hipszer et al using insulin pharmacokinetics model to study distribution and elimination of insulin in the body was found to be 15.6 ± 4.0L (Hipszer, Joseph and Kam, 2005). The basal insulin concentration observed in a non-diabetic person is ~10 mU/L (Daly, 2003) which is equivalent to a concentration of 6.01 x 10^{-8} mmol/L, assuming the body distribution volume as 19.6L the total mass of insulin present in circulation would be 1.18 x 10^{-6} mmol. Based on the flux per unit area from the device of J = 8.52 x 10^{-9} mmol/cm^2s calculated for device in presence of basal glucose, the mass transferred from the device was found to be 5.28 x 10^{-8} mmol/s. Therefore in 22.34 sec the device should be able to deliver 1.18 x 10^{-6} mmol, the basal amount required.

1IU = 0.0349 mg = 3.49x10^{-5} g
10mU/L = 3.49x10^{-7} g/L
=3.49x10^{-7}/ 5808 (RMM for insulin)
= 6.01x10^{-11}mol/L = 6.01x10^{-8}mmol/L
Total mass of basal insulin in circulation =6.01x10^{-8} x 19.6 = 1.18x10^{-6}mmol.
Mass delivered from device per sec = 5.28x 10^{-8} mmol/s
Time taken to deliver basal amount of 1.18 x 10^{-6} mmol = 1.18 x 10^{-6}/5.28x 10^{-8} = 22.34s

We can say that the insulin delivered from the device in gel state (in presence of basal glucose) can meet the basal insulin requirement (based on basal insulin concentration in non-diabetic person).

The insulin endogenously produced by the pancreatic beta cell has a half life of approximately 4 to 6 min (Duckworth, Bennett and Hamel, 1998; Hulse, Ralat and Wei-Jen, 2009). The basal insulin delivery rate from the device in presence of basal

glucose levels might seem too fast. However, a point to note here is that these are theoretical estimations based on in-vitro experiments made purely to gain some understanding of the performance window for the device.

8.2.2 Exploring different device geometries

The **gel thickness** in the device for *in vitro* diffusivity experiments using FITC-insulin with the NP gel and CL gel was 0.117 cm. The diffusion coefficients of FITC-insulin within the polymeric matrix determined experimentally are as presented in **Chapter 7**. The solution for Fick's law (TL method) which gives the total amount of solute transferred through the gel (refer to **Chapter 5, Equation 5-13)** was used to predict the impact of varying gel thickness. The drug released for the gel thickness from 0.1 to 2 cm was measured. **Figure 8-3** shows the insulin delivered from the device per day with varying gel thickness from 0.1 to 2 cm. As the gel thickness increased the drug delivered decreased due to the increasing diffusion pathlengths. **Figure 8-3** shows the performance window for the device with respect to gel thickness, gel thickness 0.1 to 1 cm showing capability for acceptable performance.

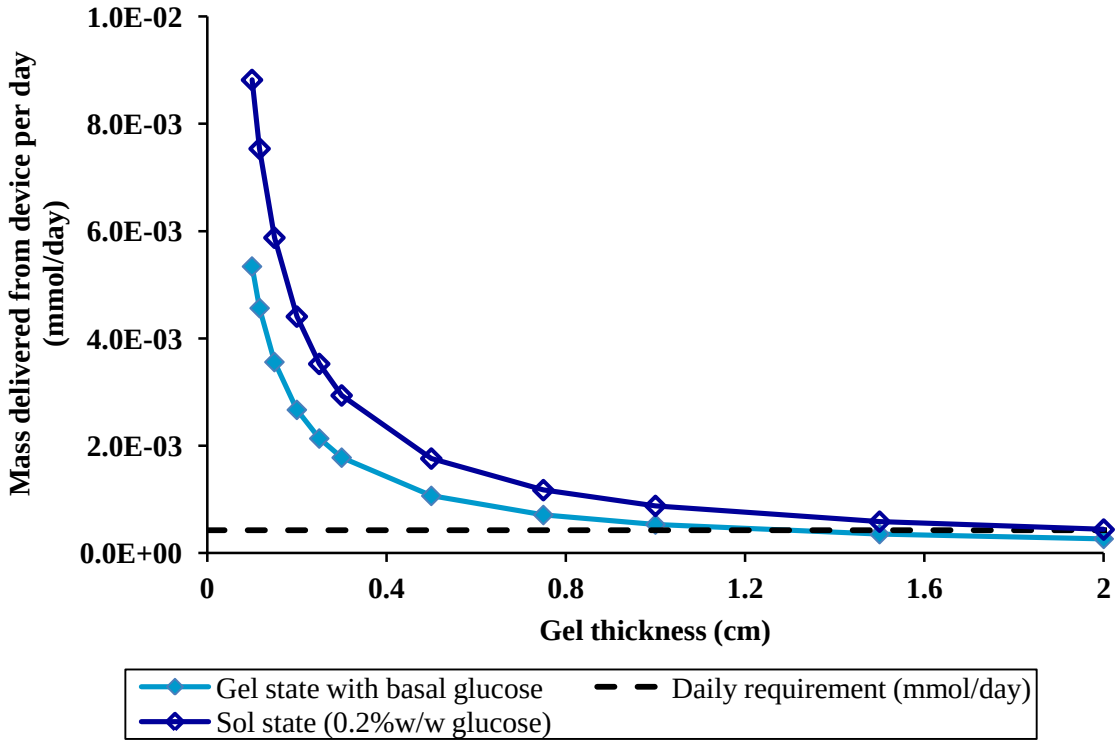

Figure 8-3: Effect of gel thickness on the insulin mass delivered from the device.

The drug delivered from the device in response to basal and post-meal glucose levels for gel thickness from 0.1 to 2 cm was also compared with the real time basal and bolus insulin levels observed (calculated from **Figure 8-2**). The real time basal insulin concentration observed in a non-diabetic person is ~10 mU/L (Daly, 2003) which is equivalent to a concentration of 6.01 x 10^{-8} mmol/L, assuming the body distribution volume as 19.6L the total mass of insulin present in circulation would be 1.18 x 10^{-6} mmol and a bolus insulin level of ~70 mU/L equates to 8.25 x 10^{-6} mmol. **Figure 8-4** shows the insulin delivered per 3 minutes meet the basal requirement with gel thickness less than 1cm. However the bolus requirement is met by a gel thickness less than 0.25cm.

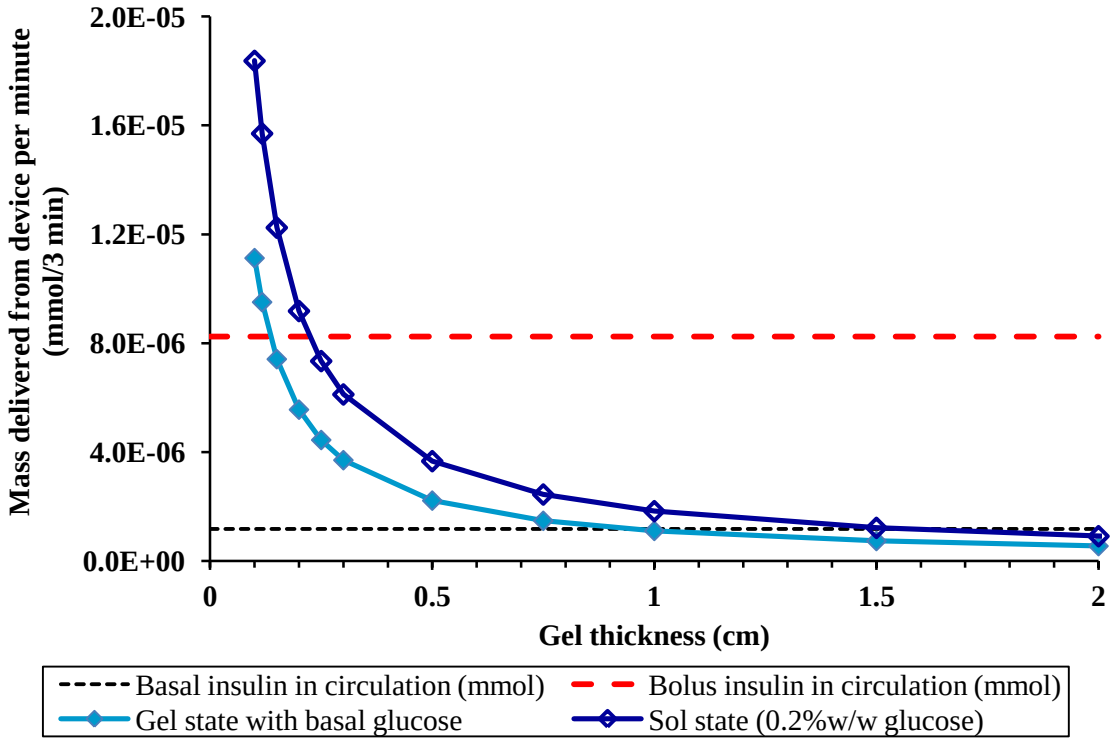

Figure 8-4: Effect of gel thickness on the insulin mass delivered from the device (mmol/3min).

The **surface area** available for diffusion in the device for *in vitro* diffusivity experiments using FITC-insulin with the NP gel and CL gel was 6.2 cm^2. The diffusion coefficient of FITC-insulin through the glucose-sensitive gel determined experimentally is as presented in **Chapter 7**. Fick's law was used to predict the impact of varying surface area and gel thickness on the amount of drug delivered. **Figure 8-5** shows the drug delivered per 10 seconds in gel state for the NP gel with increasing surface area from 1 to 50 cm^2 at gel thickness 0.05, 0.1, 0.2 and 0.5 cm. It is possible to select an appropriate combination of gel thickness and surface area to determine the ideal performance window which meets the daily basal insulin requirements.

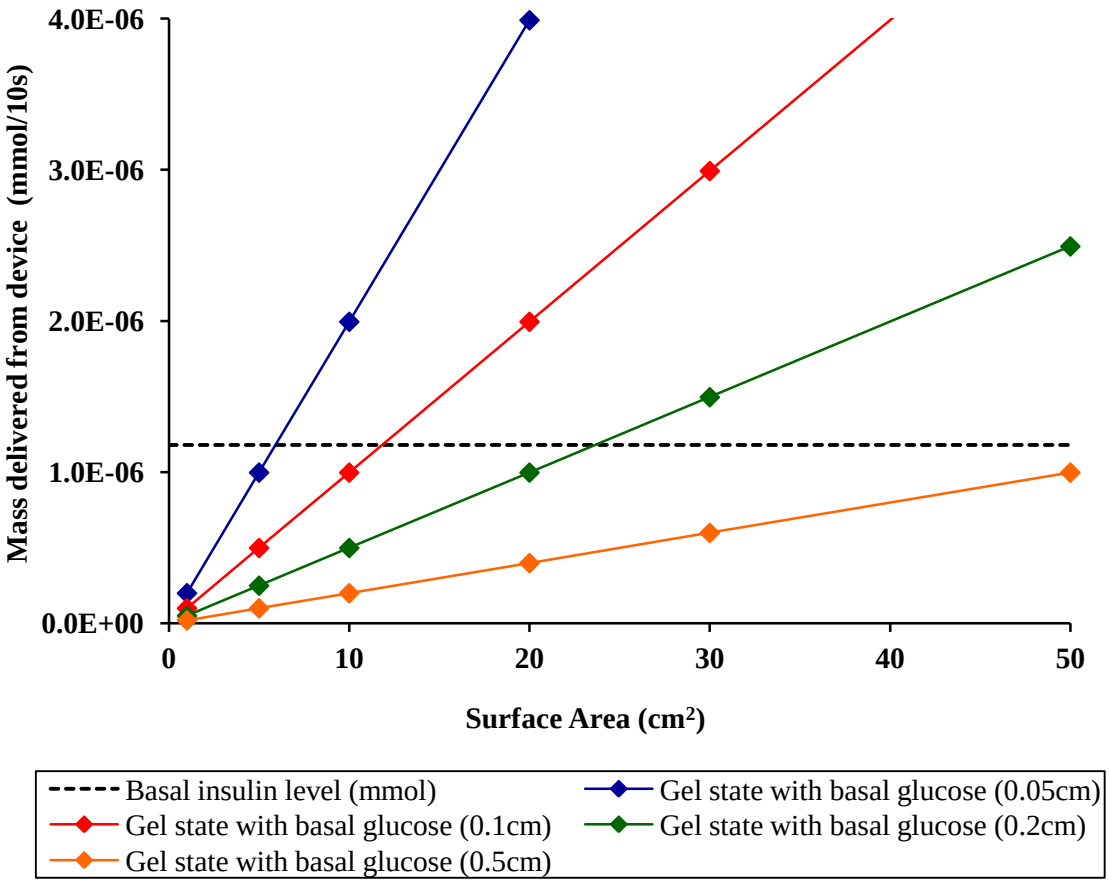

Figure 8-5: Effect of varying surface area and gel thickness on insulin delivered from the device (mmol/10s).

Figure 8-5 shows that a combination of gel thickness 0.1cm and surface areas greater than 12 cm^2 can deliver per 10 seconds the required basal insulin amount. Gel thickness less than 0.1cm with smaller surface areas and gel thicknesses greater than 0.1cm with larger surface areas can achieve the basal insulin amounts in 10 seconds. **Figure 8-6** shows that in 10 seconds the device was capable of delivering the bolus amount for 0.05 cm gel thickness with surface areas greater than 25 cm^2, 0.1 cm gel thickness with surface areas greater than 50 cm^2.

Thus if a gel thickness of 0.1 cm is selected to achieve the basal insulin levels in not more than 10 seconds, a range of surface area greater than 50 cm^2 can be explored depending on desired response times from 10 s to 3 min to deliver bolus insulin levels.

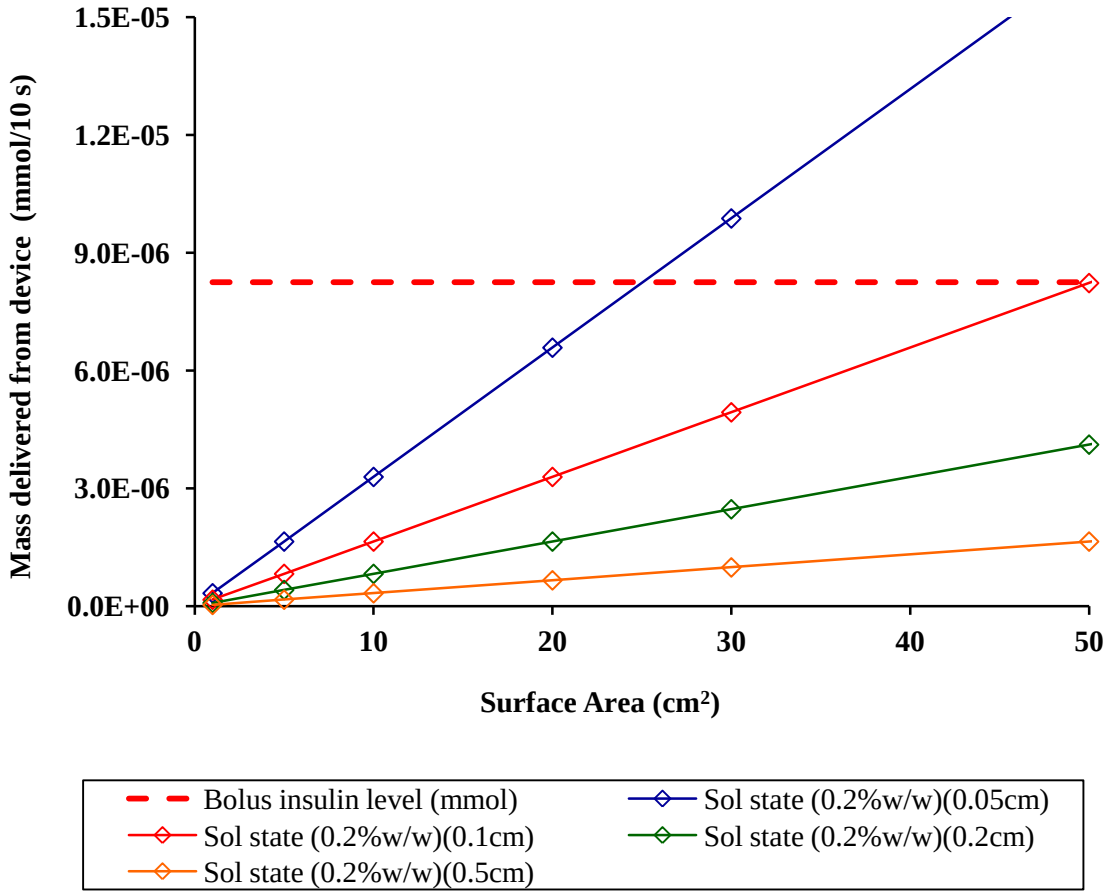

Figure 8-6: Effect of varying surface area and gel thickness on insulin delivered from the device (mmol/10s).

This theoretically selected ideal performance window which meets the daily basal and bolus insulin requirement provides an opportunity for increasing the surface area and thus exploring different device geometries in place of the current device geometry as shown in **Figure 8-7**. Based on the daily insulin requirements and the bolus insulin required to be delivered in response to postprandial glucose levels, the optimum dimensions for the device could have gel thickness from 0.05 to 0.1 cm with surface area greater than 12 cm^2.

Current device design **Device with gel slab double sided**

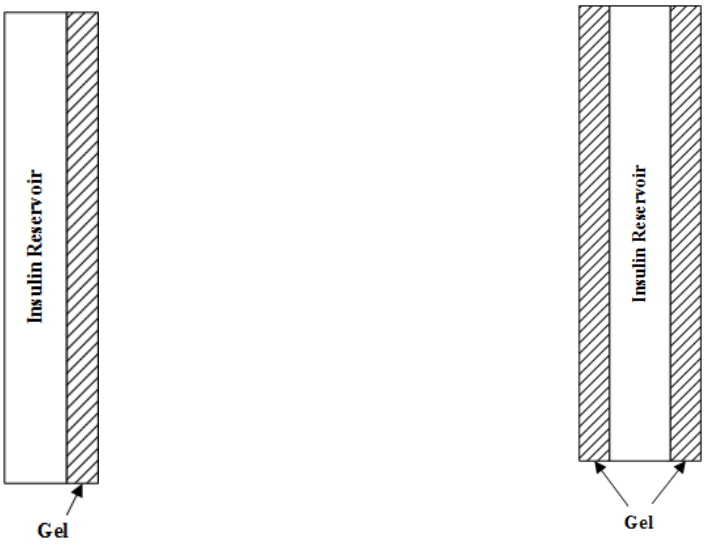

Spherical device design

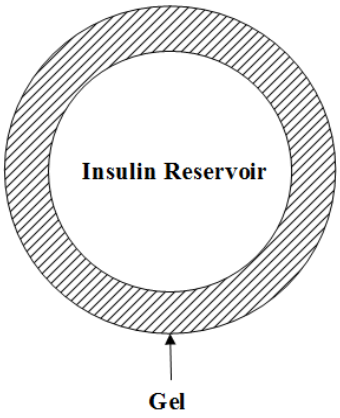

Cylindrical device design

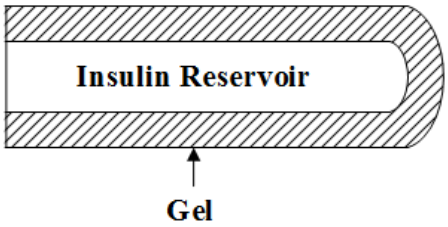

Figure 8-7: Current and potential device designs.

Figure 8-7 shows the current gel as a slab design, the current device design (INsmart, working design) has a diameter of approximately 4.5 cm with effective surface area of 6.2 cm^2. Double sided gel slab design with double the surface area can also be explored to increase the drug delivered and improve response times.

The spherical device design could be advantageous in terms of increased surface area for quicker response times. Also a smooth device surface finish can be advantageous in terms of lesser chances of lesions forming at the implantation site. As an example if a surface area of 12 cm^2 is considered, the sphere diameter as small as 2 cm can be explored, however this design will have a limitation with respect to a small insulin reservoir in the centre. This could be overcome by decreasing the gel thickness or increasing the diameter appropriately so that the effective surface area increases with insulin levels achieved in required response times.

A cylindrical device design would substantially increase the surface area which could significantly improve its performance. The device shape could have a number of advantages in terms of ease of implant and removal procedures, comfort to the wearer and also easy refilling. Here again based on a surface area of 12 cm^2, the cylinder radius as small as 0.5 cm and height 1.7 cm or radius 0.2 cm and height 1.9 cm can be explored, however this design will again have the same limitation in terms of insulin reservoir size in the centre. This could be overcome by decreasing the gel thickness or increasing the radius and height appropriately so that the effective surface area increases with insulin levels achieved in required response times.

The optimisation of the device design in favour of reducing the overall size has a number of advantages in terms of reduced risks of infection due to smaller size and smoother finish and faster recovery times in comparison to traditional more invasive surgical implants. However, the various geometries and design have to take into account the compatibility of the materials used in terms of suitability for implantation and effect on stability of insulin solution. Further, the surface finish for these devices should also be of high quality so as not to cause formation of lesions or abrasions at the implantation site. The most appropriate design will also depend on surgical needs, plumbing limitations or even manufacturing costs and safety.

In order to evaluate the validity of these theoretical predictions, experiments with increasing pathlengths or surface area could be performed. Agreement between theoretical predictions and independent experiments could indicate the validity of this model for this type of drug delivery systems. This illustrates the practical benefit of mathematical modelling of drug release, the impact of design parameters on drug release can be simulated in silico, thus potentially replacing time- and cost-intensive series of experimental studies.

8.2.3 Realistic scenario

Meal time – can the device deliver bolus doses and how fast?

An idealised insulin release profile from the device should match the insulin responses from a normal pancreas as shown in **Figure 8-2** in response to the glucose profile shown in **Figure 8-1**.

The device parameters as used in the *in vitro* experiments with surface area of 6.2 cm^2, gel thickness 0.117 cm and donor initial insulin concentration of 3.00 x 10^{-5} mol, the D measured using the glucose trigger experiments can be used to determine the bolus insulin amount delivered by the device per sec. As shown in **Figure 8-1**, high sucrose diet shows a max glucose peak of approx 7.25 mmol/L for a non-diabetic individual; but for an individual with diabetes, levels as high as 24 mmol/L (approx 0.5% w/w glucose) could be observed. **Table 8-2** shows how long it would take for the device to deliver the appropriate amount of insulin dose in response to a high glucose meal.

Table 8-2: Time taken to deliver post-prandial insulin amounts in response to glucose concentrations observed.

Glucose triggers	**Mass delivered by device**	**Time required to deliver 70 mUL^{-1} ($8.2x10^{-6}$ mmol for 19.6L volume)**	**Time required to deliver 80 mUL^{-1}($9.4x10^{-6}$ mmol for 19.6L volume)**
	(mmol/s)	(s)	(s)
~5.5 $mmolL^{-1}$	5.28×10^{-08}	156.1	178.4
~11 $mmolL^{-1}$	8.75×10^{-08}	94.2	107.6
~27.5 $mmolL^{-1}$	2.78×10^{-07}	29.6	33.8
~55 $mmolL^{-1}$	1.20×10^{-06}	6.9	7.9

Thus in response to post prandial high glucose concentration (extreme observed in diabetic patients), the device is capable of delivering a dose in 33.8 s.

It is common knowledge that insulin is released from the pancreas *in vivo* in a biphasic manner with a first burst of insulin secretion occurring rapidly at 2-4 min and lasting 10 min and then again gradually increases progressively to a pseudo-steady state, second phase insulin release in 2-3 hours as seen in rats and humans (Gerich, 2002; Rorsman et al., 2000; Ohara-Imaizumi et al., 2002; Seino, Shibasaki and Minami, 2011). The calculations show that the device is capable of post-prandial insulin release within the time duration, in fact quicker than as seen naturally *in vivo*.

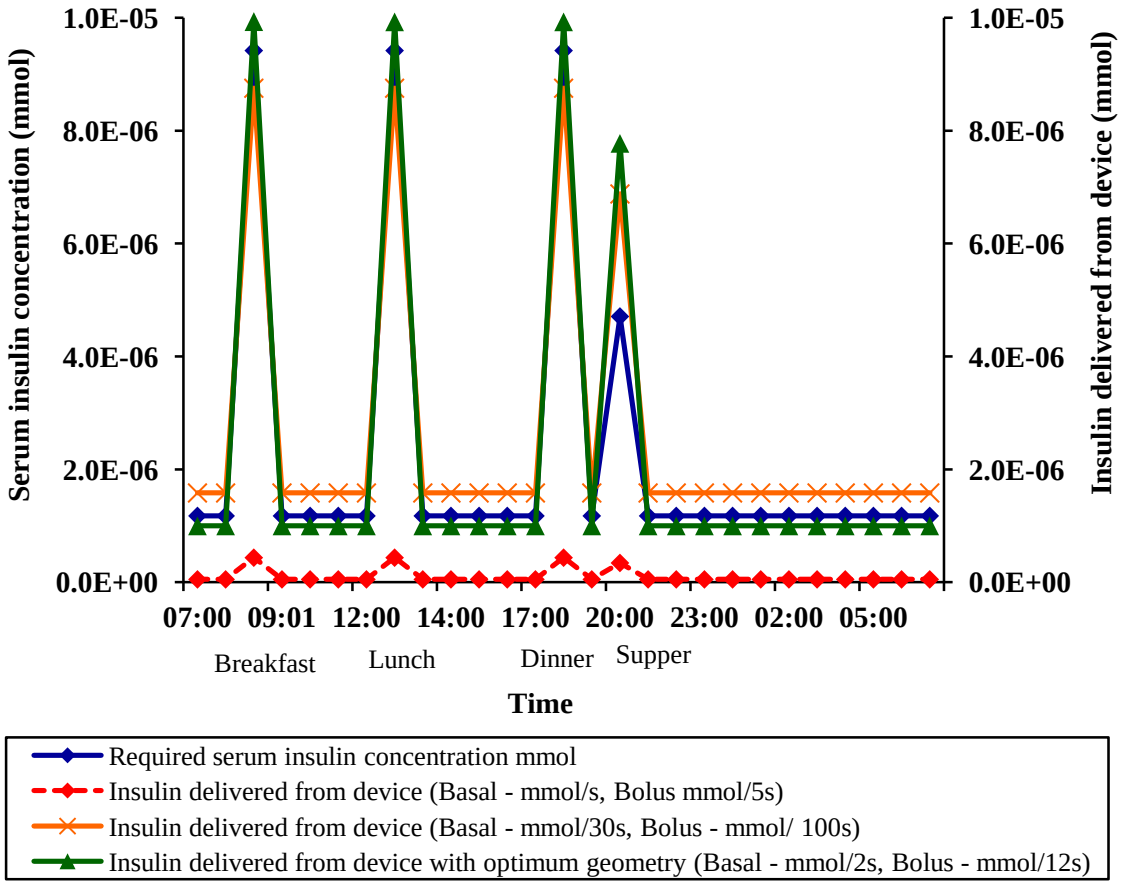

Figure 8-8: Schematic of diurnal profile of serum insulin concentration and insulin delivered from device with current geometry and optimum geometry in response to postprandial glucose concentrations.

A schematic of the diurnal profile of insulin delivered from the device with the current geometry in response to high postprandial glucose levels observed for diabetic individuals (meal time glucose level – 11 $mmolL^{-1}$ and supper – 8.3 $mmolL^{-1}$) was compared to the required serum insulin levels (from **Figure 8-2** as presented by Daly (2003)) and is presented in **Figure 8-8**.

Figure 8-8 shows that the device with the current dimensions show lower amounts of basal insulin per second and bolus insulin delivered per 5 second. The device with the current geometry is capable of delivering the required basal amount in 30 s and bolus amount in 100 s. Thus the device is capable of delivering until the required amount of insulin is delivered and as the glucose level in serum drops, the gel would revert back to

gel state. Also, if the device geometry is modified to optimum dimensions of gel thickness 0.1 cm and surface area 50 cm^2 as discussed in **Section 8.2.2** it could achieve the ideal performance required to match the serum insulin concentrations with faster response times, achieving basal amount per 2s and bolus amount in 12 s.

8.2.4 Service intervals

How long will the insulin in the reservoir last?

The ‘service interval’ applies to both the glucose-responsive gel and the insulin in the reservoir, the replacement time for the gel and the replenishment of reservoir insulin solution. Long term stability studies on the glucose-responsive gels by rheological characterisation when stored with and without 0.1% w/w glucose have found the gels to have a stable complex viscosity for over 730 days at 20°C and 37°C indicating that over time the gel components do not undergo degradation when stored in dialysis membrane, molecular weight cut off 50kDa (Sahota and Taylor, 2013).This has given confidence in the long term performance capability of the gel. Ideas for future device development include compartmentalising the gel in a cartridge which can be easily replaced if needed by non-invasive means.

The service intervals for the insulin formulation in the reservoir will depend on the insulin concentration and volume of the reservoir. The depletion of insulin in the reservoir and replacement strategies depends on daily insulin consumption by the individual with diabetes. This consumption depends on a number of factors such as onset, peak and duration of action, patient factors such as individual variations in insulin absorption affecting the basal dose required, due to levels of exercise and types of meals consumed.

Based on the calculations and estimations it has been shown that the device insulin release profiles is capable of mimicking the real-time serum insulin profile in response to glucose. Therefore estimations can be made for insulin replenishment regimens.

Based on the insulin dosage requirement of 0.5 to 1.0 unit per kg per day for most patients with C-peptide–negative T1DM diabetes (Hirsch, 1999), the insulin used up for an average male with body weight of 70.8 kg can be calculated.

The daily insulin requirement for an average man with body weight of 70.8 kg and the insulin requirement from the device per day are 2.14×10^{-4} to 4.25×10^{-4} mmol. The initial insulin reservoir mass based on current device design is 3.00×10^{-2} mmol, therefore the insulin in the reservoir would be depleted in 70.7 days.

Another key consideration in deciding upon the service interval for insulin would be to determine the donor concentration when the driving force is impacted which would result in lower mass transfer (flux).Based on the diffusion coefficient data for FITC-insulin in NP gel in presence of basal glucose, as shown in **Figure 8-9** the flux from the device remains constant over a period of time but decreases as the insulin concentration in receptor increases.

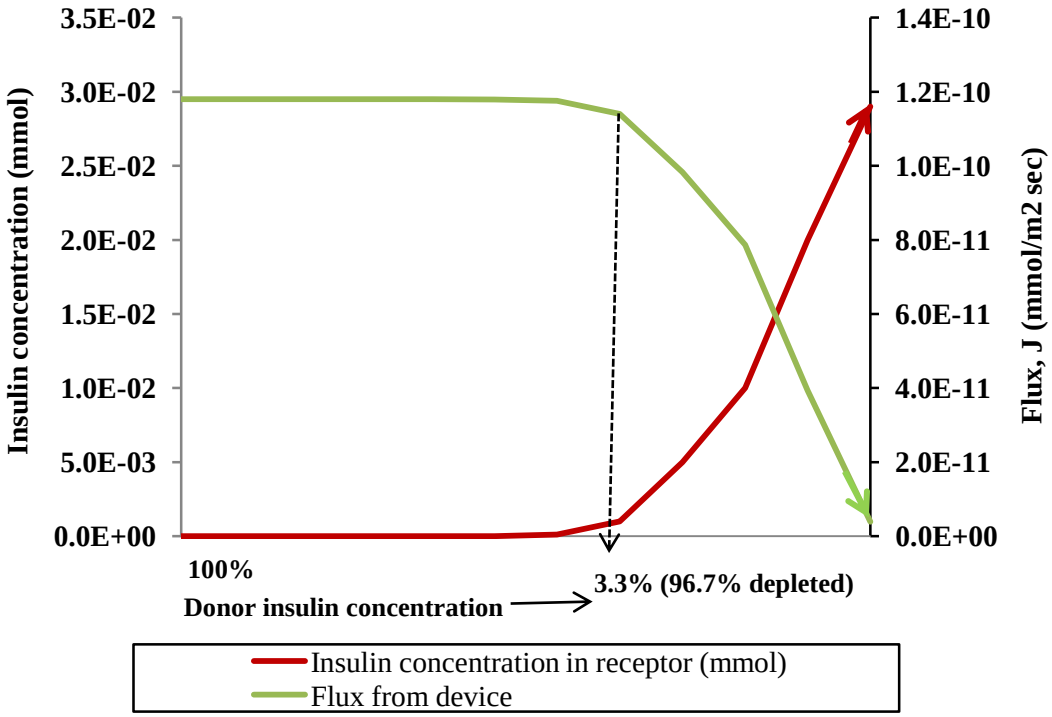

Figure 8-9: Impact of increasing receptor insulin concentration on the flux from the device.

In vivo the insulin delivered would quickly diffuse away into the tissues maintaining perfect sink conditions, thus would not affect the flux as observed in *in.vitro* condition. For the given experimental data the calculated donor concentration corresponds to 2.9 x 10^{-2} mmol (which is 96.4%). Hence when the donor concentration drops by 96.4% the flux might get affected. Based on the daily insulin requirement for an average man with body weight of 70.8 kg and the max insulin requirement from the device per day of 4.25 x 10^{-4} mmol, the donor insulin mass of 2.9 x 10^{-2} mmol corresponds to ~ 68 days. Thus here if the device insulin reservoir is replenished on a monthly basis, it should provide a safety margin of 100% in terms of amount of insulin delivered without affecting the flux.

8.3 Chapter summary

The knowledge of diffusion kinetics of FITC-insulin in the glucose-responsive gel as discussed in **Chapter 5** and **Chapter 7** have aided in understanding the capability and performance of the INsmart device along with making some design recommendations, service intervals and developing some replacement strategies for insulin solution.

Theoretical calculations have shown that the following capability and performance attributes of the INsmart device,

- The device is capable of delivering the daily required insulin amount in gel and sol state (in response to different glucose challenges) using the current experimental device design comprising of gel thickness 0.117 cm and surface area 6.2 cm^2.
- Calculations show that the insulin delivered from the device in gel state (in presence of basal glucose) meets the *in vivo* basal insulin requirement (based on basal insulin concentration in a non-diabetic person).
- The ideal performance window with respect to gel thickness was identified as less than 0.25 cm for the current device design (surface area 6.2 cm^2) to deliver the required basal and bolus insulin amounts per 3 minutes.
- The ideal performance window with respect to different combination of gel thickness and surface area which meets the basal and bolus insulin requirement

provides an opportunity for exploring different device geometries in place of the current device geometry. Based on the basal and bolus insulin amounts required to be delivered, the optimum dimensions for the device could have gel thickness from 0.05 to 0.1 cm with surface area greater than 12 cm^2 in 10 s. Device with gel thickness of 0.1cm and surface are of 50 cm^2 achieving basal amounts per 2 s and bolus amounts per 12 s.

- The device design could be modified to achieve the ideal diurnal performance required to match the serum insulin concentrations observed in a non-diabetic person. A double sided gel slab design can be explored to increase the amount of drug delivered. A spherical device design with surface area of 12 cm^2 and diameter as small as 2 cm or a cylindrical device design based on surface area of 12 cm^2 with the cylinder radius as small as 0.5 cm and height 1.7 cm or radius 0.2 cm and height 1.9 cm can also be explored. The design can be optimised appropriately to house the required insulin reservoir by increasing the size whilst maintaining the optimum surface area. The cylindrical design can provide a number of advantages in with respect to ease of implant and reduced risks of infection and recovery times associated with traditional more invasive surgical implants.
- The current device design with a donor insulin concentration of 10 ml of 500 IU would last for 70.7 days based on the daily insulin requirement for an average man with body weight of 70.8 kg. Taking into consideration the effect of decreasing driving force (concentration gradient) on flux based on *in vitro* calculation, the insulin in the reservoir would need to be replaced in ~ 68 days. Thus a monthly service interval (insulin replenishment) should provide a 100% safety margin.

Chapter 9 Overall Conclusions and Future work

9.1 Overall Conclusions

In this investigation, the aim was to assess the key INsmart device reliability and performance criteria for successful future clinical use. Returning to the questions posed at the beginning of this study, in **Chapter 2**, it is now possible to draw the following conclusions;

- An investigation into insulin stability and compatibility with materials that formed part of the device or have a potential to be considered for use in future device designs was conducted using three validated RP-HPLC methods to determine insulin loss and degradants formed and loss of FITC-insulin conjugates. The study highlighted the necessity for presence of phenolic compound *(m*-cresol) for maintaining the stability of insulin solution and showed greater loss in insulin recovery at 37°C.
- The material compatibility have shown that PC (polycarbonate, thermoplastic polymer with monomer bisphenolA) and SS (stainless steel Grade 316) are compatible with insulin solution remaining stable for up to 31 days (study period) at 20°C, however at 37°C, insulin solution was stable with SS for up to 21 days and with PC up to 11 days. Ti (titanium, 99.99% purity) was found to be the most stable; Ti is a good material to consider in future device designs. R (resin, polyurethane two part thermosetting resin, polyol and isocyanate mixed) might not be the best material to consider and PU (polyurethane, long chain thermoplastic polymer, polyol and isocyanate mixed) is definitely the least compatible and hence not suitable for future device designs.
- The compatibility study of the device materials with FITC-insulin solution which is being used in the *in vitro* studies has revealed that the device materials were compatible up to only 3 days. This finding did not pose a problem for the *in vitro* studies as such as FITC-insulin solutions were always freshly prepared just before use and the same solution was never used for periods greater than 3days. The

findings from this study has highlighted the fact that FITC-insulin solution needs formulation adjuncts and stabilisers, which should be assessed for stability if it is intended to be used in experiments with the device over a longer period.

- FITC-labelled insulin was synthesised in-house for use in *in vitro* diffusion experiments, to improve analytical quantification and aid detection to understand release profiles from the closed loop insulin delivery device. The major limitation to producing singly labelled biologically active mono-labelled FITC-insulin conjugate (B1) using human insulin was the presence of unlabelled native insulin at shorter reaction time.
- For the purposes of the in-vitro experiments, reaction time of 25 hrs was selected for production of FITC-insulin where predominantly di-labelled FITC-insulin conjugate (over 75%) was produced with the absence of any unlabelled native insulin. For the *in vitro* diffusion experiments, it was more important to know the size of the FITC-insulin conjugate produced and presence of any unlabelled native insulin was undesirable.
- The presence of phenol or *m*-cresol there appears to be a 10% decrease in amount of mono-labelled conjugate and a slight increase in di-labelled conjugate produced.
- It was hugely advantageous to synthesise FITC-insulin in-house as product with predominantly di-labelled conjugate was successfully produced without presence of any unreacted FITC or native insulin in comparison to the commercially available Sigma FITC-insulin product which was predominantly tri-labelled conjugate (most biologically inactive conjugate species) and had unreacted FITC in the product which is highly undesirable. Also, clinically used insulin analogues were successfully fluorescently labelled to produce FITC-insulin conjugates with potential future applicability, in biological and *in vitro* applications for tracing and relevant specific receptor binding studies.

- An experimental protocol was developed and four mathematical methods were investigated for determining insulin (FITC-insulin) diffusivity through the glucose-responsive gel in the INsmart device. The Laplace transform, diffusion cell-QSS, TL, slope and intercept analysis were assessed and compared for their applicability using the tube model and model dye (tartrazine) and gel (agarose) initially.

- The QSS and the TL slope and intercept methods were found to give similar results, however the unreliability of using only the TL intercept method for determination of diffusion coefficient in some instances was also highlighted.
- The diffusivity of fluorescein sodium salt was determined in order to develop the experimental method using the Luminescence spectrometer and to understand the diffusional properties of glucose through the NP gel due to the difficulty in determining its diffusivity in the NP gel as free glucose dismantles the gelatinous three- dimensional complex of the gel by competitive displacement thus dropping its viscosity which forms the basis for the responsiveness of the gel. The diffusivities of fluorescein sodium in NP gel with 0 and 0.1% w/w glucose concentration were found to be *D*: 0.81-0.91x10^{-10} and 0.84-0.85x10^{-10} m^2/s respectively.
- Pathlength was shown not to affect the diffusivity of fluorescein sodium salt.
- Batch to batch variability in conA was highlighted during experimental work. Rheological assessments of the gels formed using the two conA batches further highlighted the need to consider the conA batch to batch variation when preparing and using these gels.
- Rheological studies on the NP gel and CL gel have shown that viscoelastic changes occur in response to increasing glucose concentration further confirming that the underlying mechanism of the smart glucose responsive gel is functioning. This was further demonstrated by the relationship between diffusion coefficient values for FITC-insulin in NP gel and the complex viscosity of the gel measured in response to increasing glucose concentration which gave a third order polynomial fit. The results for the NP mixtures suggest their suitability for *in vitro* diffusion studies. The comparison of the gels at 20°C and 37°C suggest that the viscoelastic behaviours of the different gels are suitable for the intended use in the device. The CL mixture shows ~90% drop in complex viscosity between the physiologically useful glucose concentration range (0.1-1% w/w) at 20°C and ~80% drop at 37°C thus confirming its suitability for use in the closed-loop insulin delivery device for the management of diabetes.
- The drug release mechanism of FITC-insulin from the glucose sensitive gel held in the INsmart device, studied using fluorescein sodium was found to be diffusion controlled. Fluorescein sodium release from the NP gel over time demonstrated the

Peppas equation (power law) fit, for n=0.5 thus indicating a Fickian diffusion controlled release mechanism.

- The *D* for FITC-insulin in the NP gel determined using mathematical models, QSS and TL slope methods was 1.05 ± 0.02 x 10^{-11} m^2/ and in the CL gel was 0.75 ± 0.06 x 10^{-11} m^2/s.
- In presence of 0.1% glucose the FITC-insulin *D* seems to be lower than in its absence, the reason for which could be the micro viscosity created by glucose within the gel structure contributing towards interference in the diffusion of FITC-insulin. However, the *D* values do show an increase with increasing glucose concentration as expected, approximately 48% from 0.1 to 1% w/w for NP gel and approximately 23% from 0.2 to 1% w/w for CL gel, the increase in glucose having a greater effect on the macroviscosity of the gel.
- In response to physiologically relevant glucose triggers in the NP gel, the diffusivity of FITC-insulin increases (from 0.33 to 7.55 x 10^{-11} m^2/s) with increasing glucose concentrations (from 0.1% to 1% w/w), showing a polynomial fit, device thus showing glucose sensitivity and graded response, mimicking pancreas.
- It also showed that the diffused glucose molecules in the gel drop the viscosity of the gel but do not hinder the diffusivity of FITC-insulin in the gel thus the release kinetics are controlled entirely by the diffusivity of FITC-insulin in the gel.

- The knowledge of diffusion kinetics of FITC-insulin in the glucose-responsive gel has aided in understanding the capability and performance of the INsmart device and in making some design recommendations and developing some replacement strategies for insulin solution. The device is capable of delivering the daily required insulin amount in gel and sol state (in response to different glucose challenges) using the current experimental device design comprising of gel thickness 0.117 cm and surface area 6.2 cm^2.
- Calculations show that the insulin delivered from the device in gel state (in presence of basal glucose) meets the *in vivo* basal insulin requirement (based on basal insulin concentration in a non-diabetic person).

- The ideal performance window with respect to gel thickness was identified as less than 0.25 cm for the current device design (surface area 6.2 cm^2) to deliver the required basal and bolus insulin amounts per 3 minutes.
- Based on the basal and bolus insulin amounts required to be delivered, the optimum dimensions for the device could have gel thickness from 0.05 to 0.1 cm with surface area greater than 12 cm^2. Device with gel thickness of 0.1cm and surface are of 50 cm^2 achieved basal amounts per 2 s and bolus amounts per 12 s. This understanding provides an opportunity for exploring different device geometries in place of the current device geometry.
- Different device designs can be explored, from a double sided design, spherical design or cylindrical design with increased surface areas depending on the response time needed to meet daily basal and bolus insulin demands.
- The current device design with a donor insulin concentration of 10 ml of 500 IU would last for ~ 68 days based on the daily insulin requirement and consideration made for effect of decreasing flux. Thus a monthly service interval (insulin replenishment) should provide a 100% safety margin.

9.2 Future work plans

This research has revealed several opportunities for further work.

- It was very difficult to produce a sample with purely 100% mono-labelled conjugate without presence of any unlabelled insulin using the FITC-insulin synthesis method. Therefore a method to isolate the monolabelled conjugate produced needs to be explored in the future. Moreover, it couldn't be ascertained if the mono-labelled conjugate produced at short reaction times was A1 or B1 labelled conjugate from the chromatogram and mass spectra alone. In order to locate the exact positions where FITC were attached, a *Staphylococcus aureous* digestion of the separated/isolated conjugates as described by Hentz et al would need to be employed. Also, a biological test, an autophosphorylation assay using insulin receptor would aid in confirming the biological activity of the conjugates produced.

- The diffusion kinetics experiments had to be restricted due to unavailability of conA. Further diffusion experiments using FITC-insulin to confirm the diffusion mechanism and determine the kinetics at 37°C would be advantageous.
- From previous *in vivo* experiments in pigs it was observed that the BG levels were maintained in diabetic pig even when the solution from the device reservoir had almost no insulin left in it, which implied that insulin had migrated into the gel and deposited insulin in the gel which acted as a depot in the smart gel. Thus a sustained release insulin delivery system can be explored with solid insulin precipitate in the CL gel, which allows the gel still to switch on and off by its viscosity change and thus enabling to modulate the output. Such a mechanism will allow the device to be made without a liquid reservoir of insulin and thus be safer.

- The material compatibility study performed here could be extended further to tubing material used for filling the insulin reservoir and any other material considered for future device designs.

References

FDA Guideline for Industry Q2B Validation of Analytical Procedures: MethodologyID - 1524 (1997): U.S. Department of Health and Human Services, Food and Drug Administration, ICH.

ABDEKHODAIE, M.J. and WU, X.Y. (2009) Modeling of a glucose sensitive composite membrane for closed-loop insulin delivery. *Journal of Membrane Science,* 335 (1–2), pp. 21-31.

ABEL, J.J. (1926) Crystalline Insulin. *Proceedings of the National Academy of Sciences of the United States of America,* 12 (2), pp. 132-136.

ABUHESHMEH, N. et al. (2013) A New Method for Determination of Human Insulin in Aqueous Injections. *International Journal of Research in Pharmaceutical and Biomedical Sciences,* 4 (2), pp. 428-435.

AGUILAR, M. (2004) Reversed-Phase High-Performance Liquid Chromatography. In: AGUILAR, M. (ed.)*Methods in Molecular Biology, HPLC of Peptides and Proteins: Methods and Protocols*. 251st ed. Totowa, NJ: Humana Press Inc., pp. 3-9.

AJMERA, I. et al. (2013) The impact of mathematical modeling on the understanding of diabetes and related complications. *CPT: Pharmacometrics & Systems Pharmacology,* 2 (7), pp. e54.

AMERICAN DIABETES ASSOCIATION (2008) Diagnosis and classification of diabetes mellitus. *Diabetes Care,* 31(Suppl 1), pp. S55-S60.

AXELSSON, A. and PERSSON, B. (1988) Determination of effective diffusion coefficients in calcium alginate gel plates with varying yeast cell content. *Applied Biochemistry and Biotechnology,* 18 (1), pp. 231-250.

BAILEY, C.J. et al. (2013) Dapagliflozin add-on to metformin in type 2 diabetes inadequately controlled with metformin: a randomized, double-blind, placebo-controlled 102-week trial. *BMC Medicine,* 11, pp. 43-7015-11-43.

BAILEY, C.J. and TURNER, R.C. (1996) Metformin. *The New England Journal of Medicine,* 334 (9), pp. 574-579.

BAKER, E.N. et al. (1988) The structure of 2Zn pig insulin crystals at 1.5 A resolution. *Philosophical Transactions of the Royal Society of London B: Biological Sciences,* 319 (1195), pp. 369-456.

BANTING, F.G. and BEST, C.H. (1922) Pancreatic extracts. *The Journal of Laboratory and Clinical Medicine,* 7 (8), pp. 464-472.

BENZEVAL, I., BOWYER, A. and HUBBLE, J. (2012) The influence of degree-of-branching and molecular mass on the interaction between dextran and Concanavalin A in hydrogel preparations intended for insulin release. *European Journal of Pharmaceutics and Biopharmaceutics,* 80 (1), pp. 143-148.

BERENSON, D.F. et al. (2011) Insulin analogs for the treatment of diabetes mellitus: therapeutic applications of protein engineering. *Annals of the New York Academy of Sciences,* 1243 (1), pp. E40-E54.

BERG, J.M., TYMOCZKO, J.L. and STRYER, L. (2002) 3.2.Primarystructure: Amino acids are linked by peptide bonds to form polypeptide chains. In: *Biochemistry*. 5th ed. New York: W H Freeman and Company.

BISCHOFF, R. and KOLBE, H.V. (1995) Deamidation of asparagine and glutamine residues in proteins and peptides: structural determinants and analytical methodology. *Journal of Chromatography. B, Biomedical Applications 01,* 662 (2), pp. 261-278.

BLUNDELL, T. et al. (1972) Insulin: The Structure in the Crystal and its Reflection in Chemistry and Biology by. *Advances in Protein Chemistry,* 26, pp. 279-402.

BMA (2004) *Diabetes mellitus: an update for health care professionals*. [Online] British Medical Association. www.bma.org.uk [Accessed 28/09/14].

BRANDL, F. et al. (2010) Hydrogel-based drug delivery systems: comparison of drug diffusivity and release kinetics. *Journal of Controlled Release,* 142 (2), pp. 221-228.

BRANGE, J. (1997) The new era of biotech insulin analogues. *Diabetologia,* 40 (2), pp. S48-S53.

BRANGE, J. et al. (1982) Formulation of physically stable neutral solutions for continous infusion by delivery systems. *Hormone Drugs,* pp. 96-105.

BRANGE, J., HAVELUND, S. and HOUGAARD, P. (1992a) Chemical stability of insulin. 2. Formation of higher molecular weight transformation products during storage of pharmaceutical preparations. *Pharmaceutical Research,* 9 (6), pp. 727-734.

BRANGE, J. et al. (1992b) Chemical stability of insulin. 1. Hydrolytic degradation during storage of pharmaceutical preparations. *Pharmaceutical Research,* 9 (6), pp. 715-726.

BRANGE, J. et al. (1987) *Galenics of insulin: the physico-chemical and pharmaceutical aspects of insulin and insulin preparations*. Berlin: Springer-Verlag.

BRANGE, J. (1992c) Chemical stability of insulin. 4. Mechanisms and kinetics of chemical transformations in pharmaceutical formulation. *Acta Pharmaceutica Nordica,* 4 (4), pp. 209-222.

BRANGE, J. and LANGKJAER, L. (1993) Insulin structure and stability. *Pharmaceutical Biotechnology,* 5, pp. 315-350.

BRANGE, J. and LANGKJAER, L. (1992e) Chemical stability of insulin. 3. Influence of excipients, formulation, and pH. *Acta Pharmaceutica Nordica,* 4 (3), pp. 149-158.

BRANGE, J. et al. (1990) Monomeric insulins and their experimental and clinical implications. *Diabetes Care,* 13 (9), pp. 923-954.

BRANGE, J. and VØLUND, A. (1999) Insulin analogs with improved pharmacokinetic profiles. *Advanced Drug Delivery Reviews,* 35 (2-3), pp. 307-335.

BRITISH PHARMACOPOEIA VOLUME III (2014) *Formulated Preparations: Specific Monographs: Insulin Preparations (Ph. Eur. monograph 0854).*

BRODIN, B., STEFFANSEN, B. and NIELSEN, C.U. (2009) Passive diffusion of drug substances: the concepts of flux and permeability. In: BRODIN, B. and NIELSEN, C.U. (eds.) *Molecular Biopharmaceutics*. 1st ed. London: Pharmaceutical Press, pp. 135-152.

BROWN, H., SANGER, F. and KITAI, R. (1955) The structure of pig and sheep insulins. *Biochemical Journal,* 60 (4), pp. 556-550.

BROWNLEE, M. (2001) Biochemistry and molecular cell biology of diabetic complications. *Nature,* 414 (6865), pp. 813-820.

BROWNLEE, M. (2005) The pathobiology of diabetic complications: a unifying mechanism. *Diabetes,* 54 (6), pp. 1615-1625.

BÜRGI, W. et al. (1988) One-step sandwich enzyme immunoassay for insulin using monoclonal antibodies. *Clinical Biochemistry,* 21 (5), pp. 311-314.

CAHILL JR, G.F. (1971) The Banting Memorial Lecture 1971. Physiology of insulin in man 20, pp. 785-799.

CASSIDY, J.P. et al. (2012) Quantification of human serum insulin concentrations in clinical pharmacokinetic or bioequivalence studies: what defines the "best method"?. *Clinical Chemistry and Laboratory Medicine,* 50 (4), pp. 663-666.

CHANG, X. et al. (1997) Solution structures of the R6 human insulin hexamer. *Biochemistry,* 36 (31), pp. 9409-9422.

CHEN, J., LOO, L.S. and WANG, K. (2012) A Novel Time Lag Method to Measure the Permeation of Vapor-Gas Mixtures. *Journal of Membrane and Separation Technology,* 1, pp. 94-99.

CHEN, Z. et al. (2013) Quantitative insulin analysis using liquid chromatography-tandem mass spectrometry in a high-throughput clinical laboratory. *Clinical Chemistry,* 59 (9), pp. 1349-1356.

CHOI, J. et al. (2013) Dye-Doped Silica Nanoparticle with HIV-1 TAT Peptide for Bioimaging. *Journal of Biomedical Nanotechnology,* 9 (2), pp. 291-294.

CIENCIALOVÁ, A. et al. (2004) Preparation and characterization of two LysB29 specifically labelled fluorescent derivatives of human insulin. *Journal of Peptide Science,* 10 (7), pp. 470-478.

CONVERTI, A. et al. (1996) Evaluation of glucose diffusion coefficient through cell layers for the kinetic study of an immobilized cell bioreactor. *Chemical Engineering Science,* 51 (7), pp. 1023-1026.

CRANK, J. (1975) The Diffusion Equations. In: *The Mathematics of Diffusion*. 2nd ed. London: Oxford University Press, pp. 1-10.

CROWTHER, J.B. (2001) Validation of Pharmaceutical Test Methods. In: SATINDER AHUJA, S.S. (ed.)*Handbook of Modern Pharmaceutical Analysis*: Academic Press, pp. 415-443.

CRYER, P. (2002) Hypoglycaemia: The limiting factor in the glycaemic management of Type I and Type II Diabetes*. *Diabetologia,* 45 (7), pp. 937-948.

CUSSLER, E.L. (2009) *Diffusion: Mass transfer in fluid systems*. 3rd ed. New York: Cambridge University Press.

CUSSLER, E.L. (ed.) (1997) *Diffusion Mass Tranfer in Fluid Systems: Mass Transfer in Fluid Systems*. 2nd ed. Cambridge: Cambridge University Press.

D'AURIZIO, E. et al. (2011) Preparation and characterization of poly (lactic-co-glycolic acid) microspheres loaded with a labile antiparkinson prodrug. *International Journal of Pharmaceutics,* 409 (1), pp. 289-296.

DALY, M. (2003) Sugars, insulin sensitivity, and the postprandial state. *The American Journal of Clinical Nutrition,* 78 (4), pp. 865S-872S.

DALY, M.E. et al. (1998) Acute effects on insulin sensitivity and diurnal metabolic profiles of a high-sucrose compared with a high-starch diet. *American Journal of Clinical Nutrition,* 67 (6), pp. 1186-1196.

DANAEI, G. et al. (2011) National, regional, and global trends in fasting plasma glucose and diabetes prevalence since 1980: systematic analysis of health examination surveys and epidemiological studies with 370 country-years and 2·7 million participants. *The Lancet,* 378 (9785), pp. 31-40.

DE BRUYN, T. et al. (2011) Sodium fluorescein is a probe substrate for hepatic drug transport mediated by OATP1B1 and OATP1B3. *Journal of Pharmaceutical Sciences,* 100 (11), pp. 5018-5030.

DE MEYTS, P. (2004) Insulin and its receptor: structure, function and evolution. *BioEssays : News and Reviews in Molecular, Cellular and Developmental Biology,* 26 (12), pp. 1351-1362.

DEFELIPPIS, M.R., CHANCE, R.E. and FRANK, B.H. (2001) Insulin self-association and the relationship to pharmacokinetics and pharmacodynamics. *Critical Reviews in Therapeutic Drug Carrier Systems,* 18 (2), pp. 201-264.

DEREWENDA, U. et al. (1989) Molecular Structure of insulin: The insulin monomer and its assembly. *British Medical Bulletin,* 45 (1), pp. 4-18.

DEZIER, J.F. et al. (1987) Comparison of 2 methods of measuring microalbuminuria. Immunonephelometry and radioimmunology. *Annales De Biologie Clinique,* 45 (1), pp. 78-84.

DIABETES UK (2012) *Diabetes in the UK 2012: key statistics on diabetes*. [Online] www.diabetes.org.uk [Accessed 28/09/14].

DODSON, E. et al. (1993) Insulin assembly: its modification by protein engineering and ligand binding. *Philosophical Transactions of the Royal Society of London.Series A: Physical and Engineering Sciences,* 345 (1674), pp. 153-164.

DUCKWORTH, W.C., BENNETT, R.G. and HAMEL, F.G. (1998) Insulin Degradation: Progress and Potential 1. *Endocrine Reviews,* 19 (5), pp. 608-624.

DUNNING, B.E. and GERICH, J.E. (2007) The role of α-cell dysregulation in fasting and postprandial hyperglycemia in type 2 diabetes and therapeutic implications. *Endocrine Reviews,* 28 (3), pp. 253-283.

FAISANT, N., SIEPMANN, J. and BENOIT, J. (2002) PLGA-based microparticles: elucidation of mechanisms and a new, simple mathematical model quantifying drug release. *European Journal of Pharmaceutical Sciences,* 15 (4), pp. 355-366.

FEINGOLD, V., JENKINS, A.B. and KRAEGEN, E.W. (1984) Effect of contact material on vibration-induced insulin aggregation. *Diabetologia,* 27 (3), pp. 373-378.

FISHER, B.V. and PORTER, P.B. (1981) Stability of bovine insulin. *Journal of Pharmacy and Pharmacology,* 33 (1), pp. 203-206.

FLORENCE, A.T. (2010) An Introduction to Clinical Pharmaceutics. In: London: Pharmaceutical Press, pp. 109-110.

FOORD, S. and ATKINS, E. (1989) New x-ray diffraction results from agarose: Extended single helix structures and implications for gelation mechanism. *Biopolymers,* 28 (8), pp. 1345-1365.

FRANK, B.H., PEKAR, A.H. and VEROS, A.J. (1972) Insulin and proinsulin conformation in solution. *Diabetes,* 21 (2 Suppl), pp. 486-491.

FREEMAN, J.S. (2009) Insulin analog therapy: improving the match with physiologic insulin secretion. *The Journal of the American Osteopathic Association,* 109 (1), pp. 26-36.

FRENNING, G. and STRØMME, M. (2003) Drug release modeled by dissolution, diffusion, and immobilization. *International Journal of Pharmaceutics,* 250 (1), pp. 137-145.

FRENNING, G. (2011) Modelling drug release from inert matrix systems: From moving-boundary to continuous-field descriptions. *International Journal of Pharmaceutics,* 418 (1), pp. 88-99.

FRIDLYAND, L.E. and PHILIPSON, L.H. (2010) Glucose sensing in the pancreatic beta cell: a computational systems analysis. *Theoretical Biology & Medical Modelling,* 7, pp. 15-4682-7-15.

FRIEDMAN, M.H. (2008) Free Diffusion. In: *Principles and Models of Biological Transport*. 2nd ed. New York: Springer, pp. 1-37.

FRISCH, H. and PRAGER, S. (2003) Time lag and fluctuations in diffusion through an inhomogeneous material. *The Journal of Chemical Physics,* 54 (4), pp. 1451-1453.

GANDY, J. (ed.) (2014) *Manual of Dietetic Practice*. 5th ed. The Atrium, Southern Gate, Chichester, West Sussex PO19 8SQ,Uk: John Wiley & Sons Ltd.

GARG, S.K. et al. (2011) Use of continuous glucose monitoring in subjects with type 1 diabetes on multiple daily injections versus continuous subcutaneous insulin infusion therapy: a prospective 6-month study. *Diabetes Care,* 34 (3), pp. 574-579.

GERICH, J.E. (2002) Is reduced first-phase insulin release the earliest detectable abnormality in individuals destined to develop type 2 diabetes?. *Diabetes,* 51 Suppl 1, pp. S117-21.

GIEPMANS, B.N. et al. (2006) The fluorescent toolbox for assessing protein location and function. *Science (New York, N.Y.),* 312 (5771), pp. 217-224.

GILLIAM, L.K. and HIRSCH, I.B. (2009) Practical aspects of real-time continuous glucose monitoring. *Diabetes Technology & Therapeutics,* 11 (S1), pp. S-76-S-82.

GIOVANNUCCI, E. et al. (2010) Diabetes and cancer: a consensus report. *Diabetes Care,* 33 (7), pp. 1674-1685.

GLAESSL, B. et al. (2010) Deeper insight into the drug release mechanisms in Eudragit RL-based delivery systems. *International Journal of Pharmaceutics,* 389 (1), pp. 139-146.

GRAVES, P.M. and EISENBARTH, G.S. (1999) Pathogenesis, prediction and trials for the prevention of insulin-dependent (type 1) diabetes mellitus. *Advanced Drug Delivery Reviews,* 35 (2-3), pp. 143-156.

GROOP, L.C. (1992) Sulfonylureas in NIDDM. *Diabetes Care,* 15 (6), pp. 737-754.

HAVELUND, S. et al. (2004) The mechanism of protraction of insulin detemir, a long-acting, acylated analog of human insulin. *Pharmaceutical Research,* 21 (8), pp. 1498-1504.

HAZEL, J.R. and SIDELL, B.D. (1987) A method for the determination of diffusion coefficients for small molecules in aqueous solution. *Analytical Biochemistry,* 166 (2), pp. 335-341.

HELBLING, I.M. et al. (2010b) Modeling of dispersed-drug delivery from planar polymeric systems: optimizing analytical solutions. *International Journal of Pharmaceutics,* 400 (1), pp. 131-137.

HELBLING, I.M. et al. (2010a) Modeling of drug delivery from erodible and non-erodible laminated planar devices into a finite external medium. *Journal of Membrane Science,* 350 (1), pp. 10-18.

HELBLING, I.M., LUNA, J.A. and CABRERA, M.I. (2011) Mathematical modeling of drug delivery from torus-shaped single-layer devices. *Journal of Controlled Release,* 149 (3), pp. 258-263.

HENTZ, N.G. et al. (1997) Synthesis and characterization of insulin-fluorescein derivatives for bioanalytical applications. *Analytical Chemistry,* 69 (24), pp. 4994-5000.

HERRMANN, S. et al. (2007a) New insight into the role of polyethylene glycol acting as protein release modifier in lipidic implants. *Pharmaceutical Research,* 24 (8), pp. 1527-1537.

HERRMANN, S. et al. (2007b) Mechanisms controlling protein release from lipidic implants: effects of PEG addition. *Journal of Controlled Release,* 118 (2), pp. 161-168.

HIPSZER, B., JOSEPH, J. and KAM, M. (2005) Pharmacokinetics of intravenous insulin delivery in humans with type 1 diabetes. *Diabetes Technology & Therapeutics,* 7 (1), pp. 83-93.

HIRSCH, I.B. (2010) Insulin delivery devices--pumps and pens. *Diabetes Technology & Therapeutics,* 12 Suppl 1, pp. S115-6.

HIRSCH, I.B. (2005) Insulin analogues. *New England Journal of Medicine,* 352 (2), pp. 174-183.

HIRSCH, I.B. (1999) Type 1 diabetes mellitus and the use of flexible insulin regimens. *American Family Physician,* 60 (8), pp. 2343-2352.

HOLT, T. and KUMAR, S. (2010) Diagonising Diabetes. In: HOLT, T. and KUMAR, S. (eds.) *ABC of Diabetes*. 6th ed. Oxford: Wiley-Blackwell Publication, pp. 1-4.

HOVORKA, R. et al. (2010) Manual closed-loop insulin delivery in children and adolescents with type 1 diabetes: a phase 2 randomised crossover trial. *The Lancet,* 375 (9716), pp. 743-751.

HU, F.B. et al. (2001) Diet, Lifestyle, and the Risk of Type 2 Diabetes Mellitus in Women. *New England Journal of Medicine,* 345 (11), pp. 790-797.

HUBBARD, S.R. (2013) Structural biology: Insulin meets its receptor. *Nature,* 493 (7431), pp. 171-172.

HULSE, R.E., RALAT, L.A. and WEI-JEN, T. (2009) Structure, Function, and Regulation of Insulin-Degrading Enzyme. *Vitamins & Hormones,* 80, pp. 635-648.

HUNDAL, R.S. and INZUCCHI, S.E. (2003) Metformin. *Drugs,* 63 (18), pp. 1879-1894.

INTERNATIONAL DIABETES FEDERATION (2013) *IDF Diabetes Atlas.* 6th edn. ed. Brussels: Belgium: International Diabetes Federation. Available from: http://www.idf.org/diabetesatlas [Accessed 18/05/15].

JAMESON, D.M. and ROSS, J.A. (2010) Fluorescence polarization/anisotropy in diagnostics and imaging. *Chemical Reviews,* 110 (5), pp. 2685-2708.

JENSEN, K. (ed.) (2009) *Peptide and Protein Design for Biopharmaceutical Applications*. West Sussex,UK: John Wiley & Sons.

JOHNSON, J. et al. (2012) Diabetes and cancer (1): evaluating the temporal relationship between type 2 diabetes and cancer incidence. *Diabetologia,* 55 (6), pp. 1607-1618.

KAARSHOLM, N.C., KO, H.C. and DUNN, M.F. (1989) Comparison of solution structural flexibility and zinc binding domains for insulin, proinsulin and miniproinsulin. *Biochemistry,* 28 (10), pp. 4427-4435.

KANAMORI, T. et al. (1994) An improvement on the method of determining the solute permeability of hollow-fiber dialysis membranes photometrically using optical fibers and comparison of the method with ordinary techniques. *Journal of Membrane Science,* 88 (2), pp. 159-165.

KAUSHIK, S., MOHANTY, D. and SUROLIA, A. (2009) The role of metal ions in substrate recognition and stability of concanavalin A: a molecular dynamics study. *Biophysical Journal,* 96 (1), pp. 21-34.

KELTON, J. et al. (1978) Comparison of Chemical Composition of Peritoneal Fluid and SerumA Method for Monitoring Dialysis Patients and a Tool for Assessing Binding to Serum Proteins In Vivo. *Annals of Internal Medicine,* 89 (1), pp. 67-70.

KERR, D. and PARTRIDGE, H. (2011) Deus ex machina: The use of technology in type 1 diabetes. *Primary Care Diabetes,* 5 (3), pp. 159-165.

KHUNTI, K. et al. (2006) Randomised controlled trial of near-patient testing for glycated haemoglobin in people with type 2 diabetes mellitus. *British Journal of General Practice,* 56 (528), pp. 511-517.

KIDO, Y., NAKAE, J. and ACCILI, D. (2001) The Insulin Receptor and Its Cellular Targets 1. *The Journal of Clinical Endocrinology & Metabolism,* 86 (3), pp. 972-979.

KOSMIDIS, K. et al. (2003) Analysis of Case II drug transport with radial and axial release from cylinders. *International Journal of Pharmaceutics,* 254 (2), pp. 183-188.

KOZLER, P. and POKORNY, J. (2003) Altered blood-brain barrier permeability and its effect on the distribution of Evans blue and sodium fluorescein in the rat brain applied by intracarotid injection. *Physiological Research,* 52 (5), pp. 607-614.

KREYE, F., SIEPMANN, F. and SIEPMANN, J. (2011a) Drug release mechanisms of compressed lipid implants. *International Journal of Pharmaceutics,* 404 (1), pp. 27-35.

KREYE, F. et al. (2011b) Drug release mechanisms of cast lipid implants. *European Journal of Pharmaceutics and Biopharmaceutics,* 78 (3), pp. 394-400.

LAO, L.L. et al. (2011) Modeling of drug release from bulk-degrading polymers. *International Journal of Pharmaceutics,* 418 (1), pp. 28-41.

LAVIS, L.D. and RAINES, R.T. (2008) Bright ideas for chemical biology. *ACS Chemical Biology,* 3 (3), pp. 142-155.

LEE, P.I. (2011) Modeling of drug release from matrix systems involving moving boundaries: Approximate analytical solutions. *International Journal of Pharmaceutics,* 418 (1), pp. 18-27.

LIN, C. and METTERS, A.T. (2006) Hydrogels in controlled release formulations: network design and mathematical modeling. *Advanced Drug Delivery Reviews,* 58 (12), pp. 1379-1408.

LIN-GIBSON, S. et al. (2005) Structure-property relationships of photopolymerizable poly (ethylene glycol) dimethacrylate hydrogels. *Macromolecules,* 38 (7), pp. 2897-2902.

LIU, F., KOHN, W.D. and MAYER, J.P. (2012) Site-specific fluorescein labeling of human insulin. *Journal of Peptide Science,* 18 (5), pp. 336-341.

LOUGHEED, W.D. et al. (1983) Physical stability of insulin formulations. *Diabetes,* 32 (5), pp. 424-432.

LOUGHEED, W.D. et al. (1980) Insulin aggregation in artificial delivery systems. *Diabetologia,* 19 (1), pp. 1-9.

MACDONALD, P.E., JOSEPH, J.W. and RORSMAN, P. (2005) Glucose-sensing mechanisms in pancreatic beta-cells. *Philosophical Transactions of the Royal Society of London.Series B, Biological Sciences,* 360 (1464), pp. 2211-2225.

MAGGI, V. (1966) The localization of fluorescent insulin in mouse tissues. *Experimental Cell Research,* 44 (2), pp. 672-676.

MANNING, M.C., PATEL, K. and BORCHARDT, R.T. (1989) Stability of protein pharmaceuticals. *Pharmaceutical Research,* 6 (11), pp. 903-918.

MANNING, M.C. et al. (2010) Stability of protein pharmaceuticals: an update. *Pharmaceutical Research,* 27 (4), pp. 544-575.

MARTIN, A. (1993) Diffusion and Dissolution. In: MUNDROFF, G.H. (ed.)*Physical Pharmacy - Physical Chemical Principles in the Pharmaceutical Sciences*. 4th ed. Maryland USA: Williams and Wilkins, pp. 324-361.

MARUCCI, M. et al. (2008) Mechanistic model for drug release during the lag phase from pellets coated with a semi-permeable membrane. *Journal of Controlled Release,* 127 (1), pp. 31-40.

MARUCCI, M. et al. (2011) Polymer leaching from film coating: effects on the coating transport properties. *International Journal of Pharmaceutics,* 411 (1), pp. 43-48.

MELBERG, S.G. et al. (1988) Insulin compatibility with polymer materials used in external pump infusion systems. *Diabetic Medicine,* 5 (3), pp. 243-247.

MENEGHINI, L. and SPARROW-BODENMILLER, J. (2010) Practical aspects and considerations when switching between continuous subcutaneous insulin infusion and multiple daily injections. *Diabetes Technology & Therapeutics,* 12 (S1), pp. S-109-S-114.

MENTING, J.G. et al. (2013) How insulin engages its primary binding site on the insulin receptor. *Nature,* 493 (7431), pp. 241-245.

MEZGER, T.G. (2002) Oscillatory tests. In: ZORLL, U. (ed.)*The Rheology Handbook; For users of rotational and oscillatory rheometers*Germany: Vincentz Verlag, pp. 112-163.

MOHD HAFIZ, M. et al. (2013) A simple and sensitive HPLC method for the determination of insulin in rat plasma and its application in pharmacokinetic study. *International Journal of Pharmacy and Pharmaceutical Sciences,* 5 (2), pp. 133-137.

MONTAGUE, W. (ed.) (1983) *Diabetes and the Endocrine Pancreas.Croom Helm Biology in Medicine Series.* 1st ed. New Jersey: Springer US.

MOSER, E.G., MORRIS, A.A. and GARG, S.K. (2012) Emerging diabetes therapies and technologies. *Diabetes Research and Clinical Practice,* 97 (1), pp. 16-26.

MOSLEMI, P., NAJAFABADI, A.R. and TAJERZADEH, H. (2003) A rapid and sensitive method for simultaneous determination of insulin and A21-desamido insulin by high-performance liquid chromatography. *Journal of Pharmaceutical and Biomedical Analysis,* 33 (1), pp. 45-51.

MOUSSY, Y., DUNGEL, P. and HERSH, L. (2006) Diffusion of [3H] dexamethasone in rat subcutaneous slices after injection measured by digital autoradiography. *Biotechnology Progress,* 22 (6), pp. 1715-1719.

NARASIMHAN, B. (2001) Mathematical models describing polymer dissolution: consequences for drug delivery. *Advanced Drug Delivery Reviews,* 48 (2), pp. 195-210.

NATIONAL DIABETES SUPPORT TEAM (2006) *Diabetes in black and minority ethnic communities*. [Online] NHS Clinical Governance Support Team. www.diabetes.nhs.uk [Accessed 28/09/14].

NELSON, D.L. and COX, M.M. (2008) Hormonal Regulation and Integration of Mammalian Metabolism. In: *Lehninger Principles of Biochemistry*. 5th ed. New York: W.H.Freeman and Company, pp. 929 - 931.

NESHER, R. and CERASI, E. (2002) Modeling phasic insulin release: immediate and time-dependent effects of glucose. *Diabetes,* 51 Suppl 1, pp. S53-9.

NICE (2008) *Type 2 diabetes: the management of type 2 diabetes (NICE guideline) [Partially updated by clinical guideline 87].Clinical guideline 66.* [Online] National Institute for Health and Clinical Excellence. www.nice.org.uk [Accessed 01/07/13].

NICE (2004) *Type 1diabetes: diagnosisand management of type 1 diabetes in children, young people and adults - NICE Clinical Guideline 15.* MidCity Place, 71 High Holborn, London WC1V 6NA: National Institute for Clinical Excellence. Available from: www.nice.org.uk [Accessed 01/07/13].

NIELSEN, J.K. et al. (2005) Continuous glucose monitoring in interstitial subcutaneous adipose tissue and skeletal muscle reflects excursions in cerebral cortex. *Diabetes,* 54 (6), pp. 1635-1639.

NILSSON, M.R. and DOBSON, C.M. (2003) Chemical modification of insulin in amyloid fibrils. *Protein Science,* 12 (11), pp. 2637-2641.

NOLAN, C.J., DAMM, P. and PRENTKI, M. (2011) Type 2 diabetes across generations: from pathophysiology to prevention and management. *The Lancet,* 378 (9786), pp. 169-181.

OHARA-IMAIZUMI, M. et al. (2002) Imaging exocytosis of single insulin secretory granules with evanescent wave microscopy: distinct behavior of granule motion in biphasic insulin release. *The Journal of Biological Chemistry,* 277 (6), pp. 3805-3808.

OISHI, R. et al. (1989) Involvement of central histaminergic and cholinergic systems in the morphine-induced increase in blood-brain barrier permeability to sodium fluorescein in mice. *Naunyn-Schmiedeberg's Archives of Pharmacology,* 339 (1-2), pp. 159-165.

OLIVA, A., FARIÑA, J. and LLABRÉS, M. (2000) Development of two high-performance liquid chromatographic methods for the analysis and characterization of insulin and its degradation products in pharmaceutical preparations. *Journal of Chromatography B: Biomedical Sciences and Applications,* 749 (1), pp. 25-34.

OLIVA, A., FARIÑA, J. and LLABRÉS, M. (1996) Influence of temperature and shaking on stability of insulin preparations: Degradation kinetics. *International Journal of Pharmaceutics,* 143 (2), pp. 163-170.

OWENS, D.R. (2002) New horizons--alternative routes for insulin therapy. *Nature Reviews Drug Discovery,* 1 (7), pp. 529-540.

OWENS, D.R. (2011) Insulin preparations with prolonged effect. *Diabetes Technology & Therapeutics,* 13 (S1), pp. S-5-S-14.

OZTAN, A. and MUTLU, M. (2005) Mass transfer through meat. Part I. Determination of diffusion coefficient of nitrite by time lag method. *Journal of Food Engineering,* 67 (4), pp. 387-391.

PEPPAS, N.A. (1985) Analysis of Fickian and non-Fickian drug release from polymers. *Pharmaceutica Acta Helvetiae,* 60 (4), pp. 110-111.

PEPPER, A.R. et al. (2013) Current status of clinical islet transplantation. *World Journal of Transplantation,* 3 (4), pp. 48.

PERALE, G. et al. (2009) A new model of resorbable device degradation and drug release: Transient 1-dimension diffusional model. *Journal of Controlled Release,* 136 (3), pp. 196-205.

PHILLIPS, N.B. et al. (2012) Insulin fibrillation and protein design: Topological resistance of single-chain analogs to thermal degradation with application to a pump reservoir. *Journal of Diabetes Science and Technology,* 6 (2), pp. 277-288.

PHILO, J.S. and ARAKAWA, T. (2009) Mechanisms of Protein Aggregation. *Current Pharmaceutical Biotechnology,* 10 (4), pp. 348-351.

PURI, S. and HEBROK, M. (2012) Diabetic β cells: to be or not to be?. *Cell,* 150 (6), pp. 1103-1104.

RAJAN, D.S. et al. (2006) Development of RP-HPLC for analysis of human insulin. *Indian Journal of Pharmaceutical Sciences,* 68 (5), pp. 662-665.

RENARD, E. (2008) Clinical experience with an implanted closed-loop insulin delivery system. *Arquivos Brasileiros De Endocrinologia & Metabologia*, 52 (2), pp. 349-354.

RENEHAN, A.G. et al. (2008) Body-mass index and incidence of cancer: a systematic review and meta-analysis of prospective observational studies. *The Lancet*, 371 (9612), pp. 569-578.

RENKIN, E.M. (1954) Filtration, diffusion, and molecular sieving through porous cellulose membranes. *The Journal of General Physiology,* 38 (2), pp. 225-243.

RODRÍGUEZ-SÁINZ, C. et al. (2013) Flow Cytometry Analysis with a New FITC-Conjugated Monoclonal Antibody-3E12 for HLA-B*57:01 Rapid Screening in Prevention of Abacavir Hypersensitivity in HIV-1–Infected Patients. *HIV Clinical Trials,* 14 (4), pp. 160-164.

RORSMAN, P. et al. (2000) The Cell Physiology of Biphasic Insulin Secretion. *News in Physiological Sciences : An International Journal of Physiology Produced Jointly by the International Union of Physiological Sciences and the American Physiological Society*, 15, pp. 72-77.

SACKETT, C.K. and NARASIMHAN, B. (2011) Mathematical modeling of polymer erosion: consequences for drug delivery. *International Journal of Pharmaceutics,* 418 (1), pp. 104-114.

SAHOTA, T.S. and TAYLOR, M.J. (2013) *Long term stability and storage of acrylic derivatised glucose responsive dextran-concanavalin A gels (accepted poster).* Honolulu, Hawaii: Controlled Release Society Annual Symposium.

SALTIEL, A.R. and KAHN, C.R. (2001) Insulin signalling and the regulation of glucose and lipid metabolism. *Nature*, 414 (6865), pp. 799-806.

SARMENTO, B. et al. (2006) Development and validation of a rapid reversed-phase HPLC method for the determination of insulin from nanoparticulate systems. *Biomedical Chromatography,* 20 (9), pp. 898-903.

SCHAFFER, L. (1994) A model for insulin binding to the insulin receptor. *European Journal of Biochemistry / FEBS*, 221 (3), pp. 1127-1132.

SCOTT, D.A. (1934) Crystalline insulin. *Biochemical Journal,* 28 (4), pp. 1592-1602.

SEBTI, I. et al. (2004) Experimental study and modeling of nisin diffusion in agarose gels. *Journal of Food Engineering,* 63 (2), pp. 185-190.

SEIDENBERGER, T. et al. (2011) Simultaneous controlled vitamin release from multiparticulates: theory and experiment. *International Journal of Pharmaceutics,* 412 (1), pp. 68-76.

SEINO, S., SHIBASAKI, T. and MINAMI, K. (2011) Dynamics of insulin secretion and the clinical implications for obesity and diabetes. *The Journal of Clinical Investigation,* 121 (6), pp. 2118-2125.

SENIOR, P.A. et al. (2012) Islet Transplantation at the University of Alberta: Status Update and Review of Progress over the Last Decade. *Canadian Journal of Diabetes,* 36 (1), pp. 32-37.

SHELMA, R. and SHARMA, C.P. (2013) In vitro and in vivo evaluation of curcumin loaded lauroyl sulphated chitosan for enhancing oral bioavailability. *Carbohydrate Polymers,* 95 (1), pp. 441-448.

SHIER, D., BUTLER, J. and LEWIS, R. (eds.) (2003) *Hole's Essentials of Human Anatomy and Physiology.* 8th ed. London: McGaw-Hill Higher Education.

SHOELSON, S.E. et al. (1992) Mutations at the dimer, hexamer, and receptor-binding surfaces of insulin independently affect insulin-insulin and insulin-receptor interactions. *Biochemistry,* 31 (6), pp. 1757-1767.

SIEGEL, R.A. (2000) Theoretical analysis of inward hemispheric release above and below drug solubility. *Journal of Controlled Release,* 69 (1), pp. 109-126.

SIEPMANN, F. et al. (2010) Modeling drug release from PVAc/PVP matrix tablets. *Journal of Controlled Release,* 141 (2), pp. 216-222.

SIEPMANN, J. et al. (1998) Calculation of the dimensions of drug–polymer devices based on diffusion parameters. *Journal of Pharmaceutical Sciences,* 87 (7), pp. 827-832.

SIEPMANN, J. and GÖPFERICH, A. (2001) Mathematical modeling of bioerodible, polymeric drug delivery systems. *Advanced Drug Delivery Reviews,* 48 (2), pp. 229-247.

SIEPMANN, J., LECOMTE, F. and BODMEIER, R. (1999) Diffusion-controlled drug delivery systems: calculation of the required composition to achieve desired release profiles. *Journal of Controlled Release,* 60 (2), pp. 379-389.

SIEPMANN, J. and PEPPAS, N. (2001) Modeling of drug release from delivery systems based on hydroxypropyl methylcellulose (HPMC). *Advanced Drug Delivery Reviews,* 48 (2), pp. 139-157.

SIEPMANN, J. and PEPPAS, N. (2000) Hydrophilic matrices for controlled drug delivery: an improved mathematical model to predict the resulting drug release kinetics (the “sequential layer” model). *Pharmaceutical Research,* 17 (10), pp. 1290-1298.

SIEPMANN, J. and SIEPMANN, F. (2011) Mathematical modeling of drug release from lipid dosage forms. *International Journal of Pharmaceutics,* 418 (1), pp. 42-53.

SIEPMANN, J., SIEPMANN, F. and FLORENCE, A. (2006) Local controlled drug delivery to the brain: mathematical modeling of the underlying mass transport mechanisms. *International Journal of Pharmaceutics,* 314 (2), pp. 101-119.

SIEPMANN, J., STREUBEL, A. and PEPPAS, N. (2002) Understanding and predicting drug delivery from hydrophilic matrix tablets using the "sequential layer" model. *Pharmaceutical Research,* 19 (3), pp. 306-314.

SIEPMANN, J. and PEPPAS, N.A. (2011) Higuchi equation: derivation, applications, use and misuse. *International Journal of Pharmaceutics,* 418 (1), pp. 6-12.

SIEPMANN, J. and SIEPMANN, F. (2012) Modeling of diffusion controlled drug delivery. *Journal of Controlled Release,* 161 (2), pp. 351-362.

SIEPMANN, J. and PEPPAS, N.A. (2012) Modeling of drug release from delivery systems based on hydroxypropyl methylcellulose (HPMC). *Advanced Drug Delivery Reviews,* 64, pp. 163-174.

SIEPMANN, J. and SIEPMANN, F. (2008) Mathematical modeling of drug delivery. *International Journal of Pharmaceutics,* 364 (2), pp. 328-343.

SIMMEN, H.P. et al. (1995) Biochemical analysis of peritoneal fluid in patients with and without bacterial infection. *The European Journal of Surgery = Acta Chirurgica,* 161 (1), pp. 23-27.

SINGH, S. and RASTOGI, A. (2008) Gestational diabetes mellitus. *Diabetes & Metabolic Syndrome: Clinical Research & Reviews,* 2 (3), pp. 227-234.

SKYLER, J.S. (2010) Continuous subcutaneous insulin infusion—an historical perspective. *Diabetes Technology & Therapeutics,* 12 (S1), pp. S-5-S-9.

SLOAN, J.H. et al. (2012) A novel high-sensitivity electrochemiluminescence (ECL) sandwich immunoassay for the specific quantitative measurement of plasma glucagon. *Clinical Biochemistry,* 45 (18), pp. 1640-1644.

SLUZKY, V., KLIBANOV, A.M. and LANGER, R. (1992) Mechanism of insulin aggregation and stabilization in agitated aqueous solutions. *Biotechnology and Bioengineering,* 40 (8), pp. 895-903.

SLUZKY, V. et al. (1991) Kinetics of insulin aggregation in aqueous solutions upon agitation in the presence of hydrophobic surfaces. *Proceedings of the National Academy of Sciences of the United States of America,* 88 (21), pp. 9377-9381.

SNYDER, K.L. et al. (2001) Diffusion and calibration properties of microdialysis sampling membranes in biological media. *Analyst,* 126 (8), pp. 1261-1268.

SRINIVASAN, B. et al. (2008) Diabetes: glycaemic control in type 2. *Clinical Evidence,* 2008.

STAUB, A. et al. (2010) Multiple injection technique for the determination and quantitation of insulin formulations by capillary electrophoresis and time-of-flight mass spectrometry. *Journal of Chromatography A,* 1217 (51), pp. 8041-8047.

STUMVOLL, M., GOLDSTEIN, B.J. and VAN HAEFTEN, T.W. (2005) Type 2 diabetes: principles of pathogenesis and therapy. *The Lancet,* 365 (9467), pp. 1333-1346.

SUNDBY, F. (1962) Separation and characterization of acid-induced insulin transformation products by paper electrophoresis in 7 M urea. *Journal of Biological Chemistry,* 237 (11), pp. 3406-3411.

TALCHAI, C. et al. (2012) Pancreatic β cell dedifferentiation as a mechanism of diabetic β cell failure. *Cell,* 150 (6), pp. 1223-1234.

TANAKA, H., MATSUMURA, M. and VELIKY, I.A. (1984) Diffusion characteristics of substrates in Ca-alginate gel beads. *Biotechnology and Bioengineering,* 26 (1), pp. 53-58.

TANNA, S. et al. (2006a) Glucose-responsive UV polymerised dextran–concanavalin A acrylic derivatised mixtures for closed-loop insulin delivery. *Biomaterials,* 27 (8), pp. 1586-1597.

TANNA, S. et al. (2006b) The effect of degree of acrylic derivatisation on dextran and concanavalin A glucose-responsive materials for closed-loop insulin delivery. *Biomaterials,* 27 (25), pp. 4498-4507.

TANTIPOLPHAN, R. et al. (2010) Elution behavior of insulin on high-performance size exclusion chromatography at neutral pH. *Journal of Pharmaceutical and Biomedical Analysis,* 52 (2), pp. 195-202.

TAYLOR, M.J. et al. (2006) Rheological characterisation of dextran–concanavalin A mixtures as a basis for a self-regulated drug delivery device. *European Journal of Pharmaceutics and Biopharmaceutics,* 62 (1), pp. 94-100.

TAYLOR, M. (2013a) *New patent P54853GB Matrix*. GB1314640.2 application number.

TAYLOR, M. (2001) *Glucose Sensing Gel.* (10 July 2001 filing; PCT filed July 2002, issued 23 01 03), GB.0116860.8.(Granted in Europe Dec 2010) and subsequently in US and Japan in 2012 and 2013. De Montfort University, UK.

TAYLOR, M. (1993) *Drug System II.* Filing & published January 1995. Patent Application 9313484.9. Patent WO 95/01186. Granted US (5,902,607 1999) (divisional

09/124,445 or alternatively US6410053 granted 2002). Granted in Europe –EP0706401 Nov 27 2002 (Now lapsed, due to time limit). De Montfort University, UK.

TAYLOR, M. (1992) *Drug System.* Filing & published July 1993.Patent Application 9200638.6 (Drug System I) Patent WO 93/13803. Granted US (5,830,506 1998) (divisional 09/124,694 still pending late 2004).Europe EP0626862 B11999 granted Sept 1 1999.(Now lapsed, due to time limit). De Montfort University, UK.

TAYLOR, M. et al. (2014) Insulin pump users would not rule out using an implantable artificial pancreas. *Practical Diabetes,* 31 (1), pp. 18-23a.

TAYLOR, M. (2013b) *New patent P54852GB Container specifications*. GB1310185.2 application number.

TAYLOR, M.J. and SAHOTA, T.S. (2012) *Closed Loop Delivery in the Pig* (accepted poster). In: *, Quebec*. Canada: Controlled Release Society Annual Symposium.

TAYLOR, M.J. and SAHOTA, T.S. (2013a) New technologies in insulin delivery. *Practical Diabetes,* 30 (1), pp. 21-26.

TAYLOR, M.J., TANNA, S. and SAHOTA, T.S. (2010a) Glucose-sensitive gel rheology of dextran-concanavalin A mixtures suitable for self-regulating insulin delivery. *Pharmaceutical Development and Technology,* 15 (1), pp. 80-88.

TAYLOR, M.J., TANNA, S. and SAHOTA, T. (2010b) In vivo study of a polymeric glucose-sensitive insulin delivery system using a rat model. *Journal of Pharmaceutical Sciences,* 99 (10), pp. 4215-4227.

TAYLOR, M. and SAHOTA, T. (2013b) New technologies in insulin delivery. *Practical Diabetes,* 30 (1), pp. 21-26.

TEDDY STUDY GROUP (2008) The Environmental Determinants of Diabetes in the Young (TEDDY) Study. *Annals of the New York Academy of Sciences,* 1150 (1), pp. 1-13.

THE COST OF DIABETES: REPORT (2014) *Cost of Diabetes Report_v2Jan 2014 V2.indd 5 28/01/2014*. Available at:http://www.diabetes.org.uk/Documents/Diabetes%20UK%20Cost%20of%20Diabetes%20Report.pdf: Diabetes UK, 0201A V2.

TIETZE, F., MORTIMORE, G.E. and LOMAX, N.R. (1962) Preparation and properties of fluorescent insulin derivatives. *Biochimica Et Biophysica Acta,* 59 (2), pp. 336-346.

UENO, T. and NAGANO, T. (2011) Fluorescent probes for sensing and imaging. *Nature Methods,* 8 (8), pp. 642-645.

VASHISTH, H. (2014) Flexibility in the Insulin Receptor Ectodomain Enables Docking of Insulin in Crystallographic Conformation Observed in a Hormone-Bound Microreceptor. *Membranes,* 4, pp. 730-746.

VENÂNCIO, A. and TEIXEIRA, J. (1997) Characterization of sugar diffusion coefficients in alginate membranes. *Biotechnology Techniques,* 11 (3), pp. 183-186.

VERHOEVEN, E. et al. (2009) Modeling drug release from hot-melt extruded mini-matrices with constant and non-constant diffusivities. *European Journal of Pharmaceutics and Biopharmaceutics,* 73 (2), pp. 292-301.

VOET, D. and VOET, J.G. (1995) *Biochemistry*. 2nd ed. New York: John Wiley & Sons.

WALPOLE, S.C. et al. (2012) The weight of nations: an estimation of adult human biomass. *BMC Public Health,* 12, pp. 439-2458-12-439.

WARD, C.W. and LAWRENCE, M.C. (2012) Similar but different: ligand-induced activation of the insulin and epidermal growth factor receptor families. *Current Opinion in Structural Biology,* 22 (3), pp. 360-366.

WARD, C.W. and LAWRENCE, M.C. (2011) Landmarks in insulin research. *Frontiers in Endocrinology,* 2, pp. 76.

WAUGH, D.F. (1946b) A fibrous modification of insulin. I. The heat precipitate of insulin. *Journal of the American Chemical Society,* 68 (2), pp. 247-250.

WAUGH, D.F. et al. (1953) Studies of the nucleation and growth reactions of selected types of insulin fibrils. *Journal of the American Chemical Society,* 75 (11), pp. 2592-2600.

WAUGH, D.F. (1946a) Reactions involved in insulin fibril formation. (Vol. 5, No. 1 Pt 2). In: *Federation proceedings*, pp. 111.

WEBER, L.M., LOPEZ, C.G. and ANSETH, K.S. (2009) Effects of PEG hydrogel crosslinking density on protein diffusion and encapsulated islet survival and function. *Journal of Biomedical Materials Research.Part A,* 90 (3), pp. 720-729.

WEISS, M. (2013) Design of ultra-stable insulin analogues for the developing world. *Journal of Health Specialties,* 1 (2), pp. 59.

WHITTAKER, L. et al. (2008) High-Affinity Insulin Binding: Insulin Interacts with Two Receptor Ligand Binding Sites†. *Biochemistry,* 47 (48), pp. 12900-12909.

WHITTINGHAM, J.L. et al. (2004) Crystallographic and solution studies of N-lithocholyl insulin: a new generation of prolonged-acting human insulins. *Biochemistry,* 43 (20), pp. 5987-5995.

WILLIAMS, G. (2003) Diabetes. In: WARRELL, D.A. et al. (ed.)*Oxford textbook of medicine*. 4th ed. Oxford: Oxford University Press, pp. 317-360.

WORLD HEALTH ORGANIZATION (2011a) *Global Status report on non communicable diseases 2010.* Geneva.

WORLD HEALTH ORGANIZATION (2011b) *WHO. Use of glycated haemoglobin (HbA1c) in the diagnosis of diabetes mellitus: abbreviated report of a WHO consultation*. Geneva: World Health Organization.

WORLD HEALTH ORGANIZATION (2009) *Global Health risks. Mortality and burden of disease attributable to selected major risks.* [Online].

WORLD HEALTH ORGANIZATION EXPERT COMMITTEE (1999) *Definition, diagnosis and classification of diabetes mellitus and its complications. Report of a WHO consultation, part 1: diagnosis and classification of diabetes mellitus.* Geneva: World Health Organization.

WRIGHT, A. et al. (2002) Sulfonylurea inadequacy: efficacy of addition of insulin over 6 years in patients with type 2 diabetes in the U.K. Prospective Diabetes Study (UKPDS 57). *Diabetes Care,* 25 (2), pp. 330-336.

YEH, H. et al. (2010) Simultaneous determination of regular insulin and insulin aspart by capillary zone electrophoresis and application in drug formulations. *Journal of Pharmaceutical and Biomedical Analysis,* 53 (2), pp. 145-150.

YIN, C. and LI, X. (2011) Anomalous diffusion of drug release from a slab matrix: Fractional diffusion models. *International Journal of Pharmaceutics,* 418 (1), pp. 78-87.

YOMOTA, C. et al. (1996) Separation of B-3 monodesamidoinsulin from human insulin by high-performance liquid chromatography under alkaline conditions. *Journal of Chromatography A,* 721 (1), pp. 89-96.

ZHANG, R. et al. (2006) Synthesis and characterization of a d-glucose sensitive hydrogel based on CM-dextran and concanavalin A. *Reactive and Functional Polymers,* 66 (7), pp. 757-767.

ZHANG, W. and FRANCO, C.M.M. (1999) Critical assessment of quasi-steady-state method to determine effective diffusivities in alginate gel membranes. *Biochemical Engineering Journal,* 4 (1), pp. 55-63.

ZHANG, W. and FURUSAKI, S. (2001) On the evaluation of diffusivities in gels using the diffusion cell technique. *Biochemical Engineering Journal,* 9 (1), pp. 73-82.

ZHOU, Y. et al. (2005) Modeling of dispersed-drug release from two-dimensional matrix tablets. *Biomaterials,* 26 (8), pp. 945-952.

Appendix 1 - Guidelines for method validation parameters

The FDA guidance document – *'Guidance for Industry, Q2B Validation of Analytical Procedures: Methodology'* details and acceptance criteria for each validation parameter;

System suitability

The FDA Document – *'Guidance for Industry, Q2B Validation of Analytical Procedures: Methodology'* states

"System suitability testing is an integral part of many analytical procedures. The tests are based on the concept that the equipment, electronics, analytical operations, and samples to be analyzed constitute an integral system that can be evaluated as such. System suitability test parameters to be established for a particular procedure depend on the type of procedure being validated."

Linearity

The FDA Document – *'Guidance for Industry, Q2B Validation of Analytical Procedures: Methodology'* states

"A linear relationship should be evaluated across the range of the analytical procedure. It may be demonstrated directly on the drug substance (by dilution of a standard stock solution) and/or separate weighings of synthetic mixtures of the drug product components, using the proposed procedure. The latter aspect can be studied during investigation of the range....."

"For the establishment of linearity, a minimum of five concentrations is recommended. Other approaches should be justified".

Range

The FDA Document – *'Guidance for Industry, Q2B Validation of Analytical Procedures: Methodology'* states

"*The specified range is normally derived from linearity studies and depends on the intended application of the procedure. It is established by confirming that the analytical procedure provides an acceptable degree of linearity, accuracy, and precision when applied to samples containing amounts of analyte within or at the extremes of the specified range of the analytical procedure.*

The following minimum specified ranges should be considered.

• For the assay of a drug substance or a finished (drug) product: Normally from 80 to 120 percent of the test concentration;....."

Accuracy

The FDA Document – *'Guidance for Industry, Q2B Validation of Analytical Procedures: Methodology'* states

"*Accuracy should be established across the specified range of the analytical procedure."*

Several methods of determining accuracy are available.

"Assay of Drug substance

a) Application of an analytical procedure to an analyte of known purity (e.g., reference material);

(b) Comparison of the results of the proposed analytical procedure with those of a second well-characterized procedure, the accuracy of which is stated and/or defined (independent procedure);

(c) Accuracy may be inferred once precision, linearity, and specificity have been established.

"Accuracy should be assessed using a minimum of 9 determinations over a minimum of 3 concentration levels covering the specified range (e.g., 3 concentrations /3 replicates each of the total analytical procedure)."

Accuracy should be reported as percent recovery by the assay of known added amount of analyte in the sample or as the difference between the mean and the accepted true value together with the confidence intervals."

Precision

The FDA Document – *'Guidance for Industry, Q2B Validation of Analytical Procedures: Methodology'* states

"*Validation of tests for assay and for quantitative determination of impurities includes an investigation of precision.*

Repeatability

Repeatability should be assessed using:

(1) A minimum of 9 determinations covering the specified range for the procedure

(e.g., 3 concentrations/3 replicates each); or

(2) A minimum of 6 determinations at 100 percent of the test concentration.

Intermediate Precision

The extent to which intermediate precision should be established depends on the circumstances under which the procedure is intended to be used. The applicant should establish the effects of random events on the precision of the analytical procedure. Typical variations to be studied include days, analysts, equipment, etc. It is not necessary to study these effects individually. The use of an experimental design (matrix) is encouraged.

Detection and Quantitation limits (Sensitivity)

The FDA Document – *'Guidance for Industry, Q2B Validation of Analytical Procedures: Methodology'* details several approaches for determining the detection limit and quantification limits such as based on visual examination, based on signal to noise ratio or based on standard deviation of the response and the slope, it states

"DETECTION LIMIT

Several approaches for determining the detection limit are possible, depending on whether the procedure is noninstrumental or instrumental. Approaches other than those listed below may be acceptable.

A. Based on Visual Evaluation

Visual evaluation may be used for noninstrumental methods but may also be used with instrumental methods.

The detection limit is determined by the analysis of samples with known concentrations of analyte and by establishing the minimum level at which the analyte can be reliably detected.

B. Based on Signal-to-Noise

This approach can only be applied to analytical procedures which exhibit baseline noise.

Determination of the signal-to-noise ratio is performed by comparing measured signals from samples with known low concentrations of analyte with those of blank samples and establishing the minimum concentration at which the analyte can be reliably detected. A signal-to-noise ratio between 3 or 2:1 is generally considered acceptable for estimating the detection limit.

C. Based on the Standard Deviation of the Response and the Slope

The detection limit (DL) may be expressed as:

$$DL = 3.3\frac{F}{S}$$ **Equation A1-1**

Where F = the standard deviation of the response

S = the slope of the calibration curve

The slope S may be estimated from the calibration curve of the analyte. The estimate of F may be carried out in a variety of ways, for example:

1. Based on the standard deviation of the blank

Measurement of the magnitude of analytical background response is performed by analyzing an appropriate number of blank samples and calculating the standard deviation of these responses.

2. Based on the calibration curve

A specific calibration curve should be studied using samples containing an analyte in the range of DL. The residual standard deviation of a regression line or the standard deviation of y-intercepts of regression lines may be used as the standard deviation.

D. Recommended Data

The detection limit and the method used for determining the detection limit should be presented. If DL is determined based on visual evaluation or based on signal-to-noise ratio, the presentation of the relevant chromatograms is considered acceptable for justification.

In cases where an estimated value for the detection limit is obtained by calculation or extrapolation, this estimate may subsequently be validated by the independent analysis of a suitable number of samples known to be near or prepared at the detection limit.

QUANTITATION LIMIT

Several approaches for determining the quantitation limit are possible, depending on whether the procedure is noninstrumental or instrumental. Approaches other than those listed below may be acceptable.

A. Based on Visual Evaluation

Visual evaluation may be used for noninstrumental methods, but may also be used with instrumental methods.

The quantitation limit is generally determined by the analysis of samples with known concentrations of analyte and by establishing the minimum level at which the analyte can be quantified with acceptable accuracy and precision.

B. Based on Signal-to-Noise

This approach can only be applied to analytical procedures that exhibit baseline noise. Determination of the signal-to-noise ratio is performed by comparing measured signals from samples with known low concentrations of analyte with those of blank samples and by establishing the minimum concentration at which the analyte can be reliably quantified.

A typical signal-to-noise ratio is 10:1.

C. Based on the standard deviation of the Response and the Slope

The quantitation limit (QL) may be expressed as:

$$QL = 10\frac{F}{S}$$ **Equation A1-2**

Where F = the standard deviation of responses

S = the slope of the calibration curve

The slope S may be estimated from the calibration curve of the analyte. The estimate of F may be carried out in a variety of ways, for example:

1. Based on standard deviation of the blank

Measurement of the magnitude of analytical background response is performed by analyzing an appropriate number of blank samples and calculating the standard deviation of these responses.

2. Based on the calibration curve

A specific calibration curve should be studied using samples containing an analyte in the range of QL. The residual standard deviation of a regression line or the standard deviation of y-intercepts of regression lines may be used as the standard deviation.

Appendix 2 – Chromatogram data and Mass spectra for Chapter 4.

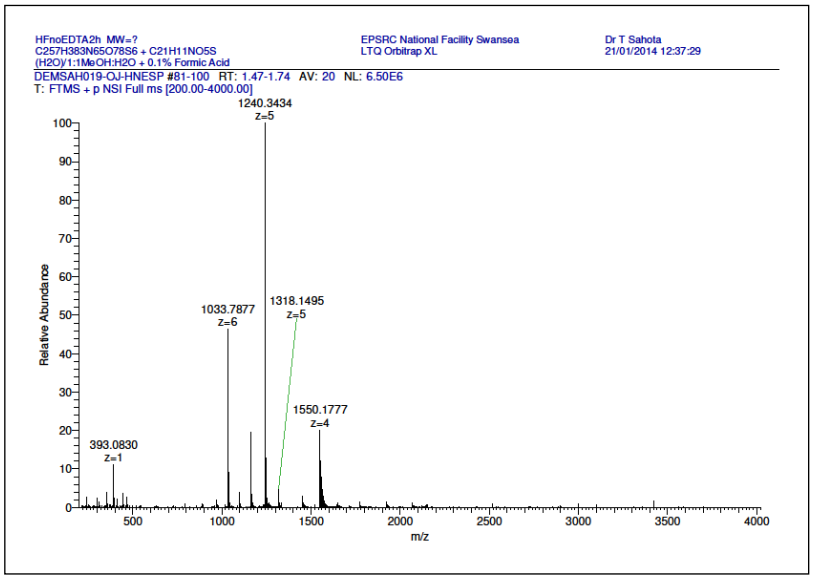

Figure A2-1: Mass spectra for FITC-insulin conjugates synthesised using Humulin®R after 2hrs reaction time (no EDTA added) (peaks present in raw data at m/z 968.7816 z6, 1162.3363 z5 and 1452.6683 z4 corresponding to unlabelled human insulin; peaks at m/z 889.5278z7, 1771.4869z7 and 2066.5662z3 corresponding to mono-labelled conjugate; peaks at m/z 1098.6266 z6 and 1647.4355 z4 corresponding to di-labelled conjugate not labelled in spectra).

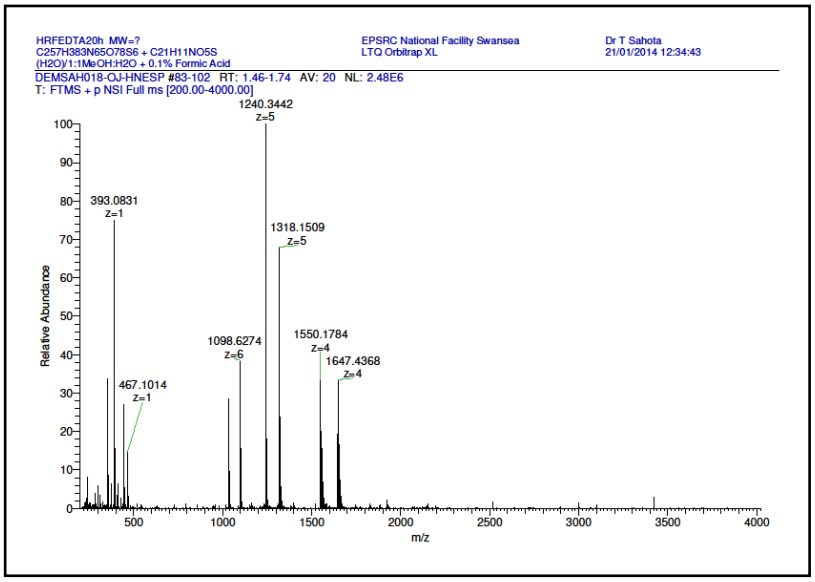

Figure A2-2: Mass spectra for FITC-insulin conjugates synthesised using Humulin®R after 20hrs reaction time (peak present in raw data at m/z 1163.4668 z6 and 1395.958 z5 corresponding to tri-labelled conjugate not labelled in spectra).

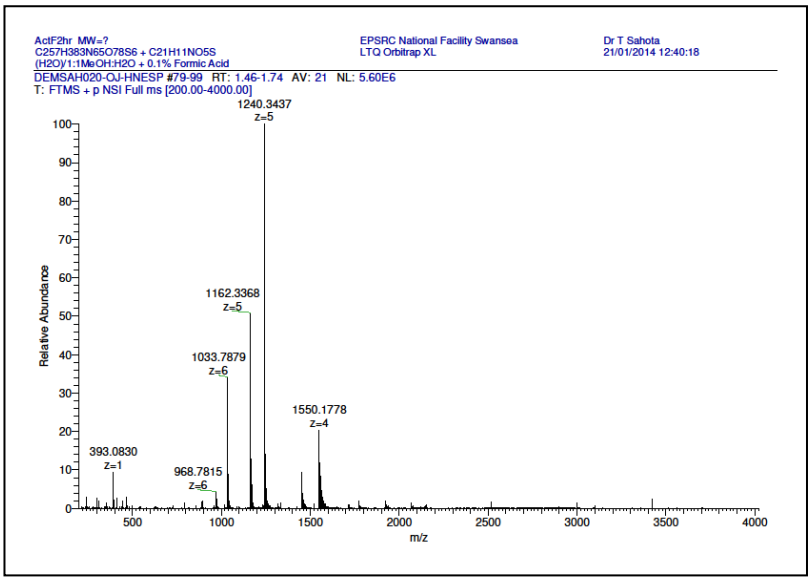

Figure A2-3: Mass spectra for FITC-insulin conjugates synthesised using Actrapid® after 2hrs reaction time(peaks present in raw data at m/z 1452.6682 z4 and 1936.5548 z3 corresponding to unlabelled human insulin; peaks at m/z 1771.6305 z7 and 2066.2323 z3 corresponding to mono-labelled conjugate; peak at m/z 2004.8541 z10 corresponding to di-labelled conjugate not labelled in spectra).

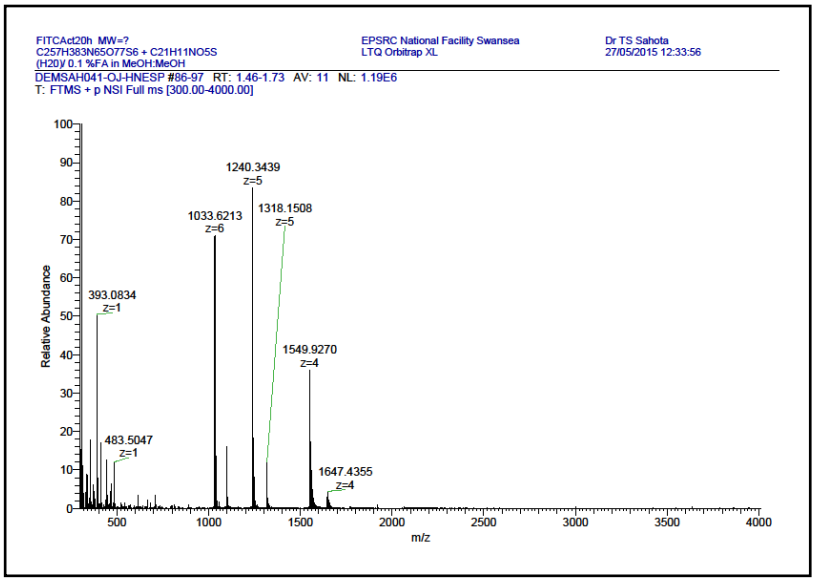

Figure A2-4: Mass spectra for FITC-insulin conjugates synthesised using Actrapid® after 20hrs reaction time (peak present in raw data at m/z 1098.7937 z6 corresponding to di-labelled conjugate not labelled in spectra).

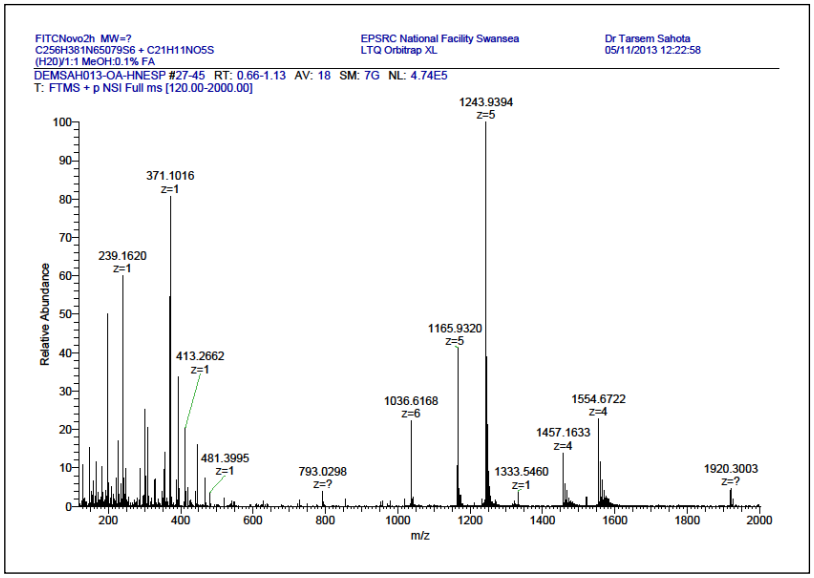

Figure A2-5: Mass spectra for FITC-insulin conjugates synthesised using NovoRapid® (insulin aspart) after 2hrs reaction time (peak present in raw data at m/z 1321.7463 z5 corresponding to di-labelled conjugate not labelled in spectra).

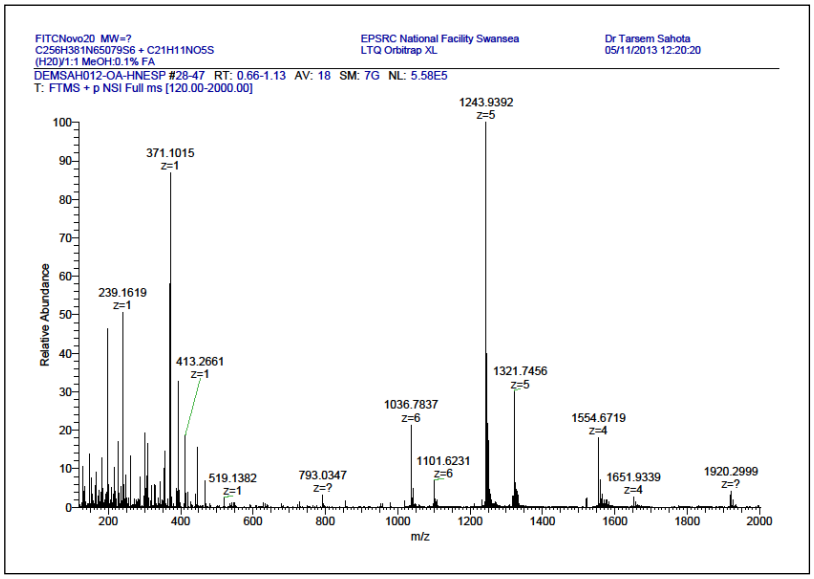

Figure A2-6: Mass spectra for FITC-insulin conjugates synthesised using NovoRapid® (insulin aspart) after 20hrs reaction time.

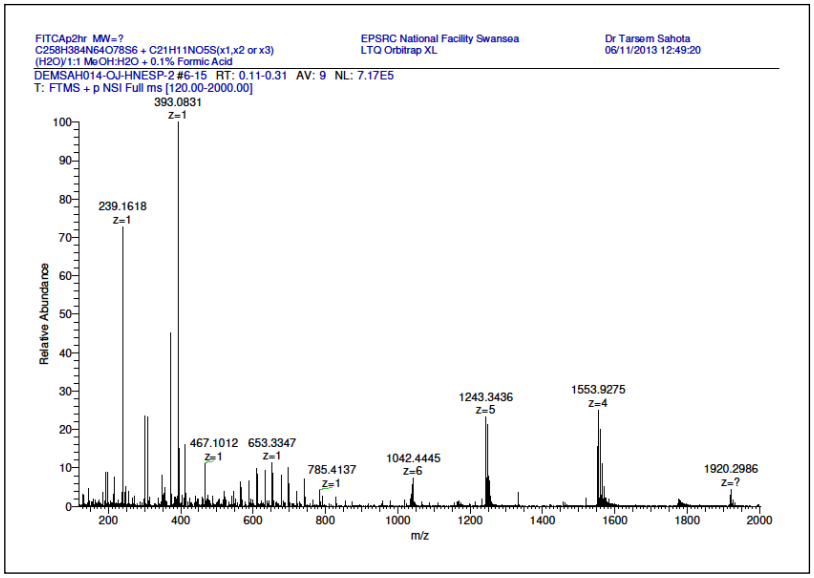

Figure A2-7: Mass spectra for FITC-insulin conjugates synthesised using Apidra® (insulin glulisine) after 2hrs reaction time (peak present in raw data at m/z 1165.7376 z5 corresponding to unlabelled insulin glulisine; peak at m/z 1775.6291 z7 corresponding to mono-labelled conjugate not labelled in spectra).

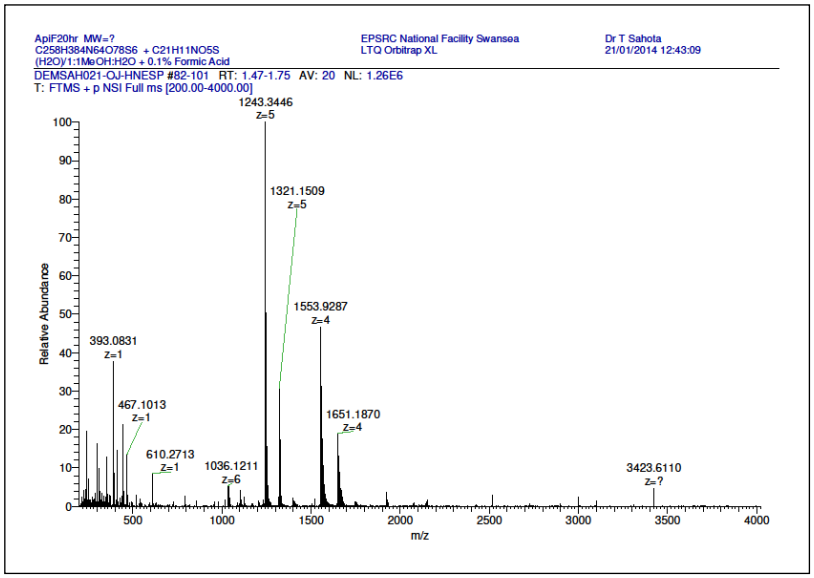

Figure A2-8: Mass spectra for FITC-insulin conjugates synthesised using Apidra® (insulin glulisine) after 20hrs reaction time (peak present in raw data at m/z 1101.1275 z6 corresponding to di-labelled conjugate; peak at m/z 1170.1286 z6 and 1399.1584 z5 corresponding to tri-labelled conjugate not labelled in spectra).

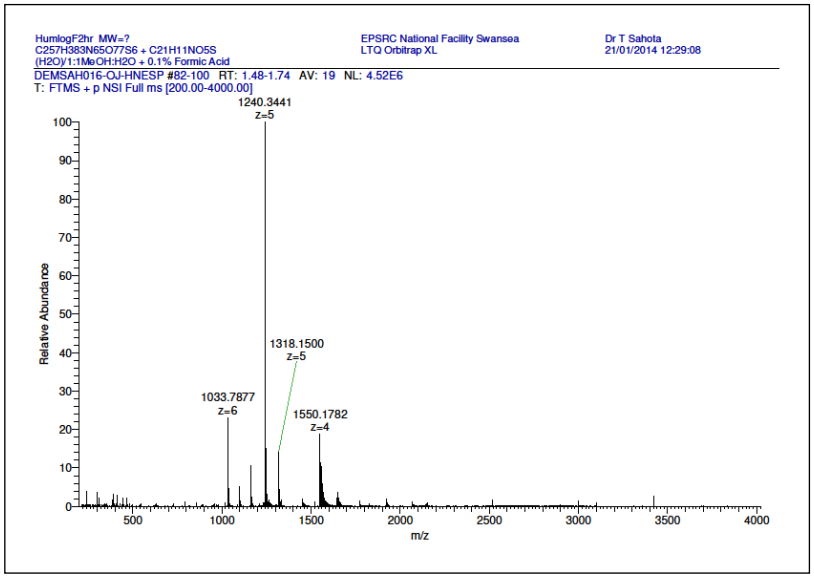

Figure A2-9: Mass spectra for FITC-insulin conjugates synthesised using Humalog® (insulin lispro) after 2hrs reaction time (peak present in raw data at m/z 1162.3364 z5 corresponding to unlabelled insulin lispro; peak at m/z 1771.3447 z7 and 2066.5680 z3 corresponding to mono-labelled conjugate; peak at m/z 1647.4363 z4 corresponding to di-labelled conjugate not labelled in spectra).

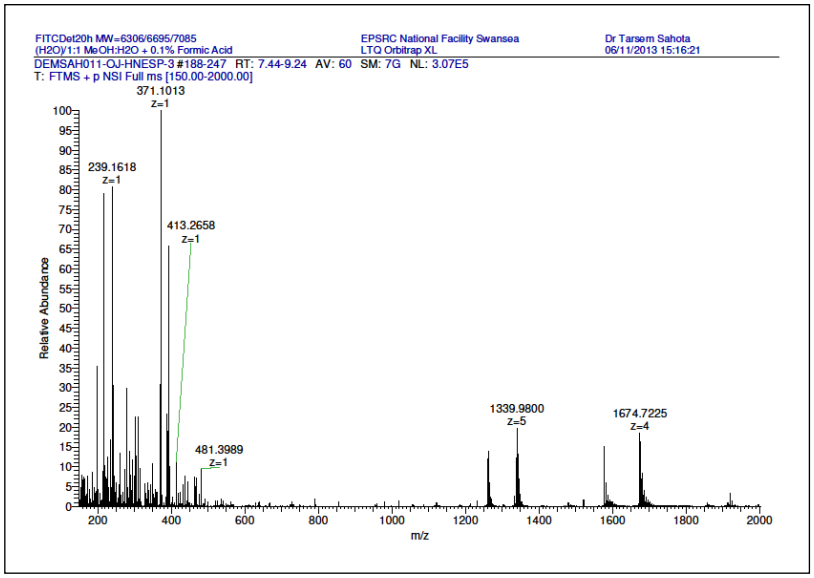

Figure A2-10: Mass spectra for FITC-insulin conjugates synthesised using Levemir® (insulin determir) after 20hrs reaction time (peak present in raw data at m/z 1262.1732 z5 and 1577.4642 z4 corresponding to mono-labelled conjugate not labelled in spectra).

Table A2-1: RP-HPLC Area % with retention times for Sigma FITC-bovine insulin commercial product.

Peak#	Ret. Time	Area	Height	Peak Start	Peak End	Area%
1	21.4	17106	1925	21.1	21.6	9.4
2	21.7	1507	175	21.6	21.8	0.8
3	22.0	33627	3686	21.8	22.3	18.5
4	22.5	7005	692	22.3	22.6	3.9
5	22.8	74886	8238	22.6	23.0	41.2
6	23.1	9082	751	23.0	23.5	5.0
7	23.9	38577	4038	23.6	24.6	21.2

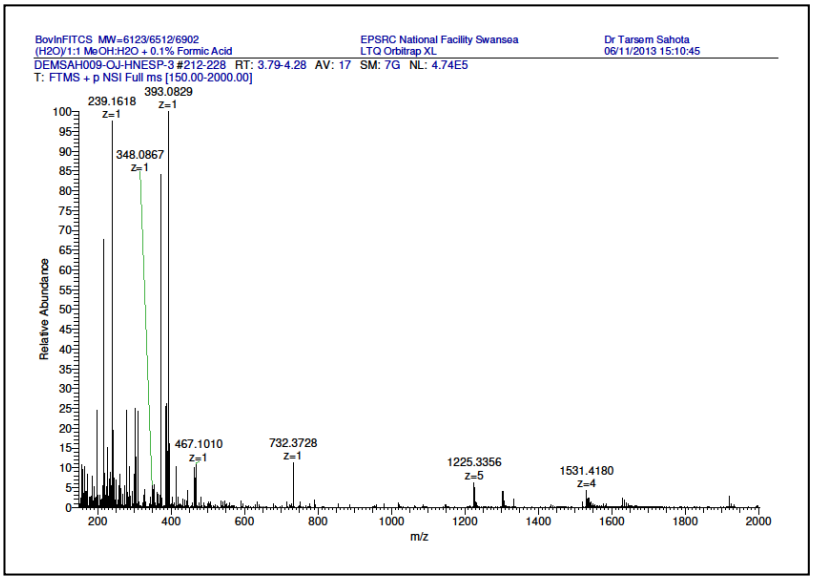

Figure A2-11: Mass spectra for Sigma FITC-bovine insulin commercial product (peaks present in raw data at m/z 1147.5280 z5 and 1434.4113 z4 corresponding to unlabelled bovine insulin; peaks at m/z 1086.1198 z6, 1303.3430 z5 and 1628.9264 z4 corresponding to di-labelled conjugate not labelled in spectra).

Table A2-2: RP-HPLC Area % with retention times for Sigma FITC-human insulin commercial product.

Peak#	Ret. Time (min)	Area	Height	Peak Start	Peak End	Area%
1	12.9	3263	318	12.7	13.2	0.5
2	22.1	17589	2036	21.9	22.3	2.5
3	22.4	22651	2694	22.3	22.6	3.2
4	22.8	10834	963	22.6	23.0	1.5
5	23.4	648351	62650	22.967	25.7	90.4
6	24.1	6743	958	24.025	24.3	0.9
7	24.6	3027	206	24.475	25.1	0.4
8	27.9	4484	526	27.7	28.2	0.6

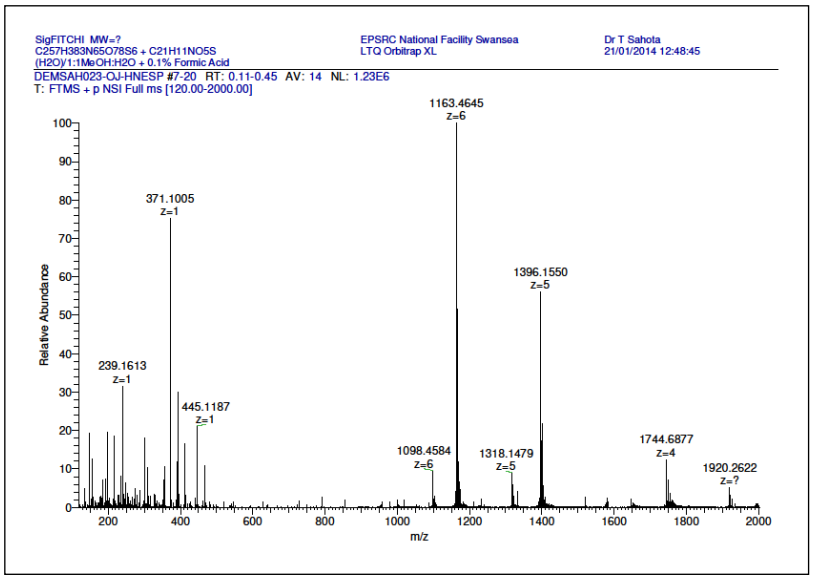

Figure A2-12: Mass spectra for Sigma FITC-human insulin commercial product (peak present in raw data at m/z 1647.4269 z4 corresponding to di-labelled conjugate not labelled in spectra).

.

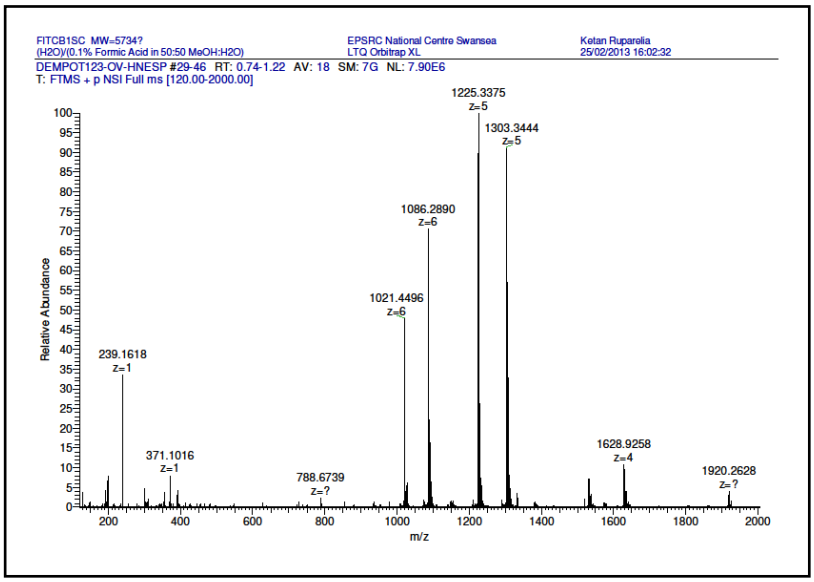

Figure A2-13: Mass spectra for FITC- bovine insulin synthesised in-house with reaction time of 20 hrs (peak present in raw data at m/z 1531.6674 z4 corresponding to mono-labelled conjugate not labelled in spectra).

Appendix 3 Figures for determination of diffusion coefficient from Chapter 5.

Appendix 3.1 Figures (representative data) for determination of diffusion coefficient of tartrazine in agarose using tube set-up

Appendix 3.1.1 Diffusion of tartrazine in 0.5% w/w agarose gel

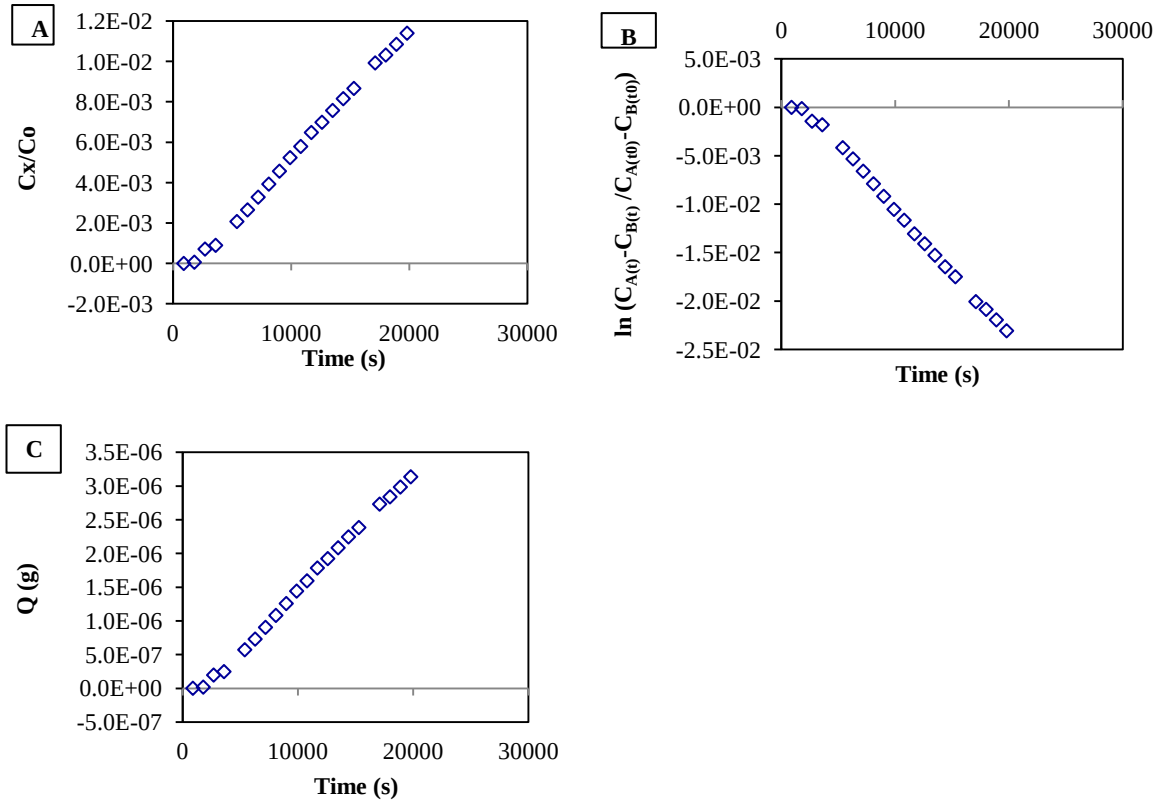

Figure A3-1: Evaluation of diffusivity D or D_e for tartrazine in 0.5% w/w agarose gel using the tube experiment from a plot of A: the Laplace transform method, B: the QSS method and C: the TL method.

Appendix 3.1.2 Diffusion of tartrazine in 0.7% w/w agarose gel

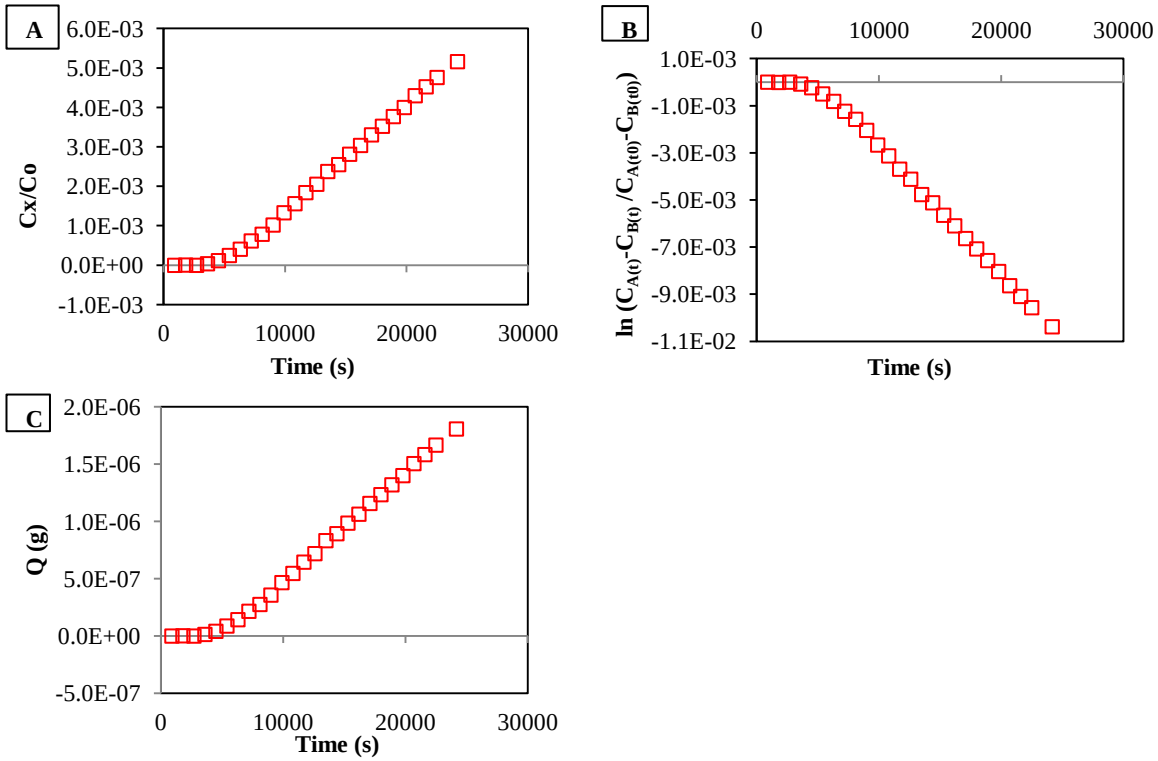

Figure A3-2: Evaluation of diffusivity D or D_e for tartrazine in 0.7% w/w agarose gel using the tube experiment from a plot of **A**: the Laplace transform method, **B**: the QSS method and **C**: the TL method.

Appendix 3.1.3 Diffusion of tartrazine in 1% w/w agarose gel

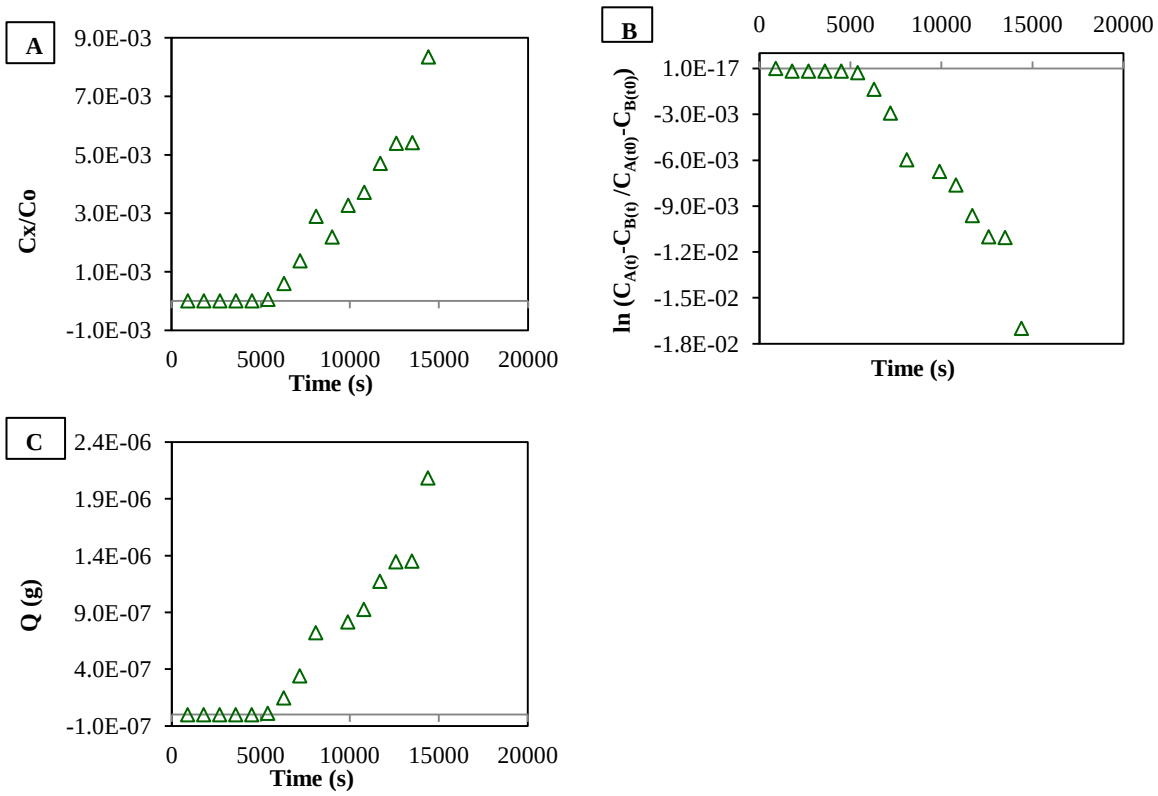

Figure A3-3: Evaluation of diffusivity D or D_e for tartrazine in 1% w/w agarose gel using the tube experiment from a plot of **A**: the Laplace transform method, **B**: the QSS method and **C**: the TL method.

Appendix 3.1.4 Diffusion of tartrazine in 2% w/w agarose Gel

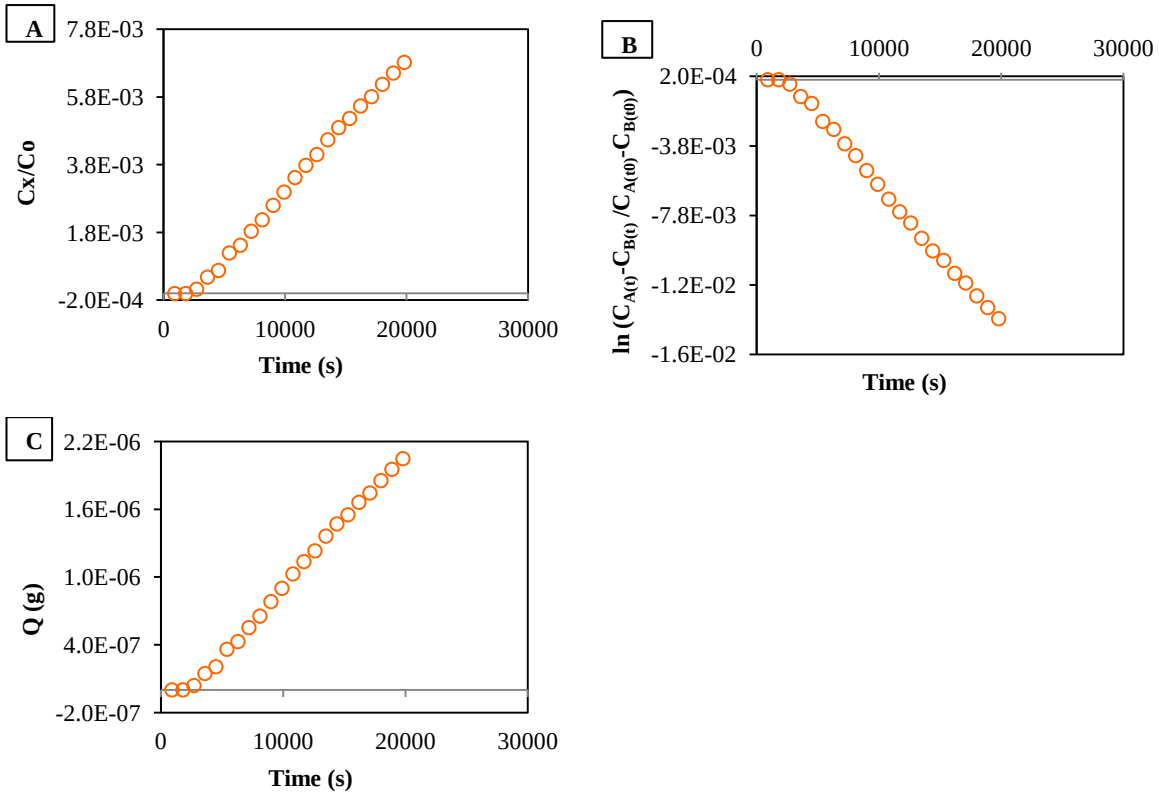

Figure A3-4: Evaluation of diffusivity D for tartrazine in 2% w/w agarose gel using the tube experiment from a plot of A: the Laplace transform method, B: the QSS method and C: the TL method.

Appendix 3.1.5 Diffusion of tartrazine in 2% w/w agarose gel with matched donor and receptor volumes

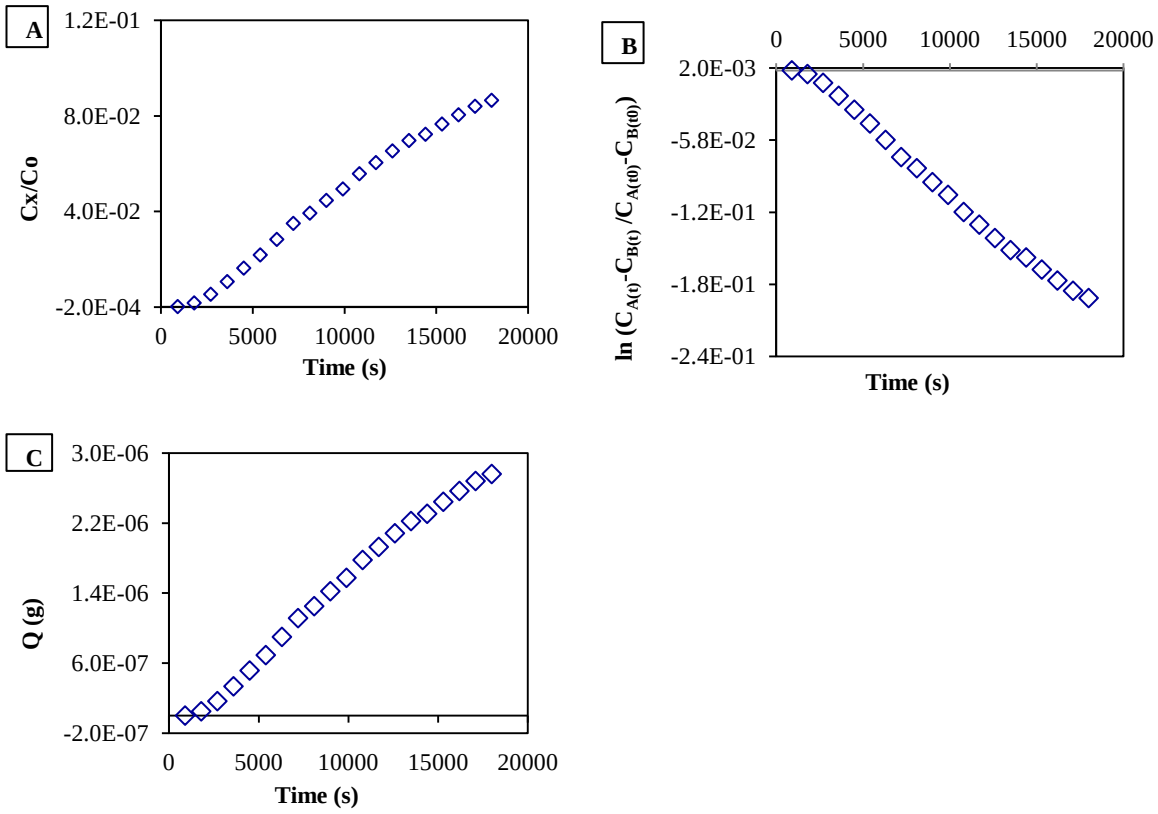

Figure A3-5: Evaluation of diffusivity *D* for tartrazine in 2% w/w agarose gel using the tube experiment with matched donor and receptor volumes from a plot of **A**: the Laplace transform method, **B**: the QSS method and **C**: the TL method.

Appendix 3.2 Figures (representative data) for determination of diffusion coefficient of tartrazine in agarose in INsmart device

Appendix 3.2.1 Diffusion of tartrazine in 2% w/w agarose gel in device

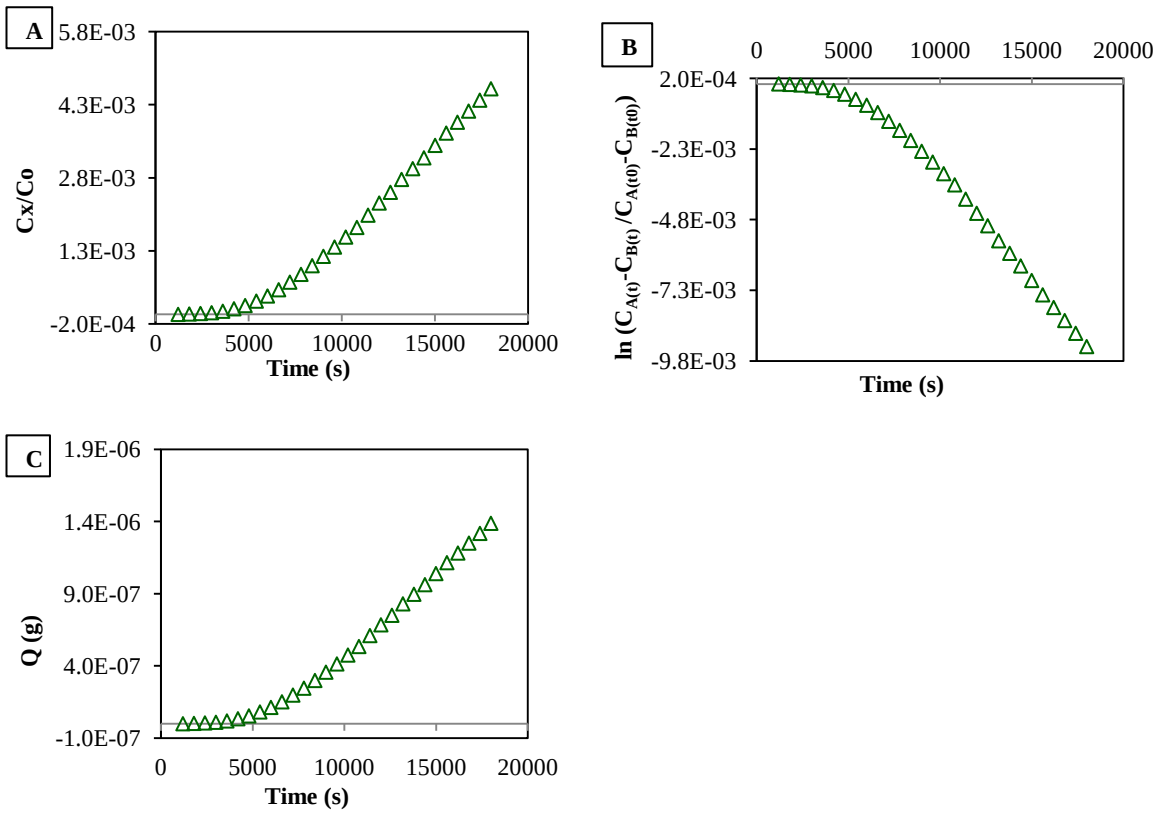

Figure A3-6: Evaluation of diffusivities *D* for tartrazine in 2% w/w agarose gel using the device from a plot of **A**: the Laplace transform method, **B**: the QSS method and **C**: the TL method. The data set presented here has been reduced to every 10th data point to aid visual clarity.

Appendix 3.2.2 Diffusion of tartrazine in 1.5% w/w agarose Gel

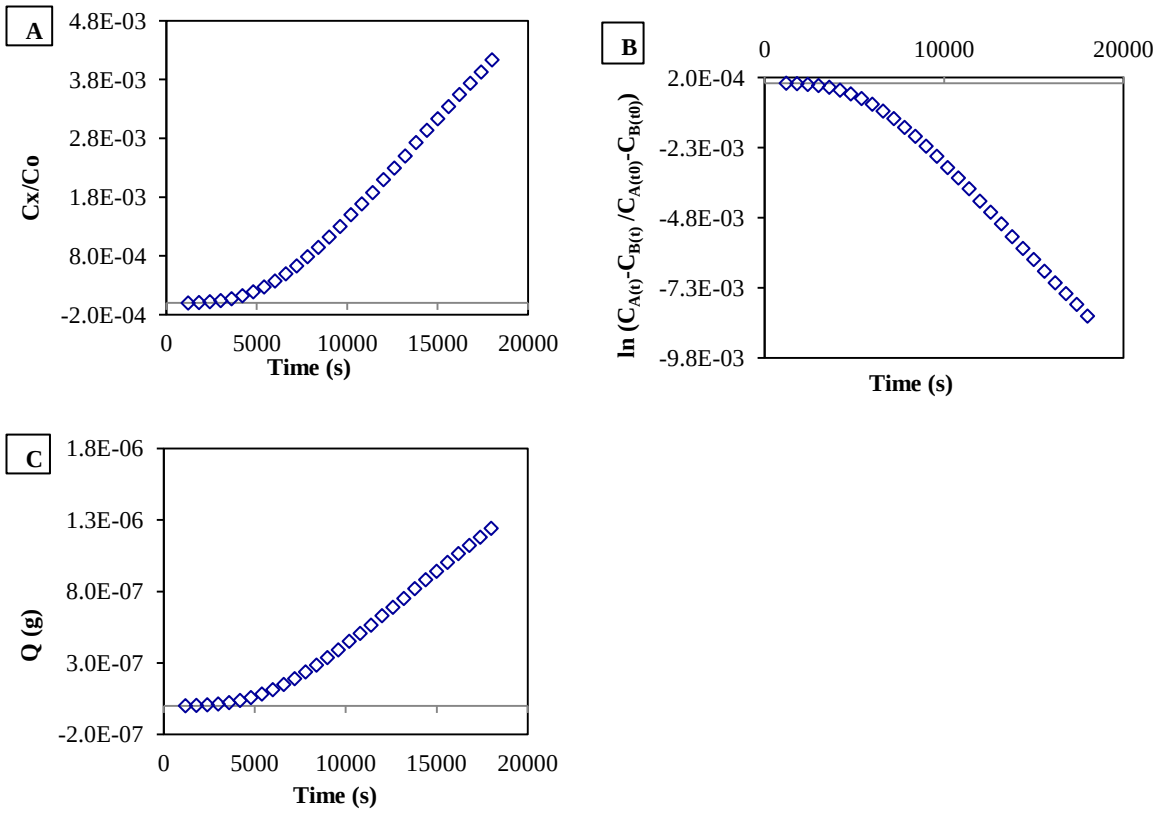

Figure A3-7: Evaluation of diffusivities *D* for tartrazine in 1.5% w/w agarose gel using the device from a plot of **A**: the Laplace transform method, **B**: the QSS method and **C**: the TL method. The data set presented here has been reduced to every 10th data point to aid visual clarity.

Appendix 3.3 Figures (representative data) for determination of diffusion coefficient of tartrazine in non-polymerised dex2M-conA mixture in INsmart device

Appendix 3.3.1 Diffusion of tartrazine in NP gel in device with no glucose

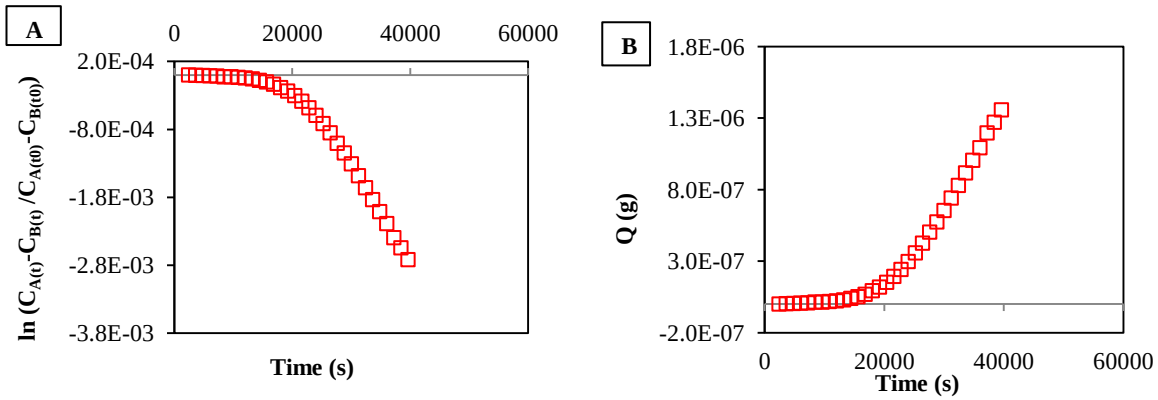

Figure A3-8: Evaluation of diffusivities *D* for tartrazine in NP gel using the device from a plot of **A:** the QSS method and **B:** the TL method. The data set presented here has been reduced to every 10th data point to aid visual clarity.

Appendix 3.3.2 Diffusion of tartrazine in NP gel in device with 0.1% w/w glucose

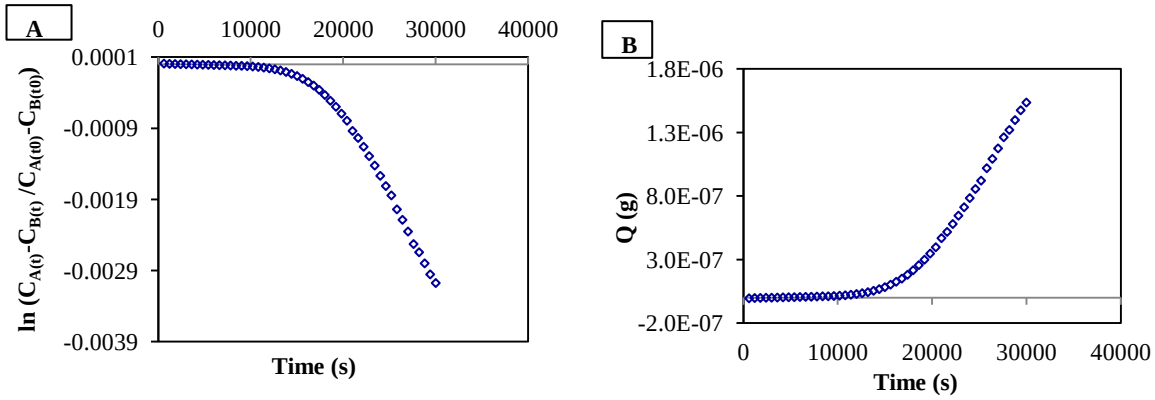

Figure A3-9: Evaluation of diffusivities *D* for tartrazine in NP gel with 0.1% w/w glucose using the device from a plot of **A**: the QSS method and **B:** the TL method. The data set presented here has been reduced to every 5th data point to aid visual clarity.

Appendix 3.3.3 Diffusion of tartrazine in NP gel in device with 0.5% w/w glucose

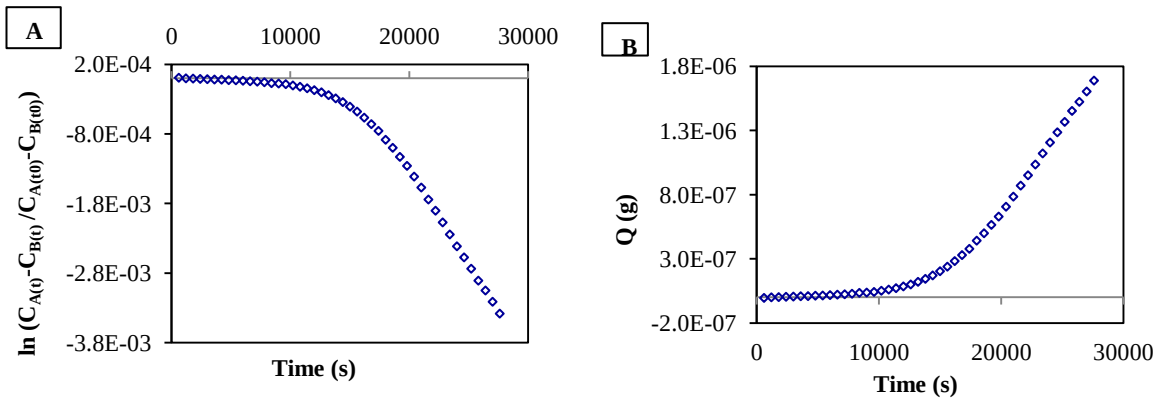

Figure A3-10: Evaluation of diffusivities *D* for tartrazine NP gel with 0.5% w/w glucose using the device from a plot of **A:** the QSS method and **B:** the TL method. The data set presented here has been reduced to every 5th data point to aid visual clarity.

Appendix 3.4 Figures (representative data) for determination of diffusion coefficient of fluorescein sodium in NP gel in INsmart device

Appendix 3.4.1 Determination of diffusion coefficient of fluorescein sodium in NP gel in device with no glucose

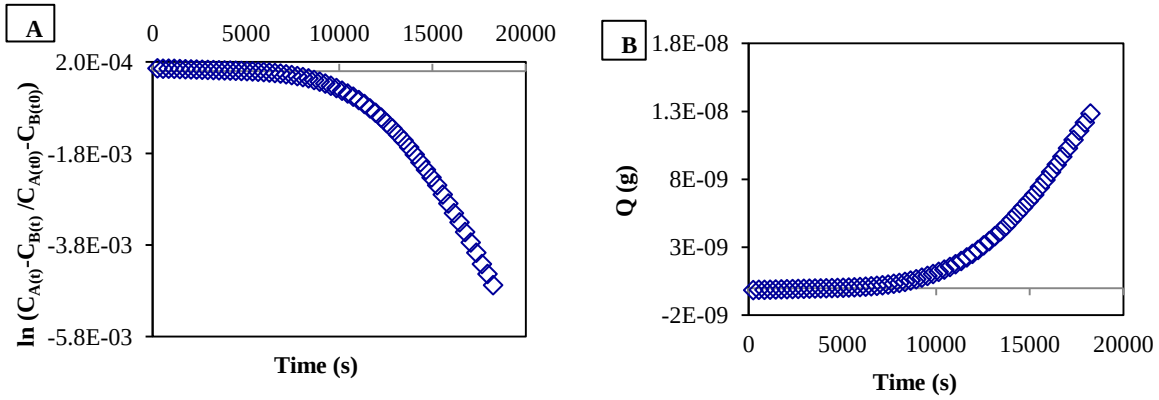

Figure A3-11: Evaluation of diffusivities D for fluorescein sodium in NP gel using the device from a plot of **A**: the QSS method and **B:** the TL method. The data set presented here has been reduced to every 5th data point to aid visual clarity.

Appendix 3.4.2 Determination of diffusion coefficient of fluorescein sodium in NP gel in device with 0.1% w/w glucose

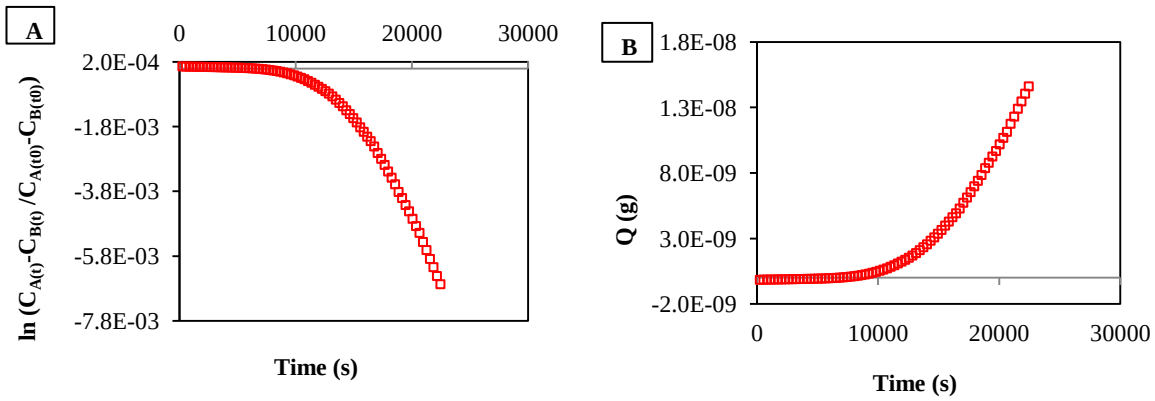

Figure A3-12: Evaluation of diffusivities D for fluorescein sodium in NP gel with 0.1% w/w glucose using the device from a plot of A: the QSS method and B: the TL method. The data set presented here has been reduced to every 5th data point to aid visual clarity.

Appendix 3.4.3 Effect of gel thickness on fluorescein sodium diffusion coefficient in NP gel in device with 0.1% w/w glucose

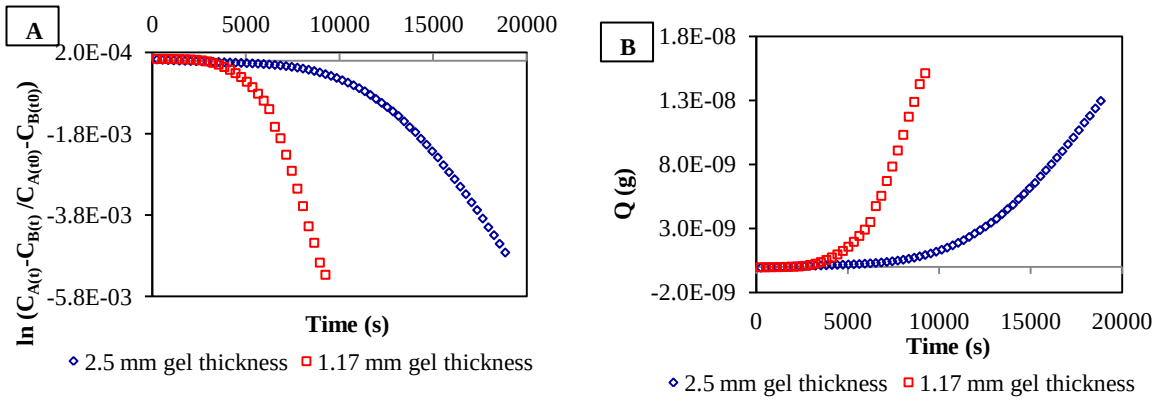

Figure A3-13: Evaluation of diffusivities *D* for fluorescein sodium in NP gel with 0.1% w/w glucose using the device with 2.50 mm and 1.17mm gel thickness from a plot of **A**: the QSS method and **B:** the TL method. The data set presented here has been reduced to every 5th data point to aid visual clarity.

Appendix 3.4.4 Comparison of effect of two different batches of conA on fluorescein sodium diffusivity in NP gel with no glucose in device

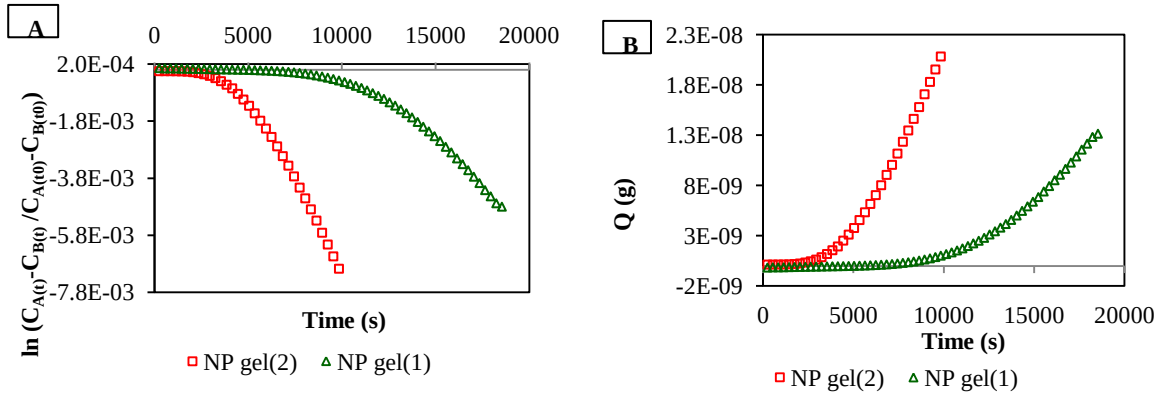

Figure A3-14: Evaluation of diffusivities *D* for fluorescein sodium in NP gel with 0.1% w/w glucose using the device with the two conA batches from a plot of **A**: the QSS method and **B:** the TL method. The data set presented here has been reduced to every 5th data point to aid visual clarity.

Appendix 4 Figures for determination of diffusion coefficient of FITC-insulin from Chapter 7.

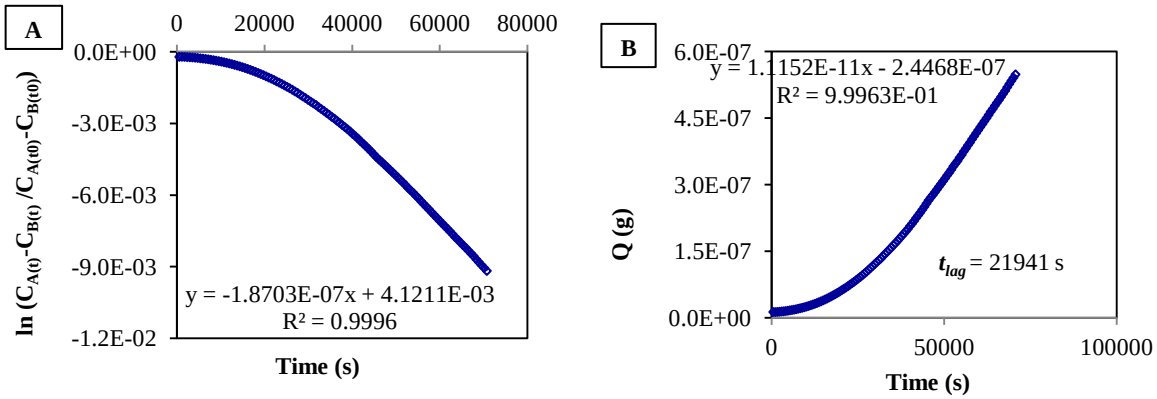

Figure A4-1: Evaluation of diffusivities *D* or D_e for FITC-insulin in NP gel with no glucose from a plot of A: the QSS method and B: the TL method. The data set presented here has been reduced to every 10th data point to aid visual clarity.

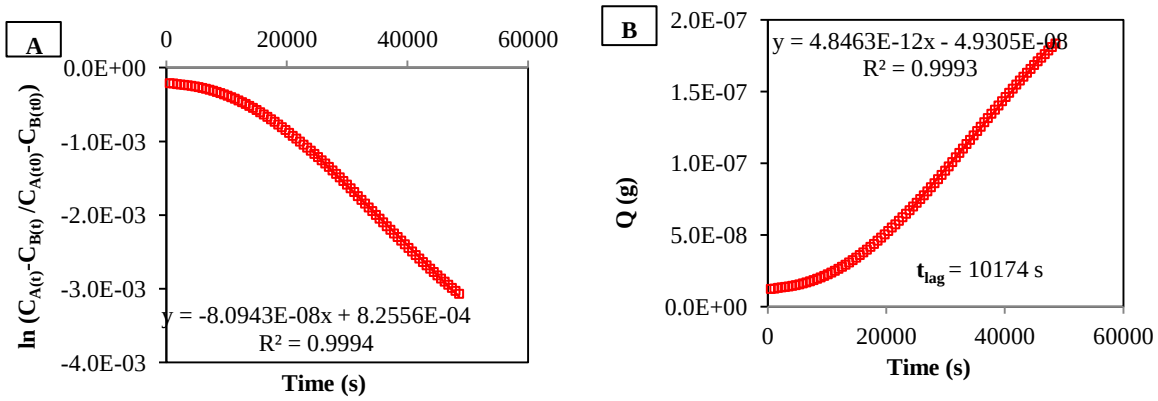

Figure A4-2: Evaluation of diffusivities D or D_e for FITC-insulin in NP gel with 0.1% w/w glucose from a plot of **A:** the QSS method and **B:** the TL method. The data set presented here has been reduced to every 10th data point to aid visual clarity.

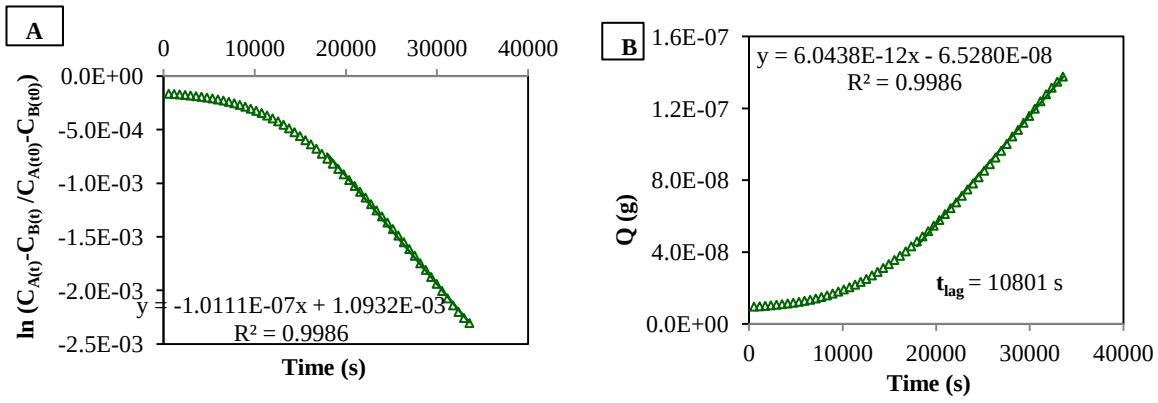

Figure A4-3: Evaluation of diffusivities D or D_e for FITC-insulin in NP gel with 0.2% w/w glucose from a plot of **A:** the QSS method and **B:** the TL method. The data set presented here has been reduced to every 10th data point to aid visual clarity.

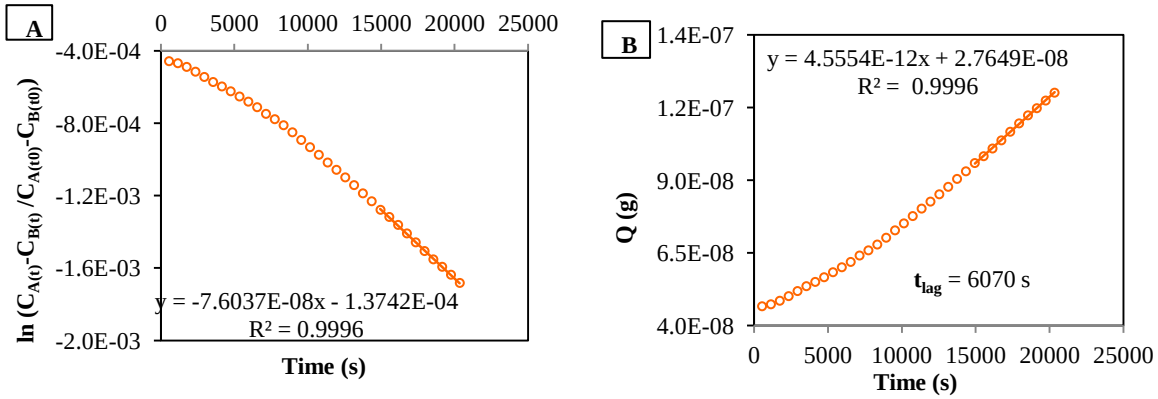

Figure A4-4: Evaluation of diffusivities D or D_e for FITC-insulin in NP gel with 0.5% w/w glucose from a plot of **A:** the QSS method and **B:** the TL method. The data set presented here has been reduced to every 10th data point to aid visual clarity.

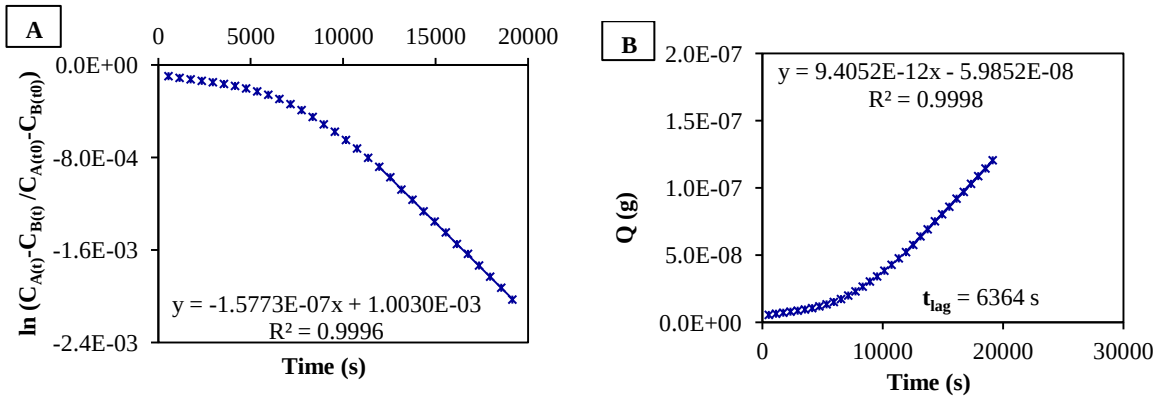

Figure A4-5: Evaluation of diffusivities D or D_e for FITC-insulin in NP gel with 1.0% w/w glucose from a plot of **A:** the QSS method and **B:** the TL method. The data set presented here has been reduced to every 10th data point to aid visual clarity.

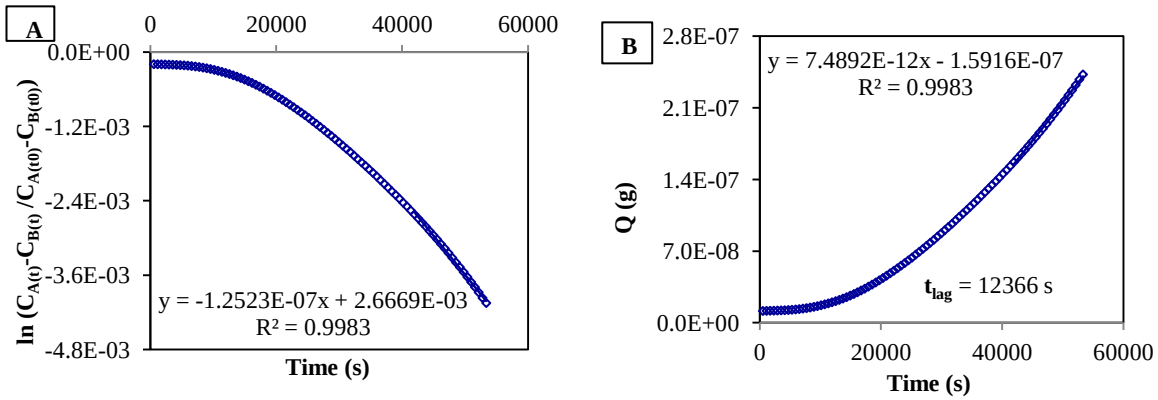

Figure A4-6: Evaluation of diffusivities D or D_e for FITC-insulin in CL gel with no glucose from a plot of **A:** the QSS method and **B:** the TL method. The data set presented here has been reduced to every 10th data point to aid visual clarity.

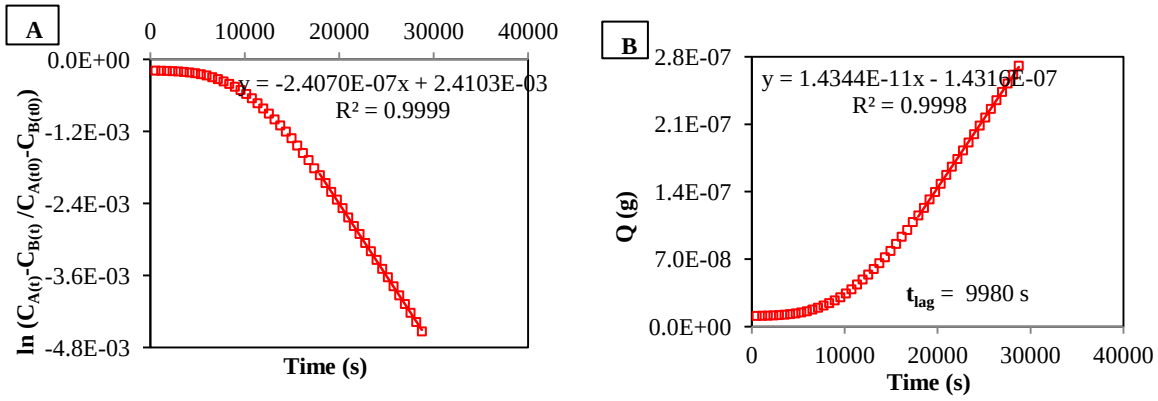

Figure A4-7: Evaluation of diffusivities D or D_e for FITC-insulin in CL gel with 0.1% w/w glucose from a plot of **A:** the QSS method and **B:** the TL method. The data set presented here has been reduced to every 10th data point to aid visual clarity.

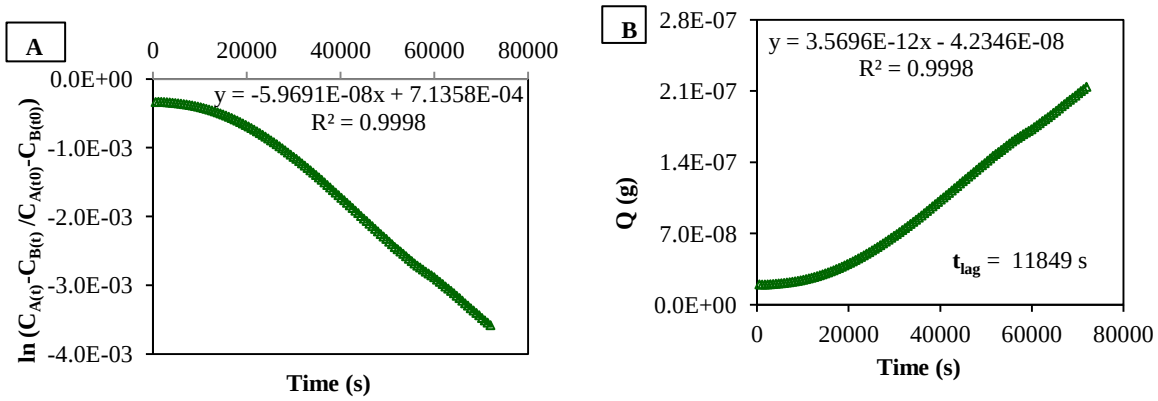

Figure A4-8: Evaluation of diffusivities D or D_e for FITC-insulin in CL gel with 0.2% w/w glucose from a plot of **A:** the QSS method and **B:** the TL method. The data set presented here has been reduced to every 10th data point to aid visual clarity.

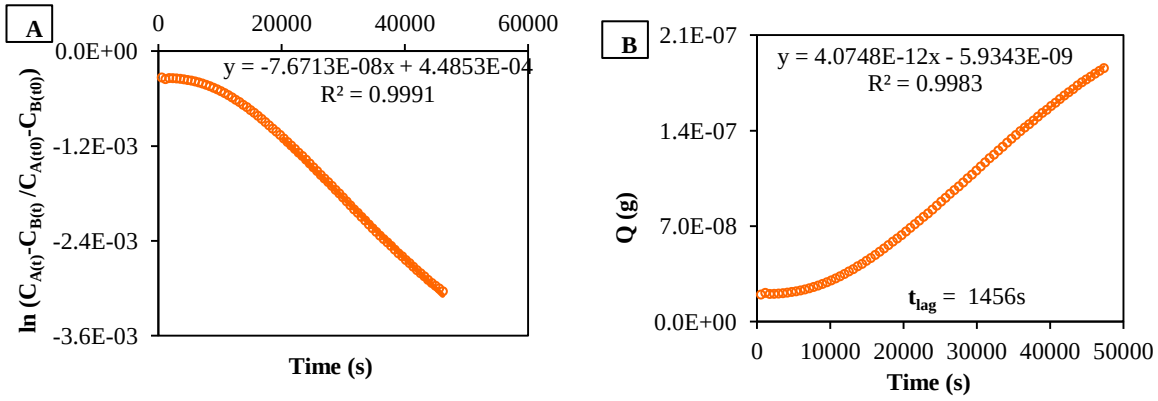

Figure A4-9: Evaluation of diffusivities D or D_e for FITC-insulin in CL gel with 0.5% w/w glucose from a plot of **A:** the QSS method and **B:** the TL method. The data set presented here has been reduced to every 10th data point to aid visual clarity.

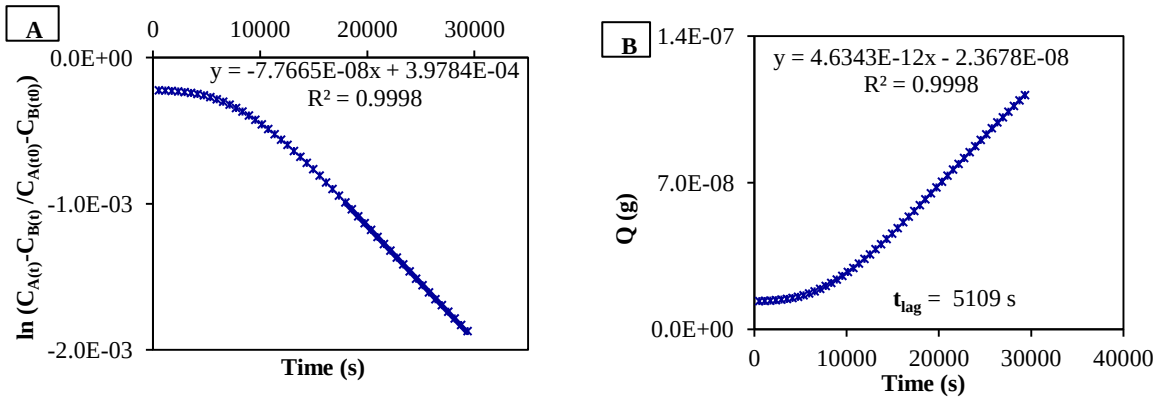

Figure A4-10: Evaluation of diffusivities D or D_e for FITC-insulin in CL gel with 1.0% w/w glucose from a plot of **A:** the QSS method and **B:** the TL method. The data set presented here has been reduced to every 10th data point to aid visual clarity.

Abstract titled 'Diffusion of fluorescent insulin from an acrylic derivatised dextran-concanavalin A gel in an implantable closed loop insulin delivery device' for **poster presentation** at the 41st Annual Meeting & Exposition of the Controlled Release Society, July 13 – 16, 2014, Chicago, USA

Diffusion of fluorescent insulin from an acrylic derivatised dextran-concanavalin A gel in an implantable closed loop insulin delivery device

D. Jacob[1], M J Taylor, P Tomlins, T S Sahota and E Jaroszkiewicz
[1]Leicester School of Pharmacy, Faculty of Health and Life Sciences, De Montfort University, the Gateway, Leicester, LE1 9BH, United Kingdom
P09050910@myemail.dmu.ac.uk

ABSTRACT SUMMARY
The drug delivery mechanism of fluorescently labelled insulin (FITC-Insulin) from a glucose sensitive gel held in an implantable closed loop insulin delivery device was found to be diffusion controlled. The diffusion coefficient of FITC-Insulin in the gel was determined and response to glucose triggers assessed.

INTRODUCTION
A fully functional implantable insulin delivery device which has shown to control blood glucose in diabetic rats and more recently in diabetic pigs has been developed [1, 2].The device encases a reversible glucose-sensitive gel of co-polymerised dextran methacrylate (dex-MA) and concanavalin A methacrylamide (conA-MA), which produces a reversible change in consistency on contact with glucose to modulate insulin transport and thus acts as a self adjusting system. The device, implanted in the peritoneal cavity, works on a very fast feedback mechanism for controlling insulin release, mimicking a normal pancreas enabling to overcome inherent problems encountered in maintaining normoglycemia with current electronically or biologically based closed loop systems. In this work we present the drug release kinetics data for FITC-Insulin from the gel used in the device.

EXPERIMENTAL METHODS

Synthesis and characterisation of fluorescently labelled insulin
Human Insulin was labelled with fluorescein isothiocyanate (FITC). Briefly, 10mg/ml human insulin in 0.1M phosphate buffer containing 200µM EDTA (pH 7.0) was prepared. FITC solution prepared in acetone (5mg/mL) was added dropwise to the human insulin stock solution (3:1 molar ratio) at pH 7.0 in the dark and stirred for 25 hours. After this time the reaction was stopped and the FITC-Insulin conjugates were fractionated by Gel Permeation Chromatography using a Sephadex G25 column. Fractionated FITC-Insulin conjugates were characterised using HPLC and EI Mass Spectroscopy [4]. The FITC-Insulin synthesised were predominantly di-labelled conjugates and contained no unlabelled insulin.

Preparation of gel
The preparation of the gel has been described previously [3]. Briefly, Con-MA (100mg) was dissolved in distilled water and photoinitiator Irgacure® (0.178 µmoles) was added. Dex-MA (RMM 500Da) (100mg) was added to the mixture and stirred to form a viscous solution, covered in foil and allowed to stand for 2 hours; the mixture was then placed between two glass plates separated by a 60µm thick gasket and was irradiated under UV-light (365nm, 10mJ cm^{-2}) for 5 minutes. The crosslinked gel (CLgel) formed was stored aseptically at 4°C for at least 24 hours prior to use. A non-polymerised version of the gel (NPgel) containing underivatised conA and dextran (RMM 2000kDa) was prepared in the same way but not irradiated.

Evaluation of drug delivery mechanism
An experimental set-up was designed using the same InSmart device as was used in *in vivo* pig trials previously [2] as shown in Figure 1.

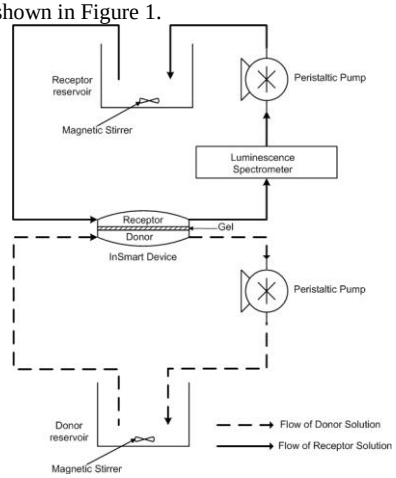

Figure 1: Schematic of the experimental set-up.

FITC-Insulin diffusing through the gel from the donor side to the receptor side was monitored over time by conversion of fluorescence intensity recordings at 518nm into concentration values using calibration curves. Preliminary experiments using probe dye fluorescein sodium and using NPgel aided selection of appropriate mathematical models.

The Power Law (Peppas equation): The release of fluorescein sodium from the NPgel was recorded over time and applied to the power law shown below to determine if the drug delivery mechanism was Fickian diffusion.

$$\frac{M_t}{M_\infty} = kt^n$$

Where, M_t and M_∞ are the absolute cumulative amount of drug released at time t and infinite time, respectively; k is

a constant incorporating structural and geometric characteristics of the system and n is the diffusional exponent, which is indicative of the mechanism of drug release.

Mathematical models for determination of Diffusion coefficient: The diffusion cell technique – Quasi steady state (QSS), the Time lag (TL) slope and the TL intercept methods based on Fick's law were identified for determination of diffusion coefficient of FITC-Insulin [5].

QSS:

$$In\frac{C_{L,A\,(t)} - C_{L,B(t)}}{C_{L,A0} - C_{L,B0}} = -\frac{D_e}{l}A_g\left(\frac{1}{V_A}+\frac{1}{V_B}\right)(t - t_0)$$

D_e is calculated from the slope of the line obtained by plotting the left-hand side of equation against time *t*.

TL slope:

$$Q_t = V_{B0}C_{L,B(t)} = \frac{A_g D C_{L,A0}}{l}\left(t - \frac{l^2}{6D}\right)$$

D is calculated by plotting the total amount of solute transferred through the gel (Q_t) against time (*t*).

TL intercept:

$$t_{lag} = \frac{l^2}{6D}$$

D is calculated from the lag time, t_{lag}, the intercept of the linear part of the TL plot.

(Key: D_e & *D* are the effective diffusion coefficient and diffusion coefficient, V_A & V_B *volumes* of the two chambers separated by the gel, A_g is effective membrane area, *l* is gel thickness, C_{LA} & C_{LB} are the concentration of the drug solute in the two chambers at initial time t_0 or at time *t*).

Glucose sensitivity of the gel was assessed by challenging the system with increasing physiologically relevant concentrations of glucose (0.1% to 1%).

RESULTS AND DISCUSSION

The Power Law: The gel (thickness 1.17mm) housed in the device can be considered as a thin film or slab with no edge effects and the power law fit for the release of fluorescein sodium through the gel indicates diffusion controlled release (Figure 2).

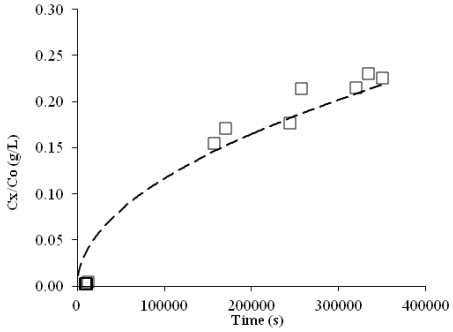

Figure 1: Power law fit for fluorescein sodium release through NPgel. Dotted line represents the power law fit for n=0.5, indicating diffusion controlled release.

Determination of Diffusion coefficient: Table 1 shows diffusion coefficients from mathematical models for FITC-Insulin in NPgel and CLgel with and without 0.1% basal glucose.

Gel	QSS method D_e(m^2/s)	TL Slope method D (m^2/s)	TL Int. method D (m^2/s)
NPgel	1.05E-11	1.04E-11	1.12E-11
NPgel + 0.1% Glucose	4.59E-12	4.58E-12	2.24E-11
CLgel	7.54E-12	7.52E-12	1.44E-11
CLgel + 0.1% Glucose	5.90E-12	5.89E-12	9.92E-11

Table 1: Diffusion coefficient values (*D* and D_e) for FITC-Insulin in NPgel and CLgel with and without 0.1% basal glucose determined using the QSS method, the TL slope method and the TL intercept method.

The QSS and TL methods gave reliable correlation in diffusion coefficient values for FITC Insulin in NPgel and CLgel. The TL intercept method gave different values, approximately a decade faster in some instances, which is consistent with the findings of others [5].

Glucose sensitivity: Figure 3 shows increasing *D* values with increasing glucose concentrations in NPgel.

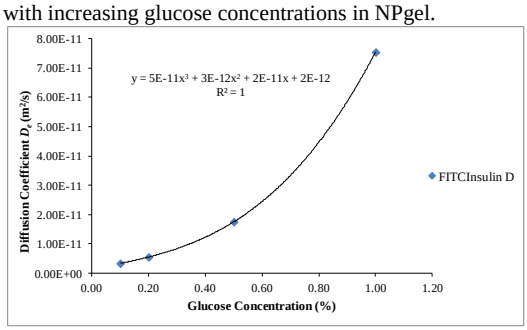

Figure 2: FITC-Insulin diffusion coefficient values with increasing glucose concentration in NPgel.

CONCLUSION

The drug release mechanism from the glucose sensitive gel held in an implantable closed loop insulin delivery device was found to be diffusion controlled. The diffusion coefficient for FITC-Insulin in the NPgel was $1.05E^{-11}$ m^2/s and in the CLgel was $7.53E^{-12}$ m^2/s. The *D* values increase with increasing glucose concentrations, device thus showing glucose sensitivity, mimicking pancreas.

REFERENCES

1.Taylor, M. J. et al. J of Pharm. Sci. 9, 10: 4215-4227 (2010).
2.Sahota, T.S. & Taylor, M. J.CRS Annual Symp 2012, Quebec, Canada.
3.Tanna, S. et al. Biomat 27: 1586-1597(2006).
4.Hentz, G. N. et al. Anal. Chem. 69: 4994-5000 (1997).
5.Zhang, W. & Furusaki, S. Biochem. Eng. J 9: 73-82 (2001).

ACKNOWLEDGMENTS

D Jacob would like to acknowledge the research studentship provided by De Montfort University.